



UNIVERSITY OF NAIROBI

FACULTY OF ENGINEERING

DEPARTMENT OF ENVIRONMENTAL & BIOSYSTEMS ENGINEERING

**Modelling Soil Erosion and Sediment Yield for Dam Reservoir Management:
A Case Study of the Maruba Dam Catchment, Kenya**

By

ALLOIS KIOKO LUVAI

F80/55100/2019

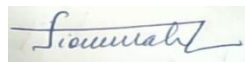
BSc. (Hons). Bios. Eng. (Nairobi), MSc. Env. & Bios. Eng. (Nairobi)

A thesis submitted for examination in partial fulfilment of the requirements for the award of the degree of **Doctor of Philosophy in Environmental & Biosystems Engineering**, in the Department of Environmental and Biosystems Engineering of the University of Nairobi

November 2022

DECLARATION

I, **Allois Kioko Luvai**, hereby declare that this thesis is my original work and to the best of my knowledge, has not been presented in any other university or academic institution.



.....

Allois Kioko Luvai

21 November 2022

.....

Date

This thesis has been submitted for examination with our approval as university supervisors.



.....

Dr. John P.O. Obiero
University of Nairobi
Nairobi, Kenya

21 November 2022

.....

Date



.....

Dr. Christian T. Omuto
University of Nairobi
Nairobi, Nairobi

21 November 2022

.....

Date

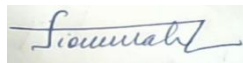
DECLARATION OF ORIGINALITY FORM

Name of student: Luvai Allois Kioko
Registration Number: F80/55100/2019
Faculty: Engineering
Department: Environmental and Biosystems Engineering
Course Name: PhD in Environmental and Biosystems Engineering
Title of the work: Modelling Soil Erosion and Sediment Yield for Dam Reservoir Management: A Case Study of Maruba Dam Catchment, Kenya

Declaration

1. I understand what plagiarism is and I am aware of the University's policy in this regard.
2. I declare that this thesis is my original work and has not been submitted elsewhere for examination, award of a degree or publication. Where other people's works or my own work has been used, this has properly been acknowledged and referenced in accordance with the University of Nairobi's requirements.
3. I have not sought or used the services of any professional agencies to produce this work
4. I have not allowed, and shall not allow anyone to copy my work with the intention of passing it off as his/her own work
5. I understand that any false claim in respect of this work shall result in disciplinary action in accordance with University Plagiarism Policy.

Signature:



Date: 21 November 2022

ACKNOWLEDGEMENT

I would want to express my gratitude to the Almighty Lord for his abundant blessings and grace throughout this research process. I am grateful to a number of people who helped this work succeed.

Dr. John P.O. Obiero and Dr. Christian T. Omutto, who embraced the challenge of guiding me through my research, deserve my gratitude. Dr. John P.O. Obiero deserves special recognition for always walking alongside me throughout data collection activities and ensuring that I did the right thing. Thank you very much for all of your help and advice. I would like to express my gratitude to Dr. Joseph K. Sang of Jomo Kenyatta University of Agriculture and Technology for his direction and assistance in utilizing the multifrequency acoustic profiling system for bathymetric data collection and analysis. You always greeted me warmly and made time for me in your busy schedule. Thank you very much.

Without some financial backing, this research would not have been able to continue. In this regard, I appreciate the financing provided by the Kenya Climate Smart Agriculture Project (KCSAP). I would also like to express my gratitude to the Water Resources Authority of Kenya (WRA), Machakos sub-branch, and the Machakos Water and Sewerage Company Limited (MAWASCO) for allowing me to collect important data inside the Maruba dam reservoir.

Finally, I would want to express my gratitude to the members of the Department of Environmental and Biosystems Engineering, headed by Eng. Dr. Duncan O.

Mbuge, for their support throughout my PhD studies. Thank you so much for your support Dorcas, Peter, and Nanje, my classmates. Thank you for your cooperation throughout field work and laboratory analysis, Mr. Boniface A. Muliro.

DEDICATION

This thesis is dedicated to my wife, Ruth Mulewa Kioko, my son, Victor Luvai Kioko, my daughter, Magdalene Mutile Kioko, and my late mother, Magdalene Mutile Luvai, for their moral support, encouragement, and patience with me while I carried out this research work to its final conclusion.

LIST OF TABLES

Table 2.1	Land-use types and erosion rates	22
Table 2.2	Average global rates of sedimentation and time period when 80 and 70 percent respectively of the capacity of the reservoir will be lost due to sedimentation	42
Table 2.3	Key parameters involved in modelling water erosion and their relevant options	52
Table 2.4	Rainfall erosivity factor algorithms	68
Table 2.5	Soil erodibility factor algorithms	71
Table 2.6	Topographic factor algorithms	76
Table 2.7	Land cover algorithms	79
Table 2.8	Conservation practices factors	80
Table 2.9	Generalized sediment delivery ratios by USSCS (1971)	89
Table 3.1	Conservation practice factors	111
Table 3.2	Guidelines for open-water transect spacing for bathymetry surveys	115
Table 4.1	Catchment's area soil properties	131
Table 4.2	Soil loss classes	140
Table 4.3	Land use and Land cover Changes between 2000 and 2020	143
Table 4.4	Physicochemical properties of bottom sediments	160
Table 4.5	Correlation matrices between physicochemical properties of bottom sediments of Maruba Reservoir	168
Table 4.6	Physicochemical properties of deposited sediments at the reservoir inlet	169
Table 4.7	Reservoir bottom sediments vs. sediment deposits at catchment outlet	177

LIST OF FIGURES

Figure 2.1	Key processes affecting soil erosion by water	19
Figure 2.2	Management of soil erosion	26
Figure 2.3	Sediment transport modes	35
Figure 2.4	Sediment equilibrium in a reservoir	50
Figure 2.5	Management strategies for reservoir sedimentation	52
Figure 2.6	Methods for assessing siltation and sedimentation processes within reservoirs and the upstream erosion dynamics	81
Figure 3.1	Research area map	99
Figure 3.2	Methodology on land use/land cover change detection	103
Figure 3.3	Derivation of the soil erodibility factor	108
Figure 3.4	Flow chart methodology for estimating annual soil loss	112
Figure 3.5	Bathymetric survey transects and ties lines orientation	115
Figure 3.6	Bathymetric survey system set up	118
Figure 3.7	Waypoints recorded during bathymetry survey exercise	118
Figure 3.8	Sediment coring procedure	123
Figure 3.9	Retrieval of the sediment sample from the core tube	123
Figure 3.10	Sampling points at the reservoir inlet	125
Figure 4.1	Rainfall erosivity factor map	129
Figure 4.2	Soil erodibility factor map	132
Figure 4.3	Topographic factor map	133
Figure 4.4	Cover management factor map	135
Figure 4.5	Support practices factor map	136

Figure 4.6	Average annual soil loss	140
Figure 4.7	Soil loss proportions	140
Figure 4.8	LULC classification maps	144
Figure 4.9a	Sediment pre-impoundment boundary	147
Figure 4.9b	Multi-frequency acoustic profiles and sediment core display in DepthPic software	148
Figure 4.10	Contour map for Maruba dam reservoir	149
Figure 4.11a	Longitudinal and transversal profiling of Maruba dam reservoir	150
Figure 4.11b	Profiled cross-sections depicting reservoir depth variation	151
Figure 4.12	Reservoir water storage characteristics	153
Figure 4.13a	Sedimentation status map for Maruba dam reservoir	154
Figure 4.13b	Sediment profiling in Maruba dam reservoir	154
Figure 4.13c	Profiled sections depicting sediment thickness	155
Figure 4.14	Reservoir sediment storage characteristics	156
Figure 4.15	Comparison of particle size distribution in sediments	181

LIST OF ABBREVIATIONS AND ACRONYMS

APS	Acoustic Profiling System
BSS	Bathymetric Survey System
CV	Coefficient of Variation
DEM	Digital Elevation Model
GIS	Geographic Information System
LiDAR	Light Detection and Ranging
LULC	Land Use and Land Cover
MLC	Maximum Likelihood Classifier
MUSLE	Modified Universal Soil Loss Equation
NDVI	Normalized Difference Vegetation Index
OLI	Operational Land Imager
PLS	Projected Lifespan
RCMRD	Regional Centre for Mapping of Resources for Development
ReSR	Volumetric Reservoir Sedimentation Rate
RS	Remote Sensing
RUSLE	Revised Universal Soil Loss Equation
sBD	Sediment Bulk Density
SCS	Stream Channel Slope
SDR	Sediment Delivery Ratio
SV	Sediment Volume
SY	Sediment Yield
TE	Trap Efficiency
TIR	Thermal Infrared

USDA	United States Department of Agriculture
USGS	United States Geological Survey
USLE	Universal Soil Loss Equation
UTM	Universal Transverse Mercator

ABSTRACT

Soil erosion is a severe land degradation issue that many developing nations continue to face. Its effects are more pronounced in catchment areas due to the combination of environmental and human factors. According to experts, soil erosion is a costly problem to fix, which is why so many attempts have been made to avoid it. However, in catchment areas, soil and water management strategies cannot be implemented without prior information of soil loss.

In Machakos town's Maruba dam catchment, soil loss is a serious problem. It has resulted in severe soil degradation in the catchment area as well as sedimentation issues in the dam reservoir. Scientific data on soil erosion in the catchment area and reservoir sedimentation rates, on the other hand, is scarce. Furthermore, the dam environment is desolate, with little evidence of soil protection measures. The Machakos County Government, the Kenya Water Resources Authority, and the Machakos Water and Sewerage Company Limited have all battled to manage the Maruba dam reservoir. The goal of this study was to model the annual soil erosion rates and sediment yield in the dam catchment, estimate annual reservoir sedimentation rates, and assess the physicochemical qualities of dam reservoir sediments for biotic or abiotic uses.

The Revised Universal Soil Loss Equation (RUSLE) was used in this study to estimate average annual soil erosion rates, as well as a bathymetric survey to determine reservoir sedimentation state and laboratory testing of the dam

sediments' physicochemical properties. Remote sensing and geographical techniques were used to determine the RUSLE model parameters. Bathymetric data was acquired using the multifrequency acoustic profiling system (APS), then analyzed in DepthPic 5.0.2 software before being imported into Golden Surfer 22 for spatial analysis. The sediment yield from bathymetric data was estimated as a ratio of the sediment volume and the catchment area, whereas that from the RUSLE model was computed as a product of the sediment delivery ratio (SDR) and the catchment's average soil loss. The physicochemical parameters of dam sediments were determined using standard laboratory procedures.

The annual soil erosion rates in the Maruba dam reservoir ranged from 0 to 29 t ha⁻¹yr⁻¹, with an average of 0.9708 t ha⁻¹yr⁻¹, according to the study. The RUSLE-based sediment output was computed as 0.1775 t ha⁻¹ yr⁻¹. The sediment deposition in the Maruba dam reservoir was estimated to be around 290435 m³, accounting for 10.8 % of the reservoir volume based on current day bathymetry. The annual rate of reservoir volume loss due to sedimentation was 1 %, which was consistent with global data. The sediment yield and the projected reservoir life, respectively, were 3.34 t ha⁻¹ yr⁻¹ and 95 years. In the study, the reservoir sedimentation rate approach was found to be a better strategy for predicting sediment yield because the RUSLE model-based was found to underestimate sediment yield. On the other hand, the RUSLE model was shown to be excellent for assessing the spatial variance of soil loss within a catchment area in this study.

The reservoir's bottom sediments were mostly clay (56.31 %) and sand particles (39.75 %), whereas the deposited sediments at the reservoir inlet were mostly sandy (54.6 %). In the bottom sediments of the Maruba dam reservoir, the mean potassium, nitrogen, and phosphorus levels were 0.46 %, 0.12 %, and 12.81 mg.kg⁻¹, respectively. Similarly, the chemical analysis of deposited sediments at the reservoir inlet showed that mean nitrogen, phosphorous and potassium contents were 0.11 and 0.10 %, 17.51 and 13.16 mg.kg⁻¹, and 0.38 and 0.43 % for the surface and subsurface horizons, respectively. According to the findings, both forms of sediment might be employed biotically to boost vegetation and plant cover around the dam and even in agricultural fields upon enrichment with nitrogen and organic carbon. More specically, bottom sediments could potentially be used to improve the water retention capacity of the catchment's sandy soils. Further, the sandy sediments at the reservoir inlet would necessitate the local government authority's coordination of sand harvesting activities as a way of sediment drenching. This process would boost the reservoir's storage capacity while also providing economic benefits to the community and local government.

LIST OF PUBLICATIONS

Published

1. Luvai, A., Obiero, J. Omuto, C. (2022). The Physicochemical Properties of Deposited Sediments at the Maruba Dam Reservoir Inlet, Machakos County, Kenya. *Applied and Environmental Soil Science (Hindawi)*, 3148073. <https://doi.org/10.1155/2022/3148073>
2. Luvai, A., Obiero, J., Omuto, C. and Sang, J. (2022). Soil Erosion and Sediment Yield Modeling for the Maruba Dam Catchment, Machakos County, Kenya. *Modeling Earth Systems and Environment (Springer)*. <https://doi.org/10.1007/s40808-022-01478-4>
3. Luvai, A., Obiero, J. Omuto, C. (2022). Physicochemical properties of bottom sediments in Maruba dam reservoir, Machakos, Kenya. *Applied and Environmental Soil Science (Hindawi)*, 2382277. <https://doi.org/10.1155/2022/2382277>
4. Luvai, A., Obiero, J. and Omuto, C. (2022). Soil Loss Assessment Using the Revised Universal Soil Loss Equation (RUSLE) Model. *Applied and Environmental Soil Science (Hindawi)*, 2122554. <https://doi.org/10.1155/2022/2122554>
5. Luvai, A.K., Obiero, J.P.O., and Omuto, C.T. (2021). Assessment of Soil Loss in a Typical Ungauged Dam Catchment using RUSLE Model (Maruba Dam, Kenya). *Journal of Environment and Earth Science (IISTE)*, 11(16): 56 – 68. <http://doi.org/10.7176/JEES/11-16-06>

6. Luvai, A.K., Obiero, J.P.O. and Omuto, C.T. (2021). Land Use and Land Cover Change Assessment for Management of a Dam Reservoir (A Case Study of Maruba Dam, Machakos). *International Journal of Engineering Research & Technology (IJERT)*, 10(8): 414 – 418.
7. Luvai, A.K., Obiero, J.P.O. and Omuto, C.T. (2020). Methods for Erosion Estimates in Assessment of Soil Degradation: A Review for Catchments in Kenya. *International Journal of Engineering Research & Technology (IJERT)*, 9(5): 489 - 494.

Conferences

1. Soil Loss Assessment in an Ungauged Dam Catchment Using RUSLE Model (A Case Study of Maruba Dam, Machakos, Kenya). A paper presented at the Kenya Climate Smart Agriculture Workshop held at Naivasha on 22-26th November, 2021.

TABLE OF CONTENTS

DECLARATION	ii
DECLARATION OF ORIGINALITY FORM.....	iii
ACKNOWLEDGEMENT	iv
DEDICATION	vi
LIST OF TABLES	vii
LIST OF FIGURES	viii
LIST OF ABBREVIATIONS AND ACRONYMS.....	x
ABSTRACT.....	xii
LIST OF PUBLICATIONS	xv
CHAPTER ONE: INTRODUCTION	1
1.1. Background.....	1
1.2. Problem Statement and Justification.....	8
1.2.1. Problem Statement	8
1.2.2. Justification	11
1.3. Objectives	14
1.3.1. Overall Objective	14
1.3.2. Specific Objectives	14
1.4. Research Questions.....	15
CHAPTER TWO: LITERATURE REVIEW	16
2.1. Soil Erosion Process	16
2.1.1. Introduction.....	16
2.1.2. Soil Erosion Due to Water	17
2.1.3. Effects of Water Erosion.....	20
2.2. Accelerated Soil Erosion.....	21
2.2.1. Impacts of Land use and/or Land Cover on Soil Erosion	21
2.2.2. Effects of Environmental Factors on Soil Erosion.....	23
2.2.3. Management Factors and Soil Erosion	24
2.2.4. Restoration Measures	25
2.3. Sediment Yield, Sediment Transfer and Sedimentation of Reservoirs.....	32
2.3.1. Sediment Yield.....	32

2.3.2. Sediment Transfer.....	34
2.3.3. Sedimentation of a Reservoir.....	36
2.3.4. Bottom Sediments.....	42
2.3.5. Beneficial Use of Reservoir Sediments	44
2.4. Reservoirs and Climate Change.....	46
2.5. Management Strategies against Sediment in Reservoirs	49
2.6. Soil Erosion Modelling.....	53
2.6.1. Why Modeling?	53
2.6.2. Soil Erosion Models.....	54
2.6.3. Model Scales.....	59
2.7. GIS and RS Applications in Modelling Soil Erosion	61
2.8. The RUSLE Model.....	63
2.8.1. Overview.....	63
2.8.2. RUSLE Parameterization.....	65
2.9. Data Simulation and Validation of Sediment Yield.....	80
2.9.1. Suspended Sediment Dynamics.....	82
2.9.2. Bathymetric Survey	90
2.10. Conclusion of Literature Review	94
CHAPTER THREE: METHODOLOGY	97
3.1. Description of the Research Area	97
3.2. Spatial Modelling of Soil Erosion.....	99
3.2.1. Data Sources	100
3.2.2. Methods	101
3.3. Sedimentation Status of the Maruba Dam Reservoir.....	113
3.3.1. Pre-bathymetric Survey	114
3.3.2. Bathymetric Survey	115
3.3.3. Post-bathymetric Survey	118
3.3.4. Determination of Sediment Accumulation Rate, Overall Storage Capacity Loss, Projected Reservoir Life, and Sediment Yield	120
3.4. Physicochemical Analysis of Sediments.....	122
3.4.1. Reservoir Bottom Sediments	122

3.4.2. Sediments at the Reservoir Inlet	124
3.4.3. Sediment Sample Preparations for Laboratory Analysis	125
3.4.4. Laboratory Analysis of Sediments	126
3.4.5. Statistical Analysis.....	127
CHAPTER FOUR: RESULTS AND DISCUSSIONS	128
4.1. RUSLE Model Parameterization	128
4.1.1. Rainfall Erosivity (R) Factor	128
4.1.2. Soil Erodibility (K) Factor	130
4.1.3. Topographic (LS) Factor.....	132
4.1.4. Land Cover (C) Factor	133
4.1.5. Support Practices (P) Factor	135
4.1.6. The Average Annual Soil Loss Potential.....	136
4.1.7. Sediment Yield.....	141
4.1.8. Land Use/ Land Cover Assessment	143
4.2. Bathymetric Survey Data.....	146
4.2.1. Acoustic Layers and Sediment Thickness	146
4.2.2. Isopach Profiles.....	147
4.2.3. Water Storage in the Dam Reservoir	148
4.2.4. Sediment Storage in Maruba Dam Reservoir	153
4.3. The Physicochemical Characteristics of Reservoir Bottom Sediments	159
4.3.1. Textural Analysis	160
4.3.2. Sediment Bulk Density	162
4.3.3. Sediment pH.....	162
4.3.4. Electrical Conductivity	164
4.3.5. Organic Matter Content	164
4.3.6. Macronutrients	166
4.3.7. Correlations.....	167
4.4. Physicochemical Characteristics of Sediments at the Reservoir's inlet.....	169
4.4.1. Sediment Texture	170
4.4.2. Sediment pH and Electrical Conductivity.....	172
4.4.3. Bulk Density and Porosity	173

4.4.4. Sediment Permeability	174
4.4.5. Sediment Organic Matter	174
4.4.6. Penetration Resistance	176
4.4.7. Micronutrients.....	176
4.4.8. Comparison between Reservoir Bottom Sediments and Sediments at the Reservoir Inlet.....	177
4.4.9. Beneficial use of Sediments.....	181
4.5. Contributions to Knowledge and Innovative Aspects.....	182
CHAPTER FIVE: CONCLUSIONS AND RECOMMENDATIONS	183
5.1. Conclusions.....	183
5.2. Recommendations.....	184
5.2.1. Recommendations for Policy	184
5.2.2. Recommendations for Future Research	185
REFERENCES	186

CHAPTER ONE: INTRODUCTION

1.1. Background

It is worth mentioning that, given the current trends in land use, which are exacerbated by climate change, fertile soils would be crucial resources for human survival, (Alewell *et al.*, 2019). In the recent decades, rapid land degradation has escalated into a major environmental problem, jeopardizing the health of natural ecosystems, (Bou-imajjane & Belfoul, 2020). Land degradation has been singled out as the greatest and most serious threat to humanity, (Jothimani *et al.*, 2022). In the twenty-first century, serious soil degradation issues have arisen, particularly in tropical and subtropical nations where soil erosion is prevalent, (Beyene, 2019; Patyal, 2022).

The majority of soils in the world have rapidly degraded as a result of soil erosion, nitrogen depletion, and other issues, (Bensekhria & Bouhata, 2022). Approximately 6 million hectares of soil are lost from agricultural fields annually, with salinization, waterlogging, and erosion being the main causes, (Beyene, 2019). The threat posed by climate change, water scarcity, and falling soil fertility affects over 95 % of the world's population, who rely on soils for their food and feed, (Panagos *et al.*, 2016; Bensekhria & Bouhata, 2022).

Soil erosion has been of global concern with negative consequences for our environment, and above all, the economy, (Devatha *et al.*, 2015; Moses, 2017; Sahu *et al.*, 2017; Thlakma *et al.*, 2018). Trigunasih *et al.* (2018) identified it as a

major issue that threatens human survival. Soil erosion, according to Yang *et al.* (2003), is a natural disaster that has contributed to deterioration in water and soil quality, as well as low agricultural production. It is a global issue that is continuing to jeopardize food security and, more importantly, ecological function, (Fayas *et al.*, 2019; Chen & Thomas, 2020; Weupper *et al.*, 2020). It has an impact on the water, air, and, most significantly, the soil, (Beyene, 2019).

The process is quite a natural one and it occurs on every arable land, (Chan & Shah, 2019), and its outcome is soil loss, (El Jazouli *et al.*, 2017). The phenomenon leads to soil degradation and it is associated with intensified agricultural activities, deforestation activities, and unsustainable human activities in the environment, (Karthick *et al.*, 2017; Roslee & Sharir, 2019). As an attribute in the degradation of land, the soil erosion process induces some on-site effects (e.g. loss of both soil and important nutrients from agricultural fields) as well as off-site effects (e.g. deposition of sediments on croplands, sedimentation in reservoirs, pollution of water bodies, etc.), (Mutua *et al.* 2006; Park *et al.*, 2011; Efthimiou *et al.*, 2014; Devatha *et al.*, 2015; Zhang *et al.*, 2017; Zhang *et al.*, 2019). Soil erosion further affects the sustainability of the ecosystem and has long-term effects on water retention capacity, plant nutrients, soil depth, organic matter content, and surface albedo, (Biasutti & Seager, 2015; Trigunasih *et al.*, 2018; Fayas *et al.*, 2019).

To be more explicit, soil erosion continues to put national, regional, and even global agriculture at danger, (Gurebiyaw *et al.*, 2018; Zhang *et al.*, 2019; Bensekhria & Bouhata, 2022). It has led to a massive loss of rich top soil and important plant nutrients resulting in reduced crop yields, (Ganasri & Ramesh, 2016). As a consequence, about a third of the entire global land that supports agriculture has been largely affected, (Thlakma *et al.*, 2018; Zhang *et al.*, 2019). Biggelaar *et al.* (2003) reported that about 12 to 15 t ha⁻¹ yr⁻¹ of soil are believed to have been lost annually worldwide due to soil erosion, a figure which translates to about 0.90 to 0.95 mm of topsoil every year, (FAO, 2015).

However, the vastness of soil loss is much influenced by the soil's type, slope, land use, land cover, among others, (Wischmeier & Smith, 1978; Renard *et al.*, 1997; Mutua *et al.*, 2006; Verheijen *et al.*, 2009; Wang *et al.*, 2022). In addition, anthropogenic activities such as development of infrastructure, expansion of urban centres, intensification of agricultural activities, removal of vegetative cover and mining have been deemed to be the key accelerators of soil erosion, (Zhang *et al.*, 2017; Sujatha & Sridhar, 2018; Thomas *et al.*, 2018). In this regard, Sujatha and Sridhar (2018) singled out climate (intense erosive precipitation), topography, and characteristics of soil as the key contributing factors in the process of soil loss.

According to Karydas *et al.* (2014), soil is dynamically at risk from water erosion due to its physical and socioeconomic importance. Water erosion, according to De

Carvalho *et al.* (2014), has led to the degradation of two crucial natural resources: soil and water, (Bečvář, 2006; Sharma & Jain, 2014), and has consequently become a global threat to agriculture, (Pimentel, 2006; Panagos *et al.*, 2018). The extent of water erosion has increased globally in the twenty-first century due to a reduction in the ratio of natural resources to population and effects associated with climate change, (Jahun *et al.*, 2015; Thlakma *et al.*, 2018; Chen & Thomas, 2020).

On the other hand, soil formation is viewed as a non-renewable resource (Rulli *et al.*, 2013) because soil loss occurs far more quickly than soil formation does, (Weupper *et al.*, 2020). One centimeter of soil can be formed in around 200 years and lost in minutes owing to a moderate storm, depending on the soil qualities, (Verheijen *et al.*, 2009). Agricultural soils are washed 10–40 times more than they are regenerated, according to Pimentel *et al.* (2009). If the current trends continue, virtually all of the world's top soil might be lost in the next 60 years, according to Blue Sky Organics (<https://blueskyorganics.com/>). The main causes of soil erosion due to water have been singled out as a combination of geomorphic and climatic elements, as well as human activity, (Panagos *et al.*, 2016).

Water erosion is arguably the most widespread kind of soil deterioration on a global scale, (Oldeman, 1991; Oldeman, 1994; Angima *et al.*, 2003; de Graffenried & Shepherd, 2009; Thlakma *et al.*, 2018; Sakuno *et al.*, 2020). It is responsible for an estimated 55 percent of the worldwide soil loss, (Bridges &

Oldeman, 1999), with soil loss being the principal result, (Misthos *et al.*, 2019). Surface runoff has been identified as a serious problem that has caused negative consequences on the environment, occupying almost 56 % of the worldwide surface area, (Gelagay & Minale, 2016; Nouri *et al.*, 2018). According to Thlakma *et al.* (2018), roughly a third of all global agricultural land has been degraded, primarily due to water. Over 2000 t km⁻² yr⁻¹ of soil has been washed from croplands, according to FAO (2015), primarily in tropical areas.

Furthermore, water-related erosion has impacted almost 1094 mega hectares of land worldwide, with around 751 mega hectares significantly deteriorating, according to statistics, (Lal, 2003). Hurni (1993) observed a 42 t ha⁻¹ yr⁻¹ mean rate of soil loss from cropped lands, and he predicted that if the current scenario continued, the amount would rise to 300 t ha⁻¹ yr⁻¹. According to Pimentel *et al.* (1995), global soil loss from farmed areas is around 30 t ha⁻¹ yr⁻¹, on average, with an estimated range of about 0.5 to 400 t ha⁻¹ yr⁻¹. Over 24 million tonnes of topsoil have been removed from agricultural fields worldwide, according to the FAO (2011). Water erosion, according to Pimentel and Burgess (2013), is responsible for the loss of around 10 million hectares of agricultural land each year around the world. Approximately 5 Mg ha⁻¹ of Africa's most productive soil ends up in rivers, lakes, seas, and oceans, according to Angima *et al.* (2003).

Sediment yields have been compiled and even analyzed for different catchment areas by several researchers all over the world. However, sediment yields in

Africa remains largely underrepresented, with smaller catchments being the worst affected, (Vanmaercke *et al.*, 2014). This has been attributed to the few sediment yield observations available in Africa, especially the lack of streamflow data, (Vanmaercke *et al.*, 2014). Vanmaercke *et al.* (2014) established that the sediment yield observations for most African catchments are between 0.002 and 157 t ha⁻¹ yr⁻¹, with an average of 6.34 t ha⁻¹ yr⁻¹.

The agricultural sector forms the backbone of Kenya's economy. As a result, any improvement in agricultural productivity is contingent on the health of the soils, (Fwamba *et al.* 2017). Around 75 % of Kenya's soils are thought to have suffered degradation as a result of environmental fragility, (Wekulo, 2017). Furthermore, around 30 % of Kenya's land area has been severely degraded due to human activity, (FAO, 2005). According to Biamah *et al.* (1997), soil erosion was pointed out as one of the primary causes of land degradation problems in Kenya, and as a result, production capacity has been significantly reduced. In Kenya, surface runoff is basically the most contributing factor in the soil erosion process, (Ongwenyi *et al.*, 1993). About 20 % of Kenya's land has permanently lost its soil fertility due to water erosion, (Dregne, 1990). It is more noticeable on slopes, particularly near rivers and streams, riparian regions, and, most crucially, in marginal areas, (Mulinge *et al.*, 2016). It gets more severe in marginal areas, owing to overstocking and increased cultivation intensity, (Ongwenyi *et al.*, 1993; Mutua & Klik, 2004; Njiru *et al.*, 2018). Furthermore, the majority of the soils are extremely bare, making them susceptible to soil erosion, (Ongwenyi *et al.*, 1993).

Kenya's annual rates of soil loss exceed the average tolerable level of $10 \text{ t ha}^{-1} \text{ yr}^{-1}$ by a substantial margin, (Ongwenyi *et al.*, 1993; Angima *et al.*, 2003). According to ICRAF (2004), the Nyando River Basin in Western Kenya was degraded at a rate of $43 \text{ t ha}^{-1} \text{ yr}^{-1}$, resulting in about 3.2 million tonnes of soil sediments entering Lake Victoria. A total of 3 mm, or $52 \text{ t ha}^{-1} \text{ yr}^{-1}$, of topsoil is lost annually, according to Mwakubo *et al.* (2004). Further, the Masinga catchment's mean annual rate of sediment yield was reported to be $57.2 \text{ t ha}^{-1} \text{ yr}^{-1}$, (Mutua *et al.*, 2006). According to reports, soil erosion rates in severely degraded places can surpass $90 \text{ t ha}^{-1} \text{ yr}^{-1}$. Fwamba *et al.* (2017) reported that the geographical variance of soil loss in Kakamega County's Isiukhu river catchment ranged from 0 to about $128 \text{ t ha}^{-1} \text{ yr}^{-1}$. According to Njiru *et al.* (2018), 279 t ha^{-1} of soil are lost each year in Marsabit County's Golole catchment.

Finally, sedimentation in reservoirs and soil erosion at the catchment level are important issues, especially in tropical climates, (Mutua *et al.*, 2006). This requires scaling up management practices for both soil and water at the catchment level, (Ongwenyi *et al.*, 1993). Moreover, catchment regions should be properly monitored by calculating soil loss from a spatiotemporal perspective, (Boix-Fayos *et al.*, 2007). In this regard, site-specific scientific information should be made available to support any planned soil and water management strategies, (Bensekhria & Bouhata, 2022). Therefore, the primary objective of any research on soil erosion should be to address soil erosion-related problems by providing appropriate solutions, (Wang *et al.*, 2022).

1.2. Problem Statement and Justification

1.2.1. Problem Statement

According to Trigunasih *et al.* (2018), catchments are segmented into upper, middle, as well as lower reaches. The upper section plays a protective role for the other basin parts. In the context of water system functions, both upper and lower reaches influence the hydrological cycle, (Trigunasih *et al.*, 2018). A catchment has distinct characteristics and it relates strongly to some of its physical conditions, which include soil type, topography, land use, etc., (Ongwenyi *et al.*, 1993; Simms *et al.*, 2003; Aglanu, 2014). Land use changes in the upper reach have an impact on the lower reach because they directly cause reservoir capacity to decline and river siltation, which raises the risk of flooding, (Tamene *et al.*, 2006).

Healthy catchments effectively serve their functions, but poor management induces some damage to them, (May & Place, 2005; Ban *et al.*, 2016). Furthermore, due to poor planning and changes brought on by land use, catchments rapidly degrade, making them vulnerable to soil erosion, flooding, and other problems, (Gratius & Chinedu, 2018). An unhealthy catchment is characterized by the occurrence of landslides, floods, high soil erosion rates, and droughts, (Aglanu, 2014; Ban *et al.*, 2016). Damage in catchments occurs more frequently if the immediate community is not sensitized to the importance of the particular environment, (Aglanu, 2014; Gratius & Chinedu, 2018). Erosion is influenced by the climate, soil, geography, plants, and humans, (Trigunasih *et al.*,

2018). However, humans can influence land and vegetation, but they have no control over topography and climate, (Aglanu, 2014).

Conservation measures can be utilized to lessen the harm caused by soil erosion in a catchment, (Ongwenyi *et al.*, 1993). As a consequence of conservation measures, soil erosion is prevented, damaged soils are repaired, and soil productivity is maintained and improved, allowing the land to be used sustainably, (Beyene, 2019). Water conservation, on the other hand, promotes greater use of rainwater by managing its flow time to reduce floods while still making water available during dry seasons. This can be accomplished by improving infiltration in high-rainfall areas and capturing rainwater in low-rainfall areas using reservoirs. However, before taking any soil and water management measures, the rate at which the soil is detached must be determined, (Jasrotia & Singh, 2006). Therefore, the effectiveness of any soil conservation program is determined by the accuracy with which soil loss is assessed, as well as the identification of critical places where management methods can be adopted, (Ganasri & Ramesh, 2016).

Despite being a small catchment, the status of the Maruba dam catchment has deteriorated because of land degradation. Soil erosion has caused land degradation in the catchment, as it has in many other catchments in Kenya and tropical countries, (Onyando *et al.*, 2005). It has been exacerbated by farming activities on steep slopes. The rapid siltation of the Maruba dam reservoir and

widespread sand harvesting along Maruba stream are both signs of soil erosion within the catchment. If the current trend continues, the situation is likely to worsen, (Ongwenyi *et al.*, 1993). However, management measures may only be implemented effectively if the vastness and spatial variations of soil loss are objectively known, (Onyando *et al.*, 2005; Salunkhe *et al.*, 2018; Sujatha & Sridhar, 2018).

The Maruba dam catchment's soil erosion state, as well as the dam reservoir's sedimentation status, has not been evaluated. To be more specific, spatial soil erosion data is still missing, which is critical for creating appropriate management plans of action, (Kale & Vadsola, 2012; Diwediga *et al.*, 2018). This obviously demonstrates that smaller catchments have received much less attention than larger ones, (Vanmaercke *et al.*, 2014). Therefore, there is both a knowledge gap and an information gap with regards to the relationship between soil erosion as well as sediment yield in small catchment areas. Soil erosion research in Kenya has primarily concentrated on large catchments, where data from gauging stations have aided in the estimation of sediment yield. Therefore, spatial assessment of soil erosion as well as sediment yield at small catchment levels is inevitable due to significant land use changes in addition to lack of management practices in such catchments, (Mutua *et al.*, 2006).

1.2.2. Justification

Huge sections of land have become economically unproductive due to land degradation and unchecked soil erosion, (Diwediga *et al.*, 2018). Decision-makers, policymakers, and land managers all across the world are concerned about land degradation, with a particular focus on soil erosion, (Holz *et al.*, 2015; Ganasri & Ramesh, 2016; Benavidez *et al.*, 2018). This concern over soil erosion has been heightened by the fact that hydrological monitoring and even proper soil surveys are in short supply, particularly in poor nations, (Steinmetz *et al.*, 2018). As a consequence, assessing the danger of soil erosion provides a valuable methodology for appropriately managing land and water resources, (Karamage *et al.*, 2016; Asadi *et al.*, 2017). Thus, a thorough prediction of erosion changes in the near future thus enables the creation of a strategy for better land management while simultaneously preserving the ecosystem, (Biasutti *et al.*, 2015; Koirala *et al.*, 2019).

Reservoir designs and catchment management action plans rely on precise geographic soil erosion data as well as sediment yield, (Korada & Vala, 2014). Hence, better management decisions will be made if soil conditions and soil erosion variables are well understood. It is important to emphasize that if soil erosion is to be effectively stopped, scientific approaches to management of watershed resources, notably vegetation, water, and soil, are required, (Korada & Vala, 2014). Therefore, scientific understanding of the elements that influence each is necessary in order to plan successfully for their management, (Njiru *et al.*,

2018; Roslee & Sharir, 2019). This aids in the delineation and, more importantly, the prioritization of erosion mitigation in erosion-prone locations, (Bewket & Teferi, 2009).

Soil erosion prevention is defined as slowing down the rate at which soil is lost in its natural form, (Korada & Vala, 2014). As a result, proper soil conservation methods must be chosen based on an understanding of the soil erosion process, (Korada & Vala, 2014). The rate of soil loss is much influenced by soil, climate, slope, vegetation cover, conservation efforts, and, most importantly, their linkages, (Ganasri & Ramesh, 2016). On the basis of the intensity of these variables, net soil loss occurs when soil erosion rates exceed the rate at which soil is formed, (Diwediga *et al.*, 2018). A catchment, on the other hand, is heterogeneous in nature, and as a result, it has a wide range of biophysical properties, (Gurebiyaw *et al.*, 2018). Because of the spatiotemporal changes therefore, determining erosion at the catchment size is extremely difficult, (Merritt *et al.*, 2003; Onyando *et al.*, 2005; Kovacs *et al.*, 2012; Amah *et al.*, 2020). The dynamics of soil erosion are determined by spatial heterogeneity elements such as elevation, soil characteristics, plant cover, land use, and above all, land cover, (Mallick *et al.*, 2014). This necessitates the employment of effective instruments and methodologies for quantifying and analyzing soil erosion in terms of its extent and magnitude, as well as, most crucially, sediment yield, (Sujatha & Sridhar, 2018).

The spatial quantification of soil loss has become necessary due to increased changes with regards land use as well as management in catchments, (Mutua *et al.*, 2006). In this sense, soil erosion can be assessed using a range of approaches used at various sizes, as well as a variety of management objectives, (Diwediga *et al.*, 2018). Therefore, quantifying soil erosion provides an estimate of its extent and magnitude, allowing for the development of effective management measures, (Bhat *et al.*, 2017; Salunkhe *et al.*, 2018; Beyene, 2019). However, because of the complicated interconnections of the many elements at play, measuring and predicting erosion is a tough task, (Bhat *et al.*, 2017; Gull *et al.*, 2017; Trigunasih *et al.*, 2018). However, if certain assumptions and simplifications are made, it is possible to measure and estimate soil erosion with a reasonable level of accuracy using soil erosion models, (Marston & Dalon, 1999).

Soil erosion modeling can simulate the erosion process by taking into account the many complex relationships that determine soil erosion rates within catchments, (Onyando *et al.*, 2005; Efthimiou *et al.*, 2014; Devatha *et al.*, 2015; Benavidez *et al.*, 2018). Most models are developed to use particular conditions from a particular area, leading to an improved understanding of such areas, (Devatha *et al.*, 2015). Therefore, soil erosion models can offer precise estimates of soil erosion, (Onyando *et al.*, 2005). To compute soil loss, the majority of models require data on the type of soil, type of land use, topography, landform, and climate, (Trigunasih *et al.*, 2018). In this regard, modeling is an excellent tool through which spatial variation of soil loss and its intensity is simulated in

addition to identifying the areas for sediment origin and above all, deposition, (Ganasri & Ramesh, 2016; Diwediga *et al.*, 2018).

Existing methods have been bolstered by current milestones in geospatial techniques, resulting in better ways for parameter analysis, monitoring and above all, management of land resources, (Hajigholizadeh *et al.*, 2018; Boufala *et al.*, 2020). Quantitative spatial datasets on soil loss at the micro-catchment level contributes significantly to developing soil conservation plans, control of erosion, and most importantly, management of the environment over the entire catchment, (Jakubínský *et al.*, 2019). However, the aims, characteristics of the catchment, data availability, and model's efficacy play an important role in the model's selection, (Pandey *et al.*, 2016).

1.3. Objectives

1.3.1. Overall Objective

The overall objective of the study was to model soil erosion, estimate sediment yield and characterize sediments for sustainable reservoir management.

1.3.2. Specific Objectives

The specific objectives of the study were to:

- a) Predict the spatial distribution of soil erosion at a catchment scale using the RUSLE model.
- b) Assess the sedimentation status of the Maruba dam reservoir over the past eleven (11) years using a multi-frequency acoustic profiling system.

- c) Assess the physicochemical characteristics of reservoir bottom sediment and sediment deposited at the inlet of the reservoir in order to inform their potential use.

1.4. Research Questions

- a) Can the average annual soil loss from a catchment be effectively predicted using the RUSLE model?
- b) Can the multi-frequency acoustic profiling system adequately model sedimentation in a dam reservoir?
- c) Can the sediments at the Maruba dam reservoir be beneficially used?
- d) How does the sediment yield estimated from the RUSLE-based sediment compare with that obtained from acoustic bathymetric measurements?

CHAPTER TWO: LITERATURE REVIEW

2.1. Soil Erosion Process

2.1.1. Introduction

Soil serves as the uppermost surface of the lithosphere, and whose depth varies according to geographical scales, and above all it is an important aspect of human existence in all the corners of world, (Abdo & Salloum, 2017). The main components are air, organic matter, water, and minerals, (Chen & Shah, 2019). It is vulnerable to a variety of degrading processes and even dangers, (Panagos *et al.*, 2018). The mechanical forces associated with water and wind damage the upper layer of many soils; this is basically the process of soil erosion, (Panagos *et al.*, 2018; Tamang *et al.*, 2018). Soil erosion is primarily caused by three factors: water, wind, and tillage, (Ghabbour *et al.*, 2017). The process is highly physical and occurs in every corner of the planet, even nearly zero slope settings, (Jakubínský *et al.*, 2019).

For a long time, the most important and urgent environmental issue has been regarded to be soil erosion, (Ochoa *et al.*, 2016; Patyal, 2022). The phenomenon is fairly gradual, and its effects may go unnoticed or be extremely severe, resulting in a rapid loss of topsoil, (Sahu *et al.*, 2017). It occurs when the soil's cohesive force is exceeded by the energy possessed by wind, drops of rain, and surface runoff water, (Lal, 1990; May & Place, 2005; Pimentel, 2006; Sahu *et al.*, 2017; Hajjizadeh *et al.*, 2018; Tsitsagi *et al.*, 2018; Dominguez & Schaldach, 2019). Soil erosion is a complicated process that involves water and wind

separating, transferring, and accumulating soil components from the land's surface, (Abdo & Hassan, 2018; Hateffard *et al.*, 2021). Soil erosion, according to Dominguez and Schaldach (2019), is a natural process whereby soil particles get separated, entrained, and transported. Due to the splashing impact of water as it rushes down the slopes and into water bodies in sloppy places, nearly half of the soil's surface is wiped away, (Pimentel, 2006). Similarly, wind's energy is sufficient to dislodge soil particles and carry them across long distances, (Pimentel, 2006). Although wind-driven erosion and raindrop impacts have a limited effect, their magnitude is smaller than that generated by water, (Kale & Vadsola, 2012). Surprisingly, while completely preventing soil erosion is difficult, it is feasible to limit it to some level, (El Jazouli *et al.*, 2017).

2.1.2. Soil Erosion Due to Water

Water erosion is simply a naturally occurring mechanism whose magnitude is determined by how agricultural fields are managed in terms of cover and surface roughness, (Carr *et al.*, 2020). It is an irreversible geomorphologic process that results in significant land degradation, (Jiang *et al.*, 2014; Dominguez & Schaldach, 2019). Water erosion is a concern in mountainous regions, tropical and subtropical climates, and dry regions, (Carr *et al.*, 2020). Suspended sediment in rivers is a good indicator of how soil erosion is dispersed around the world, (Walling & Webb, 1996). The problem is exacerbated by high-energy rainfall, extremely steep slopes, and dwindling vegetation cover, (Tamene *et al.*, 2006; Alemaw *et al.*, 2013; Carr *et al.*, 2020). Since farming is restricted in mountainous

locations, most of the harm to agricultural land brought on by water erosion occurs here, (Carr *et al.*, 2020). Different land-use activities, on the other hand, have an increasing influence on water erosion, (Tsitsagi *et al.*, 2018). However, by having appropriate vegetation cover on the soil, the erosive power's effects can be minimized, (Bekele & Gemi, 2020).

Water erosion quite is a physical mechanism in which water's erosive forces separate, transport, and deposit soil particles elsewhere within a watershed, (Wieschmeier & Smith, 1978; Lal, 1990; Jain *et al.*, 2001; Mitsova *et al.*, 2013; Hajigholizadeh *et al.*, 2018; Tsitsagi *et al.*, 2018; Chen & Shah, 2019). Erosive forces dislodge soil particles during detachment, after which they are transported and deposited following a decrease in water velocity caused by the influence of ground slope or land cover, (Yang *et al.*, 1998; Roshani *et al.*, 2013; Vantas *et al.*, 2019).

Rainfall and overland flow, according to Lal (1990), are the most powerful detaching agents. Following the contact of the raindrop with the soil's surface, shear stresses arise, and the interstitial forces that keep the soil particles together are destroyed, resulting in detachment, (Kothyari, 2008). Due to overland flow, a thin water film forms when the precipitation rate exceeds the rate of infiltration. Overland flow induces shear forces on the soil's surface, after which, when they surpass the soil's cohesive force, result in sediment detachment, (Merritt *et al.*,

2003; Kothyari, 2008). The principal processes that soil of erosion by water were summarized by Sanders (1986) as shown in figure 2.1 below.

The depletion of soil particles as a result of the effects of water through surface water runoff, rill, inter-rill, and even gulley is referred to as water-induced soil loss, (Yang *et al.*, 1998; Kothyari, 2008; Shoshany *et al.*, 2013; Wang *et al.*, 2015; Hajigholizadeh *et al.*, 2018). Rill erosion, according to Beskow *et al.* (2009), occurs when a concentrated flow detaches and moves soil particles, whereas inter-rill erosion occurs at the instant when droplets detach soil particles, which are finally transported together with surface water runoff. Sheet and inter-rill erosion were identified as the initial steps of the erosion process in catchments by Hajigholizadeh *et al.* (2018), a phenomenon that is highly widespread on bare or very bare soils in agricultural areas, pasture lands, or open places. At lower scales, such as a plot, splash and sheet erosion dominate soil loss rates, but rill and gulley erosion are the primary agents of soil loss at larger scales, such as slopes or even watersheds, (Verheijen *et al.*, 2009).

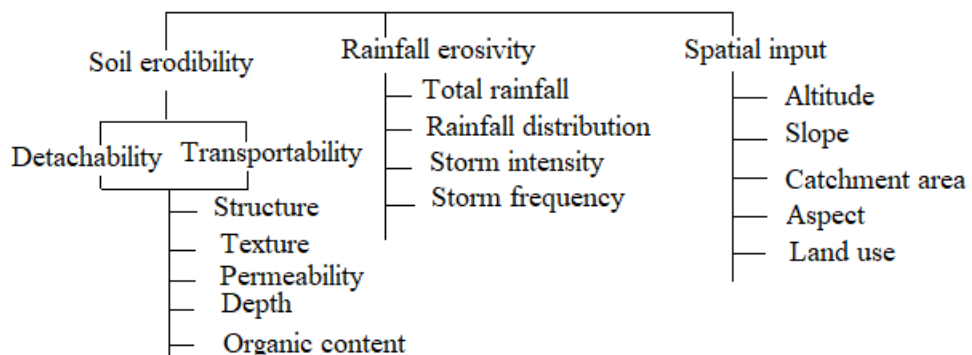


Figure 2.1: Key processes influencing soil erosion by water (Source: Sanders, 1986)

2.1.3. Effects of Water Erosion

Water-induced soil erosion causes several environmental impacts for instance reduced yields in agricultural production, hydrological cycle disruptions, reduced plant cover, and losses in biodiversity, which in turn increase the probability of the occurrence of some natural disasters, (Roslee & Sharir, 2019; López-García *et al.*, 2020). These impacts are categorized as either on-site or off-site, (Pimentel *et al.*, 1995; Kisan *et al.*, 2016; Diwediga *et al.*, 2018; Yesuph & Dagneu, 2019). For instance, it causes depletion of the topsoil, which leads to a reduced effective root depth and loss of important soil nutrients, (Lal, 1990; Yang *et al.*, 2003; Koirala *et al.*, 2019). This is an on-site soil erosion problem.

Off-site erosion problem, on the other hand, causes deposits of sediment in river channels, reservoirs and related hydraulic structures, thereby reducing their capacity, (Lal, 1990; Pandey *et al.*, 2007; Kisan *et al.*, 2016; Roslee & Sharir, 2019). Sediment is in itself a pollutant; hence, it may carry soil pollutants in adsorbed form, (Lal, 1990; Kisan *et al.*, 2016). In general, the ecosystem that surrounds wet territories is endangered by water erosion, (Abdo & Hassan, 2018). May and Place (2005) noted that a small percentage of the eroded material over a catchment is deposited in drainage systems while the rest is re-deposited in less sloping catchment areas, especially the ones with larger particles, (Haan *et al.*, 1994).

2.2. Accelerated Soil Erosion

2.2.1. Impacts of Land use and/or Land Cover on Soil Erosion

Land use as well as land cover changes indicate that the surface of the land has changed, either naturally or purposefully, (Tolessa *et al.*, 2019). The rate at which land cover is decreased influences the rate of deterioration of both land and soil resources, (Chalise *et al.*, 2019; Koirala *et al.*, 2019). In addition to shifting climate trends, the loss of land cover is exacerbated by the way the land is used, (Roshani *et al.*, 2013; Tolessa *et al.*, 2019). The key drivers of the frequency with which soil erosion occurs have been recognized as land cover changes and land use activities in terms of kind, distribution, and management, (Roshani *et al.*, 2013). Rainfed agriculture has an impact on soil and land deterioration because the primary goal is to increase output, (Roshani *et al.*, 2013; Belay *et al.*, 2020). In comparison to uplands, soil erosion rates were low in farmed low-lying regions, according to Chalise *et al.* (2019).

According to Pimentel (2006), the loss of land vegetative cover is quite substantial, especially in developing nations where population growth continues, and even agricultural operations have shown to be insufficient in safeguarding topsoils. Trimble and Mendel (1995) found that when the entire ground cover was reduced from 100 % to even less than 1 %, soil erosion rates drastically increased by 200 times. According to Haigh *et al.* (1995), a minimum forest cover of 60 % is required to prevent major soil loss and landslides. Bajracharya and Sherchan (2009) calculated that annual soil loss in wooded regions is 5.1 tonnes per hectare

per year, which is 12 times less than that in shrubland. Higher soil erosion rates have been linked to sloppy topography, less plant cover, compacted soil surface layers, and the occurrence of gullies and rills in shrub regions, (Chalise *et al.*, 2019).

Table 2.1: Land-use types and erosion rates (source: Bajracharya & Sherchan, 2009)

Type of land use	Soil erosion rate (t ha ⁻¹ yr ⁻¹)	Range (t ha ⁻¹ yr ⁻¹)
Upland	28.0 ± 29	2 – 105
Lowland	0.70 ± 0.9	0 – 2.7
Shrub	58.0 ± 78	0.4 – 420
Forest	5.1 ± 4.7	0.2 – 15.3

Soil loss is much strongly influenced by long-term land use activities and above all changes in land cover, (Mallick *et al.*, 2014; Trigunasih *et al.*, 2018). Following the positive identification of the dependency between loss of soil and sediment discharge with land management, Li *et al.* (2014) stated that there has been a topical environmental argument on the link between changes in the use of land and cover. For example, Chalise *et al.* (2019) found a decline in forested land area and land occupied by water bodies in western Nepal between 1995 and 2015, but a significant rise in cultivated fields and populated areas. This resulted in a considerable rise in soil loss rates, which varied from 5.35 to 6.03 t ha⁻¹ yr⁻¹ during the same time period, (Chalise & Kumar, 2018).

2.2.2. Effects of Environmental Factors on Soil Erosion

The rate of soil loss that occurs from a given geographical landscape is influenced by the duration and intensity of rainfall that occurs in that location, (Chalise *et al.*, 2019). The energy contained in raindrops that impact the surface of land is sufficient to dislodge soil particles, and this is the basis for soil loss by water, (Verheijen *et al.*, 2009). As a result, heavy rain that lasts longer and falls on mountainous terrain is likely to cause substantial soil loss, (Pimentel, 2006; Devatha *et al.*, 2015; Sujatha & Sridhar, 2018). Chalise *et al.* (2019), on the other hand, found that the erosivity factor of rainfall remained essentially constant across the study period, whereas soil erosion rates increased significantly, (Chalise & Kumar, 2018). This phenomenon is related to climate change, since despite a drop in the number of rainy days, no substantial change in rainfall amount was seen, (Nearing *et al.*, 2004; Mondal *et al.*, 2016; Chalise *et al.*, 2019).

Fine-textured soils with little organic matter percentage and a weak structure disintegrate more quickly, (Pimentel, 2006; Ochoa *et al.*, 2016). Water erosion is exacerbated by inadequate organic matter, which diminishes the soil's infiltration ability, (Morgan, 2005). Chalise *et al.* (2019) found that the disintegration of soil particles and eventual loss of topsoil in hilly areas compromises sustainable agricultural systems. However, strengthening the structural stability of the soil and boosting plant cover might help reduce soil erosion on such sloppy terrain. Increased grazing activities have been found to degrade the physical state of the soil, particularly its ability to hold water and nutrients, and this has exposed it to

soil erosion problems and landslides as well. The process of soil erosion is accelerated by livestock grazing because an increased animal population disintegrates soil aggregates and leads to increased soil bulk density values.

Soil erosion rises when the slope gradient is relatively high and defined by longer slopes, and topography impacts the rate of soil loss from a specific terrain, (Koirala *et al.*, 2019). As a result, the discharge and velocity of runoff increase. Flat terrains, on the contrary, undergo splash erosion as a result of falling raindrops scattering soil particles in various directions, whereas sloppy terrains experience downhill splashing, exposing the soil to additional erosion concerns, (Li *et al.*, 2014).

2.2.3. Management Factors and Soil Erosion

Before the rains fall, most cultivated areas are tilled many times, leaving the soil barren before crop planting, (Siddique *et al.*, 2017). During certain seasons, some areas may be subjected to high-intensity storms accompanied by strong winds, increasing the soil's sensitivity to erosion, (Atreya *et al.*, 2008). The production of maize, for example, is said to need a variety of soil tillage practices, (Chalise *et al.*, 2019). After the harvest of the maize crop followed by the subsequent removal of maize stalks from the field, the field is ploughed repeatedly following the application of farmyard manure, (Atreya *et al.*, 2008). As a result, the soil becomes more exposed, making it more vulnerable to erosion from water and wind, (Chalise *et al.*, 2019). This necessitates the replacement of traditional tillage

techniques with measures such as minimal and/or reduced tillage, which are mostly unsustainable. In hilly farmed fields, Atreya *et al.* (2008) observed that lowering tillage activities reduced yearly soil loss by 33 percent.

The ability of vegetation cover to fight soil erosion is due to its root system, litter, and canopy, (Dominguez & Schaldach, 2019). During parts of the year when there is no rain, however, plant cover is limited, which exacerbates soil loss. Between these intervals, according to Schreier and Shah (1999), about 60 to 80 percent of the soil, as well as nutrients, are lost. Plant cover is either alive or dead, according to Chalise *et al.* (2019), and as a result, the ground is more protected and less prone to soil erosion. Therefore, in order to successfully prevent soil erosion in poor nations, soil cover must be restored, as agriculture and forestry practices are woefully inadequate, (Pimentel, 2006).

2.2.4. Restoration Measures

Three major aspects determine the severity of soil erosion: energy, resistance, and protection, (Dominguez & Schaldach, 2019). Soil erosion is a natural occurrence that cannot be completely avoided, although it may be minimized, (El Jazouli *et al.*, 2017; Dominguez & Schaldach, 2019). The most serious issue affecting the land surface is caused by rapid soil loss coupled with high rates of surface runoff, hence it is essential to develop and put into practice effective soil erosion management techniques as soon as feasible, (Chalise *et al.*, 2019).

An effective plan for the management of soil erosion can be achieved by (figure 2.2): reducing the direct effect of falling raindrops and impeding overland flow, (Morgan, 2005; Mohammad & Adam, 2010; Dominguez & Schaldach, 2019); preventing soil crusting, increasing its infiltration, and reducing surface runoff by improving the physical conditions of the soil alongside adopting agricultural practices which can enhance conservation, (Morgan, 2005; Panagos *et al.*, 2015; Dominguez & Schaldach, 2019; Koirala *et al.*, 2019); utilization of suitable engineering technologies to manage the excess overflow of water, (Morgan, 2005; Evette *et al.*, 2009; Dominguez & Schaldach, 2019) and reducing the length of the slope by adopting agricultural practices, particularly terracing as a way of minimizing surface runoff build-up, (Morgan, 2005).

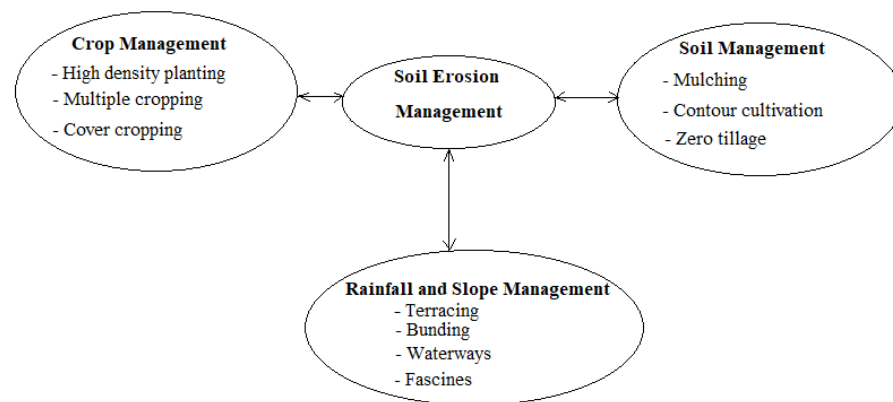


Figure 2.2: Management of soil erosion (Source: Chalise *et al.*, 2019)

Fertilizer and Manure Application

The proper use of manure and fertilizer results in a healthy crop population, (Chalise *et al.*, 2019). Plants that quickly cover the ground help to prevent soil loss, (Nasir Ahmad *et al.*, 2020). However, correct nutrient balance and tracking

is critical for crop yield and soil performance, (Chalise *et al.*, 2019). According to Ramos *et al.* (2006), introducing cow dung slurry into the soil reduced the detaching power of raindrops on soil particles by around 70 percent. Chalise *et al.* (2019) found that combining organic manures with chemical fertilizers boosts the soil's capacity to store water while also changing the physical condition of the soil, reducing soil erosion.

Mulching

Mulching, according to Dominguez and Schaldach (2019), is a popular practice that can operate as a "forest soil litter cover," protecting the soil from erosion while also increasing its physical attributes. Mulching reduces soil erosion by: minimizing surface runoff, enhancing water infiltration capacity, and reducing sediment concentrations by improving soil structure, resulting in little rill as well as inter-rill erosion, (Chalise *et al.*, 2019; Dominguez & Schaldach, 2019; Nasir Ahmad *et al.*, 2020). Mulching efficiently inhibits water erosion, although it is much dependent on variables such as soil type, slope gradient, rainfall erosivity, and mulch application rate, (Smets *et al.*, 2008).

According to Atreya *et al.* (2008), when rice straw was utilized as mulch, soil runoff was decreased by 18 percent. Farmers utilized chippings from trimming operations and distributed them on the top of the soil rather than burning them, according to Keesstra *et al.* (2016). This process, it was found to help in soil

recovery, add more organic material into the soil, and ultimately a reduction in the soil's bulk density.

Management of Cover Crop

Cover crops' thick foliage protects the soil's surface, mitigating the negative impacts caused by soil erosion, (Keesstra *et al.*, 2016; Chalise *et al.*, 2019). As a result, the volume of surface runoff water that would otherwise cause soil erosion is decreased, and the soil productivity is increased, (Vannoppen *et al.*, 2015; Nasir Ahmad *et al.*, 2020). Cover crops may reduce the splashing effect of rainfall on soil while also increasing the content of organic material into the soil, controlling weeds, and reducing microclimate changes surrounding the plants, (Ochoa *et al.*, 2016). Furthermore, soil surface cover restricts the flow of surface water, resulting in increased infiltration and less soil loss, (Vannoppen *et al.*, 2015; Chalise *et al.*, 2019). Napier grass, according to Higaki *et al.* (2005), is an efficient cover crop for restoring soil fertility and rehabilitating highly damaged catchments.

Strip Planting

Strip planting, according to Chalise *et al.* (2019), is a method in which row crops that allow erosion are cultivated alternately in strips with crops and grasses that prevent erosion. When plant strips are created on severely sloping soils, there is a reduction in runoff and subsequent soil loss, (Raya *et al.*, 2006; Gathagu *et al.*, 2018). Chalise *et al.* (2019) identified barley and lentil crops as the key erosion-

checking species because they produce thick foliage, which is important for decreasing the effects of soil erosion. Row crops prevent erosion, according to Chalise *et al.* (2019), while the eroded soil debris is contained by the erosion control strips, (Mekonnen *et al.*, 2015). The efficiency of this strategy in mitigating soil erosion, however, is dependent on how well crop rotation exercises are carried out, (Kinama *et al.*, 2007).

Contour Farming

Contour farming is a kind of farming that involves carrying out field operations like primary tillage, secondary tillage, and planting in a way that follows the land's contours, (Morgan, 2005). This method is used on sloppy soils to create a barrier against runoff water, reduce its velocity, and reduce soil loss, (Gathagu *et al.*, 2018). As a result, there is improved water conservation in the soil, resulting in increased crop output, (Farahani *et al.*, 2016). Contour cultivation is a frequently used method across the world due to its efficiency in reducing sedimentation and controlling soil erosion, (Tadesse & Morgan, 1996; Traore & Birhanu, 2019). Contour farming, according to Gathagu *et al.* (2018), decreases a catchment's annual sediment output by 36 percent. When contour farming is paired with conservation tillage methods like minimum or no-tillage, it becomes even more effective, (Farahani *et al.*, 2016). Furthermore, when some conservation tillage strategies, such as minimum or no-tillage, are combined with contour farming, it becomes more successful, (Farahani *et al.*, 2016).

Conservation Tillage

Tillage is a powerful process that produces soil dissociation, transport, and deposition despite modifying the ground surface, (Farahani *et al.*, 2016). Conservation tillage is a crop production technique that tries to leave nearly 30 % of crop residue on the surface of the land after ploughing. Surface runoff and soil loss are reduced when agricultural wastes are retained. Many people in poor nations, on the other hand, rely on crop wastes for fuel, (Pimentel, 2006). Excessive tillage disrupts the soil's structure, speeding up soil erosion, (Keesstra *et al.*, 2016; Chalise *et al.*, 2019). In addition to in situ plant remnants, adopting less frequent and vigorous tillage methods preserves the structure of the soil and prevents soil loss.

Conservation measures, notably no-till and limited tillage, increase the biological and physicochemical features of the soil, according to Mupangawa *et al.* (2007), and hence improve the soil's water holding capacity. Reduced tillage practice, according to Tiwari *et al.* (2008), reduced soil erosion as well as sediment flow by around 23 and 9 percent, respectively. According to Nyssen *et al.* (2011), conservation tillage reduced runoff by 51 percent and soil erosion by 81 percent, respectively.

Bioengineering Practices

Live plant materials are used in bioengineering approaches to give simple engineering solutions, with the living plants being wisely integrated with various

soil erosion control engineering technologies, (Sriwati *et al.*, 2018; Chalise *et al.*, 2019). Live check dams, hedgerows, fascines, and brush layers are popular bioengineering approaches that have been successfully employed to reduce soil erosion, according to Rey *et al.* (2019). The use of bioengineering methods is aided by favorable climatic conditions, particularly in tropical regions, (Vianna *et al.*, 2020).

Native plants like *Dalbergia sissoo*, bamboo, and eucalyptus *camaldulensis* can be planted alongside man-made dams built on river or streambanks, (Dhital *et al.*, 2013). These plants help to stabilize the banks and decrease landslides and above all soil erosion, (Sriwati *et al.*, 2018). The use of live plants and wire-netted check dams not only stabilizes stream banks, but also narrows the flow of the stream channel, reducing erosive force, (Dhital *et al.*, 2013). Hedgerows, according to Chaowen *et al.* (2007), produce bunds that lessen steepness and eventually build natural terraces, which minimize surface runoff and soil erosion. With the implementation of contour-planted hedgerows, Ya and Nakarmi (2004) showed a considerable reduction in soil loss of 80–99 percent. Grass strips, on the other hand, were shown to be more successful in preventing soil erosion than hedgerows because the grass strips are more compact and dense, (Kinama *et al.*, 2007).

2.3. Sediment Yield, Sediment Transfer and Sedimentation of Reservoirs

2.3.1. Sediment Yield

Soil erosion and even sediment yield are major catchment challenges in many third-world nations, limiting development, (Aga *et al.*, 2020). Sediment transfer occurs primarily in suspended form or even bedload, and comprises of eroded content from the catchment area, streambed, and even stream banks, (Nyssen *et al.*, 2009; Dutta, 2016). Deposition of sediments happens throughout time, thereby causing serious issues in downstream communities, (Gelagay, 2016).

The sediment content that passes through the catchment's outlet ultimately becomes the sediment yield at that particular point, (Swarnkar *et al.*, 2018). In this regard, sediment yield refers to a fraction of sediment mobilization from a catchment area, (Hassan *et al.*, 2008), and therefore, it accounts for the net quantity of both erosion and deposition processes inside the catchment, (Sadeghi & Mizuyama, 2007; Bekele & Gemi, 2020). Thus, sediment yield serves as the ultimate product of both erosion and even deposition phenomena within the confines of the catchment, (Haregeweyn *et al.*, 2008; Boakye *et al.*, 2018). At the scale of a catchment, soil erosion strongly relates to sediment yield, (Dutta, 2016). This explains the spatiotemporal variation in sediment production, transport and above all, deposition, (Bečvář, 2006).

Typically, the overall soil loss from a given catchment area is much smaller than the generation of sediment from the same area, (Wasson *et al.*, 1996). This is an

indication that some dislodged soil particles are deposited before being transported beyond the catchment area, (Swarnkar *et al.*, 2018). Hence, estimating soil loss rates at the scale of a catchment is therefore an engineering methodology that depends on some two basic principles: prediction of sediment yield within the catchment area and prediction of sediments inside the stream channel, (Aga *et al.*, 2020).

Erosion control elements impact sediment output, including soil topographical qualities, plant cover, catchment morphology, climate, network characteristics of the drainage region, and, most importantly, land uses, (Tamene *et al.*, 2006; Hassan *et al.*, 2008). However, several human-related activities, such as urbanization, deforestation, mining, and climate change, have exacerbated its severity, (Jain *et al.*, 2010). Estimating sediment yield is therefore significant in researches that touch on sedimentation, morphology of rivers, soil and water management plans, modeling water quality, and design considerations in erosion control structures, (Kothyari, 1997; Jain & Kothyari, 2000).

Sediment comes mostly from a catchment's upper, middle, and lower sections, (Schleiss *et al.*, 2016). Sediments have been found in fields, streams, and even reservoirs, according to reports, (Bečvář, 2006; William & Smith, 2008). Erosion and weathering of rocks inside steep mountainous terrains within valleys, as well as unchanneled movement of the same through slopes by flowing water and wind, contribute to the production of sediments in the higher reaches, (Morgan, 2009).

Therefore, in order to accurately predict sediment production in the higher reaches, it is necessary to measure the quantity of rainfall or runoff, as well as, more critically, the thermodynamic activities that occur inside the catchment's boundaries, (Schleiss *et al.*, 2016).

In the middle reach of a catchment, sediment is produced via gully, rill, and riverbank erosion as well as legacy load, (Bečvář, 2006; Schleiss *et al.*, 2016). The quantity of sediment accumulated in a dispersed way within the alluvial environment is included in the legacy load, (Hargrove *et al.*, 2010). The size of the sediments in this section of the catchment diminishes owing to crashing and abrasion that happens on bigger sediments as they travel through the river channel (Dutta, 2016). According to Fox *et al.* (2016), sediment generation in the middle reach of the catchment, particularly rill, gully, and riverbank erosion, contributes considerably to reservoir sedimentation.

2.3.2. Sediment Transfer

Depending on how the sediments are supplied, flow velocity, and turbulence, river sediments come in a variety of sizes as a bed or even suspended loads, (Pelletier, 2012; Schleiss *et al.*, 2016). The unpredictability in streamflow causes large or little amounts of suspended sediment to accumulate, resulting in a wide range of suspended sediment concentrations, (Lin *et al.*, 2017). Different mechanisms are involved in the manner in which soil particles are moved on this basis, because their size varies greatly, (Pelletier, 2012; Schleiss *et al.*, 2016).

Figure 2.3 demonstrates that large particles, which make up the bedload, roll and bounce (saltate), while smaller particles (suspended load) are lifted by flow turbulence above the channel bed and carried in a manner comparable to water flow, (Pelletier, 2012; Dutta, 2016; Lin *et al.*, 2017). The creation of a channel is determined by suspended sediment load; hence, it is critical in a watercourse regime, (Gilja, 2009).

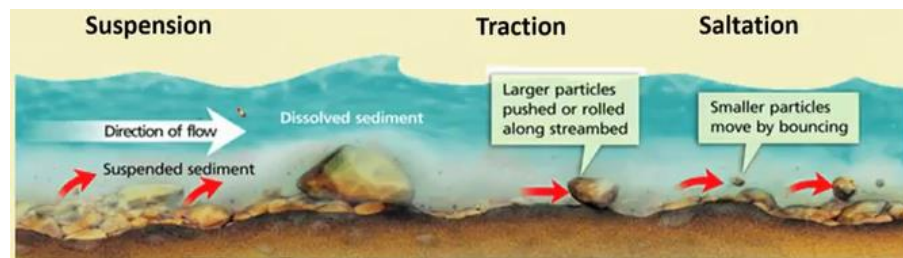


Fig. 2.3: Sediment transport modes

Sediment movement is a critical issue that must be addressed if water resources are to be used sustainably, (Khanchoul *et al.*, 2018). This is because concerns like aquatic ecosystem assessment, pollutant export estimates from catchments, and stream water quality projections all necessitate the calculation of fluctuations in suspended load with flow over time, (Tabarestani & Zarrati, 2014). Energy conditions govern the behavior of suspended sediment in watercourses, with low flows accumulating sediment and high flows transferring it, (Dutta, 2016; Khanchoul *et al.*, 2018). However, sediment transport rates are determined by the amount of sediment available, (Asselman, 2000). As a result, understanding sediment mobility is essential for anticipating sediment and even contaminants in surface water, (James *et al.*, 2010).

2.3.3. Sedimentation of a Reservoir

Water is without a doubt the most precious natural resource on the world for all living things, (Maina *et al.*, 2018; Daus *et al.*, 2021; Palma *et al.*, 2021). However, many third-world nations have struggled to find enough water in the correct quantity and quality, (Lee *et al.*, 2022). Water shortage, for example, can lead to issues like pollution and abstraction, (Palma *et al.*, 2021). In developing countries, existing freshwater resources are insufficient to sustain the enormous need for water for households, agricultural, and more importantly, industrial operations, (Kondolf & Yi, 2022). As a result, river/stream runoff retention in reservoir facilities has been suggested as a viable alternative for addressing global water concerns, (Daus *et al.*, 2021; Koś *et al.*, 2021; Moslemzadeh *et al.*, 2022). Climate change and the seasonality of rainfall, on the other hand, have heightened the need to develop and manage water resources in order to increase conservation and make resources available for immediate use, (Ilci *et al.*, 2019; Adongo *et al.*, 2020). This awareness has awakened the development of strategies for storing water in rivers through the construction of reservoirs, allowing this wonderful goal to move forward more quickly, (Gopinath, 2010). Water storage is a tried-and-true strategy that has helped humankind survive for decades, (Do *et al.*, 2022).

Reservoirs are hydraulic structures built across rivers for a variety of purposes, including recreation, water supply on a rural and municipal scale, power generating, discharge management, and flood control, (Basson, 2009; Gopinath,

2010; Schleiss *et al.*, 2016; Feldbauer *et al.*, 2020; Basson *et al.*, 2022; Kondolf & Yi, 2022). The normal location of a reservoir is near the catchment's outlet, where inflows from rivers or stream channels accumulate, (Snyder *et al.*, 2004). Sedimentation, on the other hand, has become an inescapable phenomenon that has continued to jeopardize the operation of all reservoirs, (Ilci *et al.*, 2009; Alemaw *et al.*, 2013; Adongo *et al.*, 2020; Iradukunda *et al.*, 2020).

Natural mechanisms have been shown to have an impact on the reduction of reservoir storage capacity owing to anthropogenic pressure and climate change in studies, (Dargahi, 2012; Sojka *et al.*, 2021). Land use activities and even land cover changes have all contributed to the movement of both matter and energy within these ecosystems, with sediment deposition into lakes and reservoirs being the worst, (Norgbey *et al.*, 2021; Sojka *et al.*, 2021). Climate change-related effects, such as changes in rainfall patterns, have recently resulted in a rise in occurrences of soil loss, resulting in an increase in both sediment as well as pollutant supplies in lakes and reservoirs, (El-Radaideh *et al.*, 2014). Increased population expansion has led in more sediment and nutrients entering streams and rivers, eventually ending up in reservoirs and lakes, (Kamarudin *et al.*, 2017). Despite the fact that sedimentation is a naturally occurring process, it may probably be slowed down by implementing improved soil as well as water management methods and even better agricultural practices in catchment regions, (Gopinath, 2010). The removal of sediment, on the other hand, is a far more difficult undertaking due to technological constraints and, above all,

environmental, social, and ecological concerns, (Kazberuk *et al.*, 2021; Basson *et al.*, 2022).

Reservoir sedimentation is a natural process (Foteh *et al.*, 2018); however, it may be slowed down by better catchment management methods, (Gopinath, 2010). Sediment coming from surface runoff owing to rainfall, snowmelt, and even river channel erosion makes its way into rivers or streams within the catchment, where it is finally deposited into reservoirs, thanks to the hydraulic process, (Merina *et al.*, 2016). As a result, reservoir sedimentation can serve as an indirect way of predicting soil erosion, (Kusimi *et al.*, 2015).

River basins transport water, heat, sediments, chemicals, and even biological species from the slopes of hills to aquatic bodies such as lakes and reservoirs, (Schleiss *et al.*, 2016). Natural rivers are thought to have a rough equilibrium between sediment intake and discharge, (Turgut *et al.*, 2015). Hence, the geomorphology, hydrology, and even biological conditions in both the upper and lower sections of the river are all affected when the normal flow regime is disrupted, (Turgut *et al.*, 2015). Therefore, any structure built to impound water disrupts the aforementioned fluxes and creates sedimentation, reducing the reservoir's capacity to hold water, (George *et al.*, 2016; Merina *et al.*, 2016; Ali & Shakir, 2018). Dams generate an excellent sediment sink within a valley, to put it simply, (George *et al.*, 2016; Schleiss *et al.*, 2016; Morris, 2020). As a result, the sedimentation process has an impact on a reservoir's life. Morris (2020) found that

almost half of sediment flux is confined in controlled basins, meaning that the rest may make its way into the reservoir.

The number of reservoirs across the world has been steadily increasing, (Kondolf & Yi, 2022). However, sedimentation is expected to reduce effective storage capacity during the next several years, (Basson, 2009; George *et al.*, 2016; Merina *et al.*, 2016; Basson *et al.*, 2022). Because of the accumulation of sediment and sediment imbalances caused by soil erosion, reservoir storage capacity is dwindling, (Ali & Shakir, 2018). Furthermore, the velocity of water entering a reservoir is fairly low, and as a result, a reservoir traps sediments very well, resulting in lower transit capacity while sedimentation grows, (Dutta, 2016; Merina *et al.*, 2016).

The progressive deposition process reduces the reservoir's live storage capacity, rendering it ineffectual in achieving its goal over time, (Foteh *et al.*, 2018; Boakye *et al.*, 2020). In this regard, sedimentation reduces flood storage capacity, affecting water supply and hydroelectric energy generation, exposing downstream populations to floods, reducing water quality due to sediments and phosphatic nutrients, reducing recreational value of water due to increased algal blooms, and subjecting water turbines to wear and tear, (Odhiambo & Boss, 2004; Schleiss *et al.*, 2016; Ali & Shakir, 2018).

The way reservoirs lose capacity owing to sedimentation has presented a significant issue to dam owners, (Schleiss *et al.*, 2016). This is because dams

disrupt the flow of material via rivers, generating a buildup of sediment in the reservoir, which degrades its operation and above all, reducing storage capacity, (Kondolf *et al.*, 2014; Ali & Shakir, 2018). According to Kondolf *et al.* (2014), sedimentation deprives the river's downstream portions of sediments that are necessary for maintaining the channel's shape and supporting the riparian ecology.

The rate at which sedimentation occurs in reservoirs is influenced by factors such as the catchment's extent, soil type, land use activities, land cover alterations, and most importantly, climate, (Moriassi *et al.*, 2018). Human activities and catchment manipulations on the upstream side also exacerbate reservoir sedimentation, (Foteh *et al.*, 2018). Sedimentation issues have affected 40,000 big reservoirs worldwide, leading them to lose between 0.5 and 1 % of their storage capacity, (Mahmood, 1987; Basson, 2009; Merina *et al.*, 2016). According to Basson (2009), the rate at which the storage capacity is depleted is slower when the reservoir is larger. This, according to Kondolf and Yi (2022), is owing to the increased chance of potential sediment sinks and filters forming due to topographical influences on vast drainage basins.

The worldwide reservoir capacity is predicted to be 7000 km³, with 4000 km³ being utilised for electricity generation, agriculture, and water supply, (Basson, 2009). Reservoirs have an average age of 30 to 40 years, with around 0.5 to 1 % of their volume lost each year owing to sedimentation, (Basson, 2009; Schleiss *et al.*, 2016). If no action was taken, WCD (2000) predicted that nearly a quarter of

the dam reservoirs will have sedimentation issues within 25 to 50 years. According to Basson (2009), arid regions have the greatest average rates of sedimentation (table 2.2). Schleiss and De Cesare (2010) found that the decline in reservoir storage capacity due to sedimentation was far greater than the increase in capacity due to the building of new reservoirs on a worldwide scale. Reservoir sedimentation, as shown in Table 2.2, puts the sustainable production of energy and food at jeopardy.

The sedimentation phenomenon gives a basis for forecasting the storage capacity on which the reservoir's life may be anticipated in the context of fluvial hydraulics, (Dutta, 2016; Basson *et al.*, 2022). This demonstrates that sedimentation in any reservoir is influenced by sediment yield, (Ali & Shakir, 2018). As a result, maintaining reservoirs necessitates excellent flow regulation and sediment management, (Ilci *et al.*, 2019; Ali & Shakir, 2018; Pacina *et al.*, 2020). However, data on water depth, reservoir capacity, water surface area, sedimentation rates, and genuine practical life span are still insufficient, (Adongo *et al.*, 2020).

Table 2.2: Average global rates of sedimentation and time period when 80 and 70 percent respectively of the capacity of the reservoirs will be lost due to sedimentation, (Basson, 2009)

Region	Average rate of sedimentation (%/year)	Dams for hydroelectric power: 80 %	Dams for other uses: 70 %
Africa	0.85	2100	2090
Asia	0.79	2035	2025
Australia and Oceania	0.94	2070	2080
Central America	0.74	2060	2040
Europe – Russia included	0.73	2080	2060
Middle East	1.02	2060	2030
North America	0.68	2060	2070
South America	0.75	2080	2060

2.3.4. Bottom Sediments

Bottom sediments are extremely important in aquatic bodies, (Senze *et al.*, 2021). The catchment features, the prevailing climate, and the residence duration all influence the nature, composition, and above all, the quantity of sediment material in reservoirs, (Kazberuk *et al.*, 2021). In addition to fostering the growth of plants and algae, sediments are key transporters of nutrients, (Wondim & Mosa, 2015).

Bottom sediment material found in various water bodies are typically fine-grained, if not ultrafine-grained, and consist mostly of clay particles, silt and even fine sands, (El-Radaideh *et al.*, 2014; Kazberuk *et al.*, 2021). They are either typical inorganic substances (fractions of silt, clay, and sand) or even organic material (remains of plant and animal species) and they are basically adsorbed by nutrient elements and pollutants, according to Kamarudin *et al.* (2009).

Gałaszka *et al.* (2007) defined inorganic sediments as substances that build in reservoirs throughout time as a result of human activities. Due to the high demand for both food and even feed, majority of farmers have had to depend on artificial and even organic fertilizers to fix key minerals (mostly nitrogen and phosphorus) into the soil, (Matej-Łukowicz *et al.*, 2021). However, plants, on the other hand, do not use all of the supplied nutrients, and the balance is rejected to the environment, (Szymaski *et al.*, 2012). Total organic carbon, on the other hand, is used to express the amount of organic material in sediment material, whereas nutrient content is represented as total nitrogen or even total phosphorous, (Wondim & Mosa, 2015). Furthermore, the breakdown of organic material results in lower carbon levels in the sediment, while nutrient concentrations in the sediment are discharged into the immediate water column, (Senze *et al.*, 2021).

Despite connections and interaction between the physicochemical and even biological characteristics of bottom sediments, the water ecosystem in most lakes and reservoirs is somewhat dynamic, (Kazberuk *et al.*, 2021). As a result, the the floral and faunal species in the aquatic ecosystem is heavily reliant on the reservoir's physicochemical properties, (Madeyski & Bednarczyk, 2000; Sojka *et al.*, 2021). Furthermore, reservoir features aid in a better description of interaction that may occur between some natural processes and even activities that take place within the reservoir, thereby allowing for better protection decisions, (Zakonov *et al.*, 2019). The physical properties of reservoirs describe their non-uniformity and complexity, (Ziemińska-Stolarska *et al.*, 2020; Senze *et al.*, 2021). The

circulation of water and sedimentation are influenced by actual physical elements such as the form, depth, and temperature of the water, (Senze *et al.*, 2021). The chemical characteristics of sediments provide some crucial information about eutrophication rates within reservoirs, (Szymaski *et al.*, 2012; Ziemińska-Stolarska *et al.*, 2020; Kos *et al.*, 2021).

An appropriate equilibrium is struck in healthy reservoirs between sediment intake and that which would fairly support aquatic life, (Sang *et al.*, 2017; Ziemińska-Stolarska *et al.*, 2020). Trace elements, on the other hand, are crucial indicators for documenting how human-induced activities affect lakes and reservoirs, (Sojka *et al.*, 2021). Trace elements may contaminate sediments and endanger the living species, which have a significant impact on the aquatic environment, (Ziemińska-Stolarska *et al.*, 2020). Detailed geophysical surveys are commonly used to learn about present sedimentary activities as well as catchment processes within a range of geological contexts, and more importantly, their effect with regards to sediment distribution within any receiving body, (Sahoo *et al.*, 2017). The geochemical characteristics of sediments enable the identification of variables as well as processes that affect the occurrence and distribution of elements, (Zakonov *et al.*, 2019).

2.3.5. Beneficial Use of Reservoir Sediments

Sediment is a byproduct of erosion processes in which soil breaks down into sand, silt, or clay grains, and organic materials, which ultimately settle in receiving

water bodies after being transported, (Junakova & Balintova, 2014). In the subject of water management, sediment formation in reservoirs is regarded as a serious issue, particularly in terms of reservoir storage capacity loss and, more crucially, the beneficial use of sediment material retrieved from reservoirs, (Junakova & Balintova, 2014).

Dam reservoir maintenance necessitates dredging operations, which is an expensive procedure, (Basson *et al.*, 2022). Furthermore, the reuse of dredged sediments has the potential to make better use of huge amounts of the material. The biotic and abiotic use of dredged sediments, on the other hand, can only be done once their qualities are known, (Junakova & Balintova, 2014). Dredged sediments have distinct physicochemical properties that might be connected to past and current land usage in catchment areas. Biotic use of sediments, according to Junakova and Balintova (2014), means that they are used directly for objectives such as land reclamation and augmentation, such as horticulture and forestry.

Karanam *et al.* (2008) revealed that reservoir bottom sediments are associated with both environmental and economic benefits. In this regard, such sediments with moderate levels of macronutrients, organic carbon, and even trace elements may be utilized to improve the quality status as well as the productivity of arable land, (Tomczyk-Wydrych *et al.*, 2021). They can be used to replace inorganic fertilizers in croplands when they are proven to be quite rich in the context of nutrients and organic carbon, (Karanam *et al.*, 2008). However, the direct

utilization of bottom sediments as fertilizer, according to Matej-Łukowicz *et al.* 2021, should be discouraged, and instead, nitrogen as well as organic carbon enrichment is strongly advised.

Bottom sediments, in fact, do not fit a conventional fertilizer mixture, despite the fact that they include useful elements such as iron and sulfur, (Matej-Łukowicz *et al.*, 2021). The low phosphorus concentration, which is defined as a non-renewable resource, is the most significant disadvantage with reservoir bottom sediments in terms of their potential use in agriculture.

2.4. Reservoirs and Climate Change

Reservoirs are significant hydraulic structures that help to minimize climate change-related challenges, because of their ability to store and control water supply, (Field *et al.*, 2014; Kondolf & Yi, 2022). In this regard, new reservoirs must be built, while current ones must be managed well to avoid potential storage losses, (Schleiss *et al.*, 2016; Basson *et al.*, 2022; Kondolf *et al.*, 2022). Climate change, on the other hand, has an impact on reservoirs, as well as other connected water bodies, (Feldbauer *et al.*, 2020). Increased water temperatures, high evapotranspiration rates, and hydrological shifts are all effects of climate change on reservoirs, (Ehsani *et al.*, 2017).

Soil moisture dynamics in catchments is likely to be affected by changes in temperature, runoff, and evapotranspiration rates, (Miranda *et al.*, 2019). Changes in rainfall events and decreased plant cover are expected to exacerbate soil loss

within catchments and streams that feed reservoirs, (Furniss *et al.*, 2010). Seasonal variations in temperature and rainfall may also increase forest mortality and forest fires, which have a severe impact on vegetative communities within the catchment and even on the riparian contours that define the reservoir, (Furniss *et al.*, 2010). Hence, such alterations could have an impact on the long-term buildup of particle organic matter content and coarse wood debris from wooded areas in reservoirs, (Miranda *et al.*, 2019). As a result of the catchment's vulnerability to precipitation and temperature variations, reservoirs are at increased risk, (Miranda *et al.*, 2019).

Climate change may disrupt sediment delivery, create thermodynamic processes within the catchment, promote basin drying, and, eventually, have a direct impact on sediment output, (Schleiss *et al.*, 2016; Miranda *et al.*, 2019). Furthermore, with the increased likelihood of intense precipitation events, soil erosion and river or stream bank failure are projected to rise, (Ojima *et al.*, 2015).

Schleiss *et al.* (2016) pointed out that the effects associated with climate change may significantly affect biodiversity within reservoirs, which has some relationship with sedimentation processes. For instance, catchment changes may induce some changes in the rate at which nutrients enter the reservoir, and this may stimulate the arrival mechanism of specific invasive species, given that changes in reservoir conditions may favour exotic plants compared to native ones, (Schleiss *et al.*, 2016). Similarly, increased temperatures and changing patterns of

rainfall may interfere with the distribution of vegetation if at all it exists, and this may increase the speed of eutrophication, (Schleiss *et al.*, 2016; Miranda *et al.*, 2019). According to Rebetez *et al.* (2011), the occurrence of landslides and debris-characterized flows will rise, particularly in countries with temperate hydro-climates.

The spatiotemporal sediment distribution within river catchments is affected by climate change, (Kondolf & Yi, 2022). This is because climate change has the potential to alter soil characteristics and vegetation composition, resulting in changes in sediment loading and reservoir capacity, (Miranda *et al.*, 2019). This is due to the fact that climate change may alter sediment transport through watersheds, (Schleiss *et al.*, 2016; Dahl *et al.*, 2018). As a result, climate change is projected to jeopardize reservoir sustainability through increasing sedimentation rates, (Miranda *et al.*, 2019). In this sense, small reservoirs are likely to suffer more from the effects of climate change since they are limited by capacity, and consequently they cannot resist major flow variations, (Annandale, 2014; Armin *et al.*, 2018).

On the other hand, the accumulation of sediments in reservoirs serves as a possible sink for the carbon cycle, (Mendonça *et al.*, 2012; Imamoglu & Dengiz, 2017; Mendonça *et al.*, 2017). Organic carbon present in the atmosphere is removed during the photosynthesis process and is thus trapped by sediments; as a result, the accumulation of sediments in reservoirs serves as a possible sink for the

carbon cycle, (Mendonça *et al.*, 2017; Phyoe & Wang, 2019). Eventually, the amount of carbon stored within the sediments could be released as carbon dioxide gas or even methane gas by diffusing as emissions from surfaces, being degassed into the river, especially downstream, or finally bubbling out as emissions, (Mendonça *et al.*, 2017).

According to Prairie *et al.* (2018), when rivers are dammed, carbon emissions rise because of the buildup of terrestrial organic material and sediment rich in degradable organic matter. Because of the large amounts of biomass in tropical reservoirs, they have been observed to be strong generators of methane gas, (Barros *et al.*, 2011). Reservoirs do have an impact on the carbon cycle, but their importance is mostly determined by age, climate, and latitude, (Barros *et al.*, 2011; Phyoe & Wang, 2019). Furthermore, the carbon cycle is influenced by elements such as productivity, geology, type of water body, geology, and morphometry of the watershed, (Phyoe & Wang, 2019).

2.5. Management Strategies against Sediment in Reservoirs

Sediment trapping is the only practical remedy because soil erosion never ceases and reservoir capacity is constrained, (George *et al.*, 2016; Obialor *et al.*, 2019; Morris, 2020). Morris (2020) goes on to say that when a reservoir fills and its functionality is jeopardized, an equilibrium balance between sediment influx and outflow will be struck, or by encouraging management initiatives that would improve the reservoir's long-term functionality (figure 2.4).

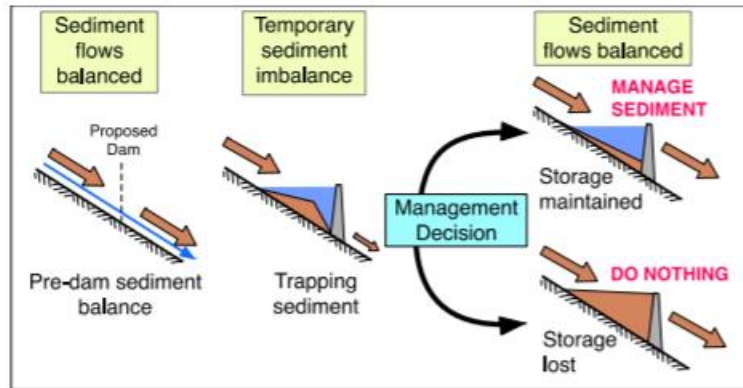


Figure 2.4: Sediment equilibrium in a reservoir (Source: Morris, 2020)

When a proper sediment management strategy is executed, a reservoir's functionality can be maintained, (George *et al.*, 2016; Morris, 2020; Basson *et al.*, 2022; Kondolf & Yi, 2022). Sustainable sediment management aims to achieve a balance between in and out of the sediment, restore sediment delivery downstream of the channel, maximize long-term storage, and derive possible advantages while keeping the environment in mind, (Morris, 2020; Sun *et al.*, 2022). Reservoirs can be characterized as low or high in this regard, depending on a variety of characteristics such as infrastructure use, volume loss due to sedimentation, and, more importantly, the rate at which sedimentation occurs, (Juracek, 2015).

Preventative and, more significantly, post-sedimentation mitigation approaches can be put in place before or even during the construction phase, (Schleiss *et al.*, 2016). There are quite a number of engineering approaches that could be used to effectively regulate sedimentation in reservoirs, (Schleiss *et al.*, 2016).

Retroactive approaches, according to Schleiss *et al.* (2016), restore reservoir volume by draining silt via or even bypassing the embankment. According to Kondolf *et al.* (2014), reservoir sedimentation mitigation methods are grouped into three categories based on where they occur within a river basin: upstream of the reservoir (C), within the reservoir (R), and most importantly at the dam (D), or even a mix of the three.

Schleiss *et al.* (2016) classified reservoir sedimentation control techniques based on the intervention process, such as where sediments are produced (upper reach, middle reach, and within the reservoir), sediment transport (within the upper network of the channel or as sediments approach the reservoir), and long-term sediment storage. As indicated in the diagram below, Morris (2020) grouped reservoir management options into four categories (figure 2.5).

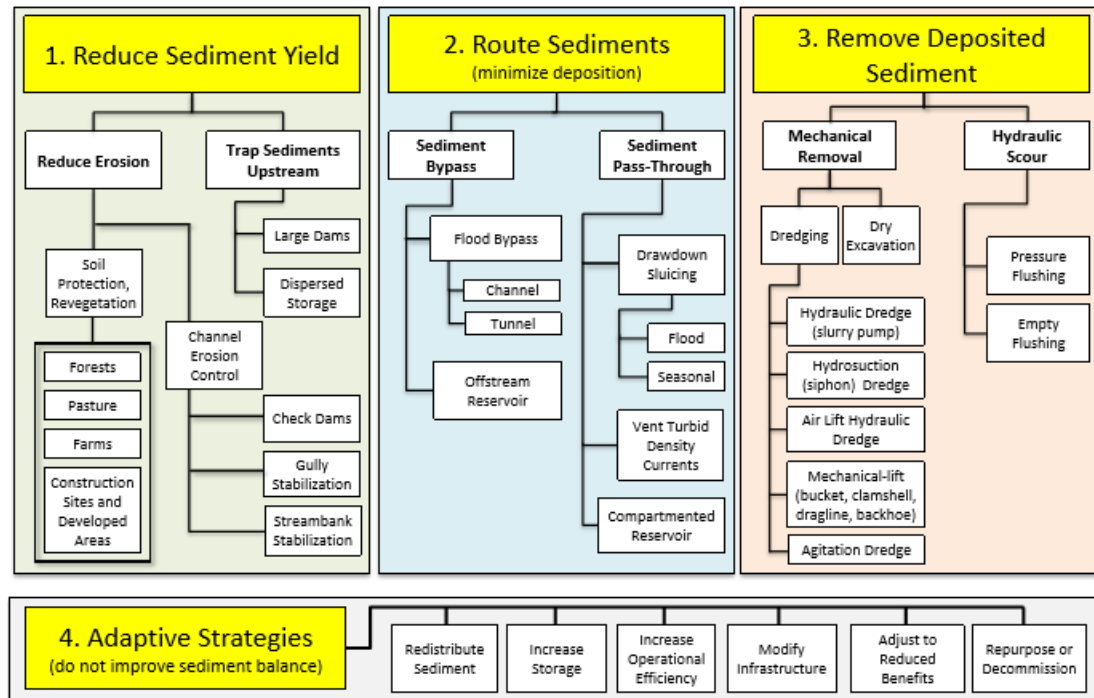


Figure 2.5: Management strategies for reservoir sedimentation (Source: Morris, 2020)

The strategy chosen for the control of sediments must take into account the following important parameters, (Schleiss *et al.*, 2016): Geographic location (climate, weather, latitude, and altitude); geometry of the catchment (hypsometry, area, river network, and topography); land cover/land use within the catchment; human activities carried out within the catchment; mineralogy of the sediment and grain size distribution; geometry of the reservoir (in relation to the area of the catchment, capacity, orography, shape and slope characteristics); type of the dam (naturally occurring or artificial, method of construction); hydro-mechanical equipment for releasing water in terms of type and even their number); age and the manner in which the infrastructure is being used; the level at which sediments have accumulated within the reservoir; the system of management of the water;

quality aspects of water and that of sediments; economic value for both the water resource as well as sediments; sensibility of geopolitics; practices at local scale in addition to the available equipment; and ecological aspects on the upstream and even on the downstream sides of the dam.

Morris (2020), on the other hand, identified technical, economic, hydrologic, environmental, and regulatory challenges as key determinants of the use of reservoir management strategies. He went on to say that adaptive and proactive techniques can be blended to come up with the best management strategy. However, the two strategies must be addressed when a long-term plan for the reservoir's sustainable usage is being prepared, as well as a foundation for moving from near-term to long-term management strategies, (Morris, 2020).

2.6. Soil Erosion Modelling

2.6.1. Why Modeling?

Managers must make decisions based on collected data in order to improve water quality and restore degraded catchments, (Jothimani *et al.*, 2022). However, data gathering can be costly, time-consuming, and inconvenient, thus modeling is considered as a superior option in these cases. A model is a representation of logic and processes, (De Roo, 1996).

In order to tackle a specific problem, a modeller employs formulations to represent a basic process or a set of processes. Some factors that are not physically observable may be included in the model, but they must be calibrated

for each case, according to De Roo (1996). This, however, does not degrade the model's quality; rather, it strikes a balance between available time, monetary resources for model creation, data collecting, and processing time. The model users should clearly identify the intended output from the modeling study. Most models that have been developed by various authors differ in complexity, data requirements, process, and application, (Pandey *et al.*, 2016).

2.6.2. Soil Erosion Models

To relate the primary causes and the key processes that occur on the ground surface, soil erosion models utilize mathematical expressions, (Jetten *et al.*, 2003; Gianinetto *et al.*, 2019). Topography, soil qualities, land use/land cover, and meteorological variables are all elements to consider, (Jetten *et al.*, 2003; Devatha *et al.*, 2015; Gianinetto *et al.*, 2019). The detachability, transportability, and deposition behaviour of soil particles on the terrestrial surface are described by these models, (Nearing *et al.*, 1994; Jetten *et al.*, 2003). They have the ability to estimate soil loss, making them valuable instruments in project planning, (Siddique *et al.*, 2017; Benavidez *et al.*, 2018). They contribute to a better apprehension of the soil erosion phenomenon and its consequences, (Nearing *et al.*, 1994; Benavidez *et al.*, 2018). Appropriate models have been chosen on the basis objectives, data availability, catchment features, and model efficiency, (Keesstra *et al.*, 2014; Pandey *et al.*, 2016).

Different types of erosion models have been developed and used on the basis of land and weather conditions, (Merritt *et al.*, 2003; Devatha *et al.*, 2015; Ganasri & Ramesh, 2016; Beyene, 2019; Bansekhria & Bouhata, 2022). For the prediction of soil erosion on fields, drainage basins, and hillslopes, some parametric models have been created, (Wischmeier & Smith, 1978; Korada & Vala, 2014). The soil type, climate, terrain, and land use features were all taken into account when creating these models, (Sharma *et al.*, 2010).

Three sorts of models are classified based on the mechanism examined during model development: physical, conceptual, and empirical models, (Merritt *et al.*, 2003; Efthimiou *et al.*, 2014; Devatha *et al.*, 2015; Ayinla & Jona, 2018; Sujatha & Sridhar, 2018; Gianinetto *et al.*, 2019). Both empirical and conceptual models are "simple," according to Merritt *et al.* (2003), however, physically-based models are "complex." Both empirical and process-based models have been used to model soil erosion, (Li *et al.*, 2017; Saha *et al.*, 2018) and, more crucially, to build conservation plans, (Ascough *et al.*, 2017). However, other aspects involved in soil erosion must be included in a model, such as influencing variables, level and implementation period, processes to be considered, characteristics to be assessed, algorithm type and assessment type, and types of hazard, (Karydas *et al.*, 2014), (Table 2.3).

Table 2.3: Key parameters involved in modelling water erosion and their relevant options (Source: Karydas *et al.*, 2014)

Parameters	Options
Magnitude	Field, hillslope, watershed or landscape
Period	Event-based or averaged
Influencing factors	Climate, topography, soil or vegetation
Soil erosion processes	Splash detachment, runoff transfer or runoff detachment
Forms of erosion	Sheet, rill, gully or bank
Algorithm	Empirical or mechanistic
Assessment	Qualitative or quantitative

Physically Based Models

In the modeling of soil erosion, physical models have frequently been used, (Malleswara Rao *et al.*, 2005). The progress of physical soil erosion models has been accelerated by increased understanding of the representation of hydrological processes, as well as the availability of measuring tools at the field level, (Ramsankaran *et al.*, 2013). Physical models solve fundamental physics equations to describe the soil erosion process in a catchment, (Merritt *et al.*, 2003; Malleswara Rao *et al.*, 2005; Roshani *et al.*, 2013). They can anticipate both runoff and even sediment yield for a given storm in terms of location, (Chandramohan *et al.*, 2015). Physical models, according to Morgan (1995), are process-based since they use an empirical method to model soil erosion. They mostly employ explicit differential equations, also commonly known as the equation of continuity, which is the theory of matter conservation in a given place for a given time, (Morgan, 2005; Mitsova *et al.*, 2013).

Physical models are effective tools because they combine elements of soil erosion, their interactions, and their temporal variability, (Zhang *et al.*, 1996; Ascough *et al.*, 2017). Physically-based models, on the other hand, do not provide an ideal set of parameters for driving models based on parameter estimation criteria, (Malleswara Rao *et al.*, 2005), despite the fact that they are extremely sophisticated and require a lot of data, (Sujatha & Sridhar, 2018). A created physically based model for a limited area, such as a catchment, cannot be transferred to a wide area, according to Malleswara Rao *et al.* (2005).

Physical models have been extensively used in studying water quality issues and erosion processes, (Sujatha & Sridhar, 2018). The common ones include: Areal Non-Point Source Watershed Environment Response Simulation model (ANSWERS), (Beasley *et al.*, 1980); Griffith University Erosion System Template model (GUEST), (Misra & Rose, 1996); Productivity, Erosion and Runoff, Functions to Evaluate Conservation Techniques model (PERFECT), (Littleboy *et al.*, 1992); European Soil Erosion Model (EUROSEM), (Morgan *et al.*, 1998), and Water Erosion Prediction Project model (WEPP), (Laflen *et al.*, 1991).

Empirical Models

Empirical models are the most basic, relying on inductive logic, experience, and experimental outcomes, (Wheater *et al.*, 1993; Merritt *et al.*, 2003; Ayinla & Jona, 2018). They have a broad range of applications because they require fewer

calculations and data, (Merritt *et al.*, 2003; Efthimiou *et al.*, 2014; Asadi *et al.*, 2017). The erosion process effect (separated amount of soil) is connected by mathematical formulae to either objectively quantifiable (temperature, catchment area, topography variables, etc.) or subjectively assignable parameters (temperature, catchment area, topographic factors, soil erodibility factor, etc).

These models are only applicable to the location and its conditions because they do not seek to understand the physics underpinning catchment dynamics, (Gianinetto *et al.*, 2019). The input data for the model is considered to be uniform across the basin. That is why they produce more consistent results when used in small areas where parameter fluctuation is minimal, (Merritt *et al.*, 2003; Efthimiou *et al.*, 2014). The models assume that the data remains constant throughout the analysis, which may be unsatisfactory in some instances.

They are, however, highly costly and time-consuming, particularly during the calibration process, because much time is required to collect the necessary data. Furthermore, empirical models are costly and necessitate extensive experiments in order to gather crucial data for calibration. Some of the most widely used examples of this type of model include: Universal Soil Loss Equation (USLE), (Wieschmeier & Smith, 1978), sediment delivery ratio (SDR), (Renfro, 1975), Modified Universal Soil Loss Equation (MUSLE), (Williams, 1975), Revised Universal Soil Loss Equation (RUSLE), (Renard *et al.*, 1997), Sediment Delivery Distributed (SEDD), (Ferro & Porto, 2000), and Agricultural Non-point Pollution

Source (AGNPS), (Young *et al.*, 1989).

Conceptual Models

Catchments are typically represented in these models as conventional periodic internal storage units, (Merritt *et al.*, 2003). The general mechanisms that govern sediment and water storage define the interface between the two, (Merritt *et al.*, 2003). Rainfall and runoff determine sediment formation; hence they are part of the model input, whereas sediment yield is the result, (Chandromohan *et al.*, 2015). The input parameters for this type of model are typically derived after calibration using field data.

The process of determining the best set of data values, on the other hand, might be time-consuming. The model may be complicated by the several sets of optimal parameter values, making it far more difficult to determine them, (Merritt *et al.*, 2003). It signifies that the parameters can not be fully translated into physical values, (Sujatha & Sridhar, 2018). Examples include the Chemical Runoff and Erosion from the Agricultural Management Systems (CREAMS), (Knisel, 1980), and Large Scale Catchment Model (LASCAM), (Viney & Sivapalan, 1999).

2.6.3. Model Scales

Soil erosion mechanisms vary in space and time due to the interplay of multiple components at each phase, (Fistikoglu & Harmacioglu, 2002; Mayor *et al.*, 2011; Santos *et al.*, 2017; Gianinetto *et al.*, 2019). Soil erosion models must account for the catchment's geographical and temporal effects, (Owen *et al.*, 2006). As a

result, the primary goal of incorporating a model into soil erosion research is to show the erosion process and sediment transport mechanism at various spatiotemporal scales, (De Vente & Poesen, 2005). Since runoff and erosion rates vary in terms of space and time, it is vital to identify the scales, as well as the processes and forces at play, (Mayor *et al.*, 2011). In order to fully represent the spatial and temporal scales, a model is designed to operate at a certain spatial extent and time interval, (Karydas *et al.*, 2014).

Examples of spatial scales include hill slopes, small, medium, and large catchments, with land area sizes ranging from less than 0.1 km² to 1,000 km², 1,000 km² to 10,000 km², and more than 10,000 km² respectively, (Owens *et al.*, 2006; Li *et al.*, 2017). According to De Vente and Poesen (2005), greater drainage area leads to enhanced sediment yield. Furthermore, Owens *et al.* (2006) pointed out that as the geographical scales rise, such as from hilltop to watershed, erosion processes and sediment transport increase. In this context, relevant data sets must be developed to aid in the modeling of soil loss and more importantly, sediment transport processes, (Owens *et al.*, 2006). Geospatial features (spatial, temporal, and even spatial methods) would, thus, constitute the basis for modeling soil erosion, according to Karydas *et al.* (2014).

In order to establish the suitable application of the model, the timing of events or even processes to be predicted must be addressed, (Merritt *et al.*, 2003). Examples of time scales include storms, daily, weekly, monthly, annual, decadal, and

holocene events, (Owens *et al.*, 2006; Li *et al.*, 2017). By building models that might function for a specific rainfall event, the behavior of an area subjected to a single storm event was explored, (Merritt *et al.*, 2003). For event-based models, the timestep ranges from minutes to hours. These models' algorithms use grid cells to describe processes at the plot or catchment level, (Merritt *et al.*, 2003). As a result, models have been used at larger temporal scales to investigate broader trends in vegetation, land management, and rainfall over time, (Merritt *et al.*, 2003). Event-based models have been modified to continuously simulate mode as computing power has increased, (Merritt *et al.*, 2003).

2.7. GIS and RS Applications in Modelling Soil Erosion

Soil erosion assessment is difficult due to the isolated nature and heterogeneity of large catchment areas, (Amah *et al.*, 2020). Hence, the use of traditional methods to map soil erosion becomes extremely difficult, (Amah *et al.*, 2020). The future success in soil erosion modeling will depend on how successfully the geographical information system (GIS) is integrated into the process, (Avwunudiogba & Hudson, 2014). At the field level, models have been used to develop plans aimed at conserving and managing catchments in a cost-effective manner, (Wieschmeier & Smith, 1978). However, given the large sets of data and parameters involved, applying models has been difficult due to the spatial extent of catchments, (Avwunudiogba & Hudson, 2014). This necessitates the use of more valuable and practical tools such as RS and GIS, among others, (Devatha *et al.*, 2015).

These geospatial tools have enhanced the quality of soil erosion modeling, (De Jong, 1994; Jain & Sharma, 2014). This is reflected in their improved ability to store, manage, analyze, and display data, (De Jong, 1994). The majority of models calculate soil loss by taking into account the relationship between the various erosion factors, (Wieschmeier & Smith, 1978). As a result of the integration of geospatial tools into these models, it is now possible to estimate the risk of soil erosion spatially as well as develop sound soil erosion prevention techniques, (Efthimiou *et al.*, 2014; Saha *et al.*, 2018).

GIS, as defined by Longley *et al.* (2004), is a computerized system that collects, stores, transforms, and displays spatial data in order to solve spatial problems. The use of GIS in erosion modeling allows for a more realistic simulation of the phenomenon, (Karydas *et al.*, 2014). Furthermore, by combining soil erosion models with GIS, the process of soil erosion can be simulated while taking into account the complexity of the factors involved, (Mallick *et al.*, 2014). When GIS is used in soil erosion models, it creates a powerful research tool, (De Roo, 1996; Devatha *et al.*, 2015; Beyene, 2019). This is due to the fact that a large number of models require manual file feeding via typing. GIS, on the other hand, can generate files for use in the model as well as display the results, (Csafordi *et al.*, 2012). De Roo (1996) went on to say that the use of DEM in GIS allows for detailed descriptions of the morphology of the catchment, which allows for successful soil erosion modeling.

In larger catchments, GIS techniques make it possible to estimate soil erosion in addition to quantifying its spatial extent at manageable costs and above all, with greater accuracy, (Jain *et al.*, 2001; Csafordi *et al.*, 2012; Manjulavani *et al.*, 2016; El Jazouli *et al.*, 2017). GIS, as demonstrated by Korada and Vala (2014), can measure parameters related to a region's topography and hydraulics at spatial scales. According to Bartsch *et al.* (2002), the GIS framework can be used to calculate a topographic factor from a DEM, which is important in calculating soil erosion loss. Some existing models, such as RUSLE, ANSWERS, and EUROSEM, have successfully integrated GIS, (Avwunudiogba & Hudson, 2014).

2.8. The RUSLE Model

2.8.1. Overview

The (R)evised (U)niversal (S)oil (L)oss (E)quation model is a mathematical model for predicting annual soil erosion that was developed and above all, it is extensively used, (Renard *et al.*, 1997; Manjulavani *et al.*, 2016; Beyene, 2019; Roslee & Sharir, 2019). It is a revised version of the (U)niversal (S)oil (L)oss (E)quation (USLE), which has been used for more than 40 years at various geospatial scales all over the world, (Farhan *et al.*, 2013). The RUSLE model's predicted amount of soil loss represents the quantity of soil lost from a user-described landscape, (Manjulavani *et al.*, 2016). The model, according to Angima *et al.* (2003), can be used to predict soil erosion in ungauged catchments.

RUSLE evaluates the loss of soil from undisturbed lands that encounter overland flow, disturbed areas, and even newly/reclaimed lands that have been recently formed, according to Renard *et al.* (1997). The RUSLE model, according to Angima *et al.* (2003), is a powerful tool for predicting the hazards associated with erosion in a specific location as well as identifying priority regions that require intervention measures. It is a common model for predicting soil erosion because it can accommodate for data management requirements to a limited extent, (Sujatha & Sridhar, 2018).

The RUSLE model accounts for the main causes of soil erosion by considering rainfall, soil, slope length, steepness, land cover management, and support practice as elements, (Farhan *et al.*, 2003; Bhat *et al.*, 2017; Sujatha & Sridhar, 2018; Phinzi & Ngetar, 2019). These characteristics vary in space and time, (Sujatha & Sridhar, 2018) and are heavily reliant on other variables, (Bhat *et al.*, 2017).

According to Bhat *et al.* (2017), the RUSLE model does not require a lot of data because it may employ satellite images with low to medium spatial resolution in addition to the restricted rainfall data. Integration of RUSLE with GIS, according to Shi *et al.* (2004), allows for the utilization and analysis of vast volumes of datasets that are difficult to handle manually. As a result, numerous countries have adopted the concept as an official conservation planning tool, (Wieschmeier & Smith, 1978; Renard *et al.*, 1997; Hudson & Fall, 2005; Farhan *et al.*, 2013).

The RUSLE model has dominated the world in predicting soil erosion because it is simple to use and has some GIS interoperability, (Pandey *et al.*, 2009; Yesuph & Dagneu, 2019).

Given that anthropogenic and natural factors are both major contributors to soil erosion (Phinzi & Ngetar, 2019), it is essential to understand these factors in order to precisely quantify soil erosion. Traditional methods, on the other hand, produce accurate predictions of soil erosion at plot proportions but are grossly inadequate at catchment dimensions, (Amah *et al.*, 2020). This is due to their inadequacy in terms of financial resources, time, and effort. As a result, Phinzi and Ngetar (2019) concluded that the RUSLE framework is excellent for assessing soil erosion and the elements that cause it. Globally, researchers have predicted soil erosion using the RUSLE model with greater success.

2.8.2. RUSLE Parameterization

RUSLE adds several enhancements for factor verification, although it keeps the latter's equation as its foundation, (Chadli, 2016; Sahu *et al.*, 2017). The model is empirically expressed as shown in equation (2.1).

$$A = (R) \times (K) \times (LS) \times (C) \times (P) \quad [2.1]$$

Where,

A = average annual soil loss time ($t \text{ ha}^{-1} \text{ yr}^{-1}$)

R = rainfall erosivity factor ($\text{MJ mm t ha}^{-1} \text{ yr}^{-1}$)

K = soil erodibility factor ($t \text{ ha h ha}^{-1} \text{ MJ}^{-1} \text{ mm}^{-1}$)

LS = slope length - steepness factor (dimensionless parameter)

C = cover management factor (dimensionless parameter)

P = support practices factor

2.8.2.1. Rainfall Erosivity (R) Factor

The energy possessed by a specific storm, which is a factor of the intensity of rainfall and the amount of precipitation, is known as rainfall erosivity, (Renard *et al.*, 1997). As a result, the rainfall factor quantifies the erosive power of a certain rainfall, (Malleswara Rao *et al.*, 2005; Tsitsagi *et al.*, 2018). There is a substantial correlation between soil erosion and rainfall, as evidenced by particle detachment and runoff contribution, (Esa *et al.*, 2018). As a result, the rainfall erosivity factor is greatly reliant on the amount and intensity of rainfall, (Phinzi & Ngetar, 2019). Therefore, the R-factor quantifies the total result of rainfall duration, volume, and severity for a certain rainfall event, (Panagos *et al.*, 2015).

The most essential aspects of rainfall, according to Foster *et al.* (2003), are the quantity and even intensity of rainfall. In this aspect, erosion is more likely when the quantity and intensity of rainfall for a specific rainfall event are both larger. Despite the fact that the rainfall erosivity factor is strongly linked to soil loss over the world, Renard and Freimund (1994) found that it varies depending on individual regions and scales. The lack of dense time series data has hampered the application of USLE and its upgraded formats. According to Vantas *et al.* (2019), a number of soil erosion models have since been developed on the basis of

rainfall's depth for certain time intervals, notably daily, monthly, and even annually, taking into account the corresponding spatial effects and climatological properties (Table 2.4).

Many researchers in many countries throughout the world have noted some good relation between R-factor values and yearly rainfall using a variety of techniques, ranging from simple equations to geo-statistical models, (Vantas *et al.*, 2019). Time periods of larger than 20 years are typically used to remove bias in the calculation of the R-factor, allowing for both wet as well as dry periods to be included, (Angima *et al.*, 2003; Vantas *et al.*, 2019).

Table 2.4: Rainfall Erosivity Factor Equations

Equation	Region of Application	Authors	Equation Number
$R = 0.55 \text{ MAR} - 24.7$	Ethiopia & Egypt	Hurni (1985)	2.2
$R = -8.12 + 0.562 \text{ MAR}$	Ethiopia	Hurni (1985)	2.3
$R = 79 + 0.363 \text{ MAR}$	Entire India	Singh <i>et al.</i> (1981)	2.4
$R = 50 + 0.389 \text{ MSR}$			2.5
$R = 0.1059 \text{ abc} + 52$	Entire India	Singh (2006)	2.6
$R = 22.8 + 0.6400 \text{ MAR}$	Dehradun, India	Rambabu <i>et al.</i> (1979)	2.7
$R = 0.5 \text{ MAR}$	Ivory Coast and Burkina Faso	Roose (1975); Morgan (1986)	2.8
$R = 23.61e^{0.0048\text{MAR}}$	Northern Jordan	Eltaif <i>et al.</i> (2010)	2.9
$R = 117.6 (1.00105^{\text{MAR}})$ for < 2000 mm	Kenya	Kassam <i>et al.</i> (1992)	2.10
$R = 0.38 + 0.35 \text{ MAR}$	Thailand	Harper (1987)	2.11
$R = \frac{2.5P^2}{100(0.073P + 0.73)}$	Indonesia	Bols (1978)	2.12

Key: MAR = average annual rainfall (mm), MSR = average seasonal rainfall (mm), and P = annual rainfall (mm), a = average annual rainfall (mm), b = maximum 24-hour rainfall (mm), and c = maximum 1-hour rainfall having a recurrence interval is 2 years

2.8.2.2. Soil Erodibility (K) Factor

When it comes to estimating soil loss and more so, implementing soil conservation measures, soil erodibility becomes an important factor to consider, (Shabani *et al.*, 2014; Zhang *et al.*, 2019). The K-factor assesses how soil attributes as well soil profile parameters influence soil loss, (Agarwal *et al.*, 2016; Chuenchum *et al.*, 2020). According to Alewell *et al.* (2019), there is a substantial statistical association between the K-factor and some soil parameters, particularly

when soil erodibility is attributable to water. These characteristics include those that affect infiltration capacity, permeability, and total content in the soil, as well as those that influence processes including abrasion, splashing, dispersion, and overland flow, (Alewell *et al.*, 2019). As a result, the K-factor has been characterized as the soil's inherent vulnerability to rainwater runoff erosion, (Ban *et al.*, 2016; Thomas *et al.*, 2017; Uddin *et al.*, 2018; Phinzi & Ngetar, 2019). It expresses the soil's inherent vulnerability to dislodgement and transfer in simple terms, (Lin *et al.*, 2019).

The erodibility of soil is much influenced by a number of physical and chemical factors, (Morgan, 1995; Esa *et al.*, 2018; Fayas *et al.*, 2019; Phinzi & Ngetar, 2019; Amah *et al.*, 2020). Organic matter content, soil particle dispersion, texture, and structural orientation are among them, (Chuenchum *et al.*, 2020). In theory, the K factor is a quantity that, despite being lumped, provides a description that quantitatively characterizes a specific soil when expressed as an annual integrated value, (Uddin *et al.*, 2018). On the basis of a typical plot, the K factor quantifies the rate of soil loss per unit index of erosion for a certain soil association, (Uddin *et al.*, 2018; Koirala *et al.*, 2019).

When exposed to water-borne erosion, however, various soils behave differently, (Phinzi & Ngetar, 2019). In this regard, finely textured clays, as well as sandy soils, have low K values; silt and loams having average texture have moderate K values; while soils with high fractions of silt have rather high K values, (Renard *et*

al., 1997). The availability of organic material in the soil, on the other hand, lowers the value of K due to its ability to bind soil particles together, and therefore, the rate of soil aggregation increases, which minimizes the effect of raindrop detachability, enhances infiltration capacity, and above all, reduces surface runoff, (Wischmeier & Smith, 1978; Renard *et al.*, 1997).

Empirical equations that have been developed using the physicochemical parameters of soils, runoff plots, and even simulation experiments on both rainfall as well as runoff have all been used to determine soil erodibility, (Shabani *et al.*, 2014). Following long-term data taken directly from runoff plots, the-K factor as described in the USLE model (Wischmeier & Smith, 1978) has been widely utilized to estimate soil erodibility. However, because the methodology is both time-consuming and costly, various ways that rely on certain soil's qualities that are easier to assess have been employed to quantify the K-factor, (Zhang *et al.*, 2019). Under some conditions, such methodologies have been used to give an estimate the K factor, (Zhang *et al.*, 2019).

K-factor values can also be obtained using erodibility and the soil nomograph, according to Wischmeier and Smith (1978). As a result, K-factors for specific sites can be found in a variety of sources, (Jain *et al.*, 2001; Agarwal *et al.*, 2016). However, if several researchers reported various K values for the same type of soil, the average values should be calculated, (Uddin *et al.*, 2018). Hurni (1985) used the color of the soil to determine K factor values. Kaltenrieder (2007), on the

other hand, claimed that this criterion was inaccurate because soils of the same color had various K values. Several studies have developed K factor algorithms based on pedological data (table 2.5).

Table 2.5: K-factor algorithms

Equation	Reference	Serial Number
$K = 27.66m^{1.14} * 10^{-8} * (12 - a) + 0.0043(b - 2) + 0.0033(c - 3)$ <p>Where, K = Soil erodibility factor (ton·hr⁻¹·ha⁻¹·MJ·mm), m = (Silt % + Sand %) × (100 – clay %), a = percent organic matter, b = soil structure code: 1) very structured or particulate, 2) fairly structured, 3) slightly structured, and 4) solid, c = soil profile permeability code: 1) rapid, 2) moderate to rapid, 3) moderate, 4) moderate to slow, 5) slow, 6) very slow</p> <p>Soil organic matter is derived by the following equation: SOM = 1.72 * OC Where, SOM = soil organic matter OC = soil percentage organic carbon content</p>	<p>Wischmeier & Smith (1978)</p> <p>Abraham, (2013)</p>	2.13
$K = 311.63 - 4.48 * (SG\% + S\%) + 613.4 + 6.45 * EC$ <p>Where, SG = coarse sand content (%) S = sand content (%)</p>	Merzoul (1985)	2.14

EC = electrical conductivity		
<p> $K = \left(0.2 + 0.3e^{-0.0256SAN \left(1 - \frac{SIL}{100} \right)} \right) *$ $\left(\frac{SIL}{CLA+SIL} \right)^{0.3} * \left[1 - \frac{0.25C}{C+e^{(3.72-2.95C)}} * \right]$ $\left[1 - \frac{0.7SN_1}{SN_1+e^{(22.9SN_1-5.51)}} \right]$ </p> <p>Where,</p> <p>SAN = sand content (%) SIL = silt content (%) CLAY = clay content (%) C = soil organic content (%) SN₁ = (1 – SAN/100)</p>	<p>Sharply and William (1990)</p>	<p>2.15</p>
<p> $K = 7.594 \left\{ 0.0034 + 0.0405 \exp \left[-\frac{1}{2} \left(\frac{\log D_g + 1.659}{0.7101} \right)^2 \right] \right\}$ </p> <p>Where,</p> <p>K is in terms of t ha h MJ⁻¹ ha⁻¹ mm⁻¹</p> <p>D_g = geometric mean particle diameter of soil texture</p>	<p>Romkens <i>et al.</i> (1986)</p>	<p>2.16</p>
<p> $K = 0.0034 + 0.0387 \exp \left[-\frac{1}{2} \frac{(\log_{10}(D_g) + 1.533)^2}{0.7671} \right]$ $D_g = \exp(0.1 * \sum_{i=1}^n f_i \ln m_i)$ </p> <p>Where,</p> <p>D_g = geometric mean diameter of the soil particles (mm) f_i = weight percentage of the particle size fraction (%), m_i = arithmetic mean of the particle size limits (mm) n = number of particle size fractions.</p>	<p>Romkens <i>et al.</i> (1997)</p>	<p>2.17</p>

<p> $K = 0.0293(0.65 - D_g + 0.24D_g^2)\exp[-0.0021\frac{OM}{Cl} - 0.00037(\frac{OM}{Cl})^2 - 4.02Cl^2 + 1.72Cl^2]$ $D_g = \sum_i f_i \ln(\sqrt{d_i d_{i-1}})$ </p> <p>Where,</p> <p> D_g = Napierian logarithm of the geometric mean of the particle size distribution OM = organic matter content (%) Cl = clay fraction (%) f_i = mass fraction in the corresponding particle size class (%) n = number of particle size fractions d_i = maximum diameter of the i^{th} class (mm) d_{i-1} = minimum diameter (mm) </p>	<p>Torri <i>et al.</i> (1997)</p>	<p>2.18</p>
<p> $K = (2.71 * 10^{-4}) * (12 - a) * M^{1.14} + 4.20 * (b - 2) + 3.23 * (c - 3)/100$ </p> <p>Where,</p> <p> M = (% silt + % fine sand) * (100 - % clay) a = organic matter content b = representative code of the soil structure type (dimensionless) c = code of soil profile permeability (dimensionless) </p>	<p>Renard <i>et al.</i> (1997)</p>	<p>2.19</p>

2.8.2.3. Topographic (LS) Factor

The topography of a specific landscape is defined by the length of the slope, in addition to its steepness, which impacts the degree of soil erosion, (Fayas *et al.*, 2019). When modeling soil erosion (Ganasri & Ramesh, 2016), slope length and slope gradient are key characteristics to consider, especially when calculating the transport power associated with surface runoff, (Koirala *et al.*, 2019). As a result, the LS factor accounts for both length as well as steepness variables, which give

an account of a landscape's topographical influence on erosion, (Sujatha & Sridhar, 2018; Chuenchum *et al.*, 2020). The topographic factor accurately represents the impacts of terrain on soil erosion processes, indicating that soil erosion rises as the angle and hence the slope length increases, (Devatha *et al.*, 2015).

The slope length (L) factor depicts the effect of slope length in the soil erosion process, (Koirala *et al.*, 2019). The slope length is defined by Ganasri and Ramesh (2016) as the cumulative distance from a given point that marks the start of surface runoff to a point that marks the start of deposition or even where runoff volume accumulates to a properly defined channel, (Gelagay & Minale, 2016; Ramesh & Ganasri, 2016). Therefore, the amount of soil removed per unit of surface rose as the slope length increased, (Ganasri & Ramesh, 2016; Koirala *et al.*, 2019).

The slope gradient, on the other hand, expresses the erosion effect of slope steepness, (Ganasri & Ramesh, 2016; Koirala *et al.*, 2019). Slope gradient parameters have a greater impact on soil erosion than slope length, (Ganasri & Ramesh, 2016; Koirala *et al.*, 2019). As a result, soil loss is much noticeable on steeper slopes, (Ganasri & Ramesh, 2016; Amah *et al.*, 2020). The most severe erosion occurs on slopes of ten to twenty-five percent, (Ganasri & Ramesh, 2016). However, the link between soil loss and slope steepness is determined by both plant cover and the distribution of particle size of the soil, (Koirala *et al.*, 2019).

The LS factor increased as the length of the slope and its steepness increased, according to Koirala *et al.* (2019).

To determine the two topographic sub-factors, digital elevation models (DEM) can be employed, (Ayalew & Selassie, 2015; Koirala *et al.*, 2019). Panagos *et al.* (2015) used both GIS and RS approaches to produce digital elevation models in order to obtain the LS factor for use in the RUSLE equation. Grid resolution, according to Wang *et al.* (2012), is critical when predicting soil erosion across a vast area. Changes in the cell size affect the steepness values either directly or indirectly, according to Chuenchum *et al.* (2020). The L sub-factor has been discovered to be dependent on the grid size and steepness, but the S sub-factor has just an effect on the steepness, (Chuenchum *et al.*, 2020). According to Liu *et al.* (2009), high-resolution DEM data may effectively be used to calculate the topographic factor accurately within the RUSLE model.

A topographic grid is produced using a filled DEM as the required input, according to Koirala *et al.* (2019). The procedure of filling a DEM entails identifying respective drains or even cells whose elevation value is lower than that of nearby cells, and then assigning greater elevation values to them. Following the filling of the sinks, each region is assigned a mean value based on the values of surrounding cells, (Shiekh *et al.*, 2011). Wischmeier and Smith (1978) established an equation (2.20) for computing and mapping slope length using a raster calculator in ArcGIS, where flow accumulation is multiplied with slope maps.

Several scholars have extensively employed equations (2.20–2.22) to estimate the topographic factor in various places, (Simms *et al.*, 2003; Panagos *et al.*, 2015; Gelagay, 2016; Gelagay & Minale 2016; Karamage *et al.*, 2016; Njiru *et al.*, 2018; Kidane *et al.*, 2019; Kogo *et al.*, 2020; Kolli *et al.*, 2021).

Table 2.6: LS-factor algorithms

Equation	Reference	Equation Number
$LS = \left(\frac{Q_a M}{22.13} \right)^y \times (0.065 + 0.045 \times S_g + 0.0065 \times S_g^2)$ <p>Where,</p> <p>LS = topographical factor; Q_a = flow accumulation grid S_g = grid slope in percentage M = grid size (vertical length x horizontal length) y = a constant which depends on the slope gradient 0.5 for slopes greater than 4.5 %, 0.4 for slopes between of 3% to 4.5% 0.3 for slopes between 1% to 3% 0.2 for slopes less than 1%.</p>	Wischmeier and Smith (1978)	2.20
$LS = \left(\frac{\text{Flow Accumulation} * \text{cell size}}{22.31} \right)^{0.4} * \left(\frac{\text{Sin (slope)}}{0.0896} \right)^{1.3}$ <p>Where, LS = topographic factor Cell size =</p>	Moore and Burch (1986)	2.21
$LS = L_{\text{factor}} * S_{\text{factor}}$ $S_{\text{factor}} = 10.8 \sin \theta + 0.03; \text{ slope gradients } < 9 \%$ $S_{\text{factor}} = 16.8 \sin \theta + 0.50; \text{ slope gradients } \geq 9 \%$	Panagos <i>et al.</i> (2015)	2.22

$L_{\text{factor}} = \left(\frac{\lambda}{22.12} \right) * \left[\frac{\frac{\left(\frac{\sin \theta}{0.0896} \right)}{\left(3 \sin \theta * 0.8 + 0.56 \right)}}{1 + \frac{\left(\frac{\sin \theta}{0.0896} \right)}{\left(3 \sin \theta * 0.8 + 0.56 \right)}} \right]$ <p>Where, λ = length of the slope L_{factor} = slope length factor S_{factor} = slope steepness factor.</p>		
---	--	--

2.8.2.4. Cover Management (C) Factor

The C-factor is a measure of how plants cover, as well as other land management methods, influences soil erosion rates, (Renard *et al.*, 1997; Ban *et al.*, 2016; Rhouma *et al.*, 2018; Koirala *et al.*, 2019). There is a substantial link between vegetation cover and C-factor, (Rhouma *et al.*, 2018). Rainfall is intercepted, infiltration is improved, and rainfall energy is absorbed by the vegetation cover, (Koirala *et al.*, 2019; Chuenchum *et al.*, 2020). As a result, the C-factor is considerably more typically linked to the percentage of vegetation cover over a specific land area, which is why Koirala *et al.* (2019) rated vegetation cover second after topography in terms of reducing erosion risks.

However, due to the impacts of rainfall, agricultural activity, and crop type, among other factors, C-factor values change from season to season, (Ganasri & Ramesh, 2016). Furthermore, historical land use activities, soil moisture content, surface roughness, canopy and surface cover all influence the factor, (Renard *et al.*, 1997; Gitas, 2009). Therefore, the C-factor denotes the ratio of soil lost from specific cropped fields to the equal quantity of soil lost from bare tilled plains, (Wischmeier & Smith, 1978; Beyene, 2019). In this case, values of 1 and less than

1 may be used for bare and covered soils, respectively. The C-factor can be described as the link between erosion effect on bare soil and erosion effect on land with a certain sort of cover and density, on this premise, (Ganasri & Ramesh, 2016; Rhouma *et al.*, 2018). As a result, the C-factor's contribution to soil loss decreases, particularly in forested areas and plantations, (Ganasri & Ramesh, 2016).

The C-factor maps were created by many researchers using both land use and land cover maps for various study locations, (Ganasri & Ramesh, 2016; Salunkhe *et al.*, 2018; Koirala *et al.*, 2019). C-factors are typically awarded by merely examining vegetation cover rather than closely analyzing cropping patterns in agriculture, according to Koirala *et al.* (2019). According to Uddin *et al.* (2018), C-factor values are assigned based on the type of vegetation cover as well as its density. According to Uddin *et al.* (2018), this method may translate land cover into unique weighted data. On the basis of percent canopy cover, ground cover, and fall height, Obiora-Okeke (2019) assigned C-factors to different types of land use.

Several approaches (table 2.7) for estimating the C-factor on the basis of the Normalized Difference Vegetation Index (NDVI) have been devised. Correlating NDVI measurements with appropriate C-factor values yielded the regression equations. De Jong (1994), for example, constructed a link between calibrated C-factors from the field and the NDVI, and then produced a continuous C-factor

showing the surface. Maps obtained by Landsat images for land use activities, in addition to land cover, can be used to determine data on vegetation cover and management, (Devatha *et al.*, 2015; Njiru *et al.*, 2018).

Table 2.7: C-factor Algorithms

Parameter	Equation	Reference	Serial Number
NDVI	$\text{NDVI} = \frac{\text{Band 5} - \text{Band 4}}{\text{Band 5} + \text{Band 4}}$ Where, Band 4 = red band Band 5 = infra-red band	Durigon <i>et al.</i> (2014)	2.23
Land cover factor	$C = 0.1 \left(\frac{-\text{NDVI} + 1}{2} \right)$ Where, C = land cover factor	Durigon <i>et al.</i> (2014)	2.24
	$C = 0.431 - 0.805 \times \text{NDVI}$	De Jong, (1994)	2.25
	$C = \exp \left[-\alpha \frac{\text{NDVI}}{(\beta - \text{NDVI})} \right]$	Van der Knijff <i>et al.</i> (1999).	2.26

2.8.2.5. Practice (P) Factor

Land use and even land cover contributions to soil erosion is expressed by support practice factors, (Chuenchum *et al.*, 2020). This factor gives a comparison between the quantity of soil lost from land surfaces that have specific management initiatives to a similar quantity lost from a landscape with an up and down slope style of tillage, (Devatha *et al.*, 2015; Rellini *et al.*, 2019). It represents the rate at which soil is lost from diverse cultivated regions, (Renard *et al.*, 1997). The P-factors, according to Ganasri and Ramesh (2016), account for the positive consequences of conservation support strategies. P-factors have been defined as the effects of practices that contribute in reducing soil erosion by

controlling the rate of runoff water, (Devatha *et al.*, 2015; López-García *et al.*, 2020).

The P-factor, according to Obiora–Okeke (2019), quantifies the efficiency of some land management strategies aimed at limiting soil loss from a certain catchment. Tillage practices along contours, strip cropping, and terracing are examples of such methods, (May & Place, 2005). P-factor values typically range from 0 to 1, where a value of zero (0) is indicative of excellent soil erosion management and a value of one (1) indicates inadequate or unavailable conservation technique, (Ganasri & Ramesh, 2016; Njiru *et al.*, 2018; Alewell *et al.*, 2019; Obiora-Okeke, 2019; Rellini *et al.*, 2019; Chuenchum *et al.*, 2020). Wischmeier and Smith (1978) recognized land slope as a primary element that influences the P-factor, (table 2.8).

Table 2.8: Conservation Practice Factors (Source: Wischmeier & Smith, 1978)

Land use	Percentage slope	P-factor
Cultivated land	0 to 5	0.10
	5 to 10	0.12
	10 to 20	0.14
	20 to 30	0.19
	30 to 50	0.25
	50 to 100	0.33
Other lands	All	1.00

2.9. Data Simulation and Validation of Sediment Yield

Sediment yield studies aim to measure the amount of sediment that moves out of a given location over time, (Boakye *et al.*, 2020). There are three parts to these studies: erosion mechanisms, sediment deposition, and delivery, (Ijam &

Tarawneh, 2012). For estimating sediment yield, a number of deterministic models have been made accessible. However, because they require large datasets, such as hydrological information and physiographic characteristics, and several field measurements to gather essential parameters for the suggested equations, most of them can only be used in small areas, (Sadeghi *et al.*, 2007).

Sediment yield is measured at the basin scale by conducting sedimentation surveys in reservoirs or monitoring erosive processes (figure 2.6), (Msadala & Basson, 2017; Millares & Moïno, 2018; Aga *et al.*, 2020). Various formulae for estimating sediment output have been developed around the world, particularly in upland watersheds, (Aga *et al.*, 2020). According to Swarnkar *et al.* (2018), sediment production is often determined using stream flow analysis, which includes sediment sampling or reservoir sedimentation surveys.

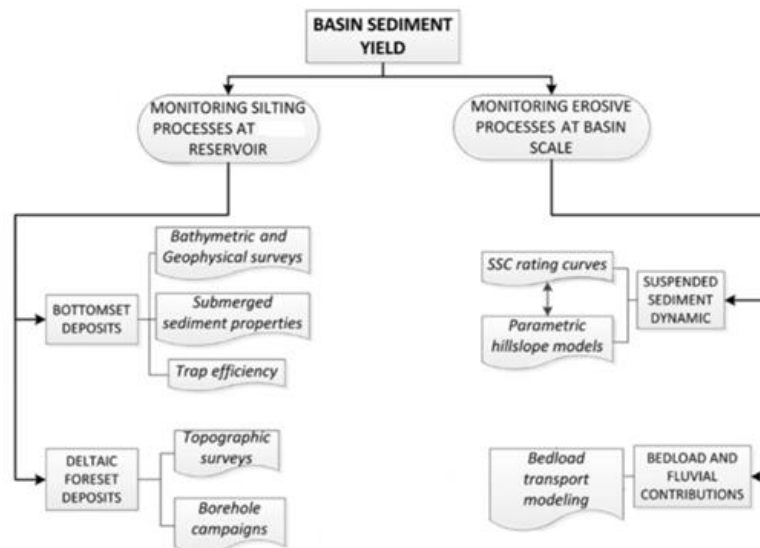


Figure 2.6: Methods for assessing siltation and sedimentation processes within reservoirs and the upstream erosion dynamics (source: Millares & Moïno, 2018).

2.9.1. Suspended Sediment Dynamics

2.9.1.1. Stream Sediment Sampling

Sediment yield, by definition, includes both bed and suspended loads, (Swarnkar *et al.*, 2018). Sediment sampling in streams, on the other hand, is mainly limited to suspended sediment loads, (Swarnkar *et al.*, 2018). Therefore, determining the amount of suspended sediment in watercourses and the fluxes associated with it is a critical stage in the development and management of water resources, (Sadeghi & Mizuyama, 2007; Tswafa & Wang, 2016; Boakye *et al.*, 2018). Suspended sediment load data is commonly utilized to assess the influence of a variety of naturalistic and anthropogenic variables on the intensity of soil erosion processes, (Dedkov, 2004).

Field measurements (direct methods) and modeling approaches (especially physical and empirical models) are commonly used to calculate sediment loads in streams and rivers, (Wu *et al.*, 2012; Boakye *et al.*, 2018). Direct sampling techniques and sediment transport equations are the most common methods for evaluating sediment loads and transport phenomena, (Tswafa & Wang, 2016). Although direct approaches are the most popular and extensively used, they are problematic during high rainstorm events due to safety considerations, making the task challenging, (Gilja *et al.*, 2009). Furthermore, these sediment monitoring programs are highly costly, (Tswafa & Wang, 2016). Rather, sediment monitoring projects are performed on a limited number of streams based on their significance, (Tswafa & Wang, 2016).

Sediment yield estimations for direct (field) measurements are based on the interconnection between the amount of suspended sediments and stream discharge (rating curve) developed at gauging stations, (Akrasi, 2005). Furthermore, direct observations include total eroded sediments, sediment deposits in local watersheds, and sediment deposition in reservoirs, (Millares & Moino, 2018). Sampling procedures and laboratory analysis are used to determine the concentration of suspended sediment, (Gilja *et al.*, 2009; Boakye *et al.*, 2018). For suspended sediment, Boakye *et al.* (2018) recognized four types of samplers: integrated, immediate, and sedimentation traps. The most popular samplers are those that integrate, (Lee *et al.*, 2014). In the unlikely event that integrating samplers are not available, the dipping approach with the Rooseboom and Annandale (1981) correction procedure may be employed, (Boakye *et al.*, 2018). The concentration of suspended sediments in the measured water is determined in a laboratory using evaporation or filtering procedures, (Boakye *et al.*, 2018). The obtained concentration of suspended sediments can be used to calculate sediment load and specific sediment yield.

2.9.1.2. Sediment Yield Modelling

Because of the economic implications, the remoteness of the site, the number of samples, and technological limitations, direct approaches do not provide continuous trends in concentration, (Edwards & Glyssen, 1999). As a result, researchers have come up with the idea of using empirical models to estimate suspended sediment load in rivers where direct observations are not possible,

(Akraasi, 2011; Kusimi *et al.*, 2015). The rating curve, erosion rate, catchment-based, and regression approaches are among these models, (Boakye *et al.*, 2018).

Sediment yield models, according to Akraasi (2011), would be a better way to assess the contribution of drainage basins to river sedimentation. These models are thought to have the capacity to forecast the impacts associated with land use and some cultural activities on both soil erosion and sediment yield in relation to catchment areas, (Akraasi, 2011). Simple climatological parameters, such as rainfall and runoff, are used in these models to link sediment yield to the catchment region, (Boakye *et al.*, 2018). These models have been developed for application in site-specific areas, by taking into account the statistical findings that result from certain field parameters, (Hajigholizadeh *et al.*, 2018). Therefore, if such models were to be implemented in certain locations that have similar conditions as to those used at the time of the model's development, then accurate results would probably be produced, (De Vente *et al.*, 2011; Aga *et al.*, 2020). However, detailed observable sediment information is required for the simulation and validation of predicted sediment yield from a catchment level, (Aga *et al.*, 2020). However, in underdeveloped nations, the use of models is hindered by a paucity of measured sediment data, (Aga *et al.*, 2020).

For example, the RUSLE model cannot be used to predict soil loss or even sediment yield on the basis of individual storm events because the R factor has been averaged during corresponding storm events for a period of not less than 22

years, (Wischmeier & Smith, 1978; Renard *et al.*, 1997). As a result, the RUSLE model cannot be used to predict both soil loss and sediment yield based on a storm event, (Lim *et al.*, 2005). The MUSLE is a frequently used model in the calculation of sediment yield on a single storm event basis, according to Williams & Berndt (1977). When it comes to estimating sediment yield, the MUSLE model methodology optimizes hydrological parameters, (Sadeghi & Mizuyama, 2007). Williams and Berndt (1977) investigated 778 single storm events from 18 catchments whose areas ranged from 15 to 1500 ha in order to construct a hydrological mechanism for estimating sediment yield. With a 92 % coefficient of variance in sediment yield estimation for single storm events, MUSLE's development was a success on this premise, (Sadeghi & Mizuyama, 2007). The following equation represents the MUSLE:

$$Y = 11.8 (Q * q_p)^{0.56} * K * C * P * LS \quad [2.27]$$

Where,

Y = Single storm event sediment yield (t)

Q = Runoff volume of the storm (m³)

q_p = Peak runoff rate (m³/s)

K = Soil erodibility factor

LS = slope length and steepness factor

C = Cover management factor

P = Support practice factor

As field scale models, USLE and RUSLE are unable to provide direct estimates of sediment yield, (Boakye *et al.*, 2018). To address this issue, the sediment delivery

ratio (SDR) for a given catchment area should be considered to calculate the total amount of sediment material transferred to the catchment's outlet, (Lim *et al.*, 2005; Pelletier, 2012; Lee & Kang, 2013; Swarnkar *et al.*, 2018). Because of their simplicity and efficiency, the RUSLE and SDR models have been extensively used to predict soil erosion as well as sediment yield in various areas, (Gelagay, 2016; Yan *et al.*, 2018).

2.9.1.3. Sediment Delivery Ratio (SDR)

Transport of sediments to river channels within basins is important for a variety of reasons, including soil conservation and reservoir siltation avoidance, (Chen & Thomas, 2020). Overland flow brings degraded soil materials into streams, affecting their functionality greatly, (Ouyang *et al.*, 2005; Chen & Thomas, 2020). The situation deteriorates, particularly in streams leading to reservoirs, (Chen & Thomas, 2020). Sediment buildup can be considered a non-point pollution source that has an impact on both the supply and demand for water in a given area. As a result, examining the manner in which sediments are carried at the catchment scale is an important component.

The SDR for a particular catchment area is a function of the time scale used to determine erosion rates and even sediment yields, (Lu *et al.*, 2005). It is therefore the proportion of total amount of soil that is moved from a specific catchment over a given length of time, (Gelagay, 2016; Panditharathne *et al.*, 2019).

Equation (2.28) represents the SDR mathematically, (Lim *et al.*, 2005; Lu *et al.*, 2005; Nyssen *et al.*, 2009; Lee & Kang, 2014; Gelagay, 2016):

$$\text{SDR} = \frac{\text{SY}}{\text{E}} \quad [2.28]$$

Where

SDR = Sediment Delivery Ratio (dimensionless)

SY = Sediment Yield ($\text{t ha}^{-1} \text{ yr}^{-1}$)

E = Watershed gross erosion ($\text{t ha}^{-1} \text{ yr}^{-1}$)

The SDR calculates the transport efficiency of sediments, which compares the quantity of sediment moved out from various eroding locations to the catchment outlet to the gross quantity of detached soil from the same area but above the outlet, (Mutua *et al.*, 2006; Gelagay, 2016; Wu *et al.*, 2018; Kidane *et al.*, 2019). SDR values, in simple terms, are a criterion for determining the quantity of sediment material stored in valleys within a catchment area, (Pelletier, 2012). SDR is a measure of a catchment's integrated ability to store and move eroded soil for a specific watershed, (Gelagay, 2016). Hence, SDR is critical in developing a thorough understanding of the phenomenon of soil loss as well as assessing the benefits of soil and water management methods, (Wu *et al.*, 2018).

Despite the usage of the inverse power law, the area of the catchment is not the only element that determines the SDR, (Pelletier, 2012). Because highly sloping catchments affect sediment storage more than less sloping catchments within the same region, the relief of the basin has an impact on SDR, (Pelletier, 2012).

Slope, sediment size, land use, vegetation cover, and runoff-rainfall characteristics are among the other influences, (Mutua *et al.*, 2006; Tamene *et al.*, 2006; Gelagay, 2016; Nguyen & Chen, 2018). SDR values for catchments have been calculated using these criteria as a starting point, (Kidane *et al.*, 2019).

A variety of SDR correlations have been developed using the combinations of different changeable physical properties of a catchment, (Ouyang & Bartholic, 1997). SDR relations for catchments have been developed in this regard, taking into account topography effects, climatic, biological, and hydrological factors, (Kidane *et al.*, 2019). Most SDR interactions, on the other hand, are limited to smaller catchment areas where data is available, (Mutua *et al.*, 2006). The determination of SDR values in Ethiopia was based on the forms of land use in the presence or absence of conservation methods, according to Nyssen *et al.* (2009). This type of estimation assumed that the major determinants were the stream's slope and hydrology, (Kidane *et al.*, 2019).

Williams and Berndt (1972) discovered that the mean gradient of a stream channel was more important in estimating SDR than the other parameters, leading to the development of equation (2.29). In different river basins, different authors have utilized equation (2.29) to estimate SDR, (Gelagay, 2016; Kidane *et al.*, 2019; Panditharathne *et al.*, 2019). In the event that data is insufficient, Onyando *et al.* (2005) confirmed that equation (2.29) yields good estimations for SDR.

$$\text{SDR} = 0.627 * (\text{SCS})^{0.403} \quad [2.29]$$

Where

SDR = Sediment delivery ratio (dimensionless)

SCS = Main stream channel gradient (%)

Furthermore, extensive study has been conducted to estimate the sediment delivery ratio, with the majority of findings relating it to the size of the catchment, (Lim *et al.*, 2005). The SDR curve has been found as a key element in the relationship between SDR and catchment size, (USDA, 1975). The SDR curve has been widely utilized because of its simplicity, (Lim *et al.*, 2005). Vanoni (1975) used data from 300 watersheds to derive a power function, from which a general SDR curve was developed (equation 2.30). USDA (1975), Boyce (1975), and USSCS (1971) table 2.19 produced more SDR curves, which are represented by equations (2.31–2.33).

$$\text{SDR} = 0.4724A^{-0.125} \quad [2.30]$$

$$\text{SDR} = 0.3750A^{-0.2382} \quad [2.31]$$

$$\text{SDR} = 0.5656A^{-0.11} \quad [2.32]$$

$$\text{SDR} = A^{-0.2} \quad [2.33]$$

Where

A = Area of the catchment (km²)

Table 2.9: Generalized sediment delivery ratios by USSCS (1971)

Catchment area (km ²)	Sediment Delivery Ratio (SDR) (dimensionless)
0.05	0.58
0.10	0.52
0.50	0.39
1	0.35
5	0.25
10	0.22
50	0.15
100	0.13
500	0.08
1000	0.06

SDR curves for a single catchment are necessary if an accurate estimate of sediment yield is to be obtained, according to Lim *et al.* (2005), yet SDR values for specific catchments are nearly difficult to get.

2.9.2. Bathymetric Survey

Suspended sediments and transported materials become trapped in reservoirs and settle, (Odhiambo & Boss, 2004). The quality and quantity of sediments, as well as the quality of water, have direct effects on reservoir management, (Hilgert *et al.*, 2016). Characterization and control of accumulated sediment quantities are critical in this regard, (Hilgert *et al.*, 2016). Therefore, the accumulation of sediments in water bodies requires periodic monitoring using appropriate techniques, (Ilci *et al.*, 2017).

Reservoir surveys are useful for determining sedimentation rates as well as determining reservoir capacity, (Elçi *et al.*, 2009). If the current bathymetric

properties and fluctuations in storage capacity were fully understood, water resources in reservoirs and lakes might be efficiently managed, (Dunbar *et al.*, 1999). Bathymetric surveys are vital when detailed information for reservoirs, lakes, and other bodies of water is required, according to Odhiambo and Boss (2004).

Bathymetric surveys offer precise information on the reservoir's depth of water, surface area, and volume connections, (Maina *et al.*, 2018; Moges *et al.*, 2018; Yan *et al.*, 2018; Maina *et al.*, 2019). Environmental changes such as reservoir sedimentation, as well as anthropogenic and biological activities, can all be evaluated, (Cross & Moore, 2014; Hassan *et al.*, 2017; Ilici *et al.*, 2017; Maina *et al.*, 2018). Multiple surveys for the same reservoir may yield valid estimates of reservoir capacity loss over time owing to sedimentation, based on variations in surface area and volume, (Rakhmatullaev *et al.*, 2011). Bathymetric studies conducted on a regular basis over a period of years can provide valuable information, notably on the overall distribution and thickness of sediment within the reservoir, allowing for a better understanding of reservoir sedimentation, (Maina *et al.*, 2019).

Pre-dam topography is compared to geophysical imaging (sonar, laser scanning, ground-penetrating radar), which gives the real topography of the bottom end, in order to analyze deposition in reservoirs, (Schleiss *et al.*, 2016). Although echosounding techniques have led to remarkable data gains in terms of quality as well

as quantity, the state of the art in surveying has not altered, (Elçi *et al.*, 2009). Surveying transects have become much faster and more accurate because of recent advances in multi-beam technology and satellite navigation employing global positioning systems, (Pratson *et al.*, 2008). As a result of the combination of GIS and geophysical imaging, reservoir monitoring has improved on a spatiotemporal scale, (Pacina *et al.*, 2020). A digital elevation model (DEM) is a crucial tool for pre-dam topography, especially when using GIS techniques to analyze sedimentary processes within reservoirs, (James *et al.*, 2012; Ibrahim *et al.*, 2022).

A variety of data gathering approaches can be used to investigate the reservoir's bottom surface, (Pacina *et al.*, 2020). The most frequent type of sonar sensor is one that is mounted on a ship, (Iradukunda & Bwambale, 2021). The survey's size is determined by the survey's established plan and, more crucially, the type of sensor utilized (single-beam, multi-beam, or side-scan), (Yan *et al.*, 2018; Pacina *et al.*, 2020). Under certain situations, remote sensing techniques including as satellite photography, airborne light detection and ranging (LiDAR), and photogrammetry can be used to map reservoir topography, (Yan *et al.*, 2018). Hence, geophysical surveying is another method of seeing the subsurface topography, (Rakhmatullaev *et al.*, 2011; Pacina *et al.*, 2020).

The thickness of sediments and the depth of water can both be estimated using detailed and reliable bathymetric data obtained using multi-frequency echo

sounders, (Dunbar *et al.*, 1999; Odhiambo & Boss, 2004; Moges *et al.*, 2018; Yan *et al.*, 2018; Maina *et al.*, 2019). Acoustic measurement techniques have been used to map underwater topography and monitor siltation in reservoirs in this regard, (Odhiambo & Boss, 2004; Elci *et al.*, 2009; Gopinath, 2010; Cross & Moore, 2014; Hassan *et al.*, 2017; Maina *et al.*, 2018; Yan *et al.*, 2018; Maina *et al.*, 2019; Iradukunda *et al.*, 2020; Iradukunda & Bwambale, 2021).

The multi-frequency acoustic profiling system (APS) works on the basis of two important frequencies: the higher one, which defines water depth, and the lower one, which has a considerably larger energy and may penetrate recently formed sediments, (Maina *et al.*, 2019). Because it does not rely on past surveys to predict loss of storage capacity or even sediment thickness, the APS technique is considerably superior to standard bathymetry techniques, (Dunbar *et al.*, 1999).

Collection of sediment cores with the help of the vibe-coring method or spud bar techniques is used to validate this procedure, (Odhiambo & Boss, 2004). Long-term rates of sedimentation and reservoir capacity loss can thus be determined with only one survey event, despite the fact that shallow locations with depths equal to or less than 50 cm are difficult to survey using acoustic techniques, (Dunbar *et al.*, 2002). The use of acoustics to examine the distribution of sediments and their thickness in a reservoir, according to Jakubauskas and de Noyelles (2008), should be double-checked using other techniques, notably sediment coring. Bathymetric approaches for determining sediment yield within a

reservoir entail subtracting pre-topographic heights from contemporary ones, (Oğuz *et al.*, 2019). This technique allows for a comparison of simulated sediment estimations to actual sediments in the reservoir, (Moges *et al.*, 2018; Oğuz *et al.*, 2019).

2.10. Conclusion of Literature Review

- 1) Soil erosion is a sluggish process whose effects can go unnoticed or be severe at times, resulting in a significant loss of top soil at a faster rate. Mathematical formulations are required to characterize the relationships between the many processes involved in the detachment, transport, and deposition of soil particles elsewhere within a catchment.
- 2) Soil erosion dynamics are influenced by spatial heterogeneity elements such as elevation, soil characteristics, vegetation cover, land use, and above all, land cover. Modeling of soil erosion in catchments is thus a vital technique for anticipating unrestricted soil loss and deposition in this regard. It also aids in the development and even in implementation of soil erosion management plans. Even in ungauged catchments, the RUSLE model is an excellent mathematical model that takes an empirical method and has been extensively refined for calculation of average annual soil loss. The model does not require a lot of data because it may employ satellite imagery with a low to medium spatial resolution, as well as rainfall data, which is limited.

- 3) Geographic information systems (GIS) are becoming more significant in soil erosion models because they allow for quick data pretreatment, data entry, analysis, and display of results. Because it can characterize the morphology of the catchment using DEM, GIS makes soil erosion modeling successful. Most notably, it allows for more accurate and cost-effective estimation of soil erosion from huge catchments.
- 4) River basins transport water, heat, sediments, chemicals, and biological species from upstream to downstream water bodies. Any construction built to impound water disrupts the above-mentioned fluxes and creates sedimentation, reducing the reservoir's capacity to store water. Dam construction, for example, generates an effective sediment sink within a valley. As a result of their ability to store and control water supply, reservoirs are key hydraulic structures that help to alleviate climate change-related difficulties. In this regard, new reservoirs must be built, while current ones must be managed well to avoid potential storage losses.
- 5) There are two basic approaches to determining sediment yield within a catchment: estimating sediment yield within the upland parts of the catchment and predicting sediment inside the stream channel. However, the lack of gauging stations makes it difficult to anticipate sediment yield in small catchments. In this regard, periodic estimations of sedimentation rates would be necessary for the management of reservoirs in such

catchments. Such information would enable comparisons with predictions from soil erosion models.

CHAPTER THREE: METHODOLOGY

3.1. Description of the Research Area

The research was conducted in Kenya's Machakos County, within the Maruba dam catchment (figure 3.1). The dam reservoir, which is built across the Maruba stream, is managed by the Machakos Water Supply and Sewerage Company Limited. The reservoir serves practically the entire town of Machakos, as well as its own neighborhood, with water, (Ngari *et al.*, 2020). The Machakos town's total population is estimated at 210,000 people, with an estimated daily water demand of about 8000 m³/day, (<https://waterauthority.go.ke>). The dam, which has a structural height of roughly 17 meters and a design yield of 4000 m³/day, was built in the 1950s, (<https://waterauthority.go.ke>). The dam reservoir's storage capacity has been lowered to almost 2000 m³/day due to the amount of silt deposited in it, (<https://waterauthority.go.ke>).

The Maruba dam reservoir catchment area is 49 km² and is located at 37 °12' 0" and 37 °20' 0" E and 1 °24' 0" to 1 °34' 0" S in Machakos County (figure 3.1). The Maruba stream flows into the Maruba dam reservoir from the Iveti hills, whose elevation is 2119 meters above the sea level. The elevation of the catchment area fluctuates between 2119 and 1576 meters above sea level (figure 3.1). The upper part of the catchment, which has rugged topography, is defined by valleys, vegetation, and human settlement, (Ngari *et al.*, 2020). The catchment area experiences a tropical type of climate with a bimodal rainfall, with short rains occurring between the months of October, November and December and longer

rains from March, April and May, (Kwena *et al.*, 2020). The annual rainfall in Machakos town is around 700 mm, and it is mostly ill distributed and, most importantly, very unreliable, according to Kwena *et al.* (2020). On average the annual temperature of the research area ranges from 17 to about 24 °C, with the hottest months being January and March, as well as August, September and October, (Agesa *et al.*, 2019). Chromic luvisols are the most common soils in the catchment area, and they are fundamentally low in fertility, resulting in low agricultural yield, (WRB, 2006). There are a variety of different land-use types that characterize the catchment area, including barren ground, villages, farming, and forest, (Ngari *et al.*, 2020). The bulk of the population in the catchment region engages in agricultural production as their primary source of income, (Agesa *et al.*, 2019). Although some areas have natural forests, the majority of the land has been and continues to be opened for agricultural activity and development, (Ngari *et al.*, 2020).

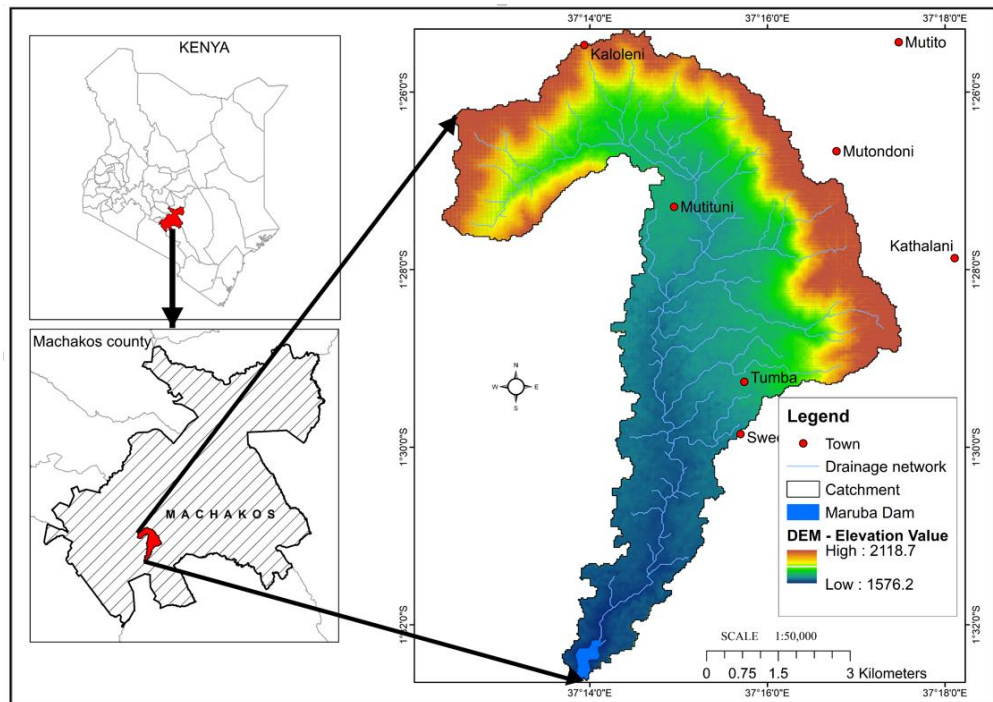


Figure 3.1: Research area map

3.2. Spatial Modelling of Soil Erosion

The RUSLE model and the spatial analytic environment of a geographic information system (GIS) were used to achieve this goal, (Beyene, 2019). The RUSLE model was selected and used for this objective because it involves land use/land cover maps generated using remotely sensed imagery, land management practices and types, and attributes, (Ganasri & Ramesh, 2015). Furthermore, the RUSLE model was chosen because of the ease with which the model's parameters integrate with GIS, allowing for improved analysis, (Kidane *et al.*, 2019; Bansekhria & Bouhata 2022; Patyal, 2022). The RUSLE model encompasses all of the major elements that cause erosion, (Rahaman *et al.*, 2015). As a result, the model's empirical principles were used to quantify the average annual loss of soil in the Maruba dam catchment, (Alewell *et al.*, 2019). The technique entailed

applying a raster-based spatial analysis to implement the empirical formula, (Beyene, 2019; Kidane *et al.*, 2019; Fenta *et al.*, 2020). Before running the RUSLE model within a GIS framework, rainfall, soil, slope, DEM, and land cover raster layers were produced, (Nouri *et al.*, 2018; Beyene, 2019).

3.2.1. Data Sources

The research was based on four separate geospatial data sets gathered from various sources, (Woldemariam *et al.*, 2018; Beyene, 2019; Woldemariam & Harka, 2020). These datasets were then converted to a raster format that was more compatible with the RUSLE model for estimating soil loss, (Amellah & Moribiti, 2021; Hateffard *et al.*, 2021). As listed below, they included soil data, meteorological data, remotely captured data, and digital elevation models:

1. Average annual rainfall data for the past 30 years (1990–2019) was provided by the Kenya Meteorological Department (KARLO Katumani, Machakos, and Jomo Kenyatta International Airport, JKIA stations) and a private station in Mua Hills.
2. A DEM with a 30 meter resolution for the research area was obtained from the Regional Centre for Mapping of Resources for Development (RCMRD), Nairobi.
3. The USGS Earth Explorer website (<https://earthexplorer.usgs.gov>) was used to retrieve Landsat 8 OLI/TIR satellite images with a resolution of 30 meters from November 2000, 2010, and 2020, respectively.

4. Soil data from the catchment area was collected during fieldwork and determined in a laboratory for critical soil parameters.

3.2.2. Methods

3.2.2.1. Digital Elevation Models (DEM) Acquisition and Processing

The DEMs were then masked in a GIS context before being registered and recalibrated to a resolution of about 30 m by 30 m. Finally, the DEMs that had been constructed were projected. The results were obtained after a maximum probability cluster was created. The freshly produced DEMs were checked for accuracy using Google Earth software. The DEMs were constructed in ArcGIS and overlaid with the Maruba dam catchment borders, after which they were truncated and the DEMs for the study were obtained. The DEMs were revised for any usage, and dummy nodes, loops, and even junctions were cleaned up across the catchment geometry.

3.2.2.2. Soil Sampling Process and Analysis

A number of reconnaissance inspections were done to find the best locations for carrying out soil sampling. The catchment area was subdivided into square grids, from which case fifteen (15) samples of topsoil were collected for laboratory investigation. Each sampling site's geographical coordinates were determined within the field using a Garmin Explorer GPS with a 3 m precision. According to equation (2.12), the parameter M denotes a soil particle variable that describes the top 15 cm of a given soil surface, therefore the study's soil samples were

collected from a depth that ranged between 0 and 15 cm, (Olaniya *et al.*, 2020). The specific sampling sites yielded both undisturbed as well as disturbed soil samples, (Oğuz *et al.*, 2019). Undisturbed samples were collected using core rings, while disturbed one were collected using the composite technique, (Oğuz *et al.*, 2019). Around 2 kg of topsoil were collected from each site using a soil auger. The samples were evaluated for organic carbon, soil texture, and permeability, using standard laboratory methods, while the structural class was determined in the field, (Didoné *et al.*, 2015; Girmay *et al.*, 2020). The soil's saturated hydraulic conductivity was assessed using the constant-head hydraulic approach, (Lin *et al.*, 2019), the grain size distribution using the hydrometer method (Gee *et al.*, 1986), and the organic carbon using the rapid wet oxidation methodology, (Walkley & Black, 1934); Nelson & Sommers (1996). The soil's organic matter content was quantified by multiplying organic carbon with a factor of 1.724, (Boyd, 1995; Abraham, 2013). The soil's structural code was 3, and this was reflection of granular state of the catchment's sandy soils.

3.2.2.3. Land Use and Land Cover Change Detection

In order to evaluate land use and land cover forms, two different types of data sets were used. The first was satellite image data for the month of November, which consisted of three-year multi-temporal Landsat satellite images (LANDSAT 8 OLI/TIR of 2000, 2010, and 2020). The second type of data was auxiliary data, which provided ground truth data for specific land use and cover classifications. Figure (3.2) depicts the detailed procedure, and the subsections that follow detail

the stages used in the methodology. The data was particularly important in image processing, picture classification, and assessment of the overall accuracy of classification results, therefore reference locations for ground truth information were mapped using a global positioning system, (Syombua, 2013; Cheruto *et al.*, 2016).

The assessment was based on the combination of ground truth data and satellite imagery, in line with the proposal by Chakraborty (2001). A GPS was used to record coordinates that represented different LULC types, including forest land, urban areas, water bodies, rainfed agricultural, and irrigated agriculture, (Syombua, 2013). Accurate detection of land use and land cover change requires at least two types of time-period data sets, (Jenson, 1986). In this study, Landsat images from the years 2000, 2010, and 2020 were used. As illustrated in figure 3.2 below, raw satellite images were subjected to preprocessing, augmentation, and classification processes, (Beyene, 2019).

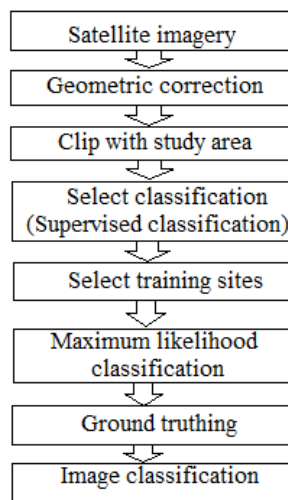


Figure 3.2: Methodology for land use and land cover change detection

Image Preprocessing

Image preprocessing is a crucial step before change detection because it creates a clear connection between biophysical elements on the land surface and recorded data, (Beyene, 2019). Due to spatial, spectral, and radiometric resolution restrictions, standard remote sensing devices are unable to adequately record the complex nature of the physical world. Therefore, any poor image attributes that emerged throughout the acquisition process should be removed, (Woldermariam *et al.*, 2018). In this regard, remotely sensed data must be preprocessed before being analyzed. Every raw Landsat imaging data point onboard the OLI and TIR sensors was preprocessed in this investigation. The Landsat images were geo-referenced, mosaicked, and sub-set based on the area of interest using the Idrisi Selva processing software, (Cheruto *et al.*, 2016; Woldermariam *et al.*, 2018).

Image Classification

Image categorization divides an image's pixels into various land use and land cover classes, from which thematic information is retrieved, (Boakye *et al.*, 2008; Boakye *et al.*, 2018; Beyene, 2019). A supervised classification technique was employed to provide different LULC classifications for the research region, (Kayet *et al.*, 2016). In this study, various spectral signatures from Landsat imagery were assigned to several types of LULC using image classification techniques, (Cheruto *et al.*, 2016). This was achieved using the reflectance characteristics of several LULC types, (Cheruto *et al.*, 2016). The visualization of image details is improved by the use of many color blends.

This form of classification made use of both local knowledge and actual geographical data, (Cheruto *et al.*, 2016; Keyet *et al.*, 2016; Woldemariam *et al.*, 2018). Preprocessed images were classified into maps of land use as well as land cover classes using a maximum likelihood classifier (MLC) technique, (Cheruto *et al.*, 2016; Sahana *et al.*, 2016; Woldemariam & Harka, 2020). The seven land use/land cover classifications were identified as being bare land, farmland, forestland, settlement, shrubland, and waterbody, (Anderson, 1976).

Accuracy Assessment

It is critical to subject image classification data to an accuracy assessment if it is to be used for identifying change, (Beyene, 2019). With the use of accuracy assessment, changes that describe diverse land uses and land cover are better understood and evaluated properly, (Cheruto *et al.*, 2016). As a result, accuracy evaluation involves a comparison of reference samples to classified images, (Cheruto *et al.*, 2016; Woldemariam & Harka, 2020). The accuracy of the Landsat 8 OLI/TIR of November 2020 was evaluated in this investigation, for which ground truth information is presumably equated. The overall accuracy was obtained as a ratio of the total number of correctly identified samples to the total number of sampled units, (Cheruto *et al.*, 2016).

3.2.2.4. Estimation of the RUSLE Model Parameters

The RUSLE model is a practical-based tool that can predict average annual soil loss over the long term, using raindrop impact and runoff as the primary causes, (Renard *et al.*, 1997). The five input parameters for the model are the following:

rainfall erosivity (R) factor, soil erodibility (K) factor, slope length and steepness (LS) factor, cover management (C) factor, and conservation practice (P) factor, (Fenta *et al.*, 2020). Each RUSLE parameter was estimated systematically using a grid-based approach, (Renard *et al.*, 1997). The parameters were estimated using precipitation data, soil data, digital elevation models, and most importantly, land cover, (Kidane *et al.*, 2019; Bekele & Gemi, 2020). Both primary as well as secondary data sources were used in this case.

Rainfall Erosivity (R) Factor

The R factor was estimated based mean annual precipitation data spanning the years 1990 to 2019. The rainfall factor was estimated in ArcGis 10.6 raster calculator using the regression equation (3.1) derived by Kassam *et al.* (1992) using annual rainfall data from 1990 to 2019. Using geostatistical interpolation techniques, long-term annual rainfall data was turned into continuous raster grids, (Kidane *et al.*, 2019; Hategekimana *et al.*, 2020). The interpolation approach used rainfall data from three rain gauge sites in the research area over a 30-year period.

$$R = 117.6 (1.00105^{\text{MAR}}) \text{ for MAR} < 2000 \text{ mm} \quad [3.1]$$

Where,

MAR = mean annual rainfall in mm

Soil Erodibility (K) Factor

The soil erodibility (K) factor was estimated in this investigation with the help of equation (3.2) devised by Wischmeier and Smith (1978). The K factor value is

calculated using the equation as a total contribution of the soil's textural class, percentage of the soil's organic material, permeability, and above all, the soil structural code, (Kidane *et al.*, 2019). As a result, soil erodibility was determined by measuring both physical as well as the chemical parameters for the various soil types found within the catchment, (Didoné *et al.*, 2015). The K factor map for the catchment was created using interpolation techniques in a GIS environment based on soil parameters (figure 3.3), (Olaniya *et al.*, 2020).

$$K = 27.66m^{1.14} * 10^{-8} * (12 - a) + 0.0043(b - 2) + 0.0033(c - 3) \quad [3.2]$$

Where,

K = Soil erodability factor (ton·hr⁻¹·ha⁻¹·MJ·mm),

m = (Silt % + Sand %) × (100 – clay %),

a = %t organic matter,

b = soil structure code: 1) very structured/ particulate, 2) fairly structured, 3) slightly structured, and 4) solid,

c = permeability code of the soil profile: 1) rapid, 2) moderate to rapid, 3) moderate, 4) moderate to slow, 5) slow, 6) very slow.

Soil organic matter was derived by the following equation:

$$SOM = 1.724 * OC \quad [3.3]$$

Where,

SOM = soil organic matter

OC = soil percentage organic carbon content

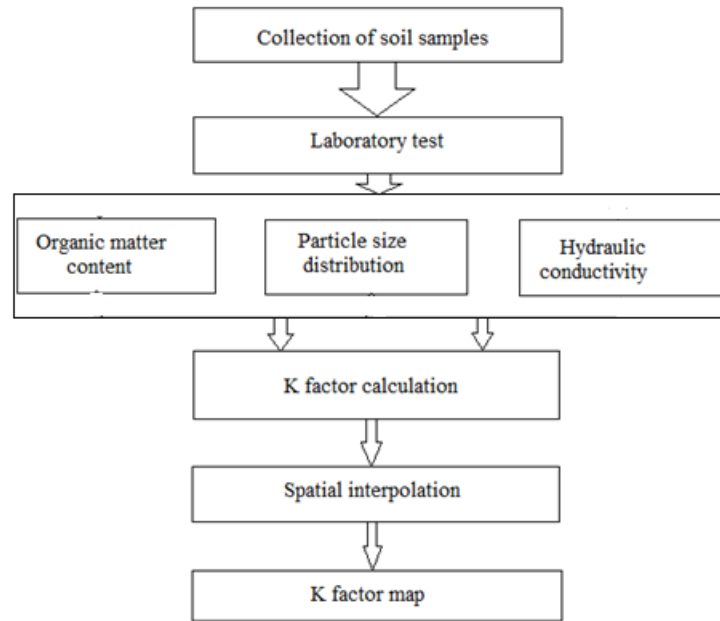


Figure 3.3: Derivation of the soil erodibility factor

The Topographic (LS) Factor

The topographic component is a combined effect of both slope length as well as slope steepness that, above all, has a significant impact on the rate of soil erosion, (Kogo *et al.*, 2020). The LS factor in this research was calculated using DEM having a resolution of about 30 m. The technique included using digital elevation models (DEMs) to derive the surface percent slope, identifying and filling of the sinks in DEMs, generating direction of flow, and, most importantly, the accumulation of flow, (Karamage *et al.*, 2016; Kogo *et al.*, 2020). LS factor was determined within a GIS framework with the help of equation (3.4), (Ganasri & Ramesh, 2015; Tessema *et al.*, 2020).

$$LS = \left(\frac{Q_{aM}}{22.13} \right)^y \times (0.065 + 0.045 \times S_g + 0.0065 \times S_g^2) \quad [3.4]$$

Where,

LS = slope length and slope steepness factor

Q_a = flow accumulation grid

Sg = grid slope (%)

M = grid size (vertical length x horizontal length)

y = a constant which depends on the slope gradient

0.5 is for slopes greater than 4.5 %,

0.4 is for slopes between of 3% to 4.5%

0.3 is for slopes between 1% to 3%

0.2 is for slopes less than 1%

Land Cover Management (C) Factor

The C factor is used to track crop effects and land management techniques that influence soil erosion process, (Ganasri & Ramesh, 2016; Kidane *et al.*, 2019).

The component as utilized within the RUSLE model, according to Renard *et al.* (1997), is obtained through the use of numerous sub-factors, specifically land use as well land cover. These two sub-factors are subject to spatial and temporal change, (Ganasri & Ramesh, 2015). The NDVI is a crucial input in calculating the land cover management factor, which is highly dynamic, (Kogo *et al.*, 2020). Therefore, when it comes to assessing the crop management aspect, remote sensing is an important instrument.

The land use and land cover map was produced using satellite images from Landsat OLI/TIR of November 2020 which had resolution of about 30 m, (Tessema *et al.*, 2020). The NDVI map was also generated using the remotely sensed data that had been interpreted, (Kogo *et al.*, 2020). Further, the spectral

indices that described the catchment area were calculated by using equation (3.5).

Finally, equation (3.6) was used to compute the spatial scattering of the C factor.

$$NDVI = \frac{\text{Band 5} - \text{Band 4}}{\text{Band 5} + \text{Band 4}} \quad [3.5]$$

Where,

Band 4 is the red band

Band 5 is the infra-red band

$$C = 0.1 \left(\frac{-NDVI + 1}{2} \right) \quad [3.6]$$

Where,

C = land cover management factor

Support Practice (P) Factor

The support practice (P) factor is basically a ratio that relates the quantity of soil lost from an agricultural field that has certain soil and water conservation methods to one that does not, (Kidane *et al.*, 2019). Traditionally, the P factor was calculated from the consideration of the different soil conservation measures implemented in a given location, (Woldemariam, 2018). Different scholars have calculated different P factor values based on percent slope and soil conservation techniques, (Karamage *et al.*, 2016). The P factor values for the catchment area were calculated in this study using the criteria established by Wischmeier and Smith (1978). The criteria entailed giving values to various land use/land cover classifications based on percent slope values (table 3.1). The slope percentages

were collected from the slope maps derived from DEM, while the LULC maps were generated from satellite images. Finally, using GIS techniques, the spatial variation of the P factors was derived, (Tessema *et al.*, 2020).

Table 3.1: Support Practice (P) Factors (Source: Wischmeier & Smith, 1978)

Land use type	Percent slope	P-factor
Cultivated land	0 – 5	0.10
	5 – 10	0.12
	10 – 20	0.14
	20 – 30	0.19
	30 – 50	0.25
	50 – 100	0.33
Other lands	All	1.00

3.2.2.5. Average Annual Soil Erosion

The potential for the dam reservoir catchment soil loss was assessed and quantified through the creation of a soil erosion risk map, (Sahu *et al.*, 2017). With the help of a raster calculator built in ArcGIS (figure 3.4), the RUSLE model parameter maps were multiplied, (Simms *et al.*, 2003; Kogo *et al.*, 2020). The outcome was a composite map that calculated the rate of soil loss in tonnes per hectare per year ($t\ ha^{-1}\ yr^{-1}$) within the catchment, (Depountis *et al.*, 2018; Kebede *et al.*, 2021). The layers were organized in a grid style, with each cell measuring 30 meters by 30 meters of the digital elevation model, (Gelagay & Minale, 2016; Tessema *et al.*, 2020). The geostatistical technique was utilized to predict the average annual soil loss potential, which was then classified to determine the risk associated with soil loss within the entire catchment, (Gelagay & Minale, 2016). Priority areas for conservation planning were identified by

categorizing the catchment's potential for soil loss into multiple severity levels, (Bekele & Gemi, 2020). The soil loss tolerance rating, (Tessema *et al.*, 2020), which varies from 5 and 11 t ha⁻¹ yr⁻¹, was used to categorize the catchment, (Mati *et al.*, 2000).

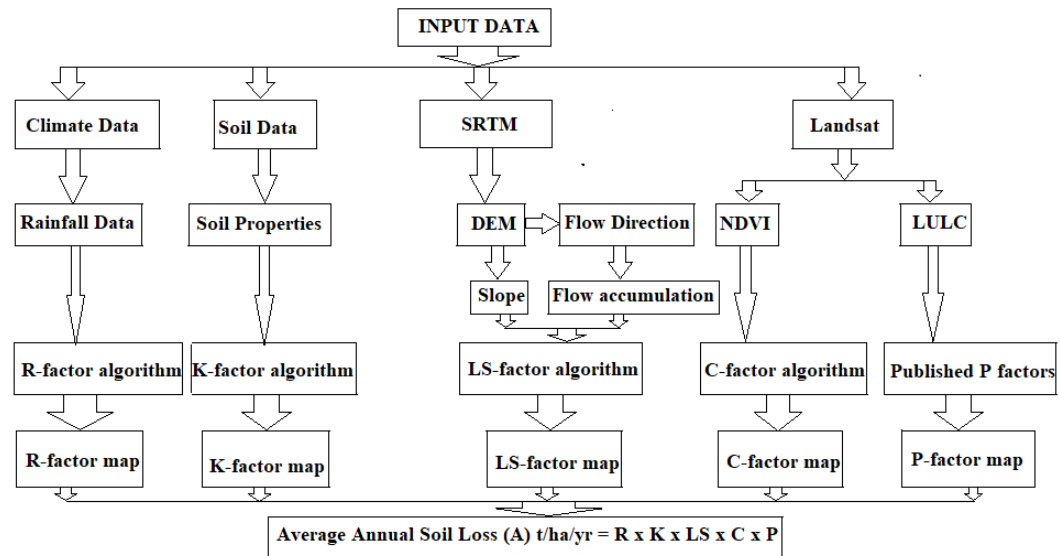


Figure 3.4: Overall methodology for estimating average annual soil loss

3.2.2.6. RUSLE-based Sediment Yield

As a field-based model, the RUSLE model basically does not provide direct estimates of sediment yield, (Boakye *et al.*, 2018). The SDR for the catchment of interest, however, should be utilized to estimate the quantity of sediment material passing through a catchment outlet, (Lim *et al.*, 2005). The SDR curve was established by the USSCS (1971), in which the SDR varied inversely to the power of 0.2 of the catchment area (equation 3.7), after which sediment yield was calculated using equation (3.8). This strategy was used for planning catchment conservation in the Ethiopian highlands, (Ayalew, 2015; Bekele and Gemi, 2020).

$$\text{SDR} = A^{-0.2} \quad [3.7]$$

Where

A = Area of the catchment (km²)

$$\text{SDR} = \frac{\text{SY}}{\text{E}} \quad [3.8]$$

Where

SDR = Sediment Delivery Ratio (dimensionless)

SY = Sediment Yield (t ha⁻¹ yr⁻¹)

E = Catchment gross erosion (t ha⁻¹ yr⁻¹)

3.3. Sedimentation Status of the Maruba Dam Reservoir

A surveying exercise should be executed out carefully right from the planning phase through the presentation of the final survey data in order to get the most accurate findings, (Samaila-Ija *et al.* 2014; Šiljeg *et al.*, 2022). If data is not adequately examined, organized, and presented in an understandable way, even the most precise and properly collected data would be meaningless, (Odhiambo & Boss, 2004). The data should be gathered, validated, checked, and most importantly, presented using clear, simple terminology in order to guarantee its recovery and understanding both immediately after the survey exercise and also in the future, (Samaila-Ija *et al.*, 2014). Consequently, hydrographic survey is the procedure of gathering, examining, displaying, and most importantly, managing spatially obtained data regarding marine structures, processes, and qualities in four basic dimensions, i.e. both space and time, (Maina *et al.*, 2019).

Bathymetric surveys are therefore defined as the measurement of water depths in water bodies, and they are required each time a complete study of the bed level is to be carried out. The procedure for estimating the depth relative to a particular water surface is known as bathymetry, (Ibrahim & Sternberg, 2021). Therefore, the sedimentation status of the Maruba dam reservoir was determined using three basic survey procedures: pre-bathymetry, the bathymetry, and post-bathymetry, (Sang *et al.*, 2017; Maina *et al.*, 2019).

3.3.1. Pre-bathymetric Survey

The dam reservoir boundary was created after the digitization process from digital globe pictures on Google Earth, (Sang *et al.*, 2017). Using ArcGIS version 10.6, the digitized reservoir border was converted to a shapefile. In a geospatial setting, survey lines (series of transects and tie lines) for directing the survey boat arrangement during the actual bathymetric survey exercise were also constructed as shapefiles (figure 3.5). Basically, the tie lines intersected with transect lines perpendicularly in order to enhance the accuracy during data collection where the water depth values at crossing places was to be cross-checked, (Hassan *et al.*, 2017; Maina *et al.*, 2018). The transect survey lines were used to guide the boat during the bathymetry survey and, more importantly, they provided sampling places where all depth measurements could be taken equitably, (Kilonzo *et al.*, 2019). Since the reservoir's area was about 40 hectares, the transect and tie lines were 50 m and 100 m apart (table 3.2) and extended from shoreline to shoreline, respectively, according to Levec and Skinner (2004). The details of the reservoir

periphery and the survey lines were loaded into the sonar device upon projection into the universal transverse Mercator (UTM) zone 37S. It would be impossible to carry out the survey exercise efficiently without the pre-bathymetry survey.

Table 3.2: Guidelines for open-water transect spacing for bathymetric surveys (source: Levec & Skinner, 2004)

Open-water surface area (ha)	Transect spacing (m)
< 200	50
200 to 1000	75
> 1000	100



Figure 3.5: Bathymetric survey transects and ties lines orientation

3.3.2. Bathymetric Survey

A detailed bathymetric survey exercise of the Maruba dam reservoir was planned and executed on 14 October 2021. According to Levec and Skinner (2004), 300 to 500 hectares of open-water area should be surveyed on a normal day. The bathymetric survey system (BSS) was used to conduct the study, which is a cutting-edge technology, (Irاندukunda *et al.*, 2020). A motor-driven Dual-Jon-boats, an echo sounder with an in-built global positioning system (GPS), the bathymetric survey system data recorder, and a vibro-coring (submersible) set of

apparatus were all part of the BSS (figure 3.6), (Levec & Skinner, 2004; Maina *et al.*, 2019). The sonar device normally obtains bathymetric data for a water body by pinging sound beams towards its bottom part, (Elçi *et al.*, 2009). The time duration taken by the sound to get reflected becomes an important factor in the measurement of the depth to the reservoir's bed and above all, determining the geographic location, (Iradukunda & Bwambale, 2021). The Specialty Devices Inc. (SDI) in Plano, Texas, has customized the boat configuration for bathymetric surveys and sediment collection using the vibro-coring system, (Sang *et al.*, 2017). During the survey, the sonar device was fastened to the boat configuration some 30 cm beneath the reservoir's water surface. Before any measurements were conducted, the sonar device was calibrated using the barcheck method because it keeps the correct depth in depth sounding, (Wilson & Richards, 2006). The procedure described by Wilson and Richards (2006) was followed during calibration. The survey boats were driven along pre-determined paths and in sections where the depth of the reservoir was quite sufficient for easier navigation (figure 3.7). The boat's cruising velocity was restricted to about 6 km/h due to safety and data quality concerns, (Levec & Skinner, 2004; Hassan *et al.*, 2017; Sang *et al.*, 2017). When the cruising speed exceeds 6 km/h, turbulence would build around the transducing element, thereby affecting the bathymetric data's quality, (Levec & Skinner, 2004; Maina *et al.*, 2018). In order to eliminate inaccuracies in depth measurement caused by wave propagation, the survey should be undertaken in some calm open-water environment, (Ortt *et al.*, 2000;

Levec & Skinner, 2004). During the survey, the inbuilt GPS device allowed us to record geographic positions that corresponded to the depths that were recorded, (Ortt *et al.*, 2000; Yesuf *et al.*, 2013; Irandukunda *et al.*, 2020). The APS was made up of three important frequencies (highest - 200 kHz, medium - 50 kHz, and smallest - 12 kHz) that were used to detect water depth and sediment thickness, (Hassan *et al.*, 2017; Maina *et al.*, 2019). The highest frequency is quite efficient in determining reservoir capacity from water depth data, (Dunbar *et al.*, 1999; Moriasi *et al.*, 2018). This frequency has enough energy to penetrate water columns and, most importantly, it has a higher resolution, (Iradukunda & Bwambale, 2021). On the other hand, the medium frequency determines a portion of the accumulated sediment horizons (sub-surface), whereas the smallest frequency is able to penetrate accumulated sediment deposits upto the pre-impoundment zone, (Sang *et al.*, 2017; Moriasi *et al.*, 2018). With the use of supplementary data acquired from the collected sediment core samples, the buildup of sediment in the post-impoundment zone was further validated, (Hassan *et al.*, 2017; Moriasi *et al.*, 2018). The customized vibro-coring system by SDI that included the vibrating core head that had a weighted rig, a check valve, as well as a core tube, was used to collect all core samples, (Dunbar *et al.*, 1999). The sediment samples were obtained at predetermined locations where sonar-based data had previously been recorded.

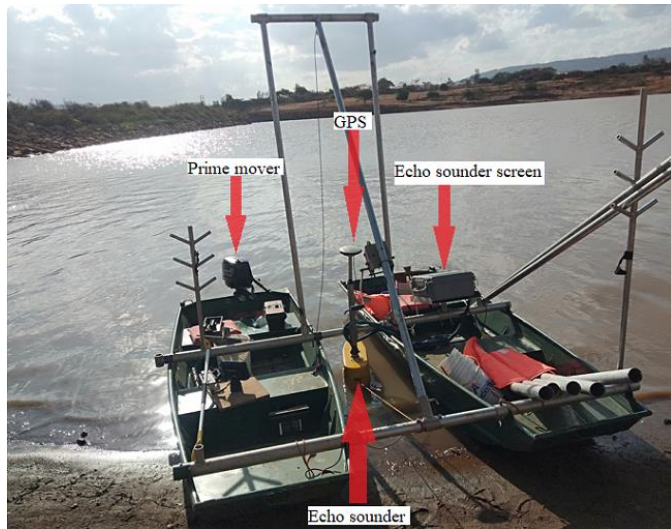


Figure 3.6: Bathymetric survey system set up

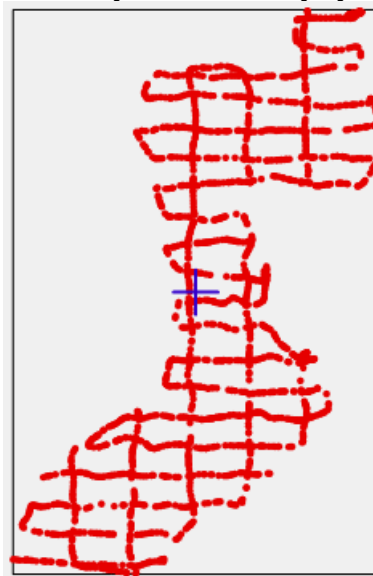


Figure 3.7: Waypoints recorded during bathymetry survey exercise

3.3.3. Post-bathymetric Survey

The geo-referenced sonar based data was downloaded from the bathymetric survey system data recorder to a computer, (Ortt *et al.*, 2000). The acoustic data was displayed, analyzed, digitized, and above all, edited using the DepthPic 5.0.2 program from the Specialty Devices, Inc. (SDI), Wyles, Texas, USA, (Moriassi *et al.*, 2018; Maina *et al.*, 2019). At every surveyed point, the X, Y, and Z variables

pertaining to latitude, longitude, and water depth, respectively, were clearly extracted, (Maina *et al.*, 2018; Iradukunda & Bwambale, 2021). The DepthPic 5.0.2 program shows bathymetry data in extremely better resolution and, and above all, in greater details, (Maina *et al.*, 2018). The program helped in removing any form of data irregularities that was captured during depth measurements as a result of inadequate GPS responses, (Hassan *et al.*, 2017). This is quite an important stage during post-bathymetry survey because the accuracy of depth measurements is improved, (Yesuf *et al.*, 2013). The acoustic data were verified with DepthPic 5.0.2 software using sediment core data. In the laboratory, the sediment cores tubes were lengthwise using a special in order to enable visual inspection. The core was then marked in accordance with the apparent stratigraphic changes in the sediment. The accumulated thickness of sediment and the depth to which the core penetrated the pre-impoundment layer were also measured. This combination of information, coupled with the geographical location of the particular core sample, helped in adequately describing the sediment core in DepthPic 5.0.2 program.

The X, Y, and Z geo-referenced data was finally imported into the Surfer 22 spreadsheet (Golden Software, Inc., Golden, CO, USA), where it was saved as a file in surfer format after validation, (Iradukunda & Bwambale, 2021). The data points were interpolated after which a grid file was created in a geospatial environment, (Adongo *et al.*, 2020). In this analysis, the Kriging interpolation method was utilized because it is quite accurate than other approaches,

(Iradukunda & Bwambale, 2021). This method of interpolation was utilized by, (Iradukunda *et al.*, 2020; Kilonzo *et al.*, 2019). The outcome of the interpolation process was grid that was used as a basis for generating contours and most importantly, the bathymetric surface. The mathematical algorithms in the Golden Surfer 22 software were used to calculate volume and surface area from the grid. The depths of water that were measured below the normal water surface described the dam reservoir's lowest surface, which basically depicted the dam reservoir like a basin, (Yesuf *et al.*, 2013). Similarly, the upper surface displayed a typical flat plane where the reservoir's normal water surface was used as the reference point, (Yesuf *et al.*, 2013). With the reservoir water surface as the reference, measurements of the reservoir's capacity and area at corresponding contours were made at intervals of 0.5 m.

3.3.4. Determination of Sediment Accumulation Rate, Overall Storage Capacity Loss, Projected Reservoir Life, and Sediment Yield

According Dunbar and Allen (2004), acoustic profiling systems provide relatively accurate bathymetric measurements with an error of $\pm 4.2\%$. Therefore, the volumetric rate of reservoir sedimentation was calculated based on sediment volume over an 11-year period according to equation (3.9) proposed by Tamene *et al.* (2006) and Moriasi *et al.* (2018). Further, the overall storage capacity loss was calculated using equation (3.10) as proposed by Allen and Naney (1991). In addition, the volumetric rate of sediment accumulation was utilized to calculate the dam reservoir's projected life, as shown in equation (3.11), (Moraisi *et al.*,

2018). According to the theories put forward by Tamene *et al.* (2006) and Moriasi *et al.* (2018), equation (3.12) was used to calculate the sediment yield (normalized reservoir sedimentation rate).

$$\text{ReSR} = \frac{\text{SV}}{\text{Yrs}} \quad [3.9]$$

Where,

ReSR = volumetric reservoir sedimentation rate (m^3/yr),

SV = sediment volume (m^3),

Yrs = period under consideration.

$$\text{Overall storage capacity loss} = \frac{\text{sediment volume}}{\text{Original reservoir capacity}} * 100 \% \quad [3.10]$$

$$\text{PLS} = \frac{\text{Original reservoir capacity}}{\text{ReSR}} \quad [3.11]$$

Where,

PLS = projected life span (years)

$$\text{ReSRa} = \frac{\text{ReSR}}{\text{A}} \quad [3.12]$$

Where,

ReSRa = normalized reservoir sedimentation rate ($\text{t ha}^{-1} \text{yr}^{-1}$)

A = catchment area (ha)

3.4. Physicochemical Analysis of Sediments

Sediments at the reservoir inlet and the reservoir bottom were used to assess the physicochemical characteristics of sediments. The sediment samples were collected and examined for physicochemical characteristics in October 2021.

3.4.1. Reservoir Bottom Sediments

3.4.1.1. Sediment Sampling

The reservoir's predetermined locations were used for sampling for sediment cores, (Maina *et al.*, 2019). The distribution of sediment depth as given by the sonar-based approach served as the basis for choosing appropriate sampling spots, (Hilgert *et al.*, 2016). These spots were chosen along transect lines, and the sediment coring method was followed as described by Maina *et al.* (2019). The twin boat was safely secured for the coring activity, following which a Vibro-coring apparatus was employed to collect sediment core samples, (Hilgert *et al.*, 2016). The penetration depth of the core tube was guided by sonar-based data when collecting sediment cores, (Maina *et al.*, 2019). In this exercise, a coring device was employed, which included a vibrating head, a weighted rig, a check valve, as well as a core tube, (Dunbar *et al.*, 1999). The Vibro-coring equipment (figure 3.8) was gently lowered vertically into the accumulated sediments with the aid of a winch until the core tube could no longer move, indicating the presence of a compacted layer of sediments, (Maina *et al.*, 2019). The sediment thickness in the core was estimated by inserting a stadia rod into the core until the sediment surface was reached after the core sample was recovered. The sediment core was

carefully capped and positioned upright during storage after the vibe-coring technique, and then taken to the laboratory for a comprehensive investigation.



Figure 3.8: Sediment coring process

3.4.1.2. Sediment Retrieval

The sediment core tubes were split lengthwise in the laboratory using a special aluminum metal cutting saw, and then meticulously sliced depending on observable stratigraphic changes (figure 3.9). The samples were properly packed in plastic containers and stored for extensive physical and chemical investigation.



Figure 3.9: Sediment core retrieval

3.4.2. Sediments at the Reservoir Inlet

3.4.2.1. Sediment Sample Collection

The sedimentation process was clearly noticeable near the Maruba dam reservoir's inlet. This area offered excellent opportunities for sampling and above all, investigating the characteristics of deposited sediments at reservoir inlet, (Turgut *et al.*, 2015). The study region was identified as the dried-up part of the reservoir, from which case, sediment samples were collected from 10 different locations as shown in figure (3.10). The sampling locations were chosen at random and georeferenced with the handheld GPS device Garmin Explorer, which had a precision of 3 m, (Olaniya *et al.*, 2020). Undisturbed sediment samples were obtained with the help of core rings, while about 2 kg of disturbed sediments was collected using some appropriate bags. The sediment samples were obtained from both the surface (0 to 10 cm) and subsurface (10 to 20 cm) horizons, respectively. In this investigation, the Turgut *et al.* (2015) criterion for determining the surface as well as the sub-surface depths was applied. This criterion utilized the sediment penetration resistance, which exhibited minimal fluctuation between the 0 and 10 cm depth, after which it started to decline. The physicochemical characteristics of the sediment samples, including penetration resistance, particle size distribution, electrical conductivity, porosity, pH, organic matter percentage, bulk density, and nutrient content, were analyzed using standard laboratory procedures, (Girmay *et al.*, 2020).

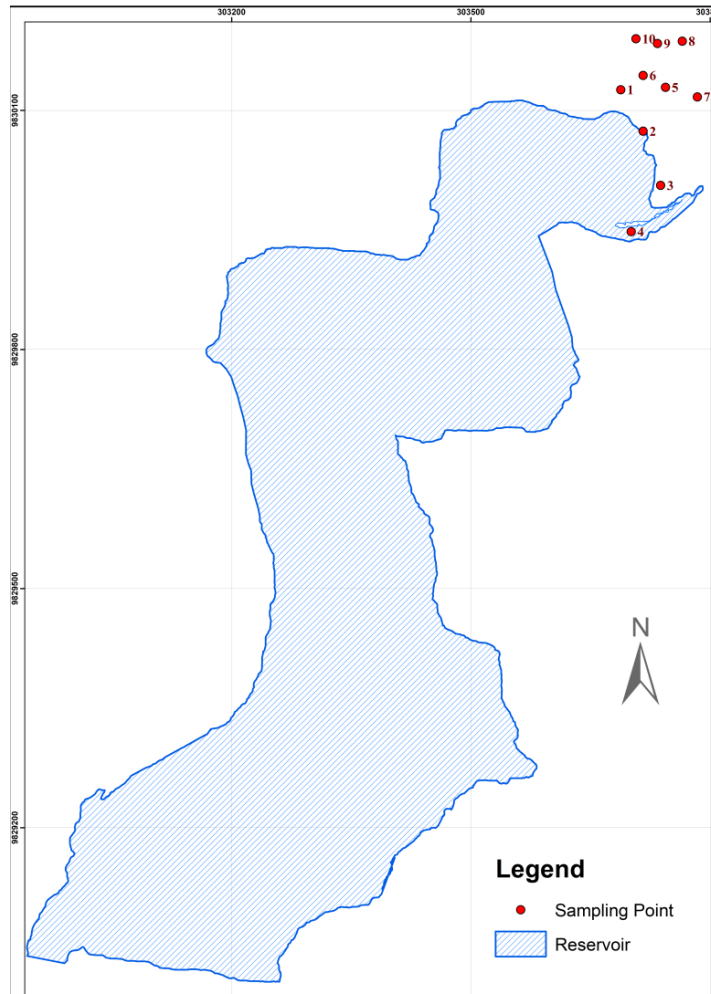


Figure 3.10: Sampling points at the reservoir inlet

3.4.3. Sediment Sample Preparations for Laboratory Analysis

The collected samples were subjected to air-drying which took place at normal room temperature for some days before being subjected to any laboratory procedures, (Junakova & Balintova, 2012). All trapped material in the sediments was carefully removed, followed by thorough mixing, (Urgesa & Yilma, 2015). Finally, the sediments were manually ground and then put through a 2 mm sieve, (Wójcikowska-Kapusta *et al.*, 2018). The Maruba dam reservoir lies within a catchment where agricultural activities are quite dominant, and therefore it was

likely that the quality of sediments could have been influenced by the non-point pollution from the crop fields. As a result, the sediment samples were tested for macronutrients, mainly, nitrogen (N), phosphorus (P), and potassium (K), (Junakova *et al.*, 2021). Other analyzed parameters included the grain size, bulk density, pH, electrical conductivity, and above all, organic matter percentage. Additionally, the sediments deposited the inlet of the reservoir were further analyzed for porosity, hydraulic conductivity, and penetration resistance.

3.4.4. Laboratory Analysis of Sediments

Gee *et al.* (1986) described the hydrometer method for determining particle size distribution. The distribution of particles was determined using this method, which is based on the rates at which particles settle in an aqueous solution, (Lin *et al.*, 2019; Hoque *et al.*, 2021). Both the sediment pH and the level of minerization of the sediment were measured using the Hach HQ40D portable multimeter. The procedure for sediment sample preparation for the two procedures is clearly outlined in Urgesa & Yilma (2015). The pH/EC meter was calibrated prior to any measurements being taken using the method described by Sha'Ato *et al.* (2020).

The organic matter content of sediments was estimated using Boyd's (1995) method. This approach determines the amount of organic carbon found in sediments, and then converts the result to organic matter content using a factor (1.724), (Abraham, 2013). The rapid wet oxidation technique has been used by researchers to estimate the level organic carbon (OC) in sediments. The Walkley

and Black (1934) procedure was used, which was later updated by Nelson and Sommers (1996). The ICP-OES procedure was used to determine phosphorus and potassium content, while the Kjeldahl method was used to determine nitrogen content, (Fonseca *et al.*, 1998; Baran *et al.*, 2019).

The bulk density and porosity of the sediment were calculated using Rowell's (1994) method. A hand penetrometer (type IB, 6000 kN.m⁻² – Eijkelkamp) was used to measure the resistance of sediment to penetration insitu. The constant or variable head tests can be used to calculate the hydraulic conductivity at saturation, (Lin *et al.*, 2019). The variable-head method is ideal for fine-grained soils, whereas the constant-head method suited for coarse-grained soils, (Iradukunda & Nyadawa, 2021). The constant head approach was used to conduct the permeability test due to the coarseness of the sediments near the reservoir inlet, (Iradukunda & Nyadawa, 2021).

3.4.5. Statistical Analysis

The minimum value, maximum value, mean value, standard deviation (SD), and coefficient of variation (CV) were used to create a descriptive evaluation of the analytical data, (Turgut *et al.*, 2015). The coefficient of variation (CV), which is basically the most relevant metric in descriptive analysis, was used to define variance in sediment properties, (Wei *et al.*, 2008). According to Wilding (1985), $CV \leq 0.15$, $0.15 \leq CV \leq 0.35$, and $\geq CV 0.35$ suggest low, moderate, and higher variability, respectively.

CHAPTER FOUR: RESULTS AND DISCUSSIONS

4.1. RUSLE Model Parameterization

4.1.1. Rainfall Erosivity (R) Factor

Rainfall has a big influence on erosion rates, especially in catchments. The R factor, which is determined using accurate and continuous precipitation data, caters for the impact of rainfall intensity, (Wischmeier & Smith, 1978). The amount and intensity of precipitation are stronger indicators of its severity, (Foster *et al.*, 2003). Soil erosion in cropped fields has a direct relationship with the energy and intensity of each storm, according to research, (Ganasri & Ramesh, 2015). As a result, using daily rainfall as the best indicator of soil loss variation, the seasonal fluctuation of sediment yield is better defined, (Ganasri & Ramesh, 2015). The use of annual precipitation data in determining the R factor, on the other hand, has the advantage of making the computation process easier and more consistent. The R factor was estimated using annual rainfall data that was averaged from 1990 to 2019.

The mean annual precipitation data for the period 1999 to 2019 ranged from 718 to 734 mm for the three rainfall stations, resulting in long-estimated erosivity values ranging from 251 to about 254 MJ mm t ha⁻¹ yr⁻¹, (figure 4.1). The lower the R factor, the lower the rainfall intensity, and vice versa (Jain *et al.*, 2001) because soil loss is heavily dependent on rainfall, (Devatha *et al.*, 2015). This suggests that the low R factor for the catchment indicated that rainfall was less erosive to erode and that rainfall intensity was low, (Devatha *et al.*, 2015).

The upper half of the catchment experienced the highest levels of rainfall erosivity due to the somewhat higher rainfall amount. The R factor slightly decreases as the land moves from steep to milder terrain as it gets closer to the dam reservoir. The R factor, on the other hand, exhibited only minor change, indicating that rainfall variance was not substantial considering the size of the catchment. As a result, the effect of rainfall on soil loss varied slightly across the entire catchment.

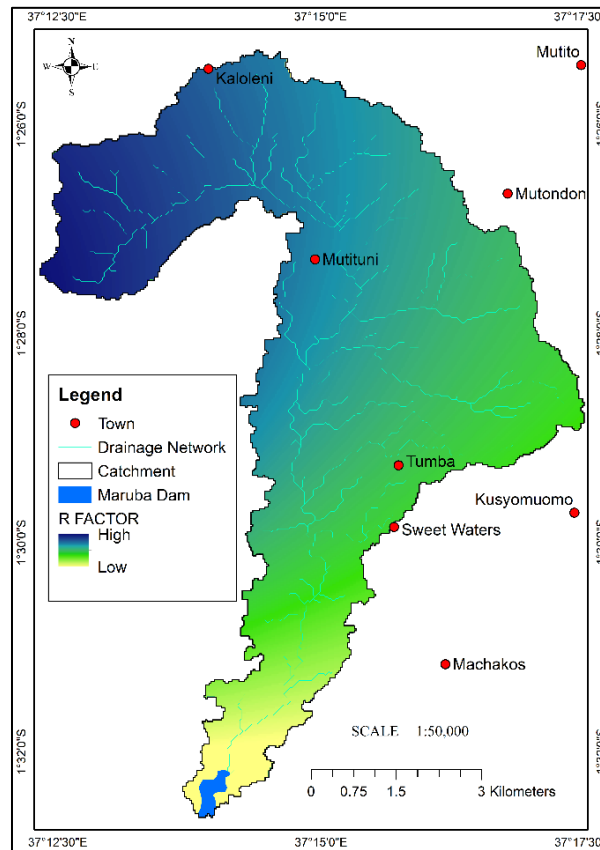


Figure 4.1: Rainfall erosivity factor

4.1.2. Soil Erodibility (K) Factor

Over the whole catchment, the soils were more or less homogenous and possessed nearly identical properties (table 4.1). This was due to the catchment's modest size (49 km²). According to field surveys, the soil's depth was around 2 meters, and particle size analysis revealed that the soil's sandy texture contained more than 59 % sand and very little silt (less than 7 %). Sandy soils have a low cohesiveness, making them susceptible to detachment and erosive movement, (Ida *et al.*, 2008). Furthermore, soils containing a lot of sand have a lot of permeability, which can lead to erosion and even landslides.

The soil erodibility (K) factor determines the soil's inherent vulnerability to erosion, (Hategekimana *et al.*, 2020). The inherent resistance to detachability and transportability of soil particles expresses their susceptibility to erosion, (Gizachew & Ayalew, 2015). Erodibility is determined by soil cohesiveness, which varies depending on vegetation cover, moisture content, and soil structure, (Gizachew & Ayalew, 2015). As a result, organic matter content, soil texture, and more importantly the soil structure all have some great influence on soil erodibility, (Pushpalatha *et al.*, 2017).

The soil erodibility factor for the Maruba dam reservoir catchment was estimated using equation 2.13 and data on soil parameters. The K-factor for the research area was calculated spatially using the Kriging interpolation techniques, (Kilonzo *et al.*, 2019), and a K-factor map was created (figure 4.2). The K factor values in

the research area ranged from about 0.0076 to 0.0125 t h MJ⁻¹ mm⁻¹. For a Kenya context, the results are equivalent to those found by Angima *et al.* (2003), Njiru *et al.* (2018), and Hategekimana *et al.* (2020). Angima *et al.* (2003) claimed that changes in K factor values are caused by factors such as time, geography, and even management techniques.

The soil particles in the research area have a low K factor, indicating that the soil was moderately susceptible to detachment, (Devatha *et al.*, 2015). The Low K factor values were related to low permeability, relatively low antecedent soil water content, and other factors in the study area soils, (Ganasri & Ramesh, 2016; Pushpalatha *et al.*, 2017). Furthermore, low K factor figures may be linked to moderate organic matter concentration as well as surface particulates, (Girmay *et al.*, 2020).

Table 4.1: Catchment's area soil properties

S. No.	Name	Sand (%)	Silt (%)	Clay (%)	Textural class	Permeability (cm/hr)	OM (%)
1	KYASILA	64	4	32	Sandy clay loam	11.9	4.4
2	MAGNETIC HILL	65	7	28	Sandy clay loam	14.4	1.91
3	NGELANI MARKET	63	3	34	Sandy clay loam	6.7	1.24
4	KIVUTINI SCH	66	3	31	Sandy clay loam	20.4	0.95
5	MARUBA DAM SITE	63	1	36	Sandy clay	70.4	1.84
6	KATUNGA FOREST	65	7	28	Sandy clay loam	3.6	5.76
7	KITITEINI SCHOOL	77	3	20	Sandy clay loam	35	1.27
8	KMTC - MANZA	59	5	36	Sandy clay	0.1	1.22
9	MUKUNI AIC CHURCH	75	5	20	Sandy clay loam	5.7	2.48
10	IVUMBUNI PRI. SCH.	71	3	26	Sandy clay loam	0.9	1.34
11	KYANGULI HIGH SCH.	63	1	36	Sandy clay	4.1	1.17
12	MUNG'ALA SEC. SCH.	75	5	20	Sandy clay loam	9.4	1.03
13	MUTITUNI	65	5	30	Sandy clay loam	18.9	3.74
14	MUA GIRLS SCH.	59	5	36	Sandy clay	10.1	1.2
15	MANZA PRI. SCH.	73	1	26	Sandy clay loam	0.3	2.41

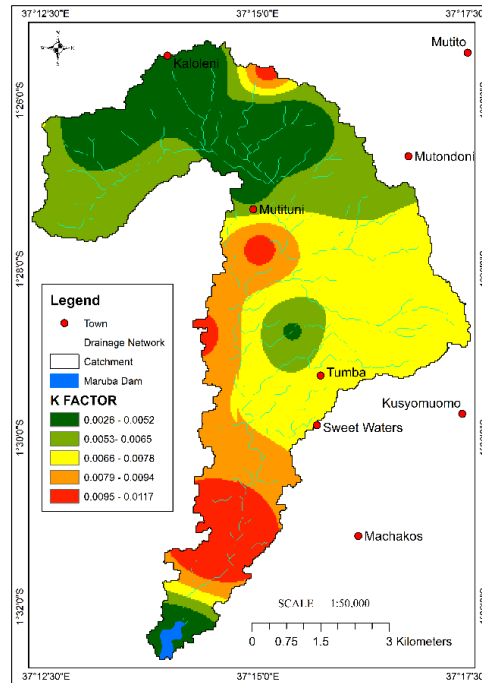


Figure 4.2: Soil erodibility factor map

4.1.3. Topographic (LS) Factor

The topographic factor takes into account the impacts of topography on soil erosion, (Ganasri & Ramesh, 2016; Balabathina *et al.*, 2019). It is the result of the interaction of two key sub-factors: slope length in addition to slope gradient. The overall amount of sediment yield generated from a specific site is influenced by the two sub-factors, (Prasannakumar *et al.*, 2012). The topographic component is an important input in the RUSLE model since it measures the rate of surface runoff and serves as a reliable indicator of soil loss in a catchment area, (Devatha *et al.*, 2015; Roslee & Sharir, 2019).

The topographic component was developed using data from digital elevation models to account for flow buildup and percent slope, (Simms *et al.*, 2003). The factor map was created using the GIS framework and equation (2.19),

(Prasannakumar *et al.*, 2012). The topographic factor's spatial distribution is depicted in the diagram below (figure 4.3). The topographic value was observed to increase from 0 to 384 with increases in flow accumulation and slope, according to this investigation, (Ganasri & Ramesh, 2016). Higher topographic factor values are indicative of areas having steep slopes and longer slope lengths. In such regions, detachment of soil particles is more pronounced since the velocity of surface runoff is higher.

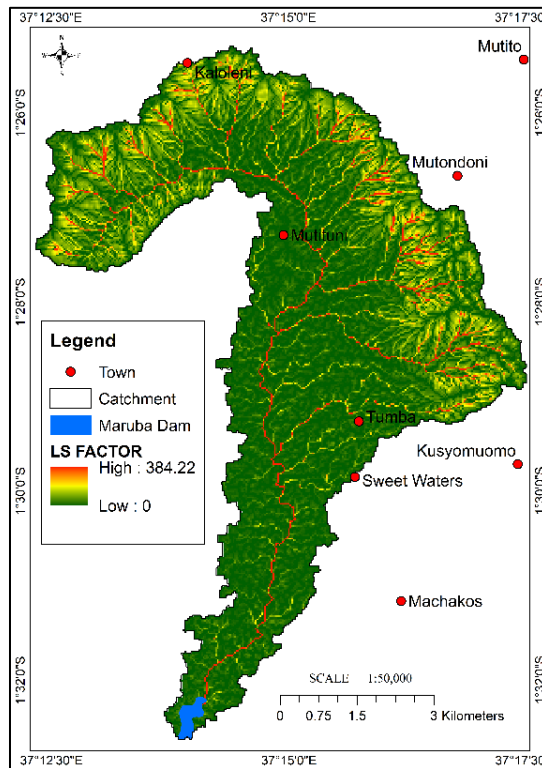


Figure 4.3: Topographic factor map

4.1.4. Land Cover (C) Factor

The C factor is a crucial input in the RUSLE model because it captures the effects brought about by crops and management strategies on soil erosion, (Jiang *et al.*, 2014). Consequently, it contrasts the relative effects of various management

alternatives with relation to conservation plans, (Roslee & Sharir, 2019). The C factor gives an account of the cumulative effect of connected soil cover and management characteristics, according to Wischmeier and Smith (1978). Land use data helps to understand how land features like cropping patterns, forests, surface water bodies, fallow land, wasteland, and so on have been used, (Ganasri & Ramesh, 2016). Such considerations are crucial in land use planning as well as soil erosion investigations. A land use and land cover map that was generated using satellite imagery was used to create data on vegetation cover and management elements, (Ganasri & Ramesh, 2016; Roslee & Sharir, 2019).

The land cover factor in this study was calculated using equation 2.24 and the NDVI, which is a reliable indication of vegetative vigor and health. The C factor would behave similarly since both land use and even land cover are subject to spatiotemporal change. The C factor for the research area varied from as low as 0.02 to 0.06 (figure 4.4). Figure 4.4 shows that the places with the lowest NDVI also had the highest C factor values. The variation in NDVI values was considered to be the cause of the C factor's variability. According to the C factor map (figure 4.4), there is a moderate amount of vegetation cover, which translates to a considerable amount of soil loss from the watershed.

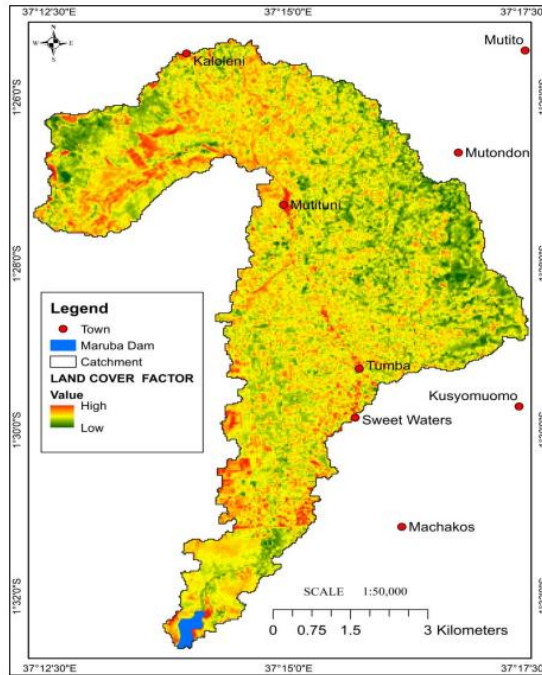


Figure 4.4: Land cover factor map

4.1.5. Support Practices (P) Factor

The conservation practice factor is also known as the support practice factor, (Jiang *et al.*, 2014). The factor compares the quantity of soil lost by specific support practices to the corresponding loss caused by up and down the slope tillage in a similar location, (Devatha *et al.*, 2015). In addition to reducing surface runoff in terms of volume and rate, the support practice component changes the flow characteristics specifically pattern, grade, and above all, direction of the runoff, (Tesfaye & Tibebe, 2018). As a result, the P factor quantifies the impact of some conservation interventions on soil loss, (Roslee & Sharir, 2019). The sorts of conservation strategies used in a given catchment region serve as the foundation for calculating P factors, (Bekele & Gemi, 2020).

Figure 4.5 depicts the factor map for support practice. The map was created using land use and land cover classes, as well as percent slope, (Tessema *et al.*, 2020). P factors ranged from 0.1 to 1, as shown in figure 4.5. The lower the value of P (0.1), the more efficient a conservation measure is, while the highest (1) indicates that there were no structures in place to stop soil erosion, (Hurni, 1985; Bekele & Gemi, 2020). According to figure 4.5, some low P factor values were noted in steep sloping areas, which indicated that agricultural activities were accompanied by some soil conservation structures.

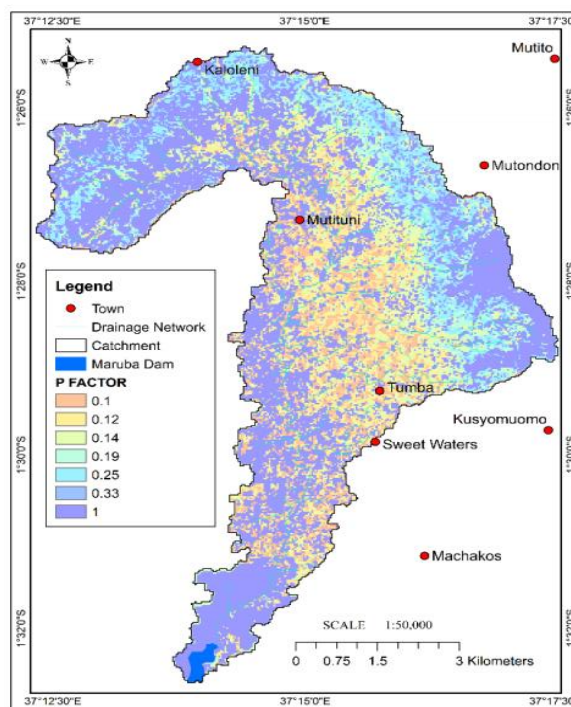


Figure 4.5: Support practices factor map

4.1.6. The Average Annual Soil Loss Potential

Using the RUSLE model to estimate potential soil loss from a catchment region necessitates the integration of a geographic information systems framework in

which the model factors are efficiently multiplied, (Hategekimana *et al.*, 2020). The anticipated soil loss on an annual basis was calculated in this way by multiplying the generated raster data for the five RUSLE model factor, (Devatha *et al.*, 2015; Depountis *et al.*, 2018; Roslee & Sharir, 2019). In a GIS system, the multiplication procedure produced a composite layout that expressed the average annual loss of soil within the catchment in tonnes per hectare per year ($\text{t ha}^{-1} \text{ yr}^{-1}$), (Fenta *et al.*, 2020). The map depicts the Maruba dam catchment's average annual soil loss potential. According to the map, the catchment's average annual rate of soil erosion varied from 0 to $29 \text{ t ha}^{-1} \text{ yr}^{-1}$, with $0.9708 \text{ t ha}^{-1} \text{ yr}^{-1}$ being the average. The lower value of the average soil loss rate was attributed to the low levels of R and C in the research area.

The research results were compared with similar ones from a similar research carried out within Machakos district (Moore, 1979) in order to validate the findings and show the efficacy of the RUSLE model methodology within the research area, according to Prasannakumar *et al.* (2012). Moore (1979) conducted a study outside the dam catchment's area using runoff plots and established that the soil was being depleted at rates that ranged from 0.22 t ha^{-1} to about 12.34 t ha^{-1} . Furthermore, Moore's (1977) prediction of soil erosion ($0\text{--}109 \text{ t ha}^{-1} \text{ yr}^{-1}$) in Machakos district was quite comparable and corresponded well with the estimated study results. Likewise, a research by Wanjiku (2015) predicted that soil loss within Katheka Kai area, which is next to Machakos town, was between 0 to $60 \text{ t ha}^{-1} \text{ yr}^{-1}$. The results of the study were compared to those of other Kenyan studies

that had similar rainfall and geo-environmental features, (Mati *et al.*, 2000; Angima *et al.*, 2003; Fenta *et al.*, 2020; Hategekimana *et al.*, 2020). According to sources, the rates of soil loss from Kenyan croplands due to sheet as well as rill erosion varies between less than 1 to greater than 100 t ha⁻¹ yr⁻¹, (Wakindiki & Ben-Hur, 2002). These studies' findings were determined to be comparable to those acquired in this investigation, and hence might be utilized to validate the findings, (Hategekimana *et al.*, 2020). Most importantly, sediment yield data estimated for the Maruba dam catchment were used to assess the veracity of the RUSLE-based estimations for soil erosion, (Fenta *et al.*, 2020).

Based on the lowest and highest values and most importantly, the spatial variance of each class, the predicted soil loss for the whole catchment was subdivided into five potential soil erosion risk classes (table 4.2). Table 4.2 demonstrates that modest soil loss (10 t ha⁻¹ yr⁻¹) occurred in around 89 % of the catchment, with the remaining areas being classed as moderate to high risk. The largest rates of soil loss are found in hilly terrain, which could be attributable to the study's high topographic factor value.

The highest risk locations are found in both the highlands and lowlands, according to the spatial variation of the erosion risk. Figure 4.6 illustrates that soil erosion within the catchment was not uniform, which was ascribed to the various terrain variations seen during the supervised categorization. The topography map and the spatial variation of the soil loss revealed a strong relationship. This

indicates that topography has an important role in regulating soil flow within catchments, (Prasannakumar *et al.*, 2012; Njiru *et al.*, 2018). Hence, sites with a high LS-factor and damaged vegetation require prompt soil conservation treatment.

The term "soil loss tolerance" is often used to refer to research on soil erosion, (Hammad, 2009). It refers to the maximum amount of permissible soil loss that supports both economic sustainability and high levels of output, (Wieschmeier & Smith 1978; Morgan, 2005). Soil loss tolerance levels typically range from 5 to 11 t ha⁻¹ yr⁻¹, (McCormack & Young, 1981). The analysis concluded that increased soil erosion was incredibly apparent, although the soil loss within the catchment was way below the acceptable limit. The study also discovered that land cover as well as land use was the primary causes of soil loss in the catchment. Environmental and managerial input components are divided into two categories in the RUSLE model. Environmental elements tend to stay the same throughout time, whereas management components change dramatically, (Rahaman *et al.*, 2015). The implication is that land cover as well as land use management can be significantly modified as a means of slowing the rate of soil loss, (Njiru *et al.*, 2018).

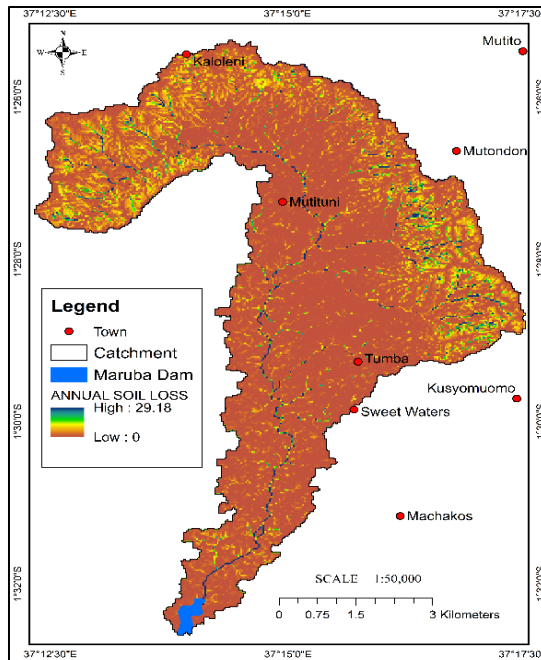


Figure 4.6: Average annual soil loss map

Table 4.2: Soil loss classes

Erosion Categories	Numeric Range ($t\ ha^{-1}\ yr^{-1}$)	Soil Loss Proportions (%)
Very Low	0 - 2	78.52
Low	2 - 5	11.04
Moderate	5 - 10	8.28
High	10 - 15	2.14
Very High	15 - 20	0.02
Extremely High	20 - 30	0.01
		100

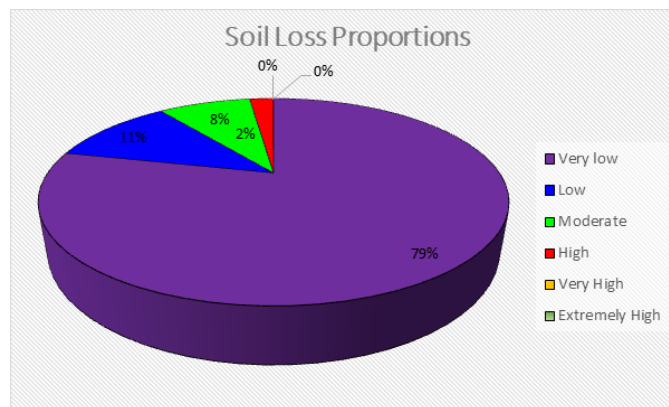


Figure 4.7: Soil loss proportions

4.1.7. Sediment Yield

The quantity of sediment discharged from a catchment's outlet is known as sediment yield, (Razad *et al.*, 2020; Kolli *et al.*, 2021). When a reservoir serves as a catchment's outlet, sediment yield is used to forecast sediment flow into the reservoir, (Razad *et al.*, 2020). Sediment yield is a crucial metric that indicates how much topsoil is lost due to overland flow, (Ayalew, 2015). It is an important consideration when identifying non-point pollution sources and designing hydraulic infrastructure, particularly dams and reservoirs, (Mutua & Klik, 2006).

Sediment yields at the catchment outlet have been found to be relatively considerable, (Ayalew, 2015). At this stage, the ability of overland flow to move sediments decreases and deposition occurs. As a result, erosion within the catchment region is often larger than the sediment yield. Therefore, estimating sediment output cannot be done using estimates of soil erosion within the watershed until more data is available, (Ayalew, 2015). Sediment yield estimates are computed using empirical relationships, just as estimates of soil erosion. The most frequent approach for predicting sediment yield is using the sediment delivery ratio, (Razad *et al.*, 2020).

The predicted average annual soil loss from the reservoir's catchment was 0.9708 t ha⁻¹ yr⁻¹, according to the findings. This represents the quantity of soil that has been removed from the catchment area by eroding agents. In this research, the SDR was 0.1828, and the RUSLE estimated sediment yield was 0.1775 t ha⁻¹ yr⁻¹.

The SDR for this investigation is comparable to the ones obtained by Mutua *et al.* (2006) and Kidane *et al.* (2019), respectively. Furthermore, the SDR figures match those given in USSCS (1971) table 2.9. The SDR values represent the catchment's overall ability to store and move erosion-related material, (Mutua *et al.*, 2006). Although empirical approaches for predicting SDR do not take into consideration the spatial range of watershed characteristics, when used in small catchments, they produce reliable findings, (Mutua *et al.*, 2006).

The catchment size, drainage network, and slope length-relief ratio are all elements that influence SDR, (Razad *et al.*, 2020). The SDR is impacted by the physical parameters of the catchment, which are highly variable in most cases. The size of the drainage area, runoff-rainfall parameters, slope, land use and/or land cover, slope, and soil qualities are all elements to consider. The transportability of sediments in catchments is heavily influenced by human activities. Soil as well as water management activities, for example, have an impact on sediment delivery in catchments, (Wu *et al.*, 2018). Catchment processes such as detachability, transport, deposition, and, most significantly, catchment sediment budgets are all affected by soil and even some water management activities. The behavior of the river channel to trap sediments causes dynamic changes in sediment delivery ratios in catchments. There are numerous factors that influence soil erosion and sediment yield, including urbanization, careless tree cutting, construction work, wetland restoration, terracing, afforestation, and grass establishment. Changes in land use mostly influence flood

frequency, peak flood volumes, runoff coefficient, and, most importantly, the dynamics associated with soil erosion as well as sediment yield relationships.

4.1.8. Land Use/ Land Cover Assessment

Table 4.3 and figure 4.8 classify and display the changes that resulted from land use in addition to land cover from 2000 to 2020. In the Maruba dam catchment, LULC classes included bodies of water, populated regions, barren ground, croplands, dense forest, sparse forest, rocks, and sand.

Table 4.3: LULC Changes between 2000 and 2020

Category	2000 (% Cover)	2010 (% Cover)	2020 (% Cover)	Change (2020 -2000)
Bare land	21.04	21.56	17.84	Negative
Built-up	0.62	2.69	3.26	Positive
Mixed	22.81	29.69	38.18	Positive
Dense Forest	9.56	6.09	4.11	Negative
Grassland	25.55	20.11	23.08	Negative
Irrigated land	0.89	2.45	1.02	Positive
Rocks and Sand	1.21	1.43	1.82	Positive
Sparse Forest	18.06	15.66	10.40	Negative
Water body	0.25	0.42	0.29	Positive
Total	100.00	100.00	100.00	

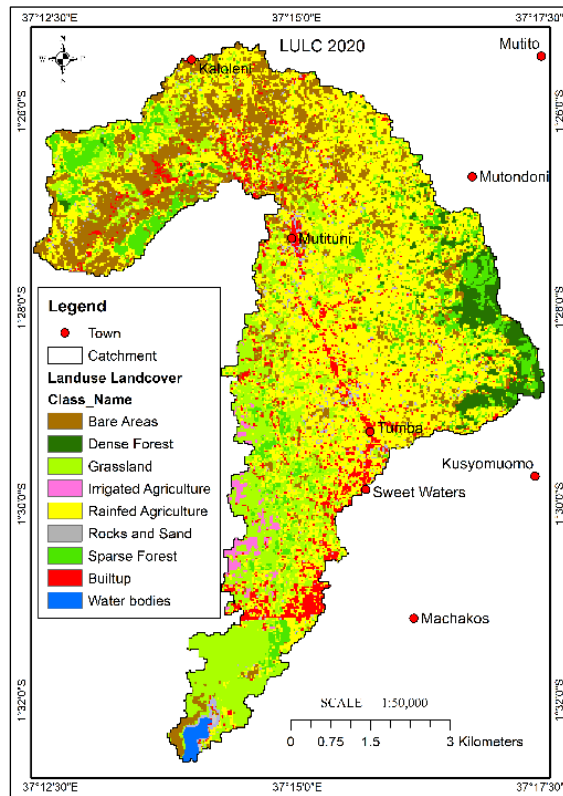
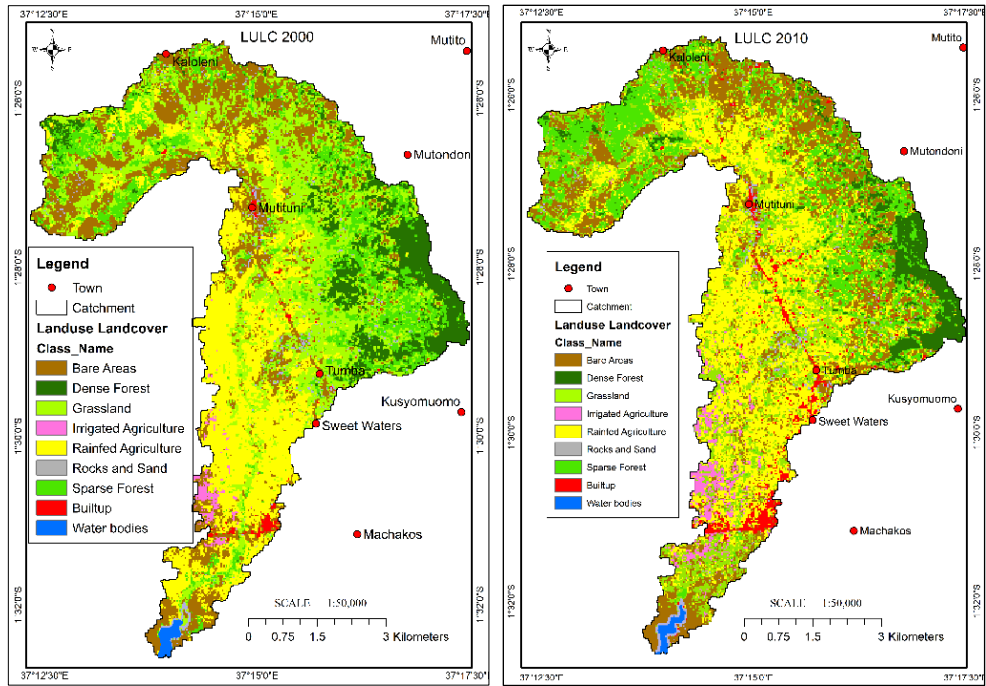


Figure 4.8: LULC maps for 2000, 2010 and 2020

Negative trends in LULC changes were recorded in bare areas, grasslands, dense, and sparse forests (table 4.3), equal to 21–18%, 26–23%, 10–43%, and 18–10%, respectively, between 2000 and 2020. On the other hand, favorable trends in LULC changes were seen in built-up areas, rainfed croplands, irrigated croplands, rocks and sands, and aquatic bodies. The percentage changes ranged from 0.6 to 3.3 percent, 23 to 38 %, 0.9 to 1 %, 1.2 to 1.8 %, and 0.25 to 0.29 %. These LULC variations are due to the human population's socioeconomic impact on the catchment surface.

Negative LULC changes suggested that the catchment was undergoing rapid change. The highest reaches of the dam catchment are made largely of bare terrain. Soil erosion is most likely to account for the bareness in these areas because of the steep slopes. Furthermore, the negative change in bare areas suggests that soil and water management systems were not successfully applied. The rate of replacement by agricultural activities and settlements is indicated by the negative trends in LULC changes in forest areas and grasslands. Syombua (2013) reported similar LULC change trends. Such changes suggest a reduction in canopy and vegetation cover, making the soil more vulnerable to erosion.

Water bodies, agriculture areas, rocks and sands, and built-up regions, all showed positive LULC alterations. The expanding human population in the catchment region is reflected in the development in built-up areas. As the human population grows, so does the demand on natural resources (soil, forests, water, and

grasslands). This explains why forests and grasslands are disappearing to satisfy socioeconomic pressures. The rise of rainfed and irrigated areas demonstrates this, (Syombua, 2013). The shallow soils were indicated by rock outcrops within the catchment region. The soil survey procedure and ground truth information both corroborated this. Soil erosion is particularly sensitive in shallow soils, which is exacerbated by a lack of plant canopy and vegetation cover.

The patterns involving the water body category revealed some fascinating dynamics. The Maruba dam reservoir was identified as the catchment area's primary water source. In the year 2000, the dam covered 0.25 % of the entire catchment area, according to the LULC classification. As a result, the percent area increased from 0.25 % to 0.42 % in 2010. However, the dam reservoir area declined from 0.42 % to 0.29 % between 2010 and 2020. This indicated that the dam's storage capacity had been reduced owing to sedimentation. The dam catchment underwent rapid terrain transformation as a result of socio-economic influences, according to the study.

4.2. Bathymetric Survey Data

4.2.1. Acoustic Layers and Sediment Thickness

In the Maruba dam reservoir, multi-frequency acoustics was used to map both soft and hard bathymetric surfaces, (Moriasi *et al.* 2018). The lowest frequency (12 kHz) has the ability to penetrate the reservoir bottom to depths of 50 meters or more, (TWDB, 2009). It does, however, produce visuals that are hazy. This

problem is solved by combining this frequency with one of 50 kHz. This phase improves the methodology for mapping sediment depth to depths of 50 meters or even more, (Maina *et al.*, 2019). As a result, the sediment thickness is quantified by using the two frequencies to estimate depth, (Odhiambo & Boss, 2004).

4.2.2. Isopach Profiles

A cross-section depicting the analyzed sediment core is shown in figure 4.9(a). There are 1.10 meters of sediment at this location, with the higher sediment layers characterized by high moisture content, minimal vegetation, and primarily clay. As illustrated in figure 4.9(b), the red box indicates significant moisture content region (0.5 m) in the sediment. The yellow box shows a 0.2 m region where notable changes in the soil structure and moisture content took place between the high moisture content section and the sediment pre-impoundment boundary. The green section on the other hand, depicts about 0.3 m section sediment pre-impoundment. The changes within sediment structure are depicted by the sediment pre-impoundment boundary. Within the sediment core, the pre-impoundment boundary was identified visually by looking for traces of terrestrial matter such as twigs, tree bark, intact roots, or leaf litter, (Hassan *et al.*, 2017).

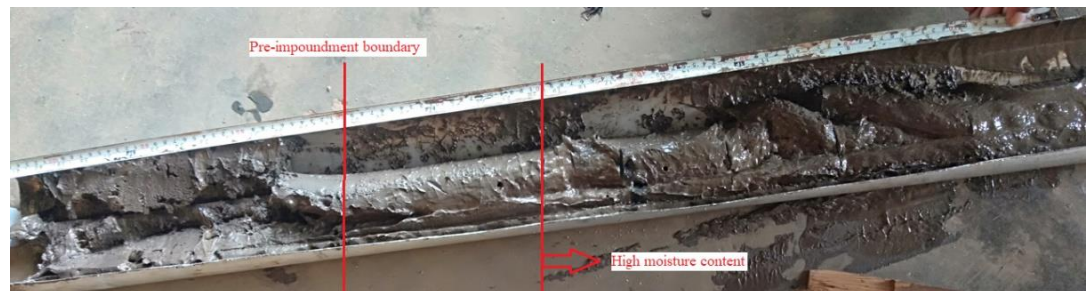


Figure 4.9(a): Pre-impoundment boundary

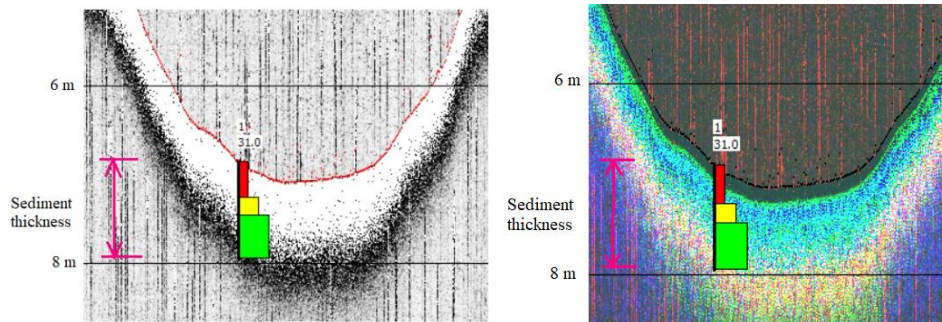


Figure 4.9(b): Multi-frequency acoustic profiles and sediment core display in DepthPic software

The current bathymetric surface in DepthPic software is determined by the 200 kHz (the highest frequency) based on acoustic signal returns. The pre-impoundment surface, on the other hand, was visually identified using the color of the displayed pixels as well as any other core data that was available, (Hassan *et al.*, 2017). The pre-impoundment surface is shown by both the red as well as the yellow pixels in figure 5(b), whereas the current one is represented by black pixels.

4.2.3. Water Storage in the Dam Reservoir

In addition to sediment deposition, a bathymetric assessment showed the reservoir's current bathymetry. On a contour map, lines are shown that link locations of equal elevations and above all they have a unique relation to volume and even area, (Odhiambo & Boss, 2004). Basically, contour maps are useful for a number of reasons, such as supply of water, irrigation activities, recreational uses, and above all, monitoring of either long-term or even temporal variations that would affect the reservoir characteristics in the context of better decision-making as well as management, (Irandukunda *et al.*, 2020; Iradukunda &

Bwambale, 2021). The reservoir's details were depicted by a succession of spatial contour lines whose interval varied from 0.5 m to 13.5 m depth (figure 4.10). The reservoir's deepest region is depicted by dark blue colour.

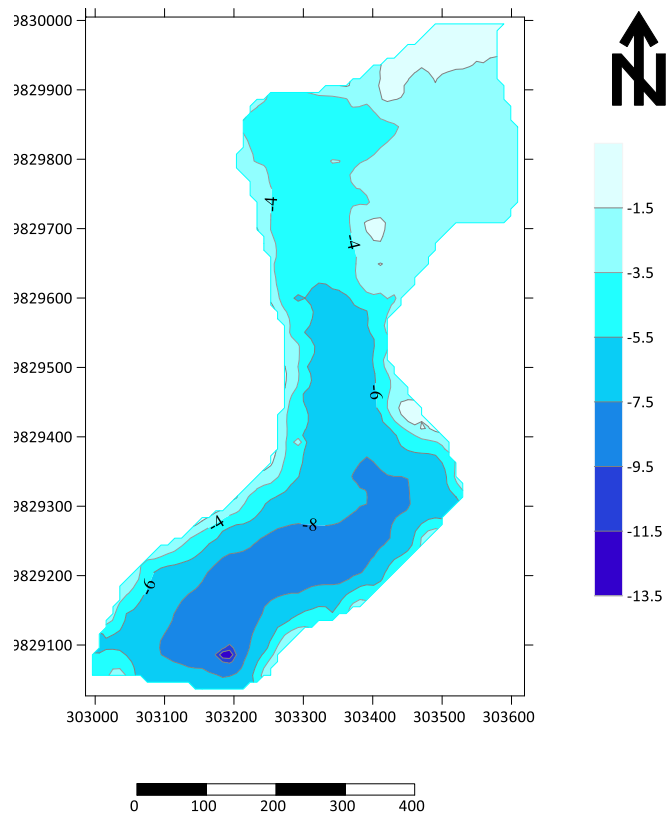


Figure 4.10: Contour map for Maruba dam reservoir

4.2.3.1. Depth Profile of Maruba Dam Reservoir

Figure 4.11 depicts the longitudinal as well as the transversal representation of the reservoir. The difference in reservoir depths from the reservoir inlet towards the dam wall is clearly depicted by the Profile A-A'. From the point A' (with a minimum reservoir depth of roughly 0.5 m) to point A, the depth increased (maximum reservoir depth of 10 m). Likewise, the transverse reservoir cross-sections are shown by the profiles B-B' and C-C', respectively. The depth of the

reservoir increased from the reservoir periphery towards its mid section, according to profile B-B' (8 m deep). Meanwhile, sediment transport dynamics were well-represented in profile C-C', which was quite close to the reservoir inlet. The variation in the reservoir depth at this particular section, where the depth was noted to increase from point C' to point C, demonstrated this. The fluctuation in water depth was a good illustration of the reservoir's topographic variability.

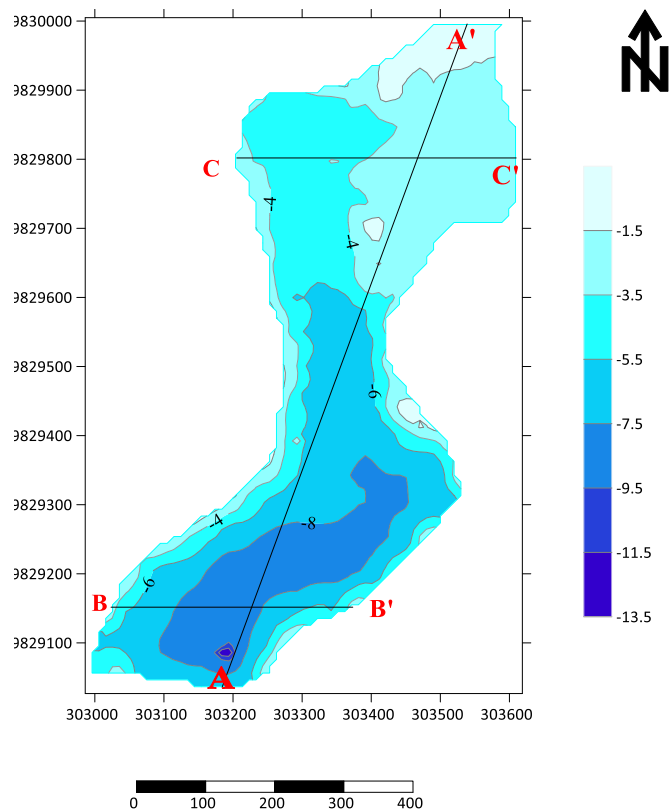


Fig. 4.11(a): Longitudinal and transversal profiling of Maruba dam reservoir

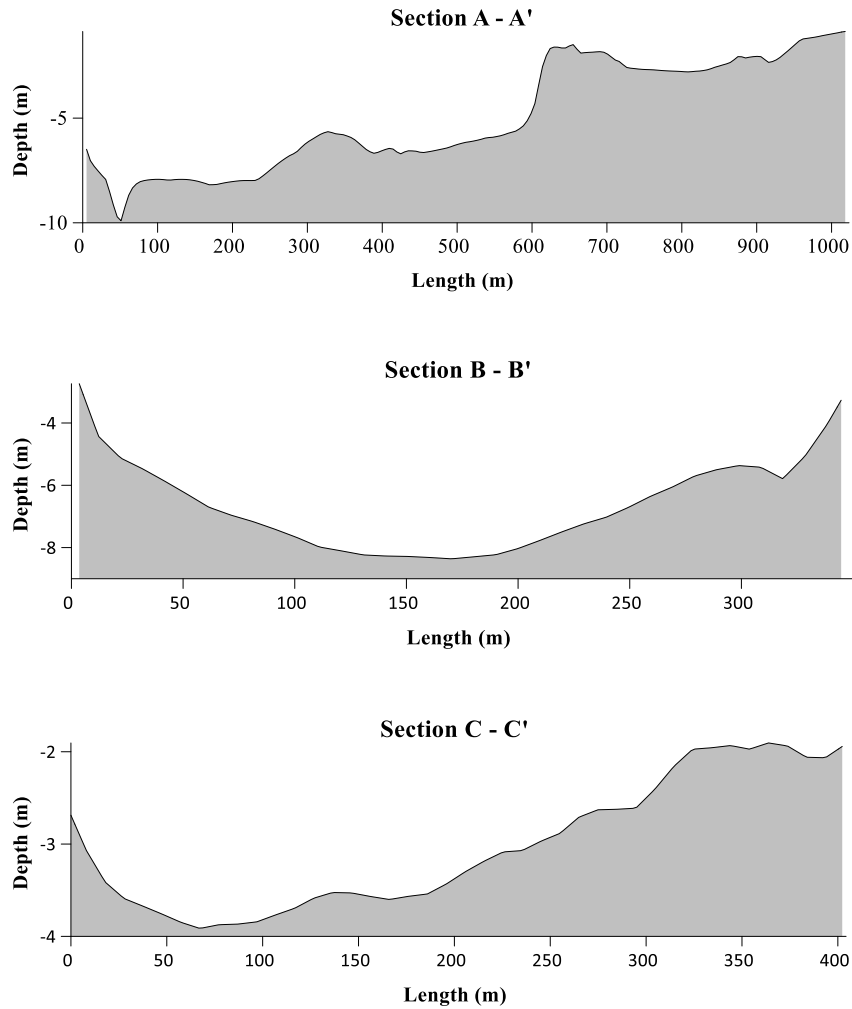


Figure 4.11(b): Profiled cross-sections depicting reservoir depth variation

4.2.3.2. Water Storage Characteristics of Maruba Dam Reservoir

The reservoir water storage properties were represented using hypsographic curves as well as related depth distributions. Basically, hypsographic curves serve as useful tool for the presentation of bathymetry survey results in a clear and understandable manner. Typically, the curves depict the some data correlations that exist between the reservoir depth, the contour surface area, and the reservoir volume, according to Sang *et al.* (2017). These correlations aid in identifying and evaluating temporal variations in the reservoir's area and volume at various

depths, and vice versa, (Yesuf *et al.*, 2013). Such data correlations result to three essential curves namely; the depth-volume, the volume-area, and most importantly, the depth-area. Moreover, the depth-volume-area curve is the result of combining these three curves (figure 8a).

The availability of these curves would serve as an important tool through which the dam reservoir would be adequately managed. The water volume and reservoir area may be assessed at specific water depths. The inverse is also possible, where the water level may be calculated from a known area of the reservoir established using remote sensing techniques. Hypsographic curves may serve as independent systems for managing day-to-day activities in a reservoir in terms of its volume and area, or they may be part of an integrated system for providing real-time as well as forecast reservoir details, (Sang *et al.*, 2017).

The combined depth, area, and volume correlations portray a more accurate image of a particular dam reservoir, which may be used to analyze reservoir operations, anticipate sediment dispersion, and, most importantly, help in understanding the dynamics in reservoir water storage capacity, (McAlister *et al.*, 2013). The reservoir capacity, and hence the water surface area, increased as the reservoir water depth increased (figure 4.12). The Maruba dam reservoir's total water volume was measured to be 2395139.5 m³. The reservoir area was also discovered to be 256622.85 m².

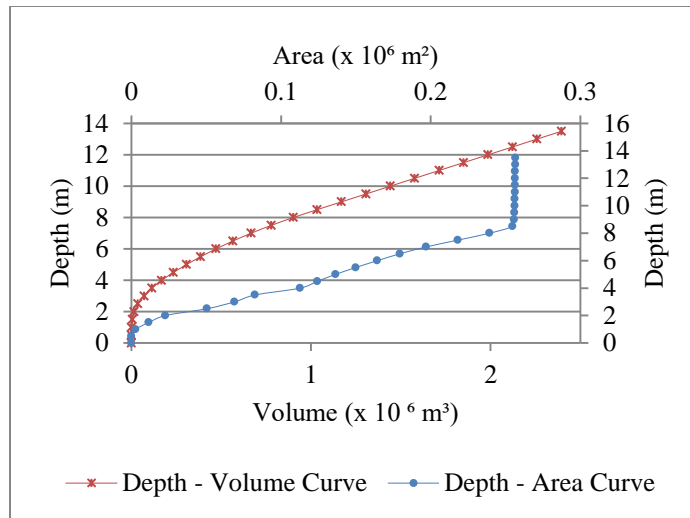


Figure 4.12: Reservoir water storage characteristics

4.2.4. Sediment Storage in Maruba Dam Reservoir

4.2.4.1. Sediment Profile

Figure 4.13(a) depicts the sedimentation state of the dam reservoir. The thickness that defines the various sediment layers describes the sediment accumulation in the reservoir, as seen in the diagram. The sediment profile was extracted by profiling the dam reservoir longitudinally, as illustrated in figure 4.13(b). Further, figure 4.13(c) is a basic spatial variation map that depicts the fluctuation of sediment within the reservoir. The thickness of the sediment is readily visible. The thickness of the respective sediment layers in the dam reservoir shows that it is rich in sediment, according to the study. The greatest thickness of sediments measured 1.7 meters, with an average of 0.60 meters. From the reservoir's mid-section to around the dam wall section, sediment accumulation was more pronounced. This explains the role of catchment activities in reservoir sedimentation.

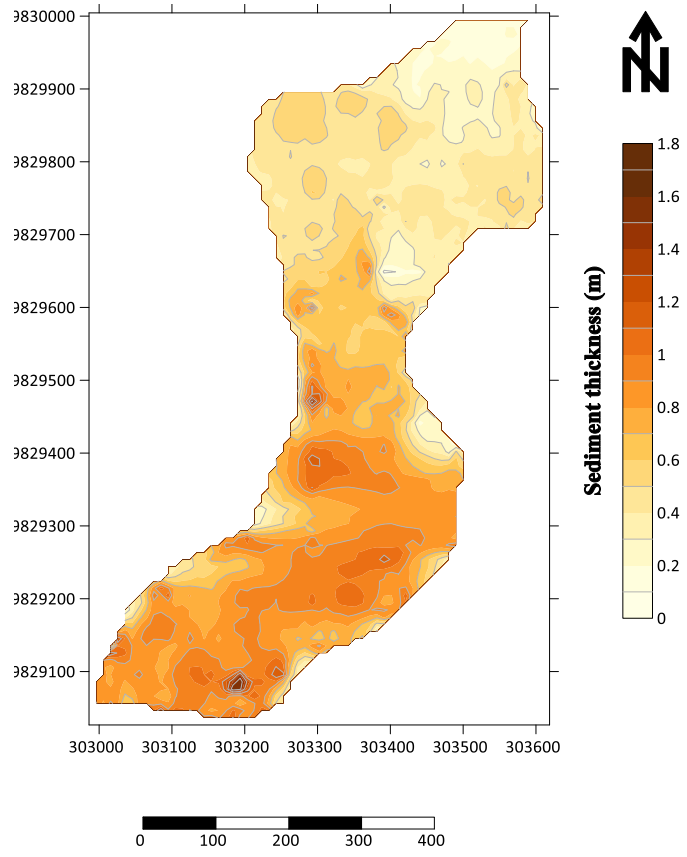


Figure 4.13(a): Sedimentation status map for Maruba dam reservoir

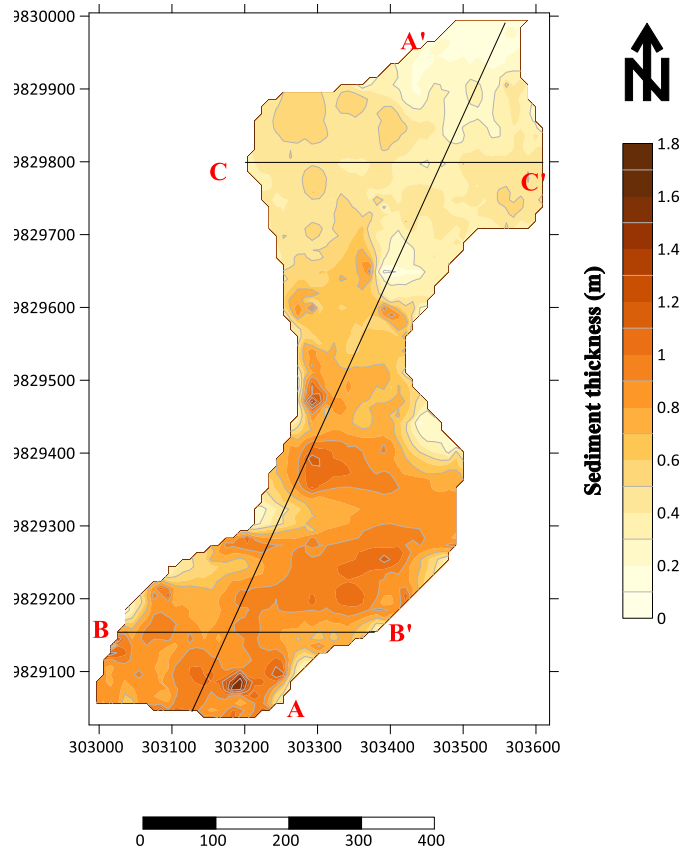
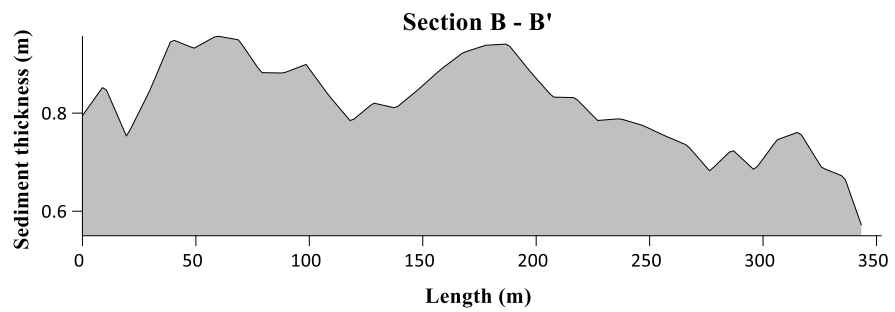
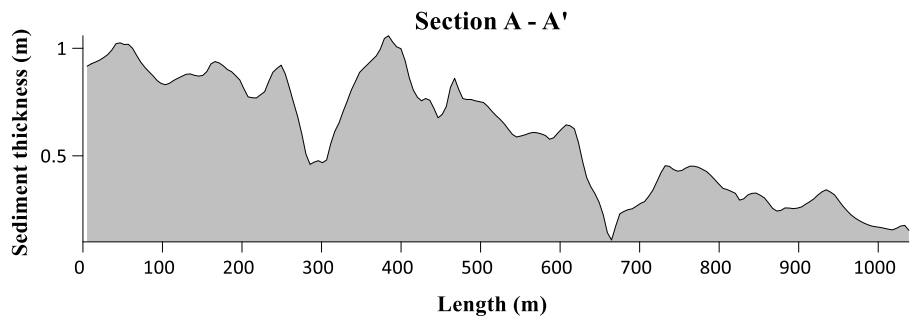


Figure 4.13(b): Sediment profiling in Maruba dam reservoir



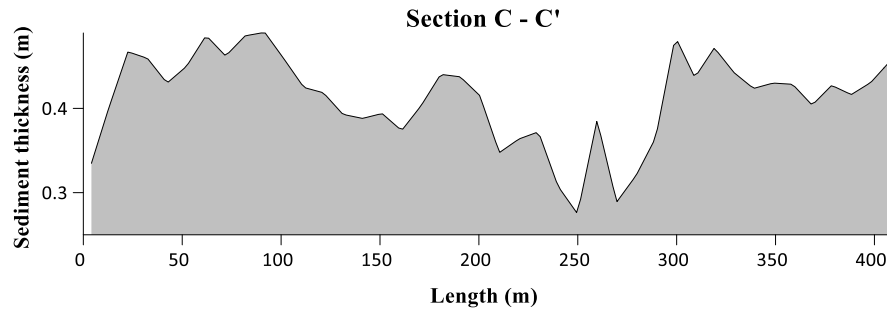


Figure 4.13(c): Profiled sections depicting sediment thickness

4.2.4.2. Sediment Storage Characteristics in the Reservoir

The thickness of the sediment layers varied from 0 m, which corresponded to the reservoir bed, to 1.7 m, which corresponded to the post-impoundment reservoir layer. A disproportionately large amount of sediment was found along the dam's wall. Figure 4.13(a) demonstrates that when the thickness of the respective sediment layer grows, the accumulation of sediments within the reservoir increases. The overall sediment deposition in the reservoir was determined to be 290434.6 m³, according to the study, a loss of nearly 11 % of the reservoir's overall storage volume. The rate of reduction of reservoir storage volume is a significant factor in determining anticipated life span of the Maruba dam reservoir, (Hassan *et al.*, 2017). Therefore, the annual loss of a reservoir's storage capacity can be calculated by dividing the amount of accumulated sediment volume by the present age of the dam reservoir, (Hassan *et al.*, 2017). Based on the study, the annual rate of the dam reservoir storage capacity loss has been 26403.15 m³, or nearly 1 % of the reservoir's storage capacity, since its commissioning and some slight extensions in 2010 and 2016, respectively. The Maruba dam reservoir's annual rate of storage capacity loss compares favorably

to international averages, (Basson *et al.*, 2009). The sedimentation rate (ReSR) of the dam reservoir was 16,370 t yr⁻¹, its anticipated life span was about 95 years, and above all, the bathymetric based sediment yield (ReSRa) was 3.34 t ha⁻¹ yr⁻¹, according to a bathymetric survey.

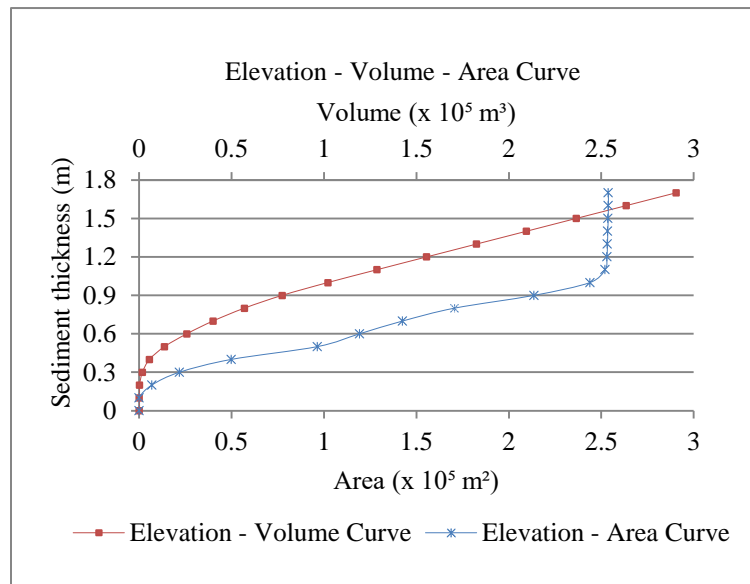


Figure 4.14: Reservoir sediment storage characteristics

4.2.5. Comparison between RUSLE-based and Reservoir Sedimentation Rate-based Sediment Yield

As a matter of fact, smaller catchment areas receive less attention than larger ones (more than 100 km²), which are deemed important in national water management actions and are adequately represented using a matrix of gauging stations, according to Vanmaercke *et al.* (2014). The sediment yield data for smaller catchments, however, is critical for a variety of reasons. The construction of reservoirs mainly for water supply is one of the most important. As a result, credible estimations of potential sediment yield are required for the construction

as well as management of reservoirs, (Vanmaercke *et al.*, 2014). Smaller catchments are preferable over bigger ones since they are less diverse and above all, they are less susceptible to some land cover alterations, (Walling 1983). Nonetheless, it might be somewhat challenging to point out the critical factors that may bring slight variabilities observed in such catchments, (Moriassi *et al.*, 2018).

Sediment outputs are known to be fairly large at catchment outlets because runoff transport capacity is limited at this point, allowing deposition to take place, (Ayalew, 2015). The total amount of erosion within catchments is much more than the quantity of sediment quantified at the respective outlet, (Bekele & Gemi, 2020). Ayalew (2015) pointed out that estimating sediment yield based on soil loss estimations necessitates some extra sediment delivery ratio data. However, because the estimation takes in to account spatially generated figures with numerous characteristics, such an approach would yield an estimate for sediment yield. In this regard, Fenta *et al.* (2020) utilized sediment yield results from distinct catchments in order to assess the trustworthiness of soil estimations using the RUSLE model methodology. Vanmaercke *et al.* (2014) established sediment yield estimates for the African continent, which were used in this particular research. The estimations were based on important data obtained from certain gauging stations as well as observable sedimentation rates in reservoirs, with a median measurement time of 4 and 17 years for both methods, respectively. Vanmaercke *et al.* (2014) further pointed out that long-term rates of sedimentation in reservoirs that have better trap efficiencies produce accurate sediment yield

estimations. The disparities in sediment yield estimations were attributed by Vanmaercke *et al.* (2014) to methodological variances since sedimentation in reservoirs includes both suspended and bedload, whereas at stream gauging points, the suspended matter is the sole concern.

The RUSLE model estimated sediment yield was $0.1775 \text{ t ha}^{-1} \text{ yr}^{-1}$ in this study, while the estimate from the bathymetric survey was $3.34 \text{ t ha}^{-1} \text{ yr}^{-1}$. The results were within Vanmaercke *et al.* (2014)'s reported range for African catchments (between 0.002 and $157 \text{ t ha}^{-1} \text{ yr}^{-1}$). However, the utilization of the RUSLE model to predict soil loss introduces a lot of uncertainty arising from the input values. In this regard, soil erosion predictions do not accurately reflect reality the in catchments. Nonetheless, Fenta *et al.* (2020) concluded that the soil loss predictions by the RUSLE model were quite reliable because there was a substantial association between estimated sediment yields and even the predicted gross soil loss, though the relationship improved for regions larger than 100 km^2 .

4.3. The Physicochemical Characteristics of Reservoir Bottom Sediments

The hydrophysical and even the biogeochemical activities that occur in catchments are strongly influenced the physicochemical qualities of reservoir bottom sediments, (Junakova *et al.*, 2021). The chemistry of bottom sediments influences their typical features and potential participation in water body activities involving contaminants, heavy metals, biogenic elements, and organic matter sorption/desorption, as well as their potential application in agriculture, (Fonseca

et al., 1998; Zakonnov *et al.*, 2019). As a result, understanding the physicochemical position of such bottom sediments in a reservoir is a key step in dam management and assessment, (Junakova & Balintova, 2014). The findings from the physicochemical investigations are shown in Table 4.4. The table summarizes the basic classical statistics of some selected physicochemical bottom sediment parameters at the Maruba dam reservoir. All of the parameters' variability was found to be in the low to moderate range on this basis.

Table 4.4: Physicochemical properties of bottom sediments

Sediment Property	Min.	Max.	Mean	SD	CV
Sand (%)	36.79	44.79	39.75	1.940	0.050
Clay (%)	48.72	59.00	56.31	2.580	0.050
Silt (%)	1.000	8.490	3.940	2.580	0.540
N (%)	0.090	0.160	0.124	0.018	0.146
P (mg kg ⁻¹)	8.684	17.034	12.809	2.164	0.169
K (%)	0.430	0.160	0.458	0.026	0.146
OM (%)	1.518	2.434	2.099	0.199	0.095
sBD (g cm ⁻³)	0.549	0.689	0.620	0.044	0.071
pH	6.270	6.800	6.630	0.151	0.023
EC (dS.m ⁻¹)	0.156	0.300	0.225	0.059	0.262

4.3.1. Textural Analysis

Sediment deposition is visible in quite water bodies, and it is made up of a variety of soil particle sizes that may range from very fine to even coarse, (Junakova & Balintova, 2014). Textural analysis is an important approach in this regard since it aids in determining the beginning of sediment transport, and most importantly deposition, (Hassan *et al.*, 2016). In table 4.4, the proportional proportions of sand, clay, and silt are shown. The reservoir's bottom sediments were mostly clay (56.31±2.580 %) and sand (39.75±1.940 %) particles. The bottom sediments'

textural class was clay. A high proportion of clay particles in bottom sediments may be utilized as an ecological indicator for identifying a catchment's land use pattern, (Hoque *et al.*, 2021). The extent of soil modification in the catchment region and the subsequent soil erosion phenomenon might be explained by the dominant soil grains within the reservoir. Clay particles are dislodged at a considerably higher rate than sand particles, which could be related to seasonal variations in flow environment that create distinct energy conditions inside the reservoir, (Fonseca *et al.*, 1998). The greater clay concentration could have been caused by urban runoff around the dam reservoir's vicinity, (Hoque *et al.*, 2021). Hassan *et al.* (2016) linked the Dukan dam reservoir's high fine-grained sediment composition (clay and silt) to lower flow energy, describing a much quiet and a calm deposition surrounding.

Typically, sediment particle size distributions vary longitudinally, with coarse material, primarily sand or even coarse silt dominating the upstream section and fine grains, primarily silt and clay, accumulating in the deepest parts and more so along the dam embankment, (Tomczyk-Wydrych *et al.*, 2021). In fact, depending on the grain size, the beneficial utilization of sediments would vary. Understanding the geographic variance of sediments inside a reservoir is important since it will aid in the development of a suitable plan for their management, (Morris, 1998). Finely-grained bottom sediments, according to Wyrwicka *et al.* (2019), are rich in both mineral elements and organic material, and so can be used as fertilizers. Consequently, sandy sediments may be useful

substrates for agricultural production, while those having higher clay content may be put into soils to improve poor soil quality, particularly sandy soils, (Fonseca *et al.*, 1998). According to Tarnawski *et al.* (2017), bottom sediments may be utilized to raise the productivity of the catchment's sandy soils by improving the water retention characteristics.

4.3.2. Sediment Bulk Density

The degree of compaction in sediments is measured by bulk density, which may not be determined by grain size analysis, (Wiesebron *et al.*, 2021). Wiesebron *et al.* (2021) also mentioned that the sediment bulk density range has some spatial orientation. The sediment bulk density measurements in this investigation well explained this proposition (table 4.4). Statistically, compacted sandy sands have bulk density range of between 1 and 2 g.cm⁻³, whereas softer sediments with increased mud fractions have a bulk density range of between 0.2 and 1.5 g.cm⁻³, (Stringer *et al.*, 2016). Bottom sediments were discovered to be rather muddy in this investigation, hence the mean bulk density (0.620±0.044 g.cm⁻³) was found to be within the reported range.

4.3.3. Sediment pH

The pH level for the reservoir bottom sediments was 6.63±0.151 on average. According to Boyd (1995), the pH level in most lakes and reservoirs is from 4 to 9, hence, the study's findings were determined to fall within that range. Different researchers have reported similar pH values in reservoirs, (Wondim &

Mosa, 2015; Wójcikowska-Kapusta *et al.*, 2018; Hoque *et al.*, 2021). The average sediments pH in this particular reservoir was somewhat acidic, which indicated the presence of soil additions and nutrients, (Donahue *et al.*, 1983). Acidic conditions are most likely caused by the acidic character of organic materials, as well as high quantities of aluminum and iron oxides, (Fonseca *et al.*, 1998). Basically, the pH test for the reservoir bottom sediments tries to link the existence of aquatic life in various environments, (Urgesa & Yilma, 2015; Boyd *et al.*, 2002). Therefore, pH is basically an index that represents the parameters associated with possible nutrient release, soil physical state, in addition toxic material effects, (Sharma *et al.*, 2013). Hence, pH as a parameter plays an essential role in determining the quality of sediments, (Wondim & Mosa, 2015; Arofi *et al.*, 2019). It is impossible to determine the catchment's land use patterns from the pH changes because they are not substantial, (Hoque *et al.*, 2021). As a result of the favorable balance that would probably have existed between organic matter material and organic carbon resulting from agricultural and forestry activities within the catchment, the pH state in the reservoir may have prevailed, (Wondim & Mosa, 2015). Furthermore, Table 4.4 showed that the pH values fluctuated from 6.5 to 8.5, and these are the suggested range for aquatic life survival, (WHO, 2014). The pH range further revealed that there are relatively few activities that promote catchment degradation, which is likely due to the fact that erosion processes largely contribute to alkalinity in both sediments and water bodies, (Gerla *et al.*, 2003).

4.3.4. Electrical Conductivity

Water reservoirs are hydraulic structures that are commonly associated with human settlements, industrial, and agricultural operations, (Diatta *et al.*, 2014). These hydraulic structures, particularly the shallow ones, are extremely vulnerable to large chemical and biological changes. The hydrochemistry of the reservoir is influenced by streamflow conditions, which have some direct interaction with reservoir bottom sediments, (Rabajczyk *et al.*, 2011). The number quantity of dissolved solids in a substance is measured using electrical conductivity, (Singare *et al.*, 2011; Chukwuemeka *et al.* 2017). Plants and animals suffer from physiological problems caused by an ion imbalance in the soil or water. The reservoir bottom sediments had an average electrical conductivity of $0.225 \pm 0.059 \text{ dS.m}^{-1}$. In their investigation in Lake Tana, Ethiopia, (Wondim & Mosa, 2015) found similar results. According to Pagenkopf (1978), most natural waters have electrical conductivity values ranging from 0.05 to even 0.5 dS.m^{-1} , with highly mineralized natural waters having values that reach 1 dS.m^{-1} . In this context, the the electrical conductivity for the bottom sediments suggested that the catchment was subjected to moderate human-related pressure, (Diatta *et al.*, 2014).

4.3.5. Organic Matter Content

The surface between the sediment and the water column is quite an important section because it has an influence on numerous processes that take place in different bodies of water, (Tomczyk-Wydrych *et al.*, 2021). Allochthonous and

even autochthonous organic substances can accumulate on this surface, (Avnimelech *et al.*, 2001). Organic matter buildup is periodic until it reaches steady-state conditions, which is determined by accumulation and sedimentation rates. Some basic features, such as adsorption capacity, are said to be influenced by the amount of organic material in sediments. The reservoir's average organic matter level was found to be 2.10 ± 0.199 % (table 4.3). Organic matter levels in typical soils should be between 2 and 7 %, (Donahue *et al.*, 1983). Sandy sediments, on the other hand, have a low organic material concentration, with less than 2 %, (Donahue *et al.*, 1983). Organically rich sediments, according to Griggs (1975), have an organic matter level more than 1 %. Going by this description, the bottom sediments in the reservoir were classified as organically rich. Essentially, organic material is added to the surface of the bottom soil via sedimentation in the reservoir, (Avnimelech *et al.*, 2001). A high energy level in the reservoir could have resulted in an elevated level of allochthonous organic materials in the reservoir environment, (Wondim & Mosa, 2015; Fonseca *et al.*, 1998). Agricultural as well as forestry activities within the catchment area are among possible sources of organic materials in the reservoir, (Sha'Ato *et al.*, 2020). In the dam reservoir, urban runoff was also cited as a possible source of organic materials, (Waltham *et al.*, 2014). Basically, the horizons layers of accumulated sediment are cut off from the organic material source. Sediment decomposition and nutrient recycling are hindered in these layers due to a lack of dissolved oxygen, (Hoque *et al.*, 2021). The decomposition of organic molecules causes an

increase in carbon concentration in sediments, (Arofi *et al.*, 2019). As a result, bottom sediment's organic carbon (OC) as well as organic matter (OM) are considered key biological factors that reveal land use patterns in a dam catchment's upper reaches, (Hoque *et al.*, 2021). Organic material content found in sediments is linked to total nitrogen, which serves as an indicator of ecosystem health, (Mondol *et al.*, 2014). Organic matter promotes cation exchange, which helps in the decomposition of non-living algae on the reservoir bottom, in which case oxygen is utilized and hazardous gases like ammonia, carbon dioxide, and hydrogen sulfide are released, (Boyd, 1995).

4.3.6. Macronutrients

The bottom sediments contained 0.458 ± 0.026 % potassium, 0.124 ± 0.018 % nitrogen, and 12.809 ± 2.164 mg.kg⁻¹ of phosphorous, respectively. These values were quite low, according to Matej-Lukowicz *et al.* (2021), when compared to single-nutrient or even multi-nutrient fertilizers. Increased human influence within the catchment area is indicated by the percentage of macronutrients found within the reservoir, (Katarzyna *et al.*, 2017). Both domestic as well as urban waste emanating from the surrounding Machakos town could have been some of the possible origins of the measured nutrient content. Additionally, surface runoff water from agricultural fields may have contaminated the reservoir with contaminants such as fertilizers and above all, pesticides. As a result, the dam reservoir is likely to be heavily polluted and contaminated with biogenic chemicals. The macronutrient content was noted to be relatively higher close to

the dam embankment in the study; similar findings were observed by, (Wójcikowska-Kapusta *et al.*, 2018). The surface movement of runoff water into the reservoir especially during flood flows most likely caused this phenomenon.

In terms of sediments, organic matter is described as a nutrient reservoir that stores and binds nutrients together, ensuring that they are not always available, (Wondim & Mosa, 2015). The amount of nitrogen in bottom sediments reveals a lot about the organic content of the sediment, (Mielnik *et al.*, 2009). In this regard, large quantities of protein in organic matter are connected with high levels of nitrogen in bottom sediments, (Mielnik *et al.*, 2009; Wondim & Mosa, 2015). The activities associated with aquatic species and most importantly, the decomposition of both floral and faunal remains contribute to the high protein content of organic materials. When compared to organic sources, the phosphorus concentration from inorganic sources, notably farming activities (phosphorous fertilizers), is quite low, (Wondim & Mosa, 2015). Phosphorous mineral rarely exists in a gaseous state, hence there is no phosphorous cycle like there is for nitrogen. Hence, phosphorus accumulates within bottom sediments as a nutrient and is released at much slower rates into the reservoir water as organic material is oxidized, (Ziemiska-Stolarska *et al.*, 2020).

4.3.7. Correlations

The electrical conductivity as well as the level of macronutrients especially N, P, and K in the sediments were influenced by the properties of the reservoir bottom

sediments, especially the sediment particle grains, organic matter, and sediment pH. Nitrogen (N) and silt were shown to have a modest relationship. Similarly, exceedingly weak correlations appeared between K nutrient and clay and silt grains and N; sediment pH and silt grains, N; total organic material and sand grains, N and K; P and sand grains; electrical conductivity and sand grains, silt grains, bulk density, pH, and P. Table 4.5 illustrates that nitrogen adsorbs on silt grains and, to a much lesser extent on sand grains, whereas potassium adsorbs on organic materials. Similarly, organic matter has been identified as the primary source of phosphorus in bottom sediments, (Baran *et al.*, 2011). Silt particles may have adsorbed acidic cations, explaining the link between silt grains and the sediment pH. As a result, finely grained sediment particles and more importantly, organic matter characteristics may have an impact on macronutrient availability in reservoir bottom sediments.

Table 4.5: Correlation matrices between physicochemical properties of bottom sediments of Maruba Reservoir

	Sand	Clay	Silt	N	K	OM	sBD	pH	P	EC
Sand	1.000									
Clay	-0.526	1.000								
Silt	-0.269	-0.677	1.000							
N	0.159	-0.593	0.534	1.000						
K	-0.190	0.042	0.117	0.203	1.000					
OM	0.092	-0.009	-0.070	0.187	0.439	1.000				
sBD	0.225	-0.019	-0.173	-0.106	-0.520	-0.488	1.000			
pH	-0.257	-0.218	0.470	0.473	-0.008	-0.344	0.110	1.000		
P	0.336	-0.230	-0.030	0.100	-0.165	0.313	-0.094	-0.560	1.000	
EC	0.203	-0.283	0.145	-0.029	-0.702	-0.485	0.413	0.175	0.026	1.000

4.4. Physicochemical Characteristics of Sediments at the Reservoir's inlet

Table 4.5 summarizes the basic classical statistics of some selected physicochemical sediment parameters measured at the deposition region in the reservoir inlet. With a CV of more than 0.35, the more variable sediment parameters were found to be percent silt at the subsurface layer, penetration resistance, hydraulic conductivity, electrical conductivity, percent nitrogen at the surface layer, and phosphorous content at the surface layer. Both environmental and anthropogenic factors were associated with the variation, (Turgut *et al.*, 2015; Kazberuk *et al.*, 2021). Furthermore, the chemical characteristics' fluctuation reflected the nature of alluvium and colluvium sediment deposits, (Moghimi *et al.*, 2013).

Table 4.6: Physicochemical properties of sediments deposited at the reservoir inlet

Sediment Property	Layer	Min	Max	Mean	SD	CV
Sand content (%)	Surface	40.30	70.30	50.60	11.50	0.23
	Subsurface	42.50	78.30	58.60	11.30	0.19
Clay content (%)	Surface	19.20	33.20	27.00	6.20	0.23
	Subsurface	16.20	30.20	23.20	4.70	0.20
Silt content (%)	Surface	8.70	30.30	22.40	6.40	0.29
	Subsurface	4.70	27.30	18.20	6.90	0.38
Bulk density (g.cm ⁻³)	Surface	1.10	1.38	1.22	0.08	0.06
	Subsurface	1.01	1.23	1.14	0.09	0.08
Porosity (%)	Surface	48.10	58.70	54.10	2.85	0.05
	Subsurface	53.40	62.00	57.10	3.23	0.06
Hydraulic conductivity (cm.hr ⁻¹)	Surface	0.07	0.73	0.35	0.25	0.71
	Subsurface	0.08	0.53	0.29	0.16	0.55
Penetration resistance (kPa)	Surface	98.00	3727.00	1563.20	1284.30	0.82
	Subsurface	75.50	2314.00	916.50	701.60	0.77
pH	Surface	6.17	6.60	6.30	0.20	0.03
	Subsurface	6.40	6.77	6.61	0.18	0.03
Electrical conductivity (dS.m ⁻¹)	Surface	0.18	0.52	0.39	0.16	0.41
	Subsurface	0.14	0.79	0.39	0.28	0.72
Organic matter (%)	Surface	1.11	2.55	1.91	0.60	0.31
	Subsurface	1.41	2.15	1.80	0.32	0.18
Nitrogen content (%)	Surface	0.03	0.14	0.11	0.05	0.45
	Subsurface	0.07	0.12	0.10	0.02	0.21
Phosphorous (mg.kg ⁻¹)	Surface	11.36	28.22	17.51	7.40	0.42
	Subsurface	11.36	16.53	13.16	2.40	0.18
Potassium (%)	Surface	0.25	0.46	0.38	0.09	0.24
	Subsurface	0.32	0.60	0.43	0.12	0.28

4.4.1. Sediment Texture

Some soil variables including permeability, infiltration capacity, structure, surface runoff, and above all, consistency are just a few that are controlled by soil textural qualities, (Kusumandari, 2014). Therefore, sediment textural features are useful instruments for assessing the effects of sediment focussing and slumping, and most importantly, inhomogeneity in the make of sediments. Uneven particle size

distribution has the ability to affect a number of soil physical characteristics, (Nsabimana *et al.*, 2020). The average proportions of sediment particles (sand, clay, and silt) in the surface horizon were 50.60 ± 11.50 , 27.40 ± 6.20 , and 22.40 ± 6.40 %, respectively, while the subsurface horizon had 58.60 ± 11.30 , 23.20 ± 4.70 , and 18.20 ± 6.90 %. The subsurface recorded the lowest sand fraction but the highest fractions of clay and silt. In both strata, sand was the most predominant soil particle, with both clay and silt fractions being less common. The sediments at reservoir inlet were categorized as basic light soil due to the sediments' high sand proportion compared to clay, (Kusumandari, 2014). Both the surface and subsurface horizons have sandy clay loam as the major textural class. The amount of sand in the sediment increased with depth, although the clay and silt fractions decreased. This phenomenon may be a sign of eluviation and above all illuviation processes. Buurman *et al.* (1998) claim that translocated clay occurs in sandy material as coatings on the surface of sand grains and even pebbles as well as as bridges between the grains, where the inter-granular space eventually fills up completely. Such clay coatings within the sediments have been attributed to the process of illuviation by soil scientists, which mostly takes place within the surface and even some several meters below, (Buurman *et al.*, 1998). The mechanical infiltration mechanism in muddy overland flow has also been recognized by geologists as the cause of coatings of translocated clay in coarse sediments, (Buurman *et al.*, 1998). Climate influences the clay illuviation process,

and it is most importantly only allowed in the vadose zone, (Buurman *et al.*, 1998).

Sandy soils have a low cohesion, making them more sensitive to eroding processes that cause separation and transport, resulting in sediment formation. Furthermore, higher quantities of sand are linked to increased permeability, resulting in a landslide effect and increased erosion, (Idah *et al.*, 2008). This is a very common occurrence with deposited sediments. Unlike sand grains, whose deposition occurs at the catchment outlet, a high fraction of finely grained sediments, primarily clay and even silt, are transported into the reservoir. The ability of the sediment to hold a significant volume of water, allow for water movement, be adequately workable, and, most importantly, be fruitful is controlled by its texture. As a result, finely grained particles have an impact on the soil's plastic index and permeability. Therefore, a higher proportion of finely grained sediment particles obstruct water transport through the soil medium, (Iradukunda & Nyadawa, 2021).

4.4.2. Sediment pH and Electrical Conductivity

The average pH of the sediments at the surface as well as the subsurface horizons was 6.30 ± 0.20 and 6.61 ± 0.18 , respectively. In the catchment area, where farming activities are the primary land uses, somewhat acidic conditions would have been linked to farming activities. The sediment pH could have resulted from mineral composition and weathering reactions due to erosion and deposition processes,

(Oshunsanya, 2018). Further, the slightly acidic conditions would have been brought about by the effects of high rainfall, fertilizer use, acid rain as well as oxidative weathering, (Oshunsanya, 2018). The pH changes in both strata may have been influenced by water circulation within the deposition area, (Hoque *et al.*, 2021).

On the other hand, the mean electrical conductivity both at the surface and the sub-surface horizons was 0.39 ± 0.16 and 0.39 ± 0.28 dS.m⁻¹, respectively. This showed that the presence of cations and anions was independent of sediment grain size. According to the results, electrical conductivity of the sediments does not indicate a highly mineralized environment (<1 dS.m⁻¹), (Pagenkopf, 1978).

4.4.3. Bulk Density and Porosity

One of the most fundamental physical qualities of soil is bulk density, which is closely related to porosity, (Huang *et al.*, 2021). The soil bulk density has an impact on the soil's ability to retain water as well as its permeability. The surface and subsurface soil sediment layers had mean bulk densities of 1.22 ± 0.08 and 1.14 ± 0.09 g.cm⁻³, respectively. In this study, it was noted, however, that the sediment bulk density was much higher on the surface horizon. The reported bulk density values suggested a binding effect that would probably been caused by presence of clay particles, which made the sediments probably less prone to erosion, (Manyiwa & Dikinya, 2013). The decrease in sediment bulk density can be explained by the fact that the sand component of sediments increased with

depth. The mean porosity for the surface and subsurface horizons, on the other hand, was 54.10 ± 2.85 and 57.10 ± 3.23 %, respectively. It was established that the relationship between sediment bulk density and porosity was inverse.

4.4.4. Sediment Permeability

The texture and structure of the soil have a big impact on its permeability. The rate at which water percolates through a specific soil media is measured by permeability, (Iradukunda & Nyadawa, 2021). It is determined by the texture, structure, and bulk density of the soil, (Kusumandari, 2014). Whenever a large storm occurs, a perched watertable was likely to build in the low-permeability subsurface zone, (Kusumandari, 2014). In this regard, infiltration is hindered, and as such, surface runoff volume becomes a main conduit for hydrologic fluxes, leading to increased erosion of deposited sediments, (Kusumandari, 2014). The surface and subsurface horizons have mean permeability values of 0.35 ± 0.25 and 0.29 ± 0.16 cm.hr⁻¹, respectively. The sediments' hydraulic conductivity was determined to be relatively poor. This was attributable to the sediments' comparatively large proportion of fine-grained particles.

4.4.5. Sediment Organic Matter

Organic material in the soil is a significant component that comes from some biological sources, both living and non-living, (Morris & Fan, 1998). It is a key soil characteristic that binds soil aggregates together, making them more stable, (Nsabimana *et al.*, 2020). The occurrence of organic material in a soil is a great

indicator of the state of the soil's health because its effects may be found in the numerous qualities and most importantly, the functions of the soil, (Lin *et al.*, 2019). Any undecomposed organic substance on a given soil surface aids in absorbing the kinetic energy possessed by the raindrops, whereas highly decomposed organic material (humus) bonds soil particles, (Manyiwa & Dikinya, 2013; Kusumandari, 2014). However, because flood water is the primary eroding agent, this phenomenon may not necessarily apply to some deposited soil. The amount of organic material in the soil has an impact on its permeability because it makes a particular soil medium more porous. Contrarily, reduced organic material in soils results in decreased porosity as well as higher bulk density, resulting in decreased infiltration. The mean organic matter percentage of the surface and subsurface sediment layers was 1.91 ± 0.60 and 1.80 ± 0.32 %, respectively. Most sandy soils and sandy loams, according to Idah *et al.* (2008), have low organic matter concentration, typically less than 2 %. Low contents of organic matter were found in the deposition area, according to the findings. The very low organic matter percentages are typical of deposited sediments at catchment outflows. This scenario could be linked to disturbances caused by recurrent storms, in which the majority of organic content ends up in the receiving water body, (N'doufou *et al.*, 2022). Furthermore, because mineralization was impeded due to poor aeration conditions, the higher percentage of clay fraction within the surface layer could have resulted in higher organic matter content, (Turgut *et al.*, 2015).

4.4.6. Penetration Resistance

Penetration resistance in soils is a parameter that helps to predict the ease with which plant roots would penetrate through, (Thomas *et al.*, 2020). For the surface and subsurface horizons, the average penetration resistances were 1546 ± 1290 and 1145 ± 1040 kPa, respectively. These values of penetration resistance were less than 2000 kPa in both layers, which is below the level that would impede plant root growth, (Kuhwald *et al.*, 2020). The penetration resistance of the surface horizon was the highest. This could be due to a compacted layer in the topsoil. It is indeed possible that the compaction was caused by animal traffic in the deposition area. Penetration resistance in a given soil medium has a direct relationship with bulk density. This was backed up by the findings of this study, where both parameters decreased with depth, (Thomas *et al.*, 2020). However, high levels of soil bulk density and penetration resistance may not have indicated severe soil compaction, (Kuhwald *et al.*, 2020).

4.4.7. Micronutrients

The mean concentrations of nitrogen, phosphorus, and potassium in the deposited sediments were 0.11 ± 0.05 and 0.10 ± 0.08 %, 17.51 ± 7.40 and 13.16 ± 2.40 mg.kg⁻¹, and 0.38 ± 0.09 and 0.43 ± 0.12 % for surface and subsurface horizons, respectively, according to chemical analyses. The concentrations of nitrogen and phosphorus within the surface horizon, but the opposite happened for potassium. Sediment deposition happens during storm occurrences, and as such is thought to be an irregular process, resulting in nutrient concentration variations. Finer particles are

frequently moved more than coarse particles, which is a sign of density current, (Junakova & Balintova, 2012). The deposition of fine-grained particles ends when the density current stops. This explains why the deposition area has the highest nutrient concentration, (Junakova & Balintova, 2012).

4.4.8. Comparison between Reservoir Bottom Sediments and Sediments at the Reservoir Inlet

The comparison between the physical and chemical characteristics of bottom sediments and those found at the reservoir inlet is shown in Table 4.7 below.

Table 4.7: Reservoir bottom sediments vs. sediment deposits at reservoir's inlet

Sediment type	Sand (%)	Clay (%)	Silt (%)	N (%)	P (mg.kg ⁻¹)	K (%)	sBD (g.cm ⁻³)	OM (%)	pH	EC (dS.m ⁻¹)
BS	39.75	56.31	3.94	0.12	12.81	0.46	0.62	2.10	6.63	0.22
	±	±	±	±	±	±	±	±	±	±
	1.95	2.58	2.12	0.018	2.16	0.026	0.044	0.199	0.151	0.059
DS	54.60	25.10	20.30	0.10	15.34	0.40	1.18	1.86	6.46	0.39
	±	±	±	±	±	±	±	±	±	±
	11.40	5.45	6.65	0.035	4.9	0.105	0.085	0.46	0.19	0.22

Key: BS – bottom sediments; DS – deposited sediments at reservoir inlet

Sediment transport patterns may have aided in the transfer of nutrients and, more importantly, served as a sink for various contaminants, (Moura *et al.*, 2020). In addition to their transformed equivalents, the size of sediment particles is an important textural property of various fragmented materials. This comparison clearly revealed the sediment movement patterns under storm rainfall. The particle size distribution in both sediment types showed some significant sedimentary variability due to spatial and seasonal variations in stream hydraulic

flow, which result in different energy conditions inside the reservoir. Similarly, when discharge is limited, the interaction between stream water and the channel bed results in sediment deposition at the reservoir's inlet. The findings reveal that finer grained particles are carried more than coarsely grained particles, (Fonseca *et al.*, 2009). The particle size measurements for bottom sediments reveal a medium-to-poor categorization, with saltation and suspension as the primary transport modes. The first is linked to fine-grained sands and silts, while the second is linked to clay, (Manassero *et al.*, 2008). Bottom sediments included 56.31 ± 2.58 % clay particles, while deposited sediments at the reservoir inlet had a 25.10 ± 5.45 % clay fraction, according to the study.

Bottom sediments had more nitrogen (N), potassium (K), organic matter content, and sediment pH than deposited sediments near the reservoir inlet, according to the comparison. This finding suggested that the finely grained particles had a substantial association with the nutrient concentration in bottom sediments, (Junakova & Bantilova, 2012). Furthermore, various environmental circumstances, hydrology, and structural aspects of the reservoir may have contributed to the differential in nutrient accumulation in the examined sediments, (Smal *et al.*, 2013). The results for phosphorus, bulk density, and electrical conductivity, on the other hand, showed that sediment deposition at the reservoir's inlet were higher than those in the bottom sediments. According to Smal *et al.* (2013), phosphorus concentrations were found to be quite high at the reservoir's inlet and near the dam wall. The first observation was related to external

phosphorous loading due to stream transport dynamics, and the second to phosphorous presence in an adsorbed form in finely grained particles, according to the study. This explanation could potentially be related to the findings of this study.

The presence of oxygen in sediment, organic matter, and chemistry are all affected by bulk density, which is said to have an inverse relationship with sediment porosity, (Dowd *et al.*, 2014). The bottom sediments were linked to notable mud fractions, which explained why the bulk density ranged from 0.2 to 1.5 g.cm⁻³, as reported by Andersen *et al.* (2005) and Stringer *et al.* (2016). The highest mean bulk density of deposited sediments at the reservoir entrance, on the other hand, was found to be 1.22 g.cm⁻³ at the surface horizon, which was within the range of 1 and 2 g cm⁻³, (Stringer *et al.*, 2016).

The mean electrical conductivity of bottom sediments (0.22±0.059 dS.m⁻¹) was nearly half that of deposited sediments at the reservoir inlet (0.39±0.22 dS.m⁻¹), indicating that there was little mineral activity in the reservoir environment, (Pagenkopf, 1978). The catchment area was found to be under considerable human pressure, according to the level of mineralization by both sediment types, (Diatta *et al.*, 2014). The variation in electrical conductivity, on the other hand, would have been caused by sedimentation during storm rainfall. The entire reservoir inlet floods during such intense storms, and after the waters subside, the

stream returns to its natural channel. This would have resulted in the deposition of dissolved solids-rich sediments.

The mean sediment pH for bottom sediments and sediment deposits at the reservoir inlet were 6.63 ± 0.151 and 6.46 ± 0.19 , respectively. The mean pH of bottom sediments was found to be within the acceptable range (6.5–8.5) for aquatic life, according to WHO (2004). Contrarily, the mean pH of the sediments that had been deposited at the reservoir inlet was slightly below the permissible limits. The pH difference between the two sediment types was attributed to the reservoir environment, where organic matter breakdown may have resulted in a modest increase in sediment pH, (Fonseca *et al.*, 1998).

The mean organic matter content of bottom sediments and deposited sediments at the reservoir entrance was 2.10 ± 0.199 % and 1.86 ± 0.46 %, respectively. Organic content was definitely related with finely grained particles in this comparison. The contrast further supports the idea that sandy sediments are characterized by lower levels of organic matter, often less than 2%, as sediments deposited near the reservoir inlet are relatively sandy, (figure 4.15).

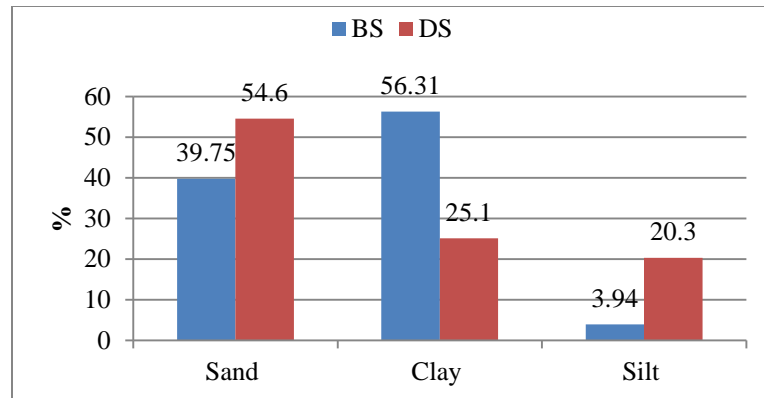


Figure 4.15: Particle size distribution in sediments

4.4.9. Beneficial use of Sediments

The macronutrient concentrations of the reservoir bottom sediments are comparable to those found in prior studies, (Fonseca *et al.*, 1998; Canet *et al.*, 2003; Baran *et al.*, 2011), in which bottom sediments were suggested for agricultural purpose and restoration of degraded lands. This suggests that the reservoir bottom sediments in this research may potentially be used to boost farming activities within the catchment region and more importantly to rehabilitate the dam's surrounding desolate land, (Tomczyk-Wydrych *et al.*, 2021).

The surrounding area of the dam reservoir is classified as having a substantial amount of bare ground, demanding quick restoration, according to some land use categorization conducted in this study (figure 4.8). Therefore, reservoir sediments could be used biotically to improve forestry activities and vegetation cover surrounding the dam, according to this study. Consequently, bottom sediments by virtual of them having high clay content (56%), they could potentially be used to

improve the productivity of the catchment's sandy soils. On the other hand, figure 4.15 further showed that the sediment deposits at the reservoir inlet were quite sandy. This would necessitate the local government authority's coordination of sand harvesting activities as a way of dam reservoir management. This process would boost the reservoir's storage capacity while also providing economic benefits to the community and local government.

4.5. Contributions to Knowledge and Innovative Aspects

The study's contribution to knowledge is summarized below:

1. Reservoirs located in small catchments lose about 1 % of their storage capacity annually.
2. The RUSLE model can be evaluated through a comparison of the model's prediction of sediment yield with measurements derived from bathymetric survey based on the multifrequency acoustic profiling system.
3. The RUSLE model underestimates the sediment yield in small catchments.
4. The reservoir sedimentation rate approach provides an accurate estimate of sediment yield in small catchments.
5. The sedimentation status of reservoirs in small catchments should be estimated within a 10-year period.

CHAPTER FIVE: CONCLUSIONS AND RECOMMENDATIONS

5.1. Conclusions

1. The Maruba dam catchment's average annual soil loss potential was adequately modelled. According to the study, a combination of the RUSLE model, remote sensing and most importantly, geographical information system resulted in a methodology for predicting spatial soil loss.
2. The current bathymetry of Maruba dam reservoir is mostly the result of high rates of sedimentation caused by surface runoff. Therefore, estimated sediment accumulation rate within the dam reservoir explains the level of anthropogenic activity in the catchment area. The study found out that acoustic and sediment core data can be used together to determine the sedimentation state of a reservoir. A multi-frequency APS offers a direct way to measure the spatial variation of sediment material in dam reservoirs and, more importantly, an accurate way to estimate the generation of sediment material in small catchments.
3. The sediments at the reservoir inlet had higher sand proportion than the reservoir bottom sediments, which had a higher percentage of clay. However, it was discovered that the concentration of macronutrients in the reservoir sediments was fairly low, suggesting that the reservoir's condition was good due to the low nutrient enrichment, particularly phosphorus. The low nutrient content further suggested that damaged

areas in the dam reservoir catchment may be restored, as well as the sandy soils of the catchment, and that bottom sediments could be used in agriculture as fertilizing medium upon enrichment. The sandy sediments at the reservoir inlet also suggested that sand harvesting might be explored for some financial gains after sediment drenching, which would aid in the management of the dam reservoir.

4. The bathymetric survey and the RUSLE model's estimated sediment yields revealed some wide variation. Sediment yield in small catchments was found to be underestimated using the RUSLE model. As a result, it was concluded that the reservoir sedimentation status technique was the most accurate method for estimating sediment yield in small catchments.

5.2. Recommendations

5.2.1. Recommendations for Policy

1. The spatial determination of soil loss within the Maruba dam catchment was a significant step toward developing a comprehensive, long-term management strategy. Higher-risk areas for soil erosion, such as those near mountainous terrains, must be prioritized for conservation.
2. The current bathymetric condition of the Maruba dam reservoir gave essential information that would aid in the creation of policies for the Maruba dam reservoir's management. The study suggests that the interested parties make use of the scientific data for improved dam reservoir and catchment area management.

5.2.2. Recommendations for Future Research

1. An assessment of nutrient release by bottom sediments into the water column in order to determine how nutrients affect water quality.
2. A detailed study of the eluviation and illuviation processes in deposited sediments at the reservoir inlet.

REFERENCES

- Abdo, H.G. and Hassan, R.M. (2018). A Statistical-spatial modeling of soil erosion: case study of Al-Sen basin, Tartous, Syria. *J. Environ Geol.*, 2(2):68–74.
- Abdo, H. and Salloum, J. (2017). Mapping the soil loss in Marqya basin: Syria using RUSLE model in GIS and RS techniques. *Environ Earth Sci.*, 76, 114. <https://doi.org/10.1007/s12665-017-6424-0>
- Abraham, J. (2013). Organic carbon estimations in soils: analytical protocols and their implications. *Rubber Science*, 26: 45–54.
- Adongo, A.T., Kyei-Baffour, N., Abagale, K.F., and Agyare, A.W. (2020). Assessment of reservoir sedimentation of irrigation dams in northern Ghana. *Lake and Reservoir Management*, 36(1): 87–105. <https://doi.org/10.1080/10402381.2019.1659461>
- Aga, O.A., Melesse, M.A., and Chane, B. (2020). An Alternative Empirical Model to Estimate Watershed Sediment Yield Based on Hydrology and Geomorphology of the Basin in Data-Scarce Rift Valley Lake Regions, Ethiopia. *Geosciences*, 10, 31. <https://doi.org/10.3390/geosciences10010031>
- Agarwal, D., Tongaria, K., Pathak, S., Ohnri, A., and Jha, M. (2016). Soil erosion mapping of watershed in Mirzapur district using RUSLE model in GIS environment. *International Journal of Students' Research in Technology & Management*, 4(3): 56–63. <http://doi.org/10.18510/ijstrtm.2016.433>
- Agesa, B.L., Onyango, C.M., Kathumo, V.M., Onwonga, R.N., and Karuku, G.N. (2019). Climate Change Effects on Crop Production in Yatta sub-County: Farmer Perceptions and Adaptation Strategies. *Afr. J. Food Agric. Nutr. Dev.*, 19(1):14010-14042. <http://doi.10.18697/ajfand.84.BLFB1017>
- Aglanu, M.L. (2014). Watersheds and Rehabilitations Measures - A Review. *Resources and Environment*, 4(2): 104–114. <http://doi.org/10.5923/j.re.20140402.04>
- Akrasi, S.A. (2011). Sediment Discharges from Ghanaian Rivers into the Sea. *West African Journal of Applied Ecology*, 18: 1–13.

- Akrasi, S.A. (2005). The assessment of suspended sediment inputs to Volta Lake. *Lakes and Reservoirs: Research & Management*, 10: 179–186.
- Aksoy, H. and Kavvas, M.L. (2005). A review of hillslope and watershed scale erosion and sediment transport models. *Catena*, 64: 247–271.
<http://doi.org/10.1016/j.catena.2005.08.008>.
- Alemaw, F.B., Majauale, M., and Simalenga, T. (2013). Assessment of Sedimentation Impacts on Small Dams -A Case of Small Reservoirs in the Lotsane Catchment. *Journal of Water Resource and Protection*, 5: 1127–1131.
- Alewell, C., Borrelli, P., Meusburger, K., and Panagos, P. (2019). Using the USLE: Chances, challenges and limitations of soil erosion modelling. *International Soil and Water Conservation Research*, 7: 203–225.
<https://doi.org/10.1016/j.iswcr.2019.05.004>
- Ali, M. and Shakir, S.A. (2018). Sustainable sediment management options for reservoirs: a case study of Chashma Reservoir in Pakistan. *Applied Water Science*, 8, 103. <https://doi.org/10.1007/s13201-018-0753-3>
- Allen, P.B. and Naney, J.W. (1991). Hydrology of the Little Washita River Watershed, Oklahoma. United States Department of Agriculture, Agricultural Research Service, ARS-90, p. 74.
ftp://164.58.150.49/pub/little_washita/ars-90.pdf.
- Amah, I.J., Aghamelu, P.O., Omonona, V.O., and Onwe, M.I. (2020). A Study of the Dynamics of Soil Erosion Using Rusle2 Modelling and Geospatial Tool in Edda-Afikpo Mesas, South Eastern Nigeria. *Pakistan Journal of Geology*, 4(2): 56–71.
- Andersen, T. J., Lund-Hansen, L. C., Pejrup, M., Jensen, K. T., and Mouritsen, K. N. (2005). Biologically induced differences in erodibility and aggregation of subtidal and intertidal sediments: a possible cause for seasonal changes in sediment deposition. *J. Mar. Syst.*, 55:123–138.
<http://doi.10.1016/j.jmarsys.2004.09.004>.
- Anderson, J. R. (1976). A land use and land cover classification system for use with remote sensor data, US Government Printing Office, 964.

- Angima, S., Stott, D., O'Neill, M., Ong, C., and Weesies, G. (2003). Soil Erosion Prediction Using RUSLE for Central Kenyan Highland Conditions. *Agricultural, Ecosystems and Environment*, 97:295–308.
[https://doi.org/10.1016/S0167-8809\(03\)00011-2](https://doi.org/10.1016/S0167-8809(03)00011-2)
- Annandale, G. (2014). Sustainable water supply, climate change and reservoir sedimentation management: Technical and economical viability. In A. J. Schleiss, G. De Cesare, M. J. Franca, & M. Pfister (Eds.), *Proceedings of River Flow 2014, Special Session on Reservoir Sedimentation* (pp.3–10). Leiden: CRC Press/Balkema
- Armin, M., Bazgir, M. and Velayatinejad, A.S. (2018). Using a special empirical model to estimate sediment yield of Koohbord dam watershed in Kohgiluyeh County. *Quarterly Journal of Environmental Erosion Research*, 30(8:2): 23–42
- Arofi, S., Rahman, M.M., Shiragi, H.K., Alam, M.A., Islam, M.M. and Biswas, J.C. (2019). Aggregate stability in soils of twelve agro-ecological zones of Bangladesh based on organic carbon and basic cations. *Ann. Bangladesh Agric.*, 23: 27–36.
- Asadi, H., Honarmand, M., Vazifiedoust, M., and Mousavi, A. (2017). Assessment of Changes in Soil Erosion Risk Using RUSLE in Navrood Watershed, Iran. *Journal of Agricultural Science and Technology*, 19: 231–244.
- Ascough, C.J., Flanagan, C.D., Tatarko, J., Nearing, A.M., and Kipka, H. (2017). Soil Erosion Modeling and Conservation Planning. *Precision Conservation: Geospatial Techniques for Agricultural and Natural Resources Conservation* J. Delgado, G. Sassenrath, and T. Mueller, editors. *Agronomy Monograph*, 59.
<http://doi.org/10.2134/agronmonogr59.2013.0011>
- Askari, A.O.K. (2017). Using SWAT Model to Determine Runoff, Sediment Yield in Maroon-Dam Catchment. *International Journal of Research Studies in Agricultural Sciences*, 3(12):31–41
- Asselman, N.E.M. (2000). Fitting and interpretation of sediment rating curves. *Journal of Hydrology*, 234, 228–248.

- Atreya, K.; Sharma, S.; Bajracharya, R.M., and Rajbhandari, N.P. (2008). Developing a sustainable agro-system for central Nepal using reduced tillage and straw mulching. *J. Environ. Manag.*, 88: 547–555.
- Avnimelech, Y., Ritvo, G., Meijer, L.E., and Kochba, M. (2001). Water content, organic carbon and dry bulk density in flooded sediments. *Aquacultural engineering*, 25: 25 - 33.
- Avwunudiogba, A. and Hudson, F.P. (2014). A Review of Soil Erosion Models with Special Reference to the needs of Humid Tropical Mountainous Environments. *European Journal of Sustainable Development*, 3(4): 299–310. <http://doi.org/10.14207/ejsd.2014.v3n4p299>.
- Ayalew, G. (2015). A Geographic information system based soil loss and sediment estimation in Zingin watershed for conservation planning, highlands of Ethiopia. *International Journal of Science, Technology and Society*, 3(1): 28–35. <https://doi.org/10.11648/j.ijsts.20150301.14>
- Ayalew, G. and Selassie, G.Y. (2015). Soil Loss Estimation for Soil Conservation Planning using Geographic Information System in Guang Watershed, Blue Nile Basin. *Journal of Environment and Earth Science*, 5(1): 126–134.
- Ayinla, I.A. and Jona, C.A. (2018). Prediction and Estimation of Sediments Discharge from Kangimi Dam Reservoir Catchment, Kaduna, Nigeria. *Universal Journal of Environmental Research and Technology*, 7(1): 19–37.
- Badil, Z.N., Eslamian, S., Sayyad, A.G., Hosseini, E.S., Asadilour, M., Askari, A.O.K., Singh, P.V. and Dehghan, S. (2017). Using SWAT Model to Determine Runoff, Sediment Yield in Maroon-Dam Catchment. *International Journal of Research Studies in Agricultural Sciences (IJRSAS)*, 3(12): 31–41.
- Bajracharya, R.M. and Sherchan, D.P. (2009). Fertility status and dynamics of soils in the Nepal Himalaya: A review and analysis. In *Soil Fertility*; Nova Science Publishers, Inc.: New York, NY, USA: 111–135.
- Ban, K.J., Yu, I., and Jeong, S. (2016). Estimation of Soil Erosion Using RUSLE Model and GIS Techniques for Conservation Planning from Kulekhani

Reservoir Catchment, Nepal. *J. Korean Soc. Hazard Mitig.*, 16(3): 323–330.

- Bansekhrria, A. and Bouhata, R. (2022). Assessment and Mapping Soil Water Erosion Using RUSLE Approach and GIS Tools: Case of Oued el-Hai Watershed, Aurès West, Northeastern of Algeria. *ISPRS Int. J. Geo-Inf.*, 11, 84. <https://doi.org/10.3390/ijgi11020084>
- Baran, A., Tarnawski, M., and Urbaniak, M. (2019). An assessment of bottom sediment as a source of plant nutrients and an agent for improving soil properties. *Emerging Engineering and Management Journal*, 18: 1647–1656.
- Barros, N., Cole, J. J., Tranvik, L. J., Prairie, Y. T., Bastviken, D., Huszar, V. L. M., and Roland, F. (2011). Carbon emission from hydroelectric reservoirs linked to reservoir age and latitude. *Nature Geoscience*, 4(9): 593–596. <http://doi.org/10.1038/ngeo1211>
- Bartsch, K.P., Mietgroet H.V., Boettinger J., and Dobrowolski, J.P. (2002). Using empirical erosion models and GIS to determine erosion at Camp Williams, Utah. *Journal of Soil & Water Conservation*, 57(1): 29–37.
- Basson, G. R. (2009). Management of siltation in existing and new reservoirs. General Report Q. 89. Proc. of the 23rd Congress of the Int. Commission on Large Dams CIGBICOLD, 2.
- Basson, G., Bosman, E., and Vonkeman, J. (2022). Reservoir sedimentation mitigation measures to deal with a severe drought at Graaff-Reinet, South Africa. *E3S Web of Conferences*, 346, 03012. <http://doi.org/10.1051/e3sconf/202234603012>
- Beasley, D. B., Huggins, F.L., and E. J. Monke, E.J. (1980). ANSWERS: a model for watershed planning. *Transactions of the ASAE*, 23(4): 938–944.
- Beck, C., Lutz, N., Lais, A., Vetsch, D., and Boes, R. (2016). Patind Hydropower Project, Pakistan – Physical model investigations on the optimization of the sediment management concept. *In Hydro 2016*. Montreux.
- Bečvář, M. (2006). Sediment Load and Suspended Sediment Concentration Prediction. *Soil & Water Res.*, 1:23–31

- Bekele, B. and Gemi, Y. (2020). Soil erosion risk and sediment yield assessment with universal soil loss equation and GIS: In Dijo watershed, Rift valley Basin of Ethiopia. *Modeling Earth Systems and Environment*.
<https://doi.org/10.1007/s40808-020-01017-z>
- Belay, T.H., Malede, A.D., and Geleta, B.F. (2020). Erosion Risk Potential Assessment Using GIS and RS for Soil and Water Resource Conservation Plan: The Case of Yisir Watershed, Northwestern Ethiopia. *Agriculture, Forestry and Fisheries*, 9(1):1–13.
<http://doi.org/10.11648/j.aff.20200901.11>
- Benavidez, R., Jackson, B., Maxwell, D. and Norton, K. (2018). A review of the (Revised) Universal Soil Loss Equation (R)USLE): with a view to increasing its global applicability and improving soil loss estimates. *Hydrol. Earth Syst. Sci.*, 22: 6059–6086. <http://doi.org/10.5194/hess-22-6059-2018>
- Beskow, S., Mello, C.R., Norton, L.D., Curi, N., Viola, M.R., and Avanzi, J.C. (2009). Soil erosion prediction in the Grande River Basin, Brazil using distributed modeling. *Catena*, 79(1): 49–59.
<http://doi.org/10.1016/j.catena.2009.05.010>
- Bewket, W. and Teferi, E. (2009) Assessment of Soil Erosion Hazard and Prioritization for Treatment at the Watershed Level: Case Study in the Chemoga Watershed, Blue Nile Basin, Ethiopia. *Land Degradation & Development*, 20: 609–622. <http://doi.org/10.1002/ldr.944>
- Beyene, A.A. (2019). Soil Erosion Risk Assessment in Nashe Dam Reservoir Using Remote Sensing, GIS and RUSLE Model Techniques in Horro Guduru Wollega Zone, Oromia Region, Ethiopia. *Journal of Civil, Construction and Environmental Engineering*, 4(1): 1–18.
<http://doi.org/10.11648/j.jccee.20190401.11>
- Bhat, A.S., Hamid, I., Dar, D.M., Rasool, D., Pandit, A.B., and Khan, S. (2017). Soil erosion modeling using RUSLE & GIS on micro watershed of J&K. *Journal of Pharmacognosy and Phytochemistry*, 6(5): 838–842.
- Biasutti, M. and Seager, R. (2015). Projected changes in US rainfall erosivity. *Hydrol. Earth Syst. Sci.*, 19: 2945–2961. <http://doi.org/10.5194/hess-19-2945-2015>

- Blue Sky Organics, (2019). <https://blueskyorganics.com/> Accessed on 29 October 2019.
- Boakye, E., Anornu, K.G., Quaye-Ballard, A.J., and Donkor, A.E. (2018). Land use change and sediment yield studies in Ghana: Review *Journal of Geography and Regional Planning*, 11(9): 122–133.
<http://doi.org/10.5897/JGRP2018.0707>
- Boakye, E., Anyemedu, K.O.F., Donkor, A.E., and Quaye-Ballard A.J. (2020). Spatial distribution of soil erosion and sediment yield in the Pra River Basin. *SN Applied Sciences*, 2, 320. <https://doi.org/10.1007/s42452-020-2129-1>
- Boakye, E., Odai, N., Adjei, A., and Annor, O. (2008). Landsat images for assessment of the impact of land use and land cover changes on the Berekese Catchment in Ghana. *European Journal of Scientific Research*, 22: 269–278.
- Bou-imajjane, L., and Belfoul, A. M. (2020). Soil Loss Assessment in Western High Atlas of Morocco: Beni Mohand Watershed Study Case. *Applied and Environmental Soil Science, Hindawi*, 6384176.
<https://doi.org/10.1155/2020/6384176>
- Boyce, R.C. (1975). Sediment routing with sediment delivery ratios. Present and Prospective Technology for ARS. *USDA*, Washington, D.C.
- Boyd, C.E. (1995). Bottom Soils, Sediment, and Pond Aquaculture. Chapman and Hall, New York, p. 348.
- Boyd, C.E., Wood, C.W., and Thunjai, T. (2002). Aquaculture pond bottom soil quality management. Department of Fisheries and Allied Aquacultures Auburn University, Alabama.
- Carr, W.T., Balkovič, J., Dodds, E.P., Folberth, C., Fulajtar, E., and Skalsky, R. (2020). Uncertainties, sensitivities and robustness of simulated water erosion in an EPIC-based global-gridded crop model. *Biogeosciences discussions*, 93. <https://doi.org/10.5194/bg-2020-93>
- Chadli, K. (2016). Estimation of soil loss using RUSLE model for Sebou watershed (Morocco). *Model. Earth. Syst. Environ.*, 2, 51.

<http://doi.org/10.1007/s40808-016-0105-y>

- Chakraborty, D. (2001). Characterization and spatial modeling for hydrological response behaviour of Birantiya Kalan watershed in western Rajasthan – remote sensing and GIS approach. PhD. Thesis. IARI, New Delhi, India.
- Chalise, D. and Kumar, L. (2018). Land Use Change Impacts on Soil Erosion Dynamics in Western Nepal; University of New England: Armidale, Australia.
- Chalise, D., Kumar, L., and Kristiansen, P. (2019). Land Degradation by Soil Erosion in Nepal: A Review. *Soil Syst.*, 3, 12.
<http://doi.org/10.3390/soilsystems3010012>
- Chandramohan, T., Venkatesh, B., and Balchand, A.N. (2015). Evaluation of Three Soil Erosion Models for Small Watershed. International Conference on Water Resources, Coastal and Ocean Engineering (ICWRCOE), *Aquatic Procedia*, 4: 1227–1234.
<http://doi.org/10.1016/j.aqpro.2015.02.156>
- Chanudet, V., Descloux, S., Harby, A., Sundt, H., Hansen, B. H., Brakstad, O., and Guerin, F. (2011). Gross CO₂ and CH₄ emissions from the Nam Ngum and Nam Leuk sub-tropical reservoirs in Lao PDR. *Science of the Total Environment*, 409(24): 5382–5391.
<http://doi.org/10.1016/j.scitotenv.2011.09.018>
- Chaowen, L., Shihua, T., Jingjing, H., and Yibing, C. (2007). Effects of plant hedgerows on soil erosion and soil fertility on sloping farmland in the purple soil area. *Acta Ecol. Sin.*, 27: 2191–2198.
[http://doi.org/10.1016/S1872-2032\(07\)60050-X](http://doi.org/10.1016/S1872-2032(07)60050-X)
- Chen, W. and Thomas, K. (2020). Sustainability. Revised SEDD (RSEDD) Model for Sediment Delivery Processes at the Basin Scale. *Sustainability*, 12, 4928. <http://doi.org/10.3390/su12124928>
- Chen, Z. and Shah, T.M. (2019). ‘An Introduction to the Global Soil Status’ in R Schaldach & R Otterpohl (eds), *RUVIVAL Publication Series*, 5:7–17.
<https://doi.org/10.15480/882.2339>

- Cheraghi, M., Jomaa, S., Sander, G.C., and Barry, D.A. (2016). Hysteretic sediment fluxes in rainfall-driven soil erosion: Particle size effects. *Water Resources Research*, 52 (11): 8613–8629. <http://doi.org/10.1002/2016WR019314>
- Cheruto, C.M., Kauti, K.M., Kisangau, D.P., and Kariuki, P. (2016). Assessment of Land Use and Land Cover Change Using GIS and Remote Sensing Techniques: A Case Study of Makueni County, Kenya. *J Remote Sensing & GIS*, 5(4). <http://doi.org/10.4175/2469-4134.1000175>
- Chuenchum, P., Xu, M., and Tang, W. (2020). Estimation of Soil Erosion and Sediment Yield in the Lancang–Mekong River Using the Modified Revised Universal Soil Loss Equation and GIS Techniques. *Water*, 12, 135. <http://doi.org/10.3390/w12010135>
- Chukwuemeka, A.N., Ngozi, V.E., Chukwuemeka, I.S. and Wirnkor, V.A. (2017). Physicochemical properties and selected metals in soils of Ohaji-Egbema, Imo State, Nigeria. *World News of Natural Sciences*, 10: 39–48.
- Cross, B. K. and Moore, B. C. (2014). Lake and reservoir volume: Hydroacoustic survey resolution and accuracy. *Lake and Reservoir Management*, 30(4): 405–411. <http://doi.org/10.1080/10402381.2014.960115>
- Csáfordi, P., Pődör, A., Bug, J., and Gribovszki, Z. (2012). Soil Erosion Analysis in a Small Forested Catchment Supported by ArcGIS Model Builder. *Acta Silv. Lign. Hung.*, 8: 39–55. <http://doi.org/10.2478/v10303-012-0004-5>
- Dahl, A.T., Kendall, D.A., and Hyndman, W.D. (2018). Impacts of projected climate change on sediment yield and dredging costs. *Hydrological Processes*, 32:1223–1234. <http://doi.org/10.1002/hyp.11486>
- Dalu, T., Tambara, M.E., Clegg, B., Chari, D.L., and Nhiwatiwa, T. (2013). Modeling sedimentation rates of Malilangwe reservoir in the south-eastern lowveld of Zimbabwe. *App Water Sci*, 3: 133–144. <http://doi.org/10.1007/s13201-012-0067-9>
- Daniel, B.E., Camp, V.J., LeBoeuf, J.E., Penrod, R.J., Dobbins, P.J., and Abkowitz, D.M. (2011). Watershed Modeling and its Applications: A State-of-the-Art Review. *The Open Hydrology Journal*, 5: 26–50. <http://doi.org/10.2174/1874378101105010026>

- Dargahi, B. (2012). Reservoir Sedimentation. In: Bengtsson L., Herschy R.W., Fairbridge R.W. (eds) *Encyclopedia of Earth Sciences Series*. Springer, Dordrecht. <http://doi.org/10.1007/978-1-4020-4410-6-215>
- Daus, M., Koberger, K., Koca, K., Beckers, F., Fernández, J.E., Weisbrod, B. *et al.* (2021). Interdisciplinary reservoir management - a tool for sustainable water resources management. *Sustainability*, 13, 4498. <https://doi.org/10.3390/su13084498>.
- De Carvalho, F.D., Durigon, L.V., Antunes, H.A.M., De Almeida, S.W., and De Oliveira, S.T.P. (2014). Predicting soil erosion using Rusle and NDVI time series from TM Landsat 5. *Pesq. agropec. bras., Brasília*, 49(3): 215–224.
- Dedkov, A. P. (2004). The relationship between sediment yield and drainage basin area. In: *Sediment Transfer Through the Fluvial System* (ed. by V. Golosov, V. Belyaev & D. E. Walling) (Proc. Moscow Symp., August 2004), 197–204. IAHS Publ. 288. IAHS Press, Wallingford, UK.
- De Graff, J. (1993). *Soil conservation and sustainable land use: An economic approach*. Amsterdam, The Netherlands: Royal Tropical Institute.
- De Jong, S.M. (1994). Applications of reflective remote sensing for land degradation studies in a Mediterranean environment. *Netherlands Geographical Studies*, 177.
- De Jong, S.M. (1994). Derivation of vegetative variables from a Landsat TM image for modelling soil erosion. *Earth Surf. Process*, 19: 165–178
- De Maisonneuve, C.B., Eisele, S., Forni, F., Hamdi, Park, E, Phua, M. *et al.* (2019). Bathymetric survey of lakes Maninjau and Diatas (West Sumatra), and Lake Kerinci (Jambi). IOP conf. Series: *J. Phys.: Conf. Ser.* <http://doi.org/10.1088/1742-6596/1185/1/012001>
- Depountis, N., Vidali, M., Kavoura, K., and Sabatakakis, N. (2018). Soil erosion prediction at the water reservoir's basin of Pineios dam, Western Greece, using the Revised Universal Soil Loss Equation (RUSLE) and GIS. *WSEAS Transactions on Environment and Development*, 14: 457–463

- De Roo, A.P.J. (1996). Soil Erosion Assessment Using G.I.S. In: Singh V.P., Fiorentino M. (eds) *Geographical Information Systems in Hydrology. Water Science and Technology Library*, 26: 339–356
- De Souza, S.L., Wambua, M.R., Raude, M.J., and Mutua, M.B. (2020). Water Flow and Sediment Flux Forecast in the Chókwè Irrigation Scheme, Mozambique. *Journal of Water Resource and Protection*, 12: 1089–1122. <http://doi.org/10.4236/jwarp.2020.1212065>
- Devatha, P.C., Deshpande, V., and Renukaprasad, S.M. (2015). Estimation of soil loss using USLE model for Kulhan Watershed, Chattisgarh - A case study. *Aquatic Procedia*, 4: 1429–1436. <http://doi.org/10.1016/j.aqpro.2015.02.185>
- De Vente, J. and Poesen, J. (2005). Predicting Soil Erosion and Sediment Yield at the Basin Scale: Scale Issues and Semi-Quantitative Models. *Earth-Science Reviews*, 71: 95–125. <http://dx.doi.org/10.1016/j.earscirev.2005.02.002>
- De Vente, J., Poesen, J., Verstraeten, G., Van Rompaey, A., and Govers, G. (2008). Spatially distributed modelling of soil erosion and sediment yield at regional scales in Spain. *Global and Planetary Change*, 60: 393–415. <http://doi.org/10.1016/j.gloplacha.2007.05.002>
- Dhital, Y.P.; Kayastha, R.B., and Shi, J. (2013). Soil bioengineering application and practices in Nepal. *Environ. Manag.* 51: 354–364. <https://dx.doi.org/10.1016/j.ecoleng.2014.11.020>
- Diatta, J., Ławniczak, A., Spsychalski, W., Kryszak, J., Choiński, A., Koralewska, I. *et al.* (2014). Geochemical evaluation of bottom sediments from two polymictic lakes of central-west Poland. *Fresenius Environmental Bulletin*, 23: 2100–2106.
- Didoné, J.E., Minella, G.P.J. and Merten, H.G. (2015). Quantifying soil erosion and sediment yield in a catchment in southern Brazil and implications for land conservation. *J. Soils Sediments*. <http://doi.10.1007/s11368-015-1160-0>.
- Dietrich, W. E., Kirchner, J. W., Ikeda, H. and Iseya, F. (1989). Sediment supply and the development of the coarse surface layer in gravel-bedded rivers. *Nature*, 340, 6230: 215–217. <http://doi.org/10.1038/340215a0>

- Diwediga, B., Le, Q.B., Agodzo, S.K. Tamene, L.D., and Wala, K. (2018). Modelling soil erosion response to sustainable landscape management scenarios in the Mo River Basin (Togo, West Africa). *Science of the Total Environment*, 625: 1309–1320.
<https://doi.org/10.1016/j.scitotenv.2017.12.228>
- Do, X.K., Nguyen, T.H., Ngo, L.A., Felix, M.L., and Jung, K. (2022). Prediction of Reservoir Sedimentation in the Long Term Period Due to the Impact of Climate Change: A Case Study of Pleikrong Reservoir. *Journal of Disaster Research*, 17(4): 552 - 560. <https://doi.org/10.20965/jdr.2022.p0552>
- Dominguez, A. and Schaldach, R. (2019). A Literature Review on Soil Erosion Quantification and Measurements. In R Schaldach & R Otterpohl (eds), *RUVIVAL Publication Series, Hamburg*, 5: 18–31.
<https://doi.org/10.15480/882.2339>
- Donahue, R.L., Miller, R.W., and Schickluna, J.C. (1983). An introduction to soils and plant growth. In: Miller J, editor. 5th ed. Englewood Cliffs (NJ): Prentice-Hall, p. 667.
- Dregne, H.E. (1990). Erosion and soil productivity in Africa. *Journal of Soil and Water Conservation*, 45(4): 431–436.
- Dunbar, J.A. and P.M. Allen (2004). Water and Sediment Volume Survey of Flood Control Reservoir, Cobb Creek #1, Washita County, Oklahoma. Waco, TX: Department of Geology, Baylor University
- Dunbar, J. A., Allen, P. M. and Higley, P. D. (1999). Multifrequency acoustic profiling for water reservoir sedimentation studies. *Journal of Sedimentary Research*, 69(2): 521–527. 7. <https://doi.org/10.2110/jsr.69.518>
- Durigon, V., Carvalho, D., Antunes, M., Almeida, W., and Oliveira, P. (2014) Predicting Soil Erosion Using RUSLE and NDVI Time Series from TM Landsat 5. *Pequisa Agropec uária Brasileira*, 49: 215–224.
<http://doi.org/10.1080/01431161.2013.871081>
- Duru, U. (2016). Assessment of Spatial Sediment Distribution and Deposition in Reservoirs: Case study of Cubuk I & II, Turkey. *Journal of Applied Geology and Geophysics (IOSR-JAGG)*, 4(5): 63–70.

- Dutta, S. (2016). Soil erosion, sediment yield and sedimentation of reservoir: A review. *Model. Earth Syst. Environ.*, 2, 123.
<https://doi.org/10.1007/s40808-016-0182-y>
- Edwards, T.K. and Glysson, G.D. (1999). Field methods for measurement of fluvial sediments. Book3, Chapter C2 U.S. Geological Survey Techniques of Water-Resources Investigations. U.S. Geological Survey, Information Services, Reston, Virginia.
- Efthimiou, N., Lykoudi, E., and Karavitis, C. (2014). Soil erosion assessment using the RUSLE model and GIS. *European Water*, 47: 15–30.
- Ehsani, N., Vorosmarty, J.C., Fekete, M.B., and Stakhiv, Z.E. (2017). Reservoir operations under climate change: storage capacity options to mitigate risk. *Journal of Hydrology*, 555: 435–446.
<http://doi.org/10.1016/j.jhydrol.2017.09.008>
- El Jazouli, A., Barakat, A., Ghafiri, A., El Moutaki, S., Ettagy, A., and Khellouk, R. (2017). *Geosci. Lett.*, 4, 25. <http://doi.org/10.1186/s40562-017-0091-6>
- Elçi, Ş., Bor, A., and Çalışkan, A. (2009). Using numerical models and acoustic methods to predict reservoir sedimentation. *Lake and Reservoir Management*, 25: 297–306. <https://doi.org/10.1080/07438140903117183>
- El-Radaideh, E., Al-Taani, A.A., Al-Momani, T., Tarawneh, K., Batayneh, A., and Taani, A. (2014). Evaluating the potential of sediments in Ziqlab Reservoir (northwest Jordan) for soil replacement and amendment. *Lake and Reservoir Management*, 30: 32–45.
<https://doi.org/10.1080/10402381.2013.870263>
- Esa, E., Assen, M., and Legass, A. (2018). Implications of land use/cover dynamics on soil erosion potential of agricultural watershed, northwestern highlands of Ethiopia. *Environmental Systems Research*, 7, 21.
<http://doi.org/10.1186/s40068-018-0122-0>
- Evette, A.; Labonne, S.; Rey, F.; Liebault, F.; Jancke, O., and Girel, J. (2009). History of bioengineering techniques for erosion control in rivers in Western Europe. *Environ. Manag.*, 43. <http://doi.org/10.1007/s00267-009-9275-y>

- Fadil, A., Rhinane, H., Kaoukaya, A., Kharchaf, Y., and Bachir, A.O. (2011). Hydrologic Modeling of the Bouregreg Watershed (Morocco) Using GIS and SWAT Model. *Journal of Geographic Information System*. 3: 279–289. <http://doi.org/10.4236/jgis.2011.34024>
- Farahani, S.S., Fard, S.F., and Asoodar, A.M. (2016). Effects of Contour Farming on Runoff and Soil Erosion Reduction: A Review Study. *Elixir Agriculture*, 101: 44089-44093.
- Farhan, Y., Zregat, D., and Ibrahim, F. (2013). Spatial Estimation of Soil Erosion Risk Using RUSLE Approach, RS, and GIS Techniques: A Case Study of Kufranja Watershed, Northern Jordan. *Journal of Water Resource and Protection*, 5: 1247–1261. <http://dx.doi.org/10.4236/jwarp.2013.512134>
- Fayas, M.C., Abeysingha, S.N., Nirmanee, S.G.K., Samaratunga, D., and Mallawatantri, A. (2019). Soil loss estimation using rusle model to prioritize erosion control in KELANI river basin in Sri Lanka. *International Soil and Water Conservation Research*. <https://doi.org/10.1016/j.iswcr.2019.01.003>.
- Feldbauer, J., Kneis, D., Hegewald, T., Berendonk, T., and Petzoldt. (2020). Managing climate change in drinking water reservoirs: potentials and limitations of dynamic withdrawal strategies. *Environmental Sciences Europe*, 32, 48. <http://doi.org/10.1186/s12302-020-020-003324-7>.
- Fernandez, C., Wu, Q.J., McCool, K.D., and Stockle, O.C. (2003). Estimating water erosion and sediment yield with GIs, RUSLE, and SEDD. *Journal of Soil and Water Conservation*, 58(3): 128–136.
- Ferro, V. and Porto, P. (2000). Sediment delivery distributed (SEDD) model. *Journal of Hydrologic Engineering*, 5: 411–422.
- Field, C., Barros, V., Dokken, D., Mach, K., Mastrandrea, M., Bilir, T., and White, L. (2014). Ipcc, 2014: Climate change 2014: Impacts, adaptation, and vulnerability. Part A: Global and sectoral aspects. Contribution of working group II to the fifth assessment report of the intergovernmental panel on climate change.
- Fistikoglu, O. and Harmacioglu, N. (2002). Integration of GIS with USLE in Assessment of Soil Erosion. *Water Resources Management*, 16: 447–476.

- Fonseca, R., Barriga, F.J.A.S., and Fyfe, W.S. (1998). Reversing desertification by using dam reservoir sediments as agriculture soils. *Episodes*, 21: 218–224.
- Fonseca, R.M.F., Barriga, F.J.A.S., and Conceicao, P.I.ST. (2009). Clay minerals in sediments of Portuguese reservoirs and their significance as weathering products from over-eroded soils: a comparative study of the Maranhao, Monte Novo and Divor Reservoirs (South Portugal). *Int J Earth Sci (Geol Rundsch)*. <http://doi.10.1007/s00531-009-0488-3>
- Foster, G. R., Meyer, L. D., and Onstad, C. A. (1977). A runoff erosivity factor and variable slope length exponents for soil loss estimates. *Trans. Am. Soc. Agric. Engrs*, Vol. 20(4): 683–687.
- Foster, G., Yoder, D.G., Weesies, G.A., McCool, D.K., McGregor, K.C., and Bingner, R.L. (2003). User's Guide: Revised universal soil loss equation. Washington DC, US Department of Agriculture, Research Service.
- Foteh, R., Garg, V., Nikam, R.B., Khadatre, Y.M., Aggarwal, P.S., and Kumar, S.A. (2018). Reservoir Sedimentation Assessment through Remote Sensing and Hydrological Modelling. *Journal of the Indian Society of Remote Sensing*, 46: 1893–1905
- Fox, G. A., Sheshukov, A., Cruse, R., Kolar, R. L., Guertault, L., Gesch, K. R., and Dutnell, R. C. (2016). Reservoir sedimentation and upstream sediment sources: Perspectives and future research needs on streambank and gully erosion. *Environmental Management*, 57: 945–955.
<http://doi.org/10.1007/s00267-016-0671-9>
- Furniss, M.J., Staab, P.B., Hazelhurst, S., Clifton, F.C., Roby, B.K., Ilhardt, L.B., Larry, B.E., Todd, H.A., Reid, M.L., Hines, J.S., Bennett, A.K., Luce, H.C., and Edwards, J.P. (2010). Water, climate change, and forests: watershed stewardship for a changing climate. *General Technical Report PNW-GTR-812*. U.S. Department of agriculture, Forest Service, Pacific Northwest Research Station, Portland, Oregon.
- Gałaszka, A. (2007). A review of geochemical background concepts and an example using data from Poland. *Environ. Geol.*, 52: 861–870.
<http://doi.org/10.1007/s00254-006-0528-2>

- Ganasri, P.B. and Ramesh, H. (2016). Assessment of soil erosion by RUSLE model using remote sensing and GIS - A case study of Nethravathi Basin. China University of Geosciences (Beijing). *Geoscience Frontiers*, 7: 953–961. <http://dx.doi.org/10.1016/j.gsf.2015.10.007>
- Garzanti E., Ando S., Vezzoli G., Ali Abdel Megid A., and El Kammar A. (2006). Petrology of Nile River sands (Ethiopia and Sudan): Sediment budgets and erosion patterns. *Earth and Planetary Science Letters*, 252 (3–4): 327–341. <http://doi.org/10.1016/j.epsl.2008.11.007>
- Gee, G.W., Bauder, J.W., and Klute, A. (1986). Particle-Size Analysis. Methods of Soil Analysis. Part 1. Physical and Mineralogical Methods. Madison WI, USA: Soil Science Society of America.
- Gelagay, S.H. (2016). RUSLE and SDR Model Based Sediment Yield Assessment in a GIS and Remote Sensing Environment; A Case Study of Koga Watershed, Upper Blue Nile Basin, Ethiopia. *Hydrol. Current Res.*, 7:2. <http://dx.doi.org/10.4172/2157-7587.1000239>
- Gelagay, S.H. and Minale, S.A. (2016). Soil loss estimation using GIS and Remote sensing techniques: A case of Koga watershed, Northwestern Ethiopia. *International Soil and Water Conservation Research*, 4: 126–136. <http://dx.doi.org/10.1016/j.iswcr.2016.01.002>
- George, W.M., Hotchkiss, H.R., and Huffaker, R. (2016). Reservoir Sustainability and Sediment Management. *Journal of Water Resources Planning and Management*, 4016077. [http://doi.org/10.1061/\(ASCE\)WR.1943-5452.0000720](http://doi.org/10.1061/(ASCE)WR.1943-5452.0000720).
- Gerla, P.J., (2003). Can pH and electrical conductivity monitoring reveal spatial and temporal patterns in wetland geochemical processes? *Hydrology and Earth System Science Discussions*, 10: 699–728.
- Ghabbour, E.A., Davies, G., Misiewicz, T., Alami, R.A., Askounis, E.M., Cuozzo, N.P., Filice, A.J., Haskell, J.M., Moy, A.K., Roach, A.C., and Shade, J. (2017). National comparison of the total and sequestered organic matter contents of conventional and organic farm. *Soils*, 146. <https://doi.org/10.1016/bs.agron.2017.07.003>.

- Ghoraba, S.M. (2015). Hydrological modeling of the Simly Dam watershed (Pakistan) using GIS and SWAT model. *Alexandria Engineering Journal*, 54: 583–594. <http://dx.doi.org/10.1016/j.aej.2015.05.018>
- Gianinetto, M., Aiello, M., Polinelli, F., Frassy, F., Rulli, C.M., Ravazzani, G. *et al.* (2019). D-RUSLE: a dynamic model to estimate potential soil erosion with satellite time series in the Italian Alps. *European Journal of Remote Sensing*. <http://doi.org/10.1080/22797254.2019.1669491>
- Gilja, G., Bekić, D., and Oskoruš, D. (2009). Processing of Suspended Sediment Concentration Measurements on Drava River. International Symposium on Water Management and Hydraulic Engineering Ohrid/Macedonia, 1-5 September 2009, Paper: A67
- Giraldez, J. V., Laguna, A., and Gonzalez, P. (1989). Soil conservation under minimum tillage techniques in Mediterranean dry farming. *Soil Technol.*, 1: 139–147.
- Girmay, G., Moges, A., and Muluneh, A. (2020). Estimation of soil loss rate using the USLE model for Agew mariyam Watershed, Northern Ethiopia. *Agric & Food Secur.*, 9(9). <https://doi.org/10.1186/s40066-020-00262-w>.
- Gitas, I. (2009). Multi temporal soil erosion risk assessment in N Chalkidiki Using a modified USLE raster model. *EARSEL EProceedings*, 8.1.
- Gomez, J. A., Battany, M., Renschler, C. S., and Fereres, E. (2003). Evaluating the impact of soil management on soil loss in olive orchards. *Soil Use Manage.*, 19: 127–134.
- Gopinath, G. (2010). Sediment stratification and bathymetric survey using sediment echo sounder in reservoirs and shallow marine areas. *Current Science*, 99 (12): 1821–1825.
- Gratius, C.U. and Chinedu, P.N. (2018). Species Composition of a Degraded Watershed in Amawbia, Anambra State, Nigeria. *American Journal of Plant Biology*, 3(1): 1 - 7.
- Griggs G. (1975). An investigation of bottom sediments in a polluted marine environment upper Saronikos Gulf, Greece. *Report of the environmental pollution control project*, Athens, Greece, 1-30.

- GSP, (2017). Global Soil Partnership Endorses Guidelines on Sustainable Soil Management <http://www.fao.org/global-soil-partnership/resources/highlights/detail/en/c/416516/>
- Gull S., Ahangar, M.A., and Dar, A.M. (2017). Prediction of Stream Flow and Sediment Yield of Lolab Watershed Using SWAT Model. *Hydrology Current Research*, 8(1): 265. <http://doi.org/10.4172/2157-7587.1000265>
- Gurebiyaw, K., Addis, K.H., and Teklay, A. (2018). Assessment of Spatial Soil Erosion Susceptibility Based on the CORINE Model in the Gumara-Maksegnit Watershed, Ethiopia. *Journal of Natural Resources and Development*, 8: 38–45. <http://doi.org/10.5027/jnrd.v8i0.05>
- Haan, C.T., Barfield, B.J., and Hayes, J.C. (1994). Design hydrology and sedimentology for small catchments. Academic Press, New York.
- Hajigholizadeh, M., Melesse, M.A., and Fuentes, R.H. (2018). Erosion and Sediment Transport Modelling in Shallow Waters: A Review on Approaches, Models and Applications. *International Journal of Environmental Research and Public Health*, 15, 518. <http://doi.org/doi:10.3390/ijerph15030518>
- Haregeweyn, N., Poesen, J., Nyssen, J., Govers, G., Verstraeten, G., De Vente, J., *et al.* (2008). Sediment yield variability in Northern Ethiopia: A quantitative analysis of its controlling factors. *Catena*, 75: 65–76. <http://doi.org/10.1016/j.catena.2008.04.011>
- Hargrove, W. L., Johnson, D., Snethen, D., and Middendorf, J. (2010). From dust bowl to mud bowl: Sedimentation, conservation measures, and the future of reservoirs. *Journal of Soil and Water Conservation*, 65(1), 14A–17A. <http://doi.org/10.2489/jswc.65.1.14A>
- Hassan, A.M., Church, M., Xu, J., and Yan, Y. (2008). Spatial and temporal variation of sediment yield in the landscape: Example of Huanghe (Yellow River). *Geophysical Research Letters*, 35, L06401. <http://doi.org/doi:10.1029/2008GL033428>, 2008
- Hassan, R., Al-Ansari, N., Ali, A.A., Ali, S.S., and Knutsson, S. (2017). Bathymetry and siltation rate for Dokan Reservoir, Iraq. *Lakes and Reservoirs and Management*, 22: 179 – 189.

[http://doi.org/ 10.1111/lre.12173](http://doi.org/10.1111/lre.12173)

- Hategekimana, Y., Allam, M., Meng, Q., Nie, Y., and Mohamed, E. (2020). Quantification of Soil Losses along the Coastal Protected Areas in Kenya. *Land*, 9, 137: <http://doi:10.3390/land9050137>.
- Hateffard, F., Mohammed, S., Alsafadi, K., Onaruvbe, G.O., Heidari, A., Abdo, H.G., and Rodrigo-Comino, J. (2021). CMIP5 climate projections and RUSLE-based soil erosion assessment in the central part of Iran. *Scientific Reports*, 11:7273. <https://doi.org/10.1038/s41598-021-86618-z>
- Hatono, M. and Yoshimura, K. (2020). Development of a global sediment dynamics model. *Progress in Earth and Planetary Science*, 7, 59. <http://doi.org/10.1186/s40645-020-00368-6>
- Higaki, D., Karki, K.K., and Gautam, C.S. (2005). Soil erosion control measures on degraded sloping lands: A case study in Midlands of Nepal. *Aquat. Ecosyst. Health Manag.*, 8: 243–249.
- Hilgert, S., Wagner, A., Kiemle, L., and Fuchs, S. (2016). Investigation of echo sounding parameters for the characterisation of bottom sediments in a subtropical reservoir. *Advances in Oceanography and Limnology*, 7(1): 93–105. <http://doi.org/10.4081/aiol.2016.5623>
- Hoque, E., Islam., M, Karmakar, S., Rahman, A., and Bhuyan, S. (2021). Sediment organic matter and physicochemical properties of a multipurpose artificial lake to assess catchment land use: a case study of Kaptai Lake, Bangladesh. *Environmental Challenges*, 3: 100070. <https://doi.org/10.1016/j.envc.2021.100070>
- Huang, J., Jiang, D., Deng, Y., Ding, S., Cai, C., and Huang, Z. (2021). Soil Physicochemical Properties and Fertility Evolution of Permanent Gully during Ecological Restoration in Granite Hilly Region of South China. *Forests*, 12, 510. <https://doi.org/10.3390/f12040510>.
- Hudson, F. (2005). Soil Erosion Modelling Using the Revised Universal Soil Loss Equation (RUSLE) in Drainage Basin in Eastern Mexico. *Environmental GIS: GRG 360G*.

- Hurni, H. (1985). Erosion-Productivity-Conservation Systems in Ethiopia. Proceedings 4th International Conference on Soil Conservation, Maracay, Venezuela, 3-9 November: 654-674.
- Hussein, M., Amien, M.I., and Kariem, H.T. (2016). Designing terraces for the rainfed farming region in Iraq using the RUSLE and hydraulic principles. *International Soil and Water Conservation Research*, 4: 39–44.
<http://dx.doi.org/10.1016/j.iswcr.2015.12.002>
- Idah, P.A., Mustapha, H.I., Musa, J.J., and Dike, J. (2008). Determination of Erodibility Indices of Soils in Owerri West Local Government Area of Imo State, Nigeria. *AU J.T.* 12(2): 130–133.
- Ijam, Z.A. and Tarawneh, R.E. (2012). Assessment of sediment yield for Wala dam catchment area in Jordan. *European Water*, 38: 43–58.
- Ilici, V., Ozulu, M.I., Alkan, M.R., Erol, S., Uysal, M., Kalkan, Y., *et al.* (2017). Determination of Reservoir Sedimentation with Bathymetric Survey: A Case Study of Obruk Dam Lake. *Fresenius Environmental Bulletin*, 28(3): 2305–2313.
- Imamoglu, A. and Dengiz, O. (2017). Determination of soil erosion risk using RUSLE model and soil organic carbon loss in Alaca catchment (Central Black Sea region, Turkey). *Rend. Fis. Acc. Lincei*, 28(1): 11–23.
<http://doi.org/10.1007/S12210-016-0556-0>.
- Iradukunda, P. and Bwambale, E. (2021). Reservoir sedimentation and its effect on storage capacity – a case study of Murera reservoir, Kenya. *Cogent Engineering*, 8, 1917329. <https://doi.org/10.1080/23311916.2021.1917329>
- Iradukunda, P. and Nyadawa, M.O. (2021). Impact of Sedimentation on Water Seepage Capacity in Lake Nakuru, Kenya. *Hindawi, Applied and Environmental Soil Science*, 8889189.
<https://doi.org/10.1155/2021/8889189>
- Iradukunda, P., Sang, K.J., Nyadawa, O.M., and Maina, W.C. (2020). Sedimentation Effect on the Storage Capacity in Lake Nakuru, Kenya. *Journal of Sustainable Research in Engineering*, 5(3): 149–158.

- Ishtiyag, A. and Verma, M. (2013) Application of USLE Model & GIS in Estimation of Soil Erosion for Tandula Reservoir. *International Journal of Emerging Technologies and Advanced Engineering*, 3: 570 – 576.
- Jahun, B.G., Ibrahim, R., Dlamini, S.N., and Musa, M.S. (2015). Review of Soil Erosion Assessment using RUSLE Model and GIS. *Journal of Biology, Agriculture and Healthcare*, 5(9): 36–47.
- Jain, M. and Sharma, D. S (2014). Hydrological Modeling of Vamsadhara River Basin, India using SWAT. *International Conference on Emerging Trends in Computer and Image Processing (ICETCIP) Dec. 15-16, Pattaya (Thailand)*.
- Jain, M.K. and Kothiyari, C.U. (2000). Estimation of soil erosion and sediment yield using GIS. *Hydrological Sciences Journal*, 45(5): 771–786.
<http://doi.org/10.1080/02626660009492376>
- Jain, S.K., Kumar, S., and Varghese, J. (2001). Estimation of Soil Erosion for a Himalayan watershed using GIS technique. *Water Resource Management*, 15: 41–54. <http://doi.org/10.1023/A:1012246029263>
- Jain, S.K., Tyagi, J., and Singh, V. (2010). Simulation of Runoff and Sediment Yield for a Himalayan Watershed Using SWAT Model. *J. Water Resource and Protection*, 2: 267–281.
- Jakubauskas, M. and deNoyelles, F. (2008). Methods for Assessing Sedimentation in Reservoirs. *Sedimentation in Our Reservoirs: Causes and Solutions*: 25–34
- Jakubínský, J., Pechanec, V., Prochazka, J., and Cudlin, P. (2019). Modelling of Soil Erosion and Accumulation in an Agricultural Landscape - A Comparison of Selected Approaches Applied at the Small Stream Basin Level in the Czech Republic. *Water*, 11, 404.
<http://doi.org/10.3390/w11030404>.
- James, C.S., Jones, A.C., Grace, D.M., and Roberts, D.J. (2010). Advances in sediment transport modelling. *Journal of Hydraulic Research*, 48(6): 754 – 763. <http://doi.org/10.1080/00221686.2010.515653>

- Jamshidi, R., Dragovich, D., and Webb, A.A. (2014). Catchment Scale Geostatistical Simulation and Uncertainty of Soil Erodibility using Sequential Gaussian Simulation. *Environmental Earth Sciences*, 71(12): 4965–4976. <http://doi.org/10.1007/s12665-013-2887-9>
- Jasrotia, S. A. and Singh, R. (2006). Modeling runoff and soil erosion in a catchment area, using the GIS, in the Himalayan region, India. *Environmental Geology*, 51(1): 29–37. <http://dx.doi.org/10.1007/s00254-006-0301-6>
- Jetten, V., Govers, G., and Hessel, R. (2003). Erosion models: quality of spatial predictions. *Hydrological Processes*, 17: 887–900. <http://doi.org/10.1002/Hyp.5519>
- Jiang, B., Bamutaze, Y., and Pilesjö, P. (2014). Climate change and land degradation in Africa: a case study in the Mount Elgon region, Uganda. *Geo-spatial Information Science*, 17(1): 39–53. <http://doi.org/10.1080/10095020.2014.889271>
- Jothimani, M., Getahun, E., and Abebe, A. (2022). Remote sensing, GIS, and RUSLE in soil loss estimation in the Kulfo river catchment, Rift valley, Southern Ethiopia. *Journal of Degraded and Mining Lands Management*, 9(2):3307–3315. <http://doi.org/10.15243/jdmlm.2022.092.3307>
- Junakova, N. and Balintova, M. (2012). Assessment of nutrient concentration in reservoir bottom sediments. In: 20th International Congress of Chemical and Process Engineering CHISA 2012 25–29 August 2012, Prague, Czech Republic. *Procedia Engineering*, 42 165–170. <http://doi.org/10.1016/j.proeng.2012.07.407>
- Junakova, N. and Balintova, M. (2014). The Study of Bottom Sediment Characteristics as a Material for Beneficial Reuse. *Chemical Engineering Transactions*, 39: 637–642. <http://doi.org/10.3303/CET1439107>
- Junakova, N., Balintova, M., Junak, K., Singovszka, E. (2021). The quality of bottom sediments in small water reservoirs located in agricultural watersheds. *IOP Conf. Ser.: Earth Environ. Sci.*, 900. <http://doi.org/10.1088/1755-1315/900/1/012016>

- Juracek, K. E. (2015). The aging of America's reservoirs: In reservoir and downstream physical changes and habitat implications. *Journal of the American Water Resources Association*, 51(1), 168–184.
- Kale, D.G. and Vadsola, N.S. (2012). Modelling of Soil Erosion by Non-Conventional Methods. World Academy of Science, Engineering and Technology. *International Journal of Geological and Environmental Engineering*, 6 (3): 139–145.
- Kalkhajeh, K.Y., Amiri, J.B., Huang, B., Khalyani, H.A., Hu, W., Gao, H., and Thompson, L.M. (2019). Methods for Sample Collection, Storage, and Analysis of Freshwater Phosphorus. *Water*, 11, 1889.
<http://doi.org/doi:10.3390/w11091889>
- Kaltenrieder, J. (2007). Adaptation and validation of the universal soil loss equation (USLE) for the Ethiopian–Eritrean Highlands. MSc Thesis, University of Berne, Centre for Development and Environment Geographisches Institut.
- Kamarudin, A.K.M., Toriman, E.M., Wahab, A.N., Rosli, H., Ata, M.F., and Faudzi, M.N.M. (2017). Sedimentation Study on Upstream Reach of Selected Rivers in Pahang River Basin, Malaysia. *International Journal on Advanced Science Engineering Information Technology*, 7(1): 35–41.
- Kamarudin, M.K.A., Toriman, M.E., Mastura, S.A.S., Idris, M., Jamil. N.R., and Gasim, M.B. (2009). Temporal variability on lowland river sediment properties and yield. *American Journal of Environmental Sciences*, 5: 657–663. <http://doi.org/10.3844/ajessp.2009.657.663>
- Karamage, F., Zhang, C., Kayiranga, A., Shao, H., Fang, X., Ndayisaba, F., Nahayo, L., Mupenzi, C., and Tian, G. (2016). USLE-Based Assessment of Soil Erosion by Water in the Nyabarongo River Catchment, Rwanda. *Int. J. Environ. Res. Public Health*, 13, 835.
<http://doi.org/10.3390/ijerph13080835>
- Karydas, G.C., Panagos, P., and Gitas, Z.I. (2014). A classification of water erosion models according to their geospatial characteristics. *International Journal of Digital Earth*, 7(3): 229–250.
<http://doi.org/10.1080/17538947.2012.671380>

- Kassam, H.A., Velthuizen, T.H., Mitchell, B.J.A., Fischer, W.G., and Shah, M.M. (1992). Agro-Ecological Land Resources Assessment for Agricultural Development Planning, A Case Study of Kenya Resources Data Base and Land Productivity. Technical Annex 2, Soil Erosion and Productivity.
- Katarzyna, R., Rafał, R., and Piotr, P. (2017). Characteristics of spatial distribution of phosphorous and nitrogen in the bottom sediments of the water reservoir Poraj. *Journal of Ecological Engineering*, 18: 178–184. <http://doi.org/10.12911/22998993/74277>
- Kavian, A., Sabet, H.S., Solaimani, K., and Jafari, B. (2017). Simulating the effects of land use changes on soil erosion using RUSLE model. *Geocarto International*, 32(1): 97–111. <http://doi.org/10.1080/10106049.2015.1130083>
- Kayet, N., Pathak, K., Chakrabarty, A., and Sahoo, S. (2016). Spatial impact of land use/land cover change on surface temperature distribution in Saranda Forest, Jharkhand. *Model. Earth Syst. Environ.* 2, 127. <http://doi.org/10.1007/s40808-016-0159-x>
- Kazberuk, W., Szulc, W. and Rutkowska, B. (2021). Use bottom sediment to agriculture - effect on plant and heavy metal content in soil. *Agronomy*, 11: 1077. <http://doi.org/10.1007/s40808-016-0159-x>
- Kebede, S.Y., Endalamaw, T.N., Sinshaw, G.B., and Atinkut, B.H. (2021). Modeling soil erosion using RUSLE and GIS at watershed level in the upper beles, Ethiopia. *Environmental Challenges*, 2, 100009. <https://doi.org/10.1016/j.envc.2020.100009>.
- Kebede, W.W. (2012). Watershed Management: An Option to Sustain Dam and Reservoir Function in Ethiopia. *Journal of Environmental Science and Technology*, 5: 262–273.
- Keesstra, S., Mol, G., De Leeuw, J., Okx, J., Molenaar, C., De Cleen, M., and Visser, S. (2018). Soil-Related Sustainable Development Goals: Four Concepts to Make Land Degradation Neutrality and Restoration Work. *Land*, 7 (133). <http://doi.org/10.3390/land7040133>

- Keesstra, S.D., Temme, A.J.A.M., Schoorl, J.M., and Visser, S.M. (2014). Evaluating the hydrological component of the new catchment-scale sediment delivery model LAPSUS-D. *Geomorphology*, 212: 97–107. <http://doi.org/10.1016/j.geomorph.2013.04.021>
- Khanchoul, K., Altschul, R., and Assassi, F. (2009). Estimating suspended sediment yield, sedimentation controls and impacts in the Mellah Catchment of Northern Algeria. *Arab J Geosci*, 2: 257–271. <http://doi.org/10.1007/s12517-009-0040-6>
- Kieti, R.N., Kauti, M.K., and Kisangau, D.P. (2016). Biophysical Conditions and Land Use Methods Contributing to Watershed Degradation in Makueni County, Kenya. *Journal of Ecosystem & Ecography*, 6(4): 1–8. <http://doi.org/10.4172/2157-7625.1000216>
- Kilonzo, W., Home, P., Sang, J., and Kakoi, B. (2019). The storage and water quality characteristics of Rungiri quarry reservoir in Kiambu, Kenya, as a potential source of urban water. *Hydrology*, 6, 93. <http://doi.org/10.3390/hydrology6040093>
- Kinama, J.M., Stigter, C.J., Ong, C.K., Ng'anga, J.K., and Gichuki, F.N. (2007). Contour Hedgerows and Grass Strips in Erosion and Runoff Control on Sloping Land in Semi-Arid Kenya. *Arid Land Research and Management*, 21(1): 1–19. <http://doi.org/10.1080/15324980601074545>
- Kinnell, P. I. A. (2005). Why the universal soil loss equation and the revised version of it do not predict event erosion well. *Hydrol. Processes*, 19: 851–854. <http://doi.org/10.1002/hyp.5816>
- Kisi, O. (2005). Suspended sediment estimation using neuro-fuzzy and neural network approaches. *Hydrol. Sci. J.* 50(4): 683–696. <http://doi.org/10.1623/hysj.2005.50.4.683>
- Knisel, G.W. (1980). CREAMS: A Field-Scale Model for Chemicals, Runoff and Erosion from Agricultural Management Systems. *USDA Conservation Research Report*, 26(1): 36–64.
- Kogo, K.B., Kumar, L., and Koech, R. (2020). Impact of Land Use/Cover Changes on Soil Erosion in Western Kenya. *Sustainability*, 12, 9740. <http://doi.org/doi:10.3390/su12229740>

- Koirala, P., Thakuri, S., Joshi S., and Chauhan, R. (2019). Estimation of Soil Erosion in Nepal Using a RUSLE Modeling and Geospatial Tool. *Geosciences*, 9, 147. <http://doi.org/10.3390/geosciences9040147>
- Kolli, K.M., Opp, C., and Groll, M. (2021). Estimation of soil erosion and sediment yield concentration across the Kolleru Lake catchment using GIS. *Environmental Earth Sciences*, 80(161): 1–16. <https://doi.org/10.1007/s12665-021-09443-7>
- Kondolf, G.M., Gao, Y., Annandale, G.W., Morris, G.L., Jiang, E., Zhang, J., and Yang, C. T. (2014). Sustainable sediment management in reservoirs and regulated rivers: Experiences from five continents. *Earth's Future*, 2(5): 256–280. <http://doi.org/10.1002/2013EF000184>.
- Kondolf, M. and Yi, J. (2022). Dam Renovation to Prolong Reservoir Life and Mitigate Dam Impacts. *Water*, 14, 1464. <https://doi.org/10.3390/w14091464>
- Koneti, S., Sunkara, L.S., and Roy, S.P. (2018). Hydrological Modeling with Respect to Impact of Land-Use and Land-Cover Change on the Runoff Dynamics in Godavari River Basin Using the HEC-HMS Model. *International Journal Geo-information*, 7, 206. <http://doi.org/10.3390/ijgi7060206>
- Korada, R.D.V.H., and Vala, R.V. (2014). Soil erosion assessment in Rangit catchment, India through a process-based model in the geospatial environment. *Geocarto International*, 29(5): 507–519. <http://dx.doi.org/10.1080/10106049.2013.798359>
- Koś K, Gruchot A., and Zawisza E. (2021). Bottom sediments from a dam reservoir as a core in embankments - filtration and stability: A case study. *Sustainability*, 13, 1221. <https://doi.org/10.3390/su13031221>
- Koshak, N. and Dawod, G. (2011). A GIS morphometric analysis of hydrological catchments within Makkah Metropolitan area, Saudi Arabia. *International Journal of Geomatics and Geosciences*, 2(2): 544–554.
- Kothyari, C.U. and Jain, K.S. (1997). Sediment yield estimation using GIS. *Hydrological Sciences Journal*, 42(6): 833–843. <https://doi.org/10.1080/02626669709492082>

- Kothyari, C.U.F. (2008). Soil erosion and sediment yield modelling. *ISH Journal of Hydraulic Engineering*, 14(1): 84–103. :
<https://doi.org/10.1080/09715010.2008.10514895>
- Kuhwald, M., Hamer, W.B., Brunotte, J. and Duttmann, R. (2020). Soil Penetration Resistance after One-Time Inversion Tillage: A Spatio-Temporal Analysis at the Field Scale. *Land*, 9, 482.
<http://doi.org/10.3390/land9120482>
- Kusimi, M.J., Yiran, B.A.G., and Attuta, M.E. (2015). Soil Erosion and Sediment Yield Modelling in the Pra River Basin of Ghana using the Revised Universal Soil Loss Equation (RUSLE). *Ghana Journal of Geography*, 7(2): 38–57
- Kusumandari, A. (2014). Soil Erodibility of Several Types of Green Open Space Areas in Yogyakarta City, Indonesia. The 4th International Conference on Sustainable Future for Human Security, SustainN 2013. *Procedia Environmental Sciences*, 20: 732–736.
<http://doi.org/doi:10.1016/j.proenv.2014.03.087>
- Kwena, K.M., Karuku, G., Ayuke. F., and Esilaba, A. (2020). Impact of Climate Change on Maize and Pigeon pea Yields in Semi-Arid Kenya. In S. Sarvajayakesavalu, & P. Charoensudjai (Eds.), *Environmental Issues and Sustainable Development*. IntechOpen.
<https://doi.org/10.5772/intechopen.93321>
- Laflen, J.M., Lane, J.L., and Foster, R.G. (1991). WEPP, a next generation of erosion prediction technology. *Journal of Soil Water Conservation*, 46(1): 34–38.
- Lal, R. (2003). Soil erosion and global carbon budget. *Environment International*, 29(4): 437–450. [http://dx.doi.org/10.1016/S0160-4120\(20\)00192-7](http://dx.doi.org/10.1016/S0160-4120(20)00192-7)
- Lee, E.S. and Kang, H.S. (2013). Estimating the GIS-based soil loss and sediment delivery ratio to the sea for four major basins in South Korea. *Water Science and Technology*, 68(1): 124–133.
<http://doi.org/10.2166/wst.2013.194>

- Lee, F-Z., Lai, J-S., and Sumi, T. (2022). Reservoir Sediment Management and Downstream River Impacts for Sustainable Water Resources—Case Study of Shihmen Reservoir. *Water*, 14, 479. <https://doi.org/10.3390/w14030479>
- Lee, M., Yu, I., Necesito, I.V., Kim, H., and Sangman, J. (2014). Estimation of Sediment Yield Using Total Sediment Yield Formulas and RUSLE. *J. Korean Soc. Hazard Mitig.*, 14(4): 279–288.
- Levec, F. and Skinner, A. (2004). Manual of instructions for bathymetric surveys, Ontario, p. 27.
- Li, L., Wang, Y., and Liu, C. (2014). Effects of land use changes on soil erosion in a fast developing area. *Int. J. Environ. Sci. Technol.*, 11: 1549–1562. <http://doi.org/10.1007/s13762-013-0341-x>
- Li, P., Mu, X., and Holden, J. (2017). Comparison of soil erosion models used to study the Chinese Loess Plateau. *Earth-Science Reviews*, 170: 17–30. <https://doi.org/10.1016/j.earscirev.2017.05.005>
- Lim, J.K., Sasong, M., Engel., A.B., Tang, Z., Choi, J., and Kim, K. (2005). GIS-based sediment assessment tool. *Catena*, 64: 61–80. <http://doi.org/10.1016/j.catena.2005.06.013>
- Lin, B., Chen, C., Thomas, K., Hsu, C. and Ho, H. (2019). Improvement of the K-Factor of USLE and Soil Erosion Estimation in Shihmen Reservoir Watershed. *Sustainability*, 11, 355. <http://doi.org/10.3390/su11020355>
- Lin, Y., Wang, Y., and Chen, S. (2017). The Variation of Sediment Discharge During Flood Period. *Top Papers*: 215–223.
- Littleboy, M., Silburn, M.D., Freebaim, D.M., Woodruff, R.D., Hammer, G.L., and Leslie, J.K. (1992). Impact of soil erosion on production in cropping systems, I. Development and validation of a simulation model. *Australian Journal of Soil Research*, 30: 757–774.
- Liu, H.H., Fohrer, N., Hormann, G., and Kiesel, J. (2009). Suitability of S factor algorithms for soil loss estimation at gently sloped landscapes. *Catena*, 77: 248–255. <http://doi.org/10.1016/j.catena.2009.02.001>
- Liu, Z.J. and Weller, D. E. (2007). A stream network model for integrated watershed modeling. *Environ Modell Assess*, 13(2): 291–303.

<http://doi.org/10.1007/s10666-007-9083-9>

- Loch, R., and Silburn, D.M. (1996). Sustainable Crop Production in the Sub-trops: An Australian Perspective. Queensland: Queensland Department of Primary & Fisheries. Chap. Constraints to sustainability-soil erosion, page 376.
- Lohani, K.A., Goel, K.N., and Bhatia, S.K.K. (2007). Deriving stage-discharge-sediment concentration relationships using fuzzy logic. *Hydrological Sciences*, 52(4): 793–807. <http://doi.org/10.1623/hysj.52.4.793>
- Longley, P.A., Goodchild, F.M., Maguire, J.D., and Rhind, W.D. (2004). *Geographic Information Systems and Science* (2nd edition), Wiley: 539
- López-García, M.E., Torres-Trejo, E., López-Reyes, L., Flores-Domínguez, D.A., Peña-Moreno, D.R., and Francisco López-Olguín, F.J. (2020). Estimation of soil erosion using USLE and GIS in the locality of Tzicatlacoyan, Puebla, México. *Soil and Water Research*, 15(1): 9–17. <https://doi.org/10.17221/165/2018-SWR>
- Loureiro, S.N. and Coutinho, A.M. (2015). A new procedure to estimate the RUSLE EI index based on monthly rainfall data and applied to the Algreve region, Portugal. *J. Hydrol.*, 250: 12–18.
- Lu, H., Moran, J.C., and Sivapalan, M. (2005). A theoretical exploration of catchment-scale sediment delivery. *Water Resources Research*, 41, W09415. <http://doi.org/10.1029/2005WR004018>, 2005
- Madeyski, M. and Bednarczyk, T. (2000). Physical, chemical and rheological characteristics of bottom sediments in reservoirs and fish ponds, Poland. The Role of Erosion and Sediment Transport in Nutrient and Contaminant Transfer (Proceedings of a symposium held at Waterloo, Canada, July 2000). *IAHS Publ.*, 263: 237–241.
- Maina, W.C., Sang, K.J., Mutua, M.B., and Raude, M.J. (2018). Bathymetric survey of Lake Naivasha and its satellite Lake Oloiden in Kenya; using acoustic profiling system. *Lakes & Reserv.* 23: 324–332. <http://doi.org/10.1111/lre.12247>

- Maina, W.C., Sang, K.J., Raude, M.J., Mutua, M.B., and Moriasi, N.D. (2019). Sediment distribution and accumulation in Lake Naivasha, Kenya over the past 50 years. *Lakes & Reserv.* 24: 162–172.
<http://doi.org/10.1111/lre.12272>
- Malleswara Rao, N.B., Umamahesh, V.N. and Reddy, T.G. (2005). GIS-Based Soil Erosion Modelling for Conservation Planning of Watersheds. *ISH Journal of Hydraulic Engineering*, 11(3): 11–23.
<https://doi.org/10.1080/09715010.2005.10514797>
- Mallick, J., Alashker, Y., Mohammad, A.S, Ahmed, M., and Hasan, A.M. (2014). Risk assessment of soil erosion in semi-arid mountainous watershed in Saudi Arabia by RUSLE model coupled with remote sensing and GIS. *Geocarto International*, 29(8): 915–940.
<https://doi.org/10.1080/10106049.2013.868044>
- Manassero, M., Camilion, C., Poire, D., Da Silva, M., and Ronco, A. (2008). Grain size analysis and clay mineral associations in bottom sediments from Parana River basin. *Latin America Journal of Sedimentary and Basin Analysis*, 15(2): 125–137.
- Manjulavani, K., Prathyusha, B., and Ramesh, M. (2016). Soil Erosion and Sediment Yield Modeling using Remote Sensing and GIS Techniques. *International Journal of Management and Applied Science*, 2(10): 59–63.
- Manyiwa, T. and Dikinya, O. (2013). Using universal soil loss equation and soil erodibility factor to assess soil erosion in Tshesebe village, north east Botswana. *African Journal of Agricultural Research*, 8(30): 4170–4178.
<http://doi.org/10.5897/AJAR2013.7081>
- Marston, R.A and Dolan, L.S. (1999). Effectiveness of sediment control structures relative to spatial patterns of soil loss in an arid upland. *Geomorphology*, 31(1): 313–324.
- Mati, M.B., Morgan, R.P.C., Gichuki, F.N., Quinton, J.N., Brewer, T.R., and Liniger, H.P. (2000). Assessment of erosion hazard with the USLE and GIS: A case study of the Upper Waso Ng'iro North basin of Kenya. *JAG*, 2(2): 78–86.

- Mavima, G.A., Soropa, G., Hodson, M., and Dzvairo, W. (2013). Sedimentation impacts on reservoir as a result of land use on a selected catchment in Zimbabwe. *International Journal of Engineering Science and Technology (IJEST)*, 3(8): 6599–6608.
- May, L. and Place, C. (2005). A GIS-based Model of Soil Erosion and Transport. *Freshwater Forum*, 23: 48–61
- Mayor, A.G., Bautista, S., Bellot, J. (2011). Scale-dependent variation in runoff and sediment yield in a semiarid Mediterranean catchment. *J. Hydrol.*, 397: 128–135. <http://doi.org/10.1016/j.jhydrol.2010.11.039>
- McAlister, J.R., Fox, W.E., Wilcox, B., and Srinivasan, R. (2013). Reservoir volumetric and sedimentation survey data: A necessary tool for evaluating historic sediment flux and appropriate mitigation response. *Lakes and Reservoirs: Research and Management*, 18: 275–283. <http://doi.org/10.1111/lre.12036>
- Mdee, O.J. (2015). Spatial distribution of runoff in ungauged catchments in Tanzania. *Water Utility Journal*, 9: 61–70.
- Megersa, S.L. (2014). Prediction of Runoff and Sediment Yield Using AnnAGNPS Model: Case of Erer-Guda Catchment, East Hararghe, Ethiopia. *ARPJ Journal of Science and Technology*, 4(10): 575–595.
- Mekonnen, M., Keesstraa, S.D., Baartmana, J.E.M., Stroosnijdera, L., and Maroulisac, J. (2016). Reducing sediment connectivity through man-made and natural sediment sinks in the Minizr Catchment, Northwest Ethiopia. *Land Degrad. Dev.*, 28: 708–717. <http://doi.org/10.1002/ldr.2308>
- Mendonça, R., Müller, A.R., Clow, D., Verpoorter, C., Raymond, P., Tranvik, J.L., and Sobek, S. (2017). Organic carbon burial in global lakes and reservoirs. *Nature Communications*, 8: 1694. <http://doi.org/10.1038/s41467-017-01789-6>
- Mendonça, R., Kosten, S., Sobek, S., Barros, N., Cole, J. J., Tranvik, L., and Roland, F. (2012). Hydroelectric carbon sequestration. *Nature Geoscience*, 5(12): 838–840. <http://doi.org/10.1038/ngeo1653>

- Merina, N. R., Sashikkumar, M., Rizvana, N., and Adlin, R. (2016). Sedimentation study in a reservoir using remote sensing technique. *Applied Ecology and Environmental Research*, 14(4): 296–304. http://doi.org/dx.doi.org/10.15666/aeer/1404_296304
- Merritt, S.W., Letcher, A.R., and Jakeman, J.A. (2003). A review of erosion and sediment transport models. *Environmental Modelling & Software*, 18: 761–799. [http://doi.org/10.1016/S1364-8152\(03\)00078-1](http://doi.org/10.1016/S1364-8152(03)00078-1)
- Merzoul, A. (1985). Relative erodibility of nine selected Moroccan soils related to their physical and chemical and mineralogical properties (Doctoral dissertation). University of Minnesota, USA (1985).
- Mielnik, L., Ryszard, P., and Klimaszyk, P. (2009). Chemical properties of bottom sediments in throughflow lakes located in Drawieński National Park. *Oceanological and Hydrobiological Studies*, 38: 69–76. <http://doi.org/10.2478/v10009-009-0033-5>
- Millares, A. and Monino, A. (2018). Sediment yield and transport process assessment from reservoir monitoring in a semi-arid mountainous river. *Hydrological Processes*, 32(19). <http://doi.org/10.1002/hyp.13237>
- Miranda, E.L., Coppola, G., and Boxrucker, J. (2019). Reservoir Fish Habits: A Toolkit for Coping with Climate Change. Reservoir Fisheries Habitat Partnership.
- Misra, R. K. and Rose, C. W. (1996). Application and Sensitivity Analysis of Process-based Erosion Model GUEST. *Euro. J. Soil Sci.*, 47: 593–604. <http://doi.org/10.1111/j.1365-2389.1996.tb01858.x>
- Mitasova, H., Barton, M., Hofierka, J., and Harmon, R.S. (2013). GIS-Based Soil Erosion Modelling. In: John, F. Shroder (Editor-in-chief), Bishop, M.P. (volume editor). *Treatise on Geomorphology*, 3: Remote Sensing and GIScience in Geomorphology, San Diego: Academic Press: 228–258.
- Moges, M.M., Abay, D., and Engidayehu, H. (2018). Investigating reservoir sedimentation and its implications to watershed sediment yield: The case of two small dams in datascarce upper Blue Nile Basin, Ethiopia. *Lakes & Reserv.*, 23:217–229. <http://doi.org/10.1111/lre.12234>

- Moghimi, A.H., Hamdan, J., Shamsuddin, J., Samsuri, A.W., and Abtahi, A. (2013). Physicochemical Properties and Surface Charge Characteristics of Arid Soils in Southeastern Iran. *Applied and Environmental Soil Science, Hindawi*, 252861. <http://dx.doi.org/10.1155/2013/252861>
- Mohammad, A.G. and Adam, M.A. (2010). The impact of vegetative cover type on runoff and soil erosion under different land uses. *Catena*, 81: 97–103. <http://doi.org/10.1016/j.catena.2010.01.008>
- Mondol, M.N., Chamon, A.S., Faiz, B. and Elahi, S.F. (2014). Chromium in urban soil-plant-water ecosystems. *J. Bangladesh Acad. Sci.*, 37: 173–187. <http://doi.org/10.3329/jbas.v37i2.17558>
- Moore, I. and Burch, F. (1986). Physical basic of the length–slope factor in the universal soil loss equation. *Soil Science Society of America Journal*, 50: 1294–1298.
- Moore, R.T. (1979). Land Use and Erosion in the Machakos Hills. *Annals of the Association of American Geographers*, 69(3): 419–431.
- Moore, T.R. (1977). Soil Erosion. Miscellaneous Paper No. 1. Department of Soil Science, University of Nairobi.
- Morgan, C.P.R., Quinton, N.J., Smith, E.R., Govers, G., Poesen, A.W.J., Auerswald, K., Chisci, G., Torri, D., and Styczen, E.M., (1998). The European soil erosion model (EUROSEM): A dynamic approach for predicting sediment transport from fields and small catchments. *Earth Surface Processes and Landforms*, 23: 527–544. [http://doi.org/10.1002/SICI1096-9837\(199806\)23:6<527::AID-ESP868>3.0.CO;2-5](http://doi.org/10.1002/SICI1096-9837(199806)23:6<527::AID-ESP868>3.0.CO;2-5)
- Morgan, R.P.C. (2005). Soil Erosion and Conservation. Third edition. Blackwell Publishing, Malden, U.S.A
- Morgan, R.P.C. (2009). Soil Erosion and Conservation, 3rd ed.; Blackwell Publishing: Massachusetts, MA, USA.
- Morgan, R.P.C., Morgan, D.D.V. and Finney, H.J. (1984). A predictive model for the assessment of soil erosion risk. *J. Agric. Eng. Res.*, 30: 245–253. [http://doi.org/10.1016/S0021-8634\(84\)80025-6](http://doi.org/10.1016/S0021-8634(84)80025-6)

- Moriasi, N.D. Steiner, L.J., Duke, E.S., Starks, J.P., and Verser, J.A. (2018). Reservoir Sedimentation Rates in the Little Washita River Experimental Watershed, Oklahoma: Measurement and Controlling Factors. *Journal of the American Water Resources Association*, 54(5): 1011–1023
- Morris, L.G. (2020). Classification of Management Alternatives to Combat Reservoir Sedimentation. *Water*, 12, 861.
<http://doi.org/doi:10.3390/w12030861>
- Morris, L.G. and Fan, J. (1998). *Reservoir sedimentation handbook*. New York: McGraw-Hill
- Moslemzadeh, M., Roueinian, K., and Salarijazi, M. (2022). Improving the estimation of sedimentation in multi-purpose dam reservoirs, considering hydrography and time scale classification of sediment rating curve (case study: Dez Dam). *Arabian Journal of Geosciences*, 15:226.
<https://doi.org/10.1007/s12517-021-09292-5>
- Moura, D.S., De Almeida, A.S.O., Pestana, C.J., Girão, L.G. and Capelo-Neto, J. (2020). Internal loading potential of phosphorus in reservoirs along a semiarid watershed. *Brazilian Journal of Water Resources*, 25:13.
<https://doi.org/10.1590/2318-0331.252020180023>
- Mouri, G., Ros, C.F. and Chalov, S. (2014). Characteristics of suspended sediment and river discharge during the beginning of snowmelt in volcanically active mountainous environments. *Geomorphology*, (213): 266–276. <http://dx.doi.org/10.1016/j.geomorph.2014.02.001>
- Msadala, V.C. and Basson, R.G. (2017). Revised regional sediment yield prediction methodology for ungauged catchments in South Africa. *Journal of the South African Institution of Civil Engineering*, 59(20): 28–36.
- Muia, V.K. and Ndunda, E. (2013). Evaluating the impact of direct anthropogenic activities on land degradation in arid and semi-arid regions in Kenya. *Wudpecker Journal of Agricultural Research*.
- Mulinge, W., Gicheru, P., Murithi, F., Maingi, P., Kihui, E., Kirui, K.O. *et al.*, (2016). Economics of Land Degradation and Improvement in Kenya. In: Nkonya E., Mirzabaev A., von Braun J. (eds) Economics of Land Degradation and Improvement – A Global Assessment for Sustainable

Development. *Springer, Cham*. <http://doi.org/10.1007/978-3-319-19168-3-16>.

Mupangwa, W.; Twomlow, S.; Walker, S., and Hove, L. (2007). Effect of minimum tillage and mulching on maize (*Zea mays* L.) yield and water content of clayey and sandy soils. *Phys. Chem. Earth Parts A/B/C.*, 32: 1127–1134. <http://10.1016/j.pce.2007.07.030>

Mushir, A., and Kedru, S. (2012). Soil and water conservation management through indigenous and traditional practices in Ethiopia: A case study. *Ethiopian Journal of Environmental Studies and Management*, 5 (4): 343–355. <http://doi.org/10.4314/ejesm.v5i4.3>

Mutua, M.B., Klik, A., and Loiskandl, W. (2006). Modelling Soil Erosion and Sediment Yield at a Catchment Scale: The Case of Masinga Catchment, Kenya. *Land Degrad. Develop.*, 17: 557–570. <http://doi.org/10.1002/ldr.753>

N’doufou, G.H.C., Nangah, K.Y., and Kouadio, K.H. (2022). Comparative Study of Physico-Chemical Properties of Sediments from Two Sectors Close to Bandama in Northern Côte D’Ivoire (Sinematiali and Niakaramadougou). *Journal of Geoscience and Environment Protection*, 10: 33–46. <https://doi.org/10.4236/gep.2022.102003>

Nasir Ahmad, B.S.N., Mustafa, B.F., Yusoff, M.Y.S., and Didams, G. (2020). A systematic review of soil erosion control practices on the agricultural land in Asia. *International Soil and Water Conservation Research*, 8: 103–115. <http://doi.org/10.1016/j.iswcr.2020.04.001>

Nasrin, Z., Saeid, E., Vijay, P., Kavesh, O., Nicolas, R., and Shahide, D. (2018). Calibration and Uncertainty of the SWAT Model Using the SUFI-2 Algorithm. *International Journal of Research Studies in Science, Engineering and Technology*, 5 (4): 4–10.

Nearing, A.M., Lane, J.L. and Lopes, L.V. (1994). Modelling soil erosion. *Soil Erosion: Research Methods*: 127–156.

Nelson, D.W. and Sommers, L.E. (1996). Methods of Soil Analysis. Part 3. Chemical Methods. *Soil Science Society of America Book Series*: 961–1010.

- Nelson, N. and Baldock, A. (2000) Soil Organic Matter. *Handbook of Soil Science*, Chapter 2, CRC Press, Boca Raton, B25-B84.
- Ngari, J.K., Nyanchaga, E.N., and Oonge, Z.I. (2020). Assessment of post expansion impacts of Maruba dam in Machakos County; a case study of Miwani estate in Machakos town. *International Journal of Innovative Science, Engineering Technology*, 7(9).
- Nguyen, A.K. and Chen, W. (2018). Estimating sediment delivery ratio by stream slope and relief ratio. *MATEC Web of Conferences*, 192, 02040.
- Njiru, N.G., Kariuki, P., and Mwetu, K. (2018). Modelling Soil Erosion for Land Management in Ungauged Golole Catchment in Marsabit County, Kenya. *Open Journal of Soil Science*, 8(11): 277–302.
<https://doi.org/10.4236/ojss.2018.811021>
- Nkonya, E., Gerber, N., Baumgartner, P., Von Braun, J., De Pinto, A., and Graw, V. (2011). The Economics of Desertification, Land Degradation, and Drought: Toward an Integrated Global Assessment. IFPRI Discussion Paper 01086.
- Nouri, A., Saffari, A., and Karami, J. (2018). Assessment of Land Use and Land Cover Changes on Soil Erosion Potential Based on RS and GIS, Case Study: Gharesou, Iran. *J. Geogr Nat Disast.* , 8(2): 1–9.
<http://doi.org/10.4172/2167-0587.1000222>
- Novotny, V. and Olem, H. (1994). *Water Quality: Prevention, Identification, and Management of Diffuse Pollution*. John Wiley & Sons, Inc., New York, USA.
- Nsabimana, G., Bao, Y., He, X., Nambajimana, J. D., Wang, M. *et al.*, (2020). Impacts of Water Level Fluctuations on Soil Aggregate Stability in the Three Gorges Reservoir, China. *Sustainability*, 12, 9107.
<http://doi.org/10.3390/su12219107>.
- Nyssen, J., Clymans, W., Poesen, J., Vandecasteele, I., De Baets, S., Haregeweyn, N., *et al.* (2009). How soil conservation affects the watershed sediment budget—a comprehensive study in the North Ethiopian Highlands. *Earth Surf Process Landforms*, 34:1216–1233.
<http://doi.org/10.1002/esp.1805>

- Nyssen, J., Govaerts, B., Araya, T., Cornelis, W., Bauer, H., Haile, M. *et al.* (2011). The use of the marashaard and plough for conservation agriculture in Northern Ethiopia. *Agronomy for sustainable Development*, 31: 287–297.
- Obiora-Okeke, O.A. (2019). Erosion Mapping using Revised Universal Soil Loss Equation Model and Geographical Information System: A Case Study of Okitipupa, Nigeria. *European Journal of Engineering and Technology*, 7(4): 73–80
- Ochoa, A.P., Fries, A., Mejia, D., Burneo, I.J., Ruiz-Sinoga, D.J., and Cerda, A. (2016). Effects of climate, land cover and topography on soil erosion risk in a semiarid basin of the Andes. *Catena*, 140: 31–42.
<http://doi.org/10.1016/j.catena.2016.01.011>
- Odhiambo, K.B. and Boss, K.S. (2004). Integrated echo sounder, GPS, and GIS for reservoir sedimentation studies: Examples from two Arkansas Lakes. *J. Am. Water Resour. Assoc.*, 40(4): 981–997.
- Oğuz, I., Susam, T., Kocyigit, R., Bicak, H., Demirkiran, O., and Demir, S. (2019). Estimation of soil erosion and river sediment yield in a rural basin of North Anatolia, Turkey. *Applied Ecology and Environmental Research*, 17(4): 7741–7763. https://doi.org/10.15666/aeer/1704_77417763
- Ojima, D., Steiner, J., McNeeley, S., Cozzetto, K. and Childress, A. (2015). *Great Plains regional technical input report*. Washington, DC: Island Press.
- Olaniya, M., Bora, K.P., Das, S., and Chanu, H.P. (2020). Soil erodibility indices under different land uses in Ri-Bhoi district of Meghalaya (India). *Scientific reports*, 10:14986. <https://doi.org/10.1038/s41598-020-72070-y>.
- Oldeman, L., Hakkeling, R., and Sombroek, W., (1990). World map of the status of soil degradation, an explanatory note. International soil reference and information center, Wageningen, The Netherlands and the United Nations Environmental Program, Nairobi, Kenya.
- Oldeman, L.R. (1997). Soil Degradation: A Threat to Food Security? Paper presented at the International Conference on Time Ecology: Time for Soil Culture Temporal Perspectives on Sustainable Use of Soil, 6–9 April, Tutzing, Germany.

- Ongwenyi, S.G., Kithiia, M.S., and Denga, O.F. (1993). An overview of the soil erosion and sedimentation problems in Kenya. *Sediment Problems: Strategies for Monitoring, Prediction and Control* (Proceedings of the Yokohama Symposium, July 1993). *IAHS Publ.* 217.
- Onyando, O.J., Kisoyan, P., and Chemilil, M.C. (2005). Estimation of Potential Soil Erosion for River Perkerra Catchment in Kenya. *Water Resources Management*, 19: 133–143. <https://doi.org/10.1007/s11269-005-2706-5>
- Ortt, R.A., Kerhin, R.T., Wells, D., and Cornwell, J. (2000). Bathymetric survey and sedimentation analysis of Loch Raven and Prettyboy reservoirs. *Coastal and estuarine geology file report no. 99-4*. Department of natural resources Maryland geological survey.
- Oshunsanya, S.O. (2018). Introductory Chapter: Relevance of Soil pH to Agriculture. Introductory Chapter: Relevance of Soil pH to Agriculture. In (Ed.), *Soil pH for Nutrient Availability and Crop Performance*. IntechOpen. <https://doi.org/10.5772/intechopen.82551>
- Ouyang, D. and Bartholic, J. (1997). Predicting sediment delivery ratio in Saginaw Bay watershed. Proceedings of the 22nd National Association of Environmental Professionals Conference. May 19–23, Orlando, FL: 659 – 671.
- Ouyang, D., Bartholic, J., and Selegean, J. (2005). Assessing Sediment Loading from Agricultural Croplands in the Great Lakes Basin. *The Journal of American Science*, 1(2): 14–21.
- Owens, N.P. and Collins, J.A. (2006). *Soil Erosion and Sediment Redistribution in River Catchments: Measurement, Modelling and Management*. *CABI Publishing Series*, 328
- Pacina, J., Lend'áková, Z., Štojdl, J., Grygar, M.T., and Dolejš, M. (2020). Dynamics of Sediments in Reservoir Inflows: A Case Study of the Skalka and Nechranice Reservoirs, Czech Republic. *International Journal of Geo-Information*, 9, 258. <http://doi.org/10.3390/ijgi9040258>.
- Pagenkopf, G.K. (1978) *Introduction to Natural Water Chemistry*. Marcel Dekker, New York, 272 pp.

- Palma, P., Penha, A.M., Novais, M.H., Fialho, S., Lima, A., Mourinha, P. *et al.* (2021). Water-Sediment Physicochemical Dynamics in a Large Reservoir in the Mediterranean Region under Multiple Stressors. *Water*, 13, 707. <https://doi.org/10.3390/w13050707>
- Panagos, P., Ballabio, C., Borrelli, P., Meusburger, K., Klik, A., Rousseva, S., *et al.* (2018). Rainfall erosivity in Europe. *Science of the Total Environment*, 511: 801–814. <https://doi.org/10.1016/j.scitotenv.2015.01.008>
- Panagos, P., Borrelli, P., Poesen, J., Ballabio, C., Lugato, E., Meusburger, K., *et al.* C. (2015). The new assessment of soil loss by water erosion in Europe. *Environmental Science & Policy*, 54: 438–447. <http://dx.doi.org/10.1016/j.envsci.2015.08.012>
- Pandey, A., Himanshu, S.K., Mishra, S.K., and Singh, V.P. (2016). Physically based soil erosion and sediment yield models revisited. *Catena*, 147: 595–620. <http://dx.doi.org/10.1016/j.catena.2016.08.002>
- Pandey. A., Mathur, A., Mishra, S.K., and Mal, B.C. (2009). Soil erosion modeling of a Himalayan watershed using RS and GIS. *Environmental Earth Sciences*, 59(2): 399–410. <http://doi.org/10.1007/s12665-00900038-0>
- Panditharanthne, D.I.D., Abeysingha, S.N., Nirmanee, S.G.K., and Mallawatantri, A. (2019): Application of Revised Universal Soil Loss Equation (Rusle) Model to Assess Soil Erosion in “Kalu Ganga” River Basin in Sri Lanka. *Applied and Environmental Soil Science*, Hindawi, 4037379
- Park, S., Oh, C., Jeon, S., Jung, H., and Choi, C. (2011). Soil erosion risk in Korean watersheds, assessed using the revised universal soil loss equation. *Journal of Hydrology*, 399: 263–273. <http://doi.org/10.1016/j.jhydrol.2011.01.004>
- Patyal, S. (2022). RUSLE-based soil erosion assessment and erosion control evaluation in the Kabul Watershed. *Central Asian Journal of Water Research*, 8(1):143-159. <https://doi.org/10.29258/CAJWR/2022-R1.v8-1/143-159.eng>.

- Pelletier, D.J. (2012). A spatially distributed model for the long-term suspended sediment discharge and delivery ratio of drainage basins. *Journal of Geophysical Research*, 117, F02028.
<http://doi.org/10.1029/2011JF002129>.
- Phinzi, K. and Ngetar, N. S. (2019). The assessment of water-borne erosion at catchment level using GIS-based RUSLE and remote sensing: A review. *International Soil and Water Conservation Research*, 7: 27–46.
<https://doi.org/10.1016/j.iswcr.2018.12.002>
- Phyoe, W.W. and Wang, F. (2019). A review of carbon sink or source effect on artificial reservoirs. *International Journal of Environmental Science and Technology*, 16: 2161–2174.
- Pimentel, D. (2006). Soil erosion: A Food and Environmental Threat. *Environment, Development and Sustainability*, 8: 119–137.
<http://doi.org/10.1007/s10668-005-1262-8>
- Pimentel, D. and Burgess, M. (2013). Soil erosion threatens food production. *Agriculture*, 3(3): 443–463. <http://doi.org/10.3390/agriculture3030443>
- Pimentel, D., Marklein, A., Toth, M.A., Karpoff, M.N., Paul, G.S., McCormack, R., *et al.*, (2009). Food versus Biofuels: Environmental and Economic Costs. *Human ecology*, 37(1): 1–12. <http://doi.org/10.1007/s10745-009-9215-8>
- Poesen, J. (2018). Soil erosion in the Anthropocene: research needs. *Earth Surf. Process. Landf.*, 43: 64–84. <http://doi.org/10.1002/esp.4250>
- Prairie, Y.T., Alm, J., Beaulieu, J., Barros, N., Battin, T., Cole, J. *et al.* (2018). Greenhouse Gas Emissions from Freshwater Reservoirs: What Does the Atmosphere See? *Ecosystems*, 21(5): 1058–1071.
<http://doi.org/10.1007/s10021-017-019-0198-9>
- Prasannakumar, V., Shiny, R., Geetha, N., and Vijith, H. (2012). Spatial prediction of soil erosion risk by remote sensing, GIS and RUSLE approach: A case study of Siruvani river watershed in Attapady valley, Kerala, India. *Environ. Earth Sci.*, 64: 965–972.
<http://doi.org/10.1016/j.gsf.2011.11.003>

- Pratson, L., Hughes-Clarke, J., Anderson, M., Gerber, T., and Twichell, D. (2008). Timing and patterns of basin infilling as documented in Lake Powell during a drought. *Geology*, 36(11): 843–846.
<http://doi.org/10.1130/G24733A.1>
- Rabajczyk, A., Józwiak, M.A., Józwiak, M., and Kozłowski, R. (2011). Heavy metal (Cd, Pb, Cd, Zn, Cr) in bottom sediments and the recultivation of Kielce Lake. *Polish Journal of Environmental Studies*, 20(4): 1013–1019.
- Rahaman, S.A., Aruchamy, S., Jegankumar, R., and Ajeez, S.A. (2015) Estimation of Annual Average Soil Loss Based on RUSLE Model in Kallar Watershed, Bhavani Basin, Tamil Nadu, India. *ISPRS Annals of the Photogrammetry, Remote Sensing and Spatial Information Sciences*, II-2/W2, 207-214. Joint International Geoinformation Conference 2015, 28-30 October 2015, Kuala Lumpur, Malaysia
<http://doi.org/10.5194/isprsannals-II-2-W2-207-2015>
- Rakhmatullaev, S., Marache, A., Huneau, F., Le Coustumer, P., Bakiev, M., and Motelica-Heino, M. (2011). Geostatistical approach for the assessment of the water reservoir capacity in arid regions: a case study of the Akdarya reservoir, Uzbekistan. *Environmental Earth Sciences*, 63(3): 447–460.
<http://doi.org/10.1007/s12665-010-0711-3ff.insu-00524538f>
- Ramos, M.C., Quinton, J.N., and Tyrrel, S.F. (2006). Effects of cattle manure on erosion rates and runoff water pollution by faecal coliforms. *J. Environ. Manag.*, 78, 97–101.
- Ramsankaran, J.A.A.R., Kothiyari, U.C., Ghosh, S.K., Malcherek, A., and Mugesan, K. (2013). Physically-based distributed soil erosion and sediment yield model (DREAM) for simulating individual storm events. *Hydrological Sciences Journal*, 58(40):872–891.
<http://doi.10.1080/0262667.2013.781606>.
- Raya, A.M., Zuazo, V. and Martínez, J. (2006). Soil erosion and runoff response to plant-cover strips on semiarid slopes (SE Spain). *Land Degrad. Dev.*, 17: 1–11.
- Razad, A.Z.A., Samsudin, S.H., Setu, A., Abbas, N.A., Sidek, L.M., and Basri, H. (2020). Investigating the Impact of Land Use Change on Sediment Yield for Hydropower Reservoirs through GIS Application. *IOP Conf. Series:*

Earth and Environmental Science 540, 012037.<http://doi:10.1088/1755-1315/540/1/012037>

- Rebetez, M., Lugon, R., and Baeriswyl, P. A. (1997). Climatic change and debris flows in high mountain regions: The case study of the Ritigraben torrent (Swiss Alps). *Climatic Change*, 36 (3–4), 371–389.
- Rellini, I., Scopesi, C., Olivari, S., Firpo, M., and Maerker, M. (2019). Assessment of soil erosion risk in a typical Mediterranean environment using a high resolution RUSLE approach (Portofino promontory, NW-Italy). *Journal of Maps*, 15(2): 356–362.
<https://doi.org/10.1080/17445647.2019.1599452>
- Renard, G.K. and Freimund, R., J. (1994). Using monthly precipitation data to estimate the R-factor in the revised USLE. *J. Hydrol.*, 157: 287–306.
[http://dx.doi.org/10.1016/0022-1694\(94\)90110-4](http://dx.doi.org/10.1016/0022-1694(94)90110-4)
- Renard, K., Foster, G., Weesies, G., McDool, D., and Yoder, D. (1997). Predicting Soil Erosion by Water: A Guide to Conservation Planning with the Revised Universal Soil Loss Equation (RUSLE). Agricultural Handbook 703, USDA-ARS.
- Renfro, G.W. (1975). Use of erosion equation and sediment delivery ratios for predicting sediment yield. Present and Prospective Tecnology for Predicting Sediment Yields and Sources, pp. 33–45, US Dept. Agric, Publ. ARS-S-40, Washington, DC, USA, 1975.
- Rey, F., Bifulco, C., Bischetti, G.B., Bourrier, F., De Cesare, G., Florineth, F. *et al.* (2019). Soil and water engineering: Practice and research needs for reconciling natural hazard control and ecological restoration. *Science of the Total Environment*, 648: 1210–1218.
<http://doi.org/10.1016/j.scitotenv.2018.08.217>
- Rhouma, B.A, Hermassi, T., and Habaieb, H. (2018). Water Erosion modeling in a Mediterranean semi-arid catchment using USLE/GIS (El Gouazine, Central Tunisia). *Journal of new sciences*, 50(7): 3071–3081.
- Ritchie, J.C., Walling, D.E., and Peters, J. (2003). Application of geographic information systems and remote sensing for quantifying patterns of erosion and water quality. *Hydrological Processes*, 17: 885–886.

- Romkens, M.J.M., Prasad, N.S., and Poesen, J. (1986). Soil erodibility and properties. *Transactions of the XIII Congress of the International Soc. of Soil Sci.* 5: 492–504.
- Romkens, M.J.M., Young, A.R., Poesen, A.W.J., McCool, K.D., El-Swaify, A.S., and Bradford, J.M. (1997). Chapter 3. Soil erodibility factor (K) in Predicting Soil Erosion by Water: A Guide to Conservation Planning with the Revised Universal Soil Equation (RUSLE). Agriculture Handbook No. 703, K. G. Renard, G. R. Foster, G. A. Weesies, D. K. McCool, and D. C. Yoder, Eds., pp. 65–99, US Department of Agriculture, Washington, DC, USA.
- Roose, E. (1975). Use of the universal soil loss equation to predict erosion in West Africa. In: *Soil Erosion: Prediction and Control*, Soil and Water Conservation Society, Ankeny, IA: 60–74
- Rooseboom, A. and Annandale, G.W. (1981). Techniques applied in determining sediment loads in South African rivers. *Erosion and Sediment Transport Measurement (Proceedings of the Florence Symposium, June 1981)*. *IAHS Publ.*, 133:219–224.
<http://agris.fao.org/agrissearch/search.do?recordID=US19840095155>
- Roshan, H.M., Solaimani, K., Piri, A., Ahmadi, M., and Lofti, S. (2007). Optimization of the Relationship between Water and Sediment Discharge Rates (Case Study: Amameh Indicator Watershed of Iran). *Pakistan Journal of Biological Sciences*, 10(2): 356–362.
- Roshani, R.M., Rangavar, A., Javadi, R.M., and Ziyadee, A. (2013). A new mathematical model for estimation of soil erosion. *Intl. Res. J. App. Basic. Sci.*, 5(4): 491–495.
- Roslee, R. and Sharir, K. (2019). Soil Erosion Analysis using RUSLE Model at the Minitod Area, Penampang, Sabah, Malaysia. *Journal of Physics: Conference Series* 1358 012066.
<http://doi.org/10.1088/1742-6596/1358/1/012066>.
- Rowell, D.L. (1994). *Soil Science: Methods and Applications*, Longman Scientific and technical, England.
- Rzetala, M., Babicheva, V.A. and Rzetala, M.A. (2019). Composition and physico-chemical properties of bottom sediments in the southern part of the Bratsk Reservoir (Russia). *Scientific reports* 9, 12790.

<https://doi.org/10.1038/s41598-019-49228-4>.

- Sadeghi, R.H.S. and Mizuyama, T. (2007). Applicability of the Modified Universal Soil Loss Equation for prediction of sediment yield in Khanmirza watershed, Iran. *Hydrological Sciences Journal*, 52(5): 1068–1075. <https://doi.org/10.1623/hysj.52.5.1068>
- Sadeghi, S. H. R., Singh, J. K., and Das, G. (2004). Efficacy of annual soil erosion models for storm-wise sediment prediction: a case study. *Int. Agric. Engng J.* 13(1/2): 1–14.
- Saha, A., Ghosh, P., and Mitra, B. (2018). GIS Based Soil Erosion Estimation Using Rusle Model: A Case Study of Upper Kangsabati Watershed, West Bengal, India. *International Journal of Environmental Sciences & Natural Resources*, 13(5): 119–126. <http://doi.org/10.19080/IJESNR.2018.13.555871>.
- Sahana, M., Ahmed, R., and Sajjad, H. (2016). Analyzing land surface temperature in response to land use/land cover change using split window algorithm and spectral radiance model in Sundarban Biosphere Reserve, India. *Model. Earth Syst. Environ.* 2(81). <http://doi.org/10.1007/s40808-016-0135-5>. <http://doi.org/10.1007/s40808-016-013-5>
- Sahoo, K., Jee, P.K., Dhal, N.K., and Das, R. (2017). Physico-chemical sediment properties of mangroves of Odisha, India. *Journal of Oceanography and Marine Research*. 5(2). <http://doi.org/10.4172/2572-3103.1000162>
- Sahu, A., Baghel, T., Sinha, K.M., Ahmad, I., Verma, K.M. (2017). Soil Erosion Modelling using RUSLE and GIS on Dudhawa Catchment. *International Journal of Applied Environmental Sciences*, 12(6): 1147–1158.
- Salunkhe, S.S., Nandgude, B.S., Mahale, M.D., Bhambure, V.T., Bhattacharya, T., and Wandre, S.S. (2018). Estimation of Soil Erosion and Nutrient Loss by USLE Model for Ratnagiri District. *Advanced Agricultural Research & Technology Journal*, 2(1): 53–61
- Samaila-Ija, H.A., Ajayi, O.G., Zitta, N., Odumosu, J.O., and Kuta, A.A. (2014). Bathymetric Survey and Volumetric Analysis for Sustainable Management Case Study of Suleja Dam, Niger State, Nigeria. *Journal of Environment and Earth Science*, 4(18): 24–32

- Sanders, D.W. (1986). Sloping land: soil erosion problems and soil conservation requirements. In: Land evaluation for land use planning and conservation in sloping areas (ed. W. Siderius), pp. 40-50. International Workshop, Enschede, The Netherlands, 17-21 December, 1984.
- Sang, J.K., Raude, J.M., Mati, B.M., Mutwiwa, U.N. and Ochieng, F. (2017). Dual Echo Sounder Bathymetric Survey for Enhanced Management of Ruiru Reservoir, Kenya. *Journal of sustainable research in engineering*, 3(4): 113–118.
- Santos, N.C.J., Andrade, M.E., Medeiros, A.H.P., Guerreiro, S.J.M., and Palacio, Q.A.H. (2017). Land use impact on soil erosion at different scales in the Brazilian semi-arid. *Revista Ciência Agronômica*, 48 (2); 251–260.
<http://doi.org/10.5935/1806-6690.20170029>
- Schleiss, A.J., and De Cesare, G. (2010). Physical model experiments on reservoir sedimentation. *IAHR Hydrolink*, 4, 54–57.
- Schleiss, A.J., Franca, J.M., Juez, C., and De Cesare, G. (2016). Reservoir Sedimentation. *Journal of Hydraulic Research*, 54 (6): 595–614.
<http://dx.doi.org/10.1080/00221686.2016.1225320>
- Schreier, H. and Shah, P. (1999). Soil fertility status and dynamics in the Jhikhu and Yarsha Khola watersheds. In Proceedings of the People and Resource Dynamics Project: The First Three Years (1996–1999), Baoshan, China, 2–5: 281–289.
- Sha'Ato, R., Benibo, A.G., Itodo, A.U., and Wuana, R.A. (2020). Evaluation of bottom sediment qualities in Ihetutu Minefield, Ishiagu, Nigeria. *Journal of Geoscience and Environment Protection*, 8: 125–142.
<https://doi.org/10.4236/gep.2020.84009>
- Shabani, F., Kumar, L., and Esmaili, A. (2014). Improvement to the prediction of the USLE K factor. *Geomorphology*, 204: 229–234.
<http://doi.org/10.1016/j.geomorph.2013.08.008>
- Sharma, A. (2010). Integrating and vegetation indices for identifying potential soil erosion risk area. *Geol. Spat. Info. Sci.*, 13: 201–209.
<http://doi.org/10.1007/s11806-0100342-6>

- Sharma, V., Sharma, K.K., and Sharma, A. (2013). Sediment Characterization of Lower sections of a Central Himalayan river, Tawi, Jammu (J&K), India. *International Research Journal of Environment Sciences*, 2: 51–55.
- Sharply, N.A. and Williams, R.J. (1990). EPIC-erosion/productivity impact calculator I, Model documentation. U.S. Department of Agriculture Technical Bulletin, Beltsville, MD, No.1768.
- Sheikh, A.H., Palria, S., and Alam, A. (2011). Integration of GIS and Universal Soil Loss Equation (USLE) for soil loss estimation in a Himalayan watershed. *Recent Res. Sci. Tech.*, 3: 51–57.
- Shi, Z., Cai, C., Ding, S., Wang, T., and Chow, T. (2004). Soil Conservation Planning at the Small Watershed Level Using RUSLE with GIS: A Case Study in the Three Gorge Area of China. *Catena*, 55: 33–48.
[http://doi.org/10.1016/S0341-8162\(03\)00088-2](http://doi.org/10.1016/S0341-8162(03)00088-2)
- Shoshany, M., Goldshleger, N., and Chudnovsky, A. (2013). Monitoring of agricultural soil degradation by remote-sensing methods: A review. *Int. J. Remote Sens.*, 34 (17): 6152–6181.
<http://doi.org/10.1080/01431161.2013.793872>
- Siddique, A.N.M., Sultana, J., Abdullah, R.M., and Azad, N.K. (2017). Modelling of Soil Loss through RUSLE2 for Soil Management in an Agricultural Field of Uccle, Belgium. *British Journal of Environment & Climate Change*, 7(4): 252–260. <http://doi.org/10.9734/BJECC/2017/35336>
- Šiljeg, A., Maric, I., Domazetovic, F., Cukrov, N., Lovric, M., and Panda, L. (2022). Article Bathymetric Survey of the St. Anthony Channel (Croatia) Using Multibeam Echosounders (MBES)—A New Methodological Semi-Automatic Approach of Point Cloud Post-Processing. *J. Mar. Sci. Eng.*, 10, 101. <https://doi.org/10.3390/jmse10010101>
- Simms. D.A., Woodroffe, D.C., and Jones, G.B. (2003). Application of RUSLE for erosion management in a coastal catchment, southern NSW, , in Proceedings of MODSIM 2003: International Congress on Modelling and Simulation, Integrative Modelling of Biophysical, Social and Economic Systems for Resource Management Solutions, Townsville, Queensland, 14-17 July, 2: 678–683.

- Simons, D.B. and Şentürk, F. (1992). Sediment transport technology: water and sediment dynamics. *Water Resources Publication*. Colorado, USA.
- Singare, P.U., Trivedi, M.P. and Mishra, R.M. (2011). Assessing the Physico-Chemical Parameters of Sediment Ecosystem of Vasai Creek at Mumbai, India. *Marine Science*, 1(1): 22–29.
<http://doi.org/10.5923/j.ms.20110101.03>
- Singh, G. and Panda, R.K. (2017). Grid-cell based assessment of soil erosion potential for identification of critical erosion prone areas using USLE, GIS and remote sensing: A case study in the Kapgari watershed, India. *International Soil and Water Conservation Research*, 5(3): 202–211.
<http://doi.org/10.1016/j.iswcr.2017.05.006>
- Singh, R., Tiwari, N.K., and Mal, C.B. (2006). Hydrological Studies for Small Watershed in India using the ANSWERS Model. *Journal of Hydrology*, 318: 184–199. <http://doi.org/10.1016/j.jhydrol.2005.06.011>
- Sivapalan, M. (2003). Process Complexity at Hillslope Scale, Process Simplicity at the Watershed Scale: Is there a connection? *Hydrological Processes*, 17 (5): 1037–104.
- Smal, H., Ligeża, S., Baran, S., Wójcikowska-Kapusta, A. and Obroślak, R. (2013). Nitrogen and Phosphorus in Bottom Sediments of Two Small Dam Reservoirs. *Pol. J. Environ. Stud.*, 22(5):1479–1489.
- Smets. T., Poesen, J., and Knapen, A. (2008). Spatial scale effects on the effectiveness of organic mulches in reducing soil erosion by water. *Earth-Science Reviews*, 89. <http://doi.org/10.1016/j.earscirev.2008.04.001>
- Snyder, N.P., Rubin, D.M., Alpers, C.N., Childs, J.R., Curtis, J.A., Flint, L.E. *et al.* (2004). Estimating accumulation rates and physical properties of sediment behind a dam: Englebright Lake, Yuba River, Northern California. *Water Resources Research*, 40(11).
<http://doi.org/10.1029/2004WR003279>
- Sojka, M., Choiński, A., Ptak, M., and Siepak, M. (2021). Causes of variations of trace and rare earth elements concentration in lakes bottom sediments in the Bory Tucholskie National Park, Poland. *Scientific reports*, 11, 244.
<https://doi.org/10.1038/s41598-020-80137-z>

- Sriniva, G. and Naik, M.G. (2017). Hydrological Modeling of Musi River Basin, India and Sensitive Parameterization of Stream Flow Using SWAT CUP. *Journal of Hydrogeology and Hydrologic Engineering*, 6(2). <http://doi.org/10.4172/2325-9647.1000153>.
- Sriwati, M., Pallu, S., Selintung, M., and Lopa. (2018). Bioengineering Technology to Control River Soil Erosion using Vetiver (*Vetiveria Zizanioides*). IOP Conf. Series: *Earth and Environmental Science*, 140, 012040 <http://doi.org/10.1088/1755-1315/140/1/012040>
- Stringer, C. E., Trettin, C. C., and Zarnoch, S. J. (2016). Soil properties of mangroves in contrasting geomorphic settings within the Zambezi River Delta, Mozambique. *Wetlands Ecol. Manage.*, 24: 139–152. <http://doi.org/10.1007/s11273-015-9478-3>.
- Sujatha, R.E. and Sridhar, V. (2018). Spatial Prediction of Erosion Risk of a Small Mountainous Watershed Using RUSLE: A Case-Study of the Palar Sub-Watershed in Kodaikanal, South India. *Water*, 10, 1608. <http://doi.org/10.3390/w10111608>
- Summer, W. (1994). GIS and soil erosion models as tools for the development of soil conservation strategies. *Transactions on Ecology and the Environment*, 6: 303–310.
- SWAG (2002). Principles of Erosion and Sediment Control. <http://www.watershedrestoration.org/erosion.htm>. Accessed on 01/02/2020
- Swarnkar, S., Malini, A., Tripathi, S., and Sinha, R. (2018). Assessment of uncertainties in soil erosion and sediment yield estimates at ungauged basins: an application to the Garra River basin, India. *Hydrol. Earth Syst. Sci.*, 22: 2471–2485. <https://doi.org/10.5194/hess-22-2471-2018>
- Syombua, J.M. (2013). Land use and land cover changes and their implications for human-wildlife conflicts in the semi-arid rangelands of southern Kenya. *Journal of Geography and Regional Planning*, 6(5): 193–199. <http://doi.org/10.5897/JGRP2013.0365>

- Szymański, D., Dunalska, J., Lopata, M., Bigaj, I., and Zieliński, R. (2012). Characteristics of bottom sediments of Lake Widryńskie. *Limnological Review*, 12: 205–210. <http://doi.org/10.2478/v10194-012-0061-5>
- Tabarestani, M.K. and Zarrati, A.R. (2014). Sediment transport during flood event: a review. *International Journal of Environmental Science and Technology*, 12(2). <http://doi.org/10.1007/s13762-014-0689-6>.
- Tadesse, L.D. and Morgan, R.P.C. (1996). Contour grass strips: A laboratory simulation of their role in erosion control using live grasses. *Soil Technol.* 9: 83–89.
- Tamang, K.S., Song, W., Fang, X., Vasconcelos, J., and Anderson, B. (2018). Framework for quantifying flow and sediment yield to diagnose and solve the aggradation problem of an ungauged catchment. *Proc. IAHS*, 379: 131–138. <https://doi.org/10.5194/piahs-379-131-2018>
- Tamene, L., Park, J.S., Dikau, R., and Vlek, G.L.P. (2006). Reservoir siltation in the semi-arid highlands of northern Ethiopia: sediment yield–catchment area relationship and a semi-quantitative approach for predicting sediment yield. *Earth Surface Processes and Landforms*, (31): 1364–1383. <http://doi.org/10.1002/esp.1338>
- Teixeira, E.C. and Caliar, P.C. (2005). Estimation of the concentration of suspended solids in rivers from turbidity measurement. Sediment Budgets 1 (Proceedings of symposium S1 held during the Seventh IAHS Scientific Assembly at Foz do Iguacu, Brazil, April 2005). *IAHS Publ.*, 291: 151–160
- Tesfaye, G. and Tibebe, D. (2018). Soil Erosion Modeling Using GIS Based RUSSEL Model in Gilgel Gibe-1 Catchment, South West Ethiopia. *Int J Environ. Sci. Nat. Res.*, 15(5): 141–148. <http://doi.org/10.19080/IJESNR.2018.15.555923>
- Tessema, M.Y., Jasinska, J., Yadeta, T.L., Switoniak, M., Puchalka, R., and Gebregeorgis, G.E. (2020). Soil Loss Estimation for Conservation Planning in the Welmel Watershed of the Genale Dawa Basin, Ethiopia. *Agronomy*, 10, 777. <http://doi.org/10.3390/agronomy10060777>.

- Tfwala, S.S. and Wang, Y. (2016). Estimating Sediment Discharge Using Sediment Rating Curves and Artificial Neural Networks in the Shiwen River, Taiwan. *Water*, 8, 53. <http://doi.org/10.3390/w8020053>.
- Thlakma, S.R., Iguisi, E.O., Odunze, A.C., and Jeb, D.N. (2018). Estimation of Soil Erosion Risk in Mubi South Watershed, Adamawa State, Nigeria. *Journal of Remote Sensing and GIS*, 7, 1. <http://doi.org/10.4172/2469-4134.1000226>.
- Thomas, J., Joseph, S., and Thrivikramji, P.K. (2018). Assessment of soil erosion in atropical mountain river basin of the southern Western Ghats, India using RUSLE and GIS. *Geoscience Frontiers*, 9: 893–906. <https://dx.doi.org/10.1016/j.gsf.2017.05.011>
- Thomas, P., Mondal, S., Roy, D., Meena, M.C., Aggarwal, B.K., Sharma, AR. et al. (2020). Exploring the relationships between penetration resistance, bulk density and water content in cultivated soils. *Journal of Agricultural Physics*, 20(1): 22-29.
- Tiwari, K.R.; Sitaula, B.K.; Bajracharya, R.M., and Borresen, T. (2008). Runoff and soil loss responses to rainfall, land use, terracing and management practices in the Middle Mountains of Nepal. *Acta Agric. Scand. B Soil Plant. Sci.*, 59: 197–207. <http://10.1080/09064710802006021>
- Tolessa, T., Dechassa, C., Simane, B., Alamerew, B., and Kidane, M. (2020). Land use/land cover dynamics in response to various driving forces in Didessa sub-basin, Ethiopia. *Geojournal*, 85: 747–760. <http://doi.org/10.1007/s10708-019-09990-4>
- Torri, D., Poesen, J., and Borselli, L. (1997). Predictability and uncertainty of the soil erodibility factor using global dataset. *Catena*, 31(1-2). [http://doi.org/10.1016/S0341-8162\(97\)00036-2](http://doi.org/10.1016/S0341-8162(97)00036-2).
- Traore, K. and Birhanu, Z.B. (2019). Soil Erosion Control and Moisture Conservation Using Contour Ridge Tillage in Bougouni and Koutiala, Southern Mali. *Journal of Environmental Protection*, 10: 1333-1360. <https://doi.org/10.4236/jep.2019.1010079>.
- Trigunasih, M.N., Kusmawati, T., and Lestari, Y.W.N (2018). Erosion Prediction Analysis and Landuse Planning in Gunggung Watershed, Bali, Indonesia.

OP Conference Series: Earth and Environmental Science, 123. <http://doi.org/10.1088/1755-1315/123/1/012025>.

Trimble, W.S. and Mendel, C.A. (1995). The cow as a geomorphic agent - A critical review. *Geomorphology*, 13: 233–253. [http://doi.org/10.1016/0169-555X\(95\)00028-4](http://doi.org/10.1016/0169-555X(95)00028-4)

Tsitsagi, M., Berdzenishvili, A., and Gugeshashvili, M. (2018). Spatial and temporal variations of rainfall-runoff erosivity (R) factor in Kakheti, Georgia. *Annals of Agrarian Science*, 16: 226–235. <https://doi.org/10.1016/j.aasci.2018.03.010>

Turgut, B., Ozalp, M., and Kose, B. (2015). Physical and chemical properties of recently deposited sediments in the reservoir of the Borçka Dam in Artvin, Turkey. *Turkish Journal of Agriculture and Forestry. Turk J Agric For*, 39: 663–678.

TWDB (2009). Volumetric and sedimentation survey of Lake Weatherford. http://www.twdb.texas.gov/hydro_survey/weatherford/2008-08/Weatherford2008_FinalReport.pdf. Accessed on 30 March 2022.

Uddin, K., Murthy, R.S.M, Wahid, M.S., and Matin, A.M. (2018). Estimation of Soil Erosion Dynamics in the Koshi Basin Using GIS and Remote Sensing to Assess Priority Areas for Conservation. *PloS One*, 11(3). <http://doi.org/10.1371/journal.pone.0150494>.

United States Geological Survey. Aster Digital Elevation Model (DEM) Resolution of 30 Metres Website. <https://gdex.cr.usgs.gov/gdex/>. Accessed on 28 February 2021.

United States Soil Conservation Service (USSCS), (1971). “Section 3, Chapter 6: Sediment sources, yields and delivery ratios.” SCS national engineering handbook, USDA Soil Conservation Service, Washington, D.C.

Urgesa, M.H. and Yilma, B. (2015). Vertical Changeability of Physico-Chemical Characteristics on Bottom Sediments in Lakes Chamosouthern Ethiopia. *G.J.L.S.B.R.*, 1: 1–6.

USDA (1975). Sediment Sources, Yields, and Delivery Ratios. National Engineering Handbook, Section 3 Sedimentation.

- Ustun, B. (2008). Soil Erosion Modelling by using GIS & Remote Sensing: A case study, Ganos Mountain. *The International Archives of the Photogrammetry, Remote Sensing and Spatial Information Sciences*, 37(7): 1681–1684.
- Van der Knijff, J. M., Jones, R. J. A., and Montanarella, L. (1999). Soil erosion risk assessment in Italy. EUR1902 EN, Office for Official Publications of the European Communities, Luxembourg, 54.
- Vannoppen, W., Vanmaercke, M., De Baets, S., and Poesen, J. (2015). A review of the mechanical effects of plant roots on concentrated flow erosion rates. *Earth-Science Reviews*, 150: 666–678.
<http://doi.org/10.1016/j.earscirev.2015.08.011>
- Vanoni, V.A. (1975). Sediment engineering. Manual and Report No. 54. American Society of Civil Engineers, New York.
- Vantas, K., Sidiropoulos, E., and Evangelides, C. (2019). Rainfall Erosivity and Its Estimation: Conventional and Machine Learning Methods, Soil Erosion - Rainfall Erosivity and Risk Assessment, *IntechOpen*.
<http://dx.doi.org/10.5772/intechopen.85937>
- Verheijen, F., Jones, R., Rickson, R., and Smith, C. (2009). Tolerable versus actual soil erosion rates in Europe. *Earth Science Review*, 94: 23–38.
<http://doi.org/10.1016/j.earscirev.2009.02.003>
- Verstraeten, G. and Poesen, J. (2000). Estimating trap efficiency of small reservoirs and ponds: methods and implications for the assessment of sediment yield. *Progress in Physical Geography* 24: 219–251.
<http://dx.doi.org/10.1177/030913330002400204>
- Vianna, F.V., Fleury, M.P., Menezes, G.B., Coelho, A.T., Bueno, C., da Silva, J.L. *et al.* (2020). Bioengineering Techniques Adopted for Controlling Riverbanks' Superficial Erosion of the Simplicio Hydroelectric Power Plant, Brazil. *Sustainability*, 12, 7886. <http://doi.org/10.3390/su12197886>.
- Viney, N.R. and Sivapalan, M. (1999). A conceptual model of sediment transport: application to the Avon River Basin in Western Australia. *Hydrological Processes*, 13: 727–743.

[http://doi.org/10.1002/\(SICI\)1099-1085\(19990415\)13:5<727::AID-HYP776>3.0.CO;2-D](http://doi.org/10.1002/(SICI)1099-1085(19990415)13:5<727::AID-HYP776>3.0.CO;2-D)

- Vrieling, A., Sterk, G., and Beaulieu, N. (2002). Erosion Risk Mapping: A Methodological Case Study in the Colombian Eastern Plains. *J. Soil Water Conserv.*, 57(3): 158–163.
- Wagari, M. and Tamiru, H. (2022). RUSLE Model Based Annual Soil Loss Quantification for Soil Erosion Protection: A Case of Fincha Catchment, Ethiopia. *Air, Soil and Water Research*, 14: 1–12.
<https://doi.org/10.1177/11786221211104623>.
- Wakindiki, I.I.C. and Ben-Hur, M. (2002). Indigenous soil and water conservation techniques: effects on runoff, erosion, and crop yields under semi-arid conditions. *Soil Res.*, 40:367–379. <http://doi.org/10.1071/SR01037>.
- Walkley, A. and Black, I.A. (1934). An examination of the Degtjareff method for determining soil organic matter and a proposed modification of the chromic acid titration method. *Soil Science* 37: 29–38.
- Walling, D.E. (1983). The sediment delivery problem. *J. Hydrol.*, 65(1– 3):209–237. [https://doi.org/10.1016/0022-1694\(83\)90217-2](https://doi.org/10.1016/0022-1694(83)90217-2)
- Walling, D.E. and Webb, B.W. (1996). Erosion and sediment yield: A global overview. In: Walling, D.E., Webb, B.W. (Eds.), *Erosion and Sediment Yield: Global and Regional Perspectives (Proceedings of the Exeter Symposium, July 1996), IAHS Publication*, 236: 3–19.
- Waltham, N.J., Reichelt-Brushett, A., McCann, D., and Eyre, B.D. (2014). Water and sediment quality, nutrient biochemistry and pollution loads in an urban freshwater lake: balancing human and ecological services. *Environ. Sci. Process. Impacts*, 16: 2804–2813.
<http://doi.org/10.1039/c4em00243a>
- Wang, J, Lu, P., Valente, D., Petrosillo, I., Babu, S., Xu, S. et al. (2022). Analysis of soil erosion characteristics in small watershed of the loess tableland Plateau of China. *Ecological Indicators*, 137, 108765.
<http://doi.org/10.1016/j.ecolind.2022.108765>

- Wang, Z.Y., Lee, J.H.W., and Melching, C.S. (2015). Vegetation-erosion dynamics. In: *River Dynamics and Integrated River Management*. Springer, Berlin, Heidelberg: 53–122
- Wasson, R.J., Olive, L.J., and Rosewell, C.J. (1996). Rates of erosion and sediment transport in Australia. *Erosion and Sediment Yield: Global and Regional Perspectives (Proceedings of the Exeter Symposium, July 1996)*. IAHS Publi., 236.
- WCD. (2000). *The report of the world commission on dams*. London: World Commission on Dams/Earthscan Publications.
- Weschmeier, W.H. and Smith, D.D. (1978). Predicting rainfall erosion losses - a guide to conservation planning. Series: agriculture handbook (3-4) Washington DC: USDA.
- Wheater, H.S., Jakeman, J., Beven, K.J., and McAleer, M.J. (1993). Progress and directions in rainfall-runoff modelling, *Modelling change in environmental systems*. New York: 101 - 132.
- Wiesebron, L.E., Steiner, N., Morys, C., Ysebaert, T., and Bouma, T.J. (2021). Sediment Bulk Density Effects on Benthic Macrofauna Burrowing and Bioturbation Behavior. *Front. Mar. Sci.* 8, 707785. <http://doi.org/10.3389/fmars.2021.707785>.
- Williams, J. R. and Berndt, H. D. (1977). Sediment yield prediction based on watershed hydrology. *Trans. Am. Soc. Agric. Engrs*, 20(6): 1100–1104.
- Wójcikowska-Kapusta, A. and Smal, H. (2018). Contents of selected macronutrients in bottom sediments of two water reservoirs and assessment of their suitability for natural use. *Journal of water and land development* 38: 147–153. <http://doi.org/10.2478/jwld-2018-0051>
- Woldemariam, W. G., Iguala, D.A., Tekalign, S., and Reddy, U.R. (2018). Spatial Modeling of Soil Erosion Risk and Its Implication for Conservation Planning: the Case of the Gobeles Watershed, East Hararge Zone, Ethiopia. *Land*, 7, 25. <http://doi.org/10.3390/land7010025>.
- Woldemariam, W.G. and Harka, E.A. (2020). Effect of Land Use and Land Cover Change on Soil Erosion in Erer Sub-Basin, Northeast Wabi Shebelle Basin, Ethiopia. *Land*, 9, 111. <http://doi.org/10.3390/land9040111>

- Wondim, Y.K. and Mosa, H.M. (2015). Spatial variation of sediment physicochemical characteristics of Lake Tana, Ethiopia. *Journal of Environment and Earth Science*, 5: 95–109
- World Health Organization (WHO), (2004) Guidelines for drinking water quality. 1; 3rd Edn., World Health Organization, Geneva, Switzerland.
- WRB (2006) World Reference Base for Soil Resources. World Soil Resources Report No. 103. Rome: Food and Agriculture Organization of the United Nations; 2006. ISBN-10: 9251055114
- Wu, L., Liu, X., and Ma, X. (2018). Research progress on the watershed sediment delivery ratio. *International Journal of Environmental Studies*, 75(4): 565–579. <https://doi.org/10.1080/00207233.2017.1392771>
- Wuepper, D., Borrelli, P., and Finger, R. (2020). Countries and the global rate of soil erosion. *Nat Sustain.*, 3: 51–55. <http://doi.org/10.1038/s41893-919-0438-4>
- Ya, T. and Nakarmi, G. (2004). Effect of contour hedgerows of nitrogen-fixing plants on soil erosion of sloping agricultural land. Impact of Contour Hedgerows: A Case Study. Presented at ICIMOD, Kathmandu, Nepal, 8–11 September 2004.
- Yahya, F., Dalal, Z., and Ibrahim F. (2013). Spatial Estimation of Soil Erosion Risk Using RUSLE Approach, RS, and GIS Techniques: A Case Study of Kufranja Catchment, Northern Jordan. *Journal of Water Resource and Protection*, 5: 1247–1261. <http://doi.org/10.4236/jwarp.2013.512134>
- Yan, Z., Qin, L., Wang, R., Wang, X., Tang, X., and An, R. (2018). The Application of a Multi-Beam Echo-Sounder in the Analysis of the Sedimentation Situation of a Large Reservoir after an Earthquake. *Water*, 10, 557. <http://doi.org/10.3390/w10050557>.
- Yang, D., Shinjiro, K., Taikano, O., Toshio, K., and Katumi, M. (2003) Global Potential Soil Erosion with Reference to Land Use and Climate. *Hydrological Process.*, 17, 2913–2928. <http://doi.org/10.1002/hyp.1441>
- Yang, T.C., Randle, J.T., and Hsu, S.K. (1998). Surface erosion, sediment transport, and reservoir sedimentation. Modelling Soil Erosion, Sediment

Transport and Closely Related Hydrological Processes (Proceedings of a symposium held at Vienna, July 1998). *IAHS Publ.* 249.

- Yasarer, L. M. and Sturm, B. S. (2016). Potential impacts of climate change on reservoir services and management approaches. *Lake and Reservoir Management*, 32(1), 13–26.
<http://doi.org/10.1080/10402381.2015.1107665>
- Yesuf, H.M., Alamirew, T., Melesse, A.M., and Assen, M. (2013). Bathymetric study of Lake Hayq, Ethiopia. *Lakes and Reservoirs; Research and Management*, 18: 155–165. <http://doi.org/10.1111/lre.12024>
- Yesuph, Y.A. and Dagneu, B.A. (2019). Soil erosion mapping and severity analysis based on RUSLE model and local perception in the Beshillo Catchment of the Blue Nile Basin, Ethiopia. *Environmental Systems Research*, 8, 17. <https://doi.org/10.1186/s40068-019-0145-1>
- Yin, S., Zhu, Z., Wang, L., Liu, B., Xie, Y., Wang, G., and Li, Y. (2018). Regional soil erosion assessment based on a sample survey and geostatistics. *Hydrol. Earth Syst. Sci.*, 22: 1695–1712.
<http://doi.org/10.5194/hess-22-1695-2018>
- Young, A.R., Onstad, A.C., Bosch, D.D., and Anderson, P.W. (1989). AGNPS: a non-point source pollution model for evaluating agricultural watersheds. *Journal of Soil and Water Conservation*, 44(2):168–173.
- Yueqing, X., Ding, L., and Jian, P. (2011). Land use change and soil erosion in the Maotiao River watershed of Guizhou Province. *J Geogr Sci.*, 21: 1138–1152. <http://doi.org/10.1007/s11442-011-0906-x>
- Yufeng, E.G., Thomasson, J.A., and Sui, R., (2011). Remote sensing of soil properties in precision agriculture: A review. *Frontiers in Earth Science*, Vol. 5(3): 229–238. <http://doi.org/10.1007/s11707-011-0175-0>
- Zakonov, V.V., Gusakov, V.A., Sigareva, L.E., and Timofeeva, N.A. (2019). Physicochemical properties of bottom sediments in water bodies in the central and southern Vietnam. *Water Resources*, 46: 87–93.
<http://doi.org/10.1134/S0097807819010159>

- Zhang, K., Yu, Y., Dong, J., Yang, Q., and Xu, X. (2019). Adapting & testing use of USLE K factor for agricultural soils in China. *Agriculture, Ecosystems and Environment*, 269: 148 – 155.
<https://doi.org/10.1016/j.agee.2018.09.033>
- Zhang, L., O'Neill, A.L., and Lacey, S. (1996). Modelling approaches to the prediction of soil erosion in catchments. *Environmental Software*, 11: 123–133. [http://doi.org/10.1016/S0266-9838\(96\)00023-8](http://doi.org/10.1016/S0266-9838(96)00023-8)
- Zi, T., Kumar, M., Kiely, G., Lewis, C., and Albertson, J. (2016). Simulating the spatio-temporal dynamics of soil erosion, deposition, and yield using a coupled sediment dynamics and 3D distributed hydrologic model. *Environmental Modelling and Software*. 83: 310–325.
<http://doi.org/10.1016/j.envsoft.2016.06.004>
- Ziemińska-Stolarska, A., Imbierowicz, E., Jaskulski, E., and Szmidt, A. (2020). Assessment of the Chemical State of bottom Sediments in the Eutrophied Dam Reservoir in Poland. *Int. J. Environ. Res. Public Health*, 17, 3424.
<http://doi.org/10.3390/ijerph17103424>